Leber Congenital Amaurosis and other autosomal recessive retinal dystrophies: A clinical and molecular genetic study

Moorfields Eye Hospital

Institute of Ophthalmology

University College London

Mr Phillip Moradi BSc MBChB FRCOphth

Supervisors: Professor AT Moore, Professor AR Webster

MD thesis to be submitted to the University of London

I, Phillip Moradi, confirm that the work presented in this thesis is my own.

Information from other sources have been referenced appropriately and indicated clearly.

Abstract

Leber congenital amaurosis (LCA) and the early onset retinal dystrophies (EORD) are a spectrum of autosomal recessively inherited genetic conditions affecting children who have visual impairment starting under the age of five years. There are currently 19 known genes that account for approximately two thirds of cases. Only two of these 19 genes (*IMPDH1* and *CRX;* not studied in this project) have been found to cause autosomal dominant LCA. This genetic heterogeneity makes the identification of these causative genes expensive and time consuming. Phenotype-genotype correlations are therefore important in directing efforts to determine the molecular cause of disease. The aims of this research project were to recruit and clinically characterise a large panel of LCA and EORD patients and to identify the underlying genetic cause of autosomal recessive disease. Patients were recruited from Moorfields Eye Hospital and Great Ormond Street Hospital. A full clinical examination was carried out. DNA samples were analysed using the Asper Ophthalmics LCA microarray chip and by direct sequencing. Large families, with several affected members, were examined using the Affymetrix gene chip arrays for regions of homozygosity and candidate gene sequencing was performed. DNA samples from 158 patients were obtained and 117 patients were examined clinically. A definitive molecular diagnosis was obtained for 26% of patients. Of the cohort of 158 patients with one or two mutated alleles identified and genotyped: *RPE65* accounts for 1% of this cohort, 6% are due to mutations in *CRB1*, 15% are due to *RDH12* mutations and 11% are due to mutations in *CEP290*. Two families were identified with novel *CRALBP* mutations. The genotype yield from the period of this research, August 2006- August

2008, is lower than that expected with newer technologies in 2014; such as next generation sequencing (NGS) or whole exome sequencing. Useful prognostic information gained will help future patients with these disorders. Patients with a molecular diagnosis may be eligible for clinical trials of gene replacement therapy.

Contents

Figures

Tables

Acknowledgments

Funding: Moorfields Special Trustees; The Eranda Foundation; EVI-GENORET

Professor Tony Moore. For all your great support. Thank you.

Professor Andrew Webster. For giving me the opportunity to do this work. Thank you.

Professor Alison Hardcastle. For all your time and help. Thank you.

Beverly Scott. Reliable, supportive and conscientious. Thank you.

Eva and Mae. For lighting up my life every day. And forever.

Eddy, Maureen and Paul. For being there always. Full of love.

1 Introduction

1.1 History

Theodor Karl Gustav von Leber (1840 - 1917) was a German ophthalmologist who initially studied in Heidelberg with Hermann von Helmholtz, the inventor of the ophthalmoscope. Leber gained international acclaim as a 24 year old at the Heidelberg Ophthalmological Society Congress with his demonstrations on the blood circulation of the eye. From 1867 until 1870 he was an assistant to Albrecht von Graefe (1828-1870) in Berlin and was subsequently director of the eye clinic in Heidelberg, where he worked as an experimental physiologist.

Despite Leber's rejection of clinical ophthalmology as a full time career he was the first to describe Leber's congenital amaurosis in 1869 and Leber's hereditary optic neuropathy in 1871. Further eponymous contributions include: Leber's plexus, a small venous plexus in the eye located adjacent to Schlemm's canal, Leber's miliary aneurysm and the Fransechetti-Leber phenomenon or oculo-digital sign of early-acquired or congenital blindness.

In 1869, Leber was working as an ophthalmic consultant for the Ilvesheim school for the blind in Germany. His original description of an 'intrauterine' form of retinitis pigmentosa (RP), "Ueber Retinitis pigmentosa und angeborene Amaurose"[1] is still used today and included: severe visual loss at or near birth , wandering nystagmus, amaurotic pupils and a pigmentary retinopathy. Leber classified this new diagnosis as part of the retinitis pigmentosa (RP) spectrum and termed it "*tapetoretinale Degeneration mit Amblyopie"* and suggested the name 'amaurosis congenita' for this condition with a notably high incidence of hereditary factors.

Franceschetti and Dieterle in 1957 recognised an important diagnostic feature of LCA, the severely reduced or absent electroretinogram (ERG) measured early in the disease process.[2] Later Waardenburg presented 32 congenitally blind children and concluded that half of them had features consistent with Leber's original description.[3] Sixteen of the children in his group had a high incidence of keratoconus/keratoglobus and all had retinal dysfunction. Waardenburg hypothesised that an aplasia or a dysgenesis was the causative pathology and proposed the name "*dysgenesis neuroepithelialis retinae"*. The same year, Alstrom and Olson reported an extensive study from Sweden in which 20% of blind children had LCA. This condition was described as condition heredoretinopathia congenitalis monohybrida recessiva autosomalis.[4] In 1958, Schappert-Kimmijser and colleagues reviewed 227 cases of LCA. Most of the ERGs performed were reported as abolished responses or demonstrated small photopic responses with very high intensities, with only two patients showing a small scotopic response.[5]

In 1956 Waardenburg described children with very poor vision and a high incidence of keratoglobus,[3] a sign not reported by Leber. In addition they described its autosomal recessive inheritance, various 'biotypes', intrafamilial variability and the poorly understood association with keratoconus and mental retardation.[6] Although LCA is now broadly accepted as a retinal dysfunction, there were initial proposals that three underlying pathological processes may be represented: aplasia or agenesis, a dysplasia (or biochemical defect/dysfunction more accurately) and a degeneration. During the incremental understanding of LCA there have been many terms used to describe the same condition. Historically the descriptions have included: amaurosis congenita, heredoretinopathia congenitalis, dysgenesis neuroepithelialis retinae, hereditary epithelial

aplasia, optic atrophy-amaurosis-pituitary syndrome, pituitary-amaurosis syndrome, congenital amaurosis syndrome, neuroepithelial dysgenesis of retina, congenital amaurosis I and II, congenital retinal blindness, retinal aplasia and tapetoretinal dystrophy. The disease is now uniformly known as Leber congenital amaurosis (LCA) (MIM:204000,204100,608553,604393).

1.2 Prevalence and Incidence

LCA accounts for 3.5% of childhood blindness in the developed world[7] and has a reported incidence of 2-3 per 100 000 live births.[8;9] LCA is more common in cultures with frequent consanguineous marriages.[10] In a UK based survey to identify the incidence and causes of all cases of childhood blindness, children with retinal and macula dystrophies accounted for 14%, of which LCA represented 3.4%.[7]

1.3 Clinical spectrum

For the purposes of this research project, LCA is characterised if vision was poor or absent in the first 3 months after birth, and where there was a severely reduced or non-detectable electroretinogram (ERG) measured early in the disease process, as a diagnostic prerequisite.[11-13] Other signs included sensory/wandering nystagmus, amaurotic pupils, and a fundus appearance that is either normal or reveals a pigmentary retinopathy with or without macular atrophy. Ocular features may include eye poking or the oculodigital sign of Franceschetti, ptosis, strabismus, high hyperopia/myopia,[14] cataracts, keratoconus/keratoglobus,[15] microphthalmos, macular coloboma, pigmentary retinopathy and maculopathy, optic disc swelling and attenuated retinal vasculature.

1.4 Differential diagnosis

LCA represents the most severe end of the spectrum of early onset retinal dystrophies. Some genes have been described as causing an early onset retinal dystrophy with a less severe clinical phenotype with milder nystagmus, normal pupil reactions and better vision despite an absent ERG.[16] This led to severe rod-cone dystrophies of early onset being described as early onset severe retinal dystrophy in the literature (EOSRD or EORD). For the purposes of this research project, electrophysiological diagnostic verification was used to diagnose early onset retinal dystrophy patients, A diagnosis of early-onset retinal dystrophy was made when symptoms and/or signs were present before the age of 5 years, and subsequently, on electroretinography, there was evidence of a severe cone/rod or rod/cone dystrophy (CRD and RCD respectively). Those patients that presented with an early retinal dystrophy at presentation, that was too severe for an electrophysiological diagnosis and with symptomatic onset after the first 3 months of infancy but less than 5 years old, were diagnosed as early onset retinal dystrophy with unknown electrophysiology data (written as EORD in the collected phenotyping data; see Results Chapter 3 in this thesis).

1.4.1 Clinically similar non-syndromic eye diseases

Other retinal degenerations forming part of the differential diagnosis when considering LCA because of early onset visual loss, infantile nystagmus and initial retinal appearances include the various forms of achromatopsia (ACHM),[17] and congenital stationary night blindness (CSNB),[18] which are both early onset static retinal conditions. Albinism and optic nerve hypoplasia may also be considered among the differential

diagnoses.[19] However the clinical features and, in particular the ERG findings, allow these disorders to be distinguished from LCA. In addition the molecular pathology, prognosis, inheritance and treatment possibilities differ significantly from LCA and therefore accurate diagnosis is paramount.

1.4.2 Clinically overlapping syndromic eye diseases

An LCA-like ocular phenotype can be found in several autosomal recessive syndromes (Table 1.4). Usually other systemic findings allow differentiation from LCA but in certain disorders such as Alstrom syndrome[20] and juvenile nephronophthisis[21;22] the systemic features may not become apparent until late childhood.

Table 1.4 Syndromic disorders associated with LCA

a)Miscellaneous syndromic diseases:	
Alstrom Syndrome	Dilated cardiomyopathy, deafness, obesity and diabetes
Infantile Batten disease	Abnormal accumulation of phytanic acid leading to peripheral neuropathy, ataxia, impaired hearing, skin and bone changes
Mainzer-Saldino syndrome	Skeletal anomalies with cone shaped epiphyses of the hand bones and ataxia
L'Hermitte-Duclos	Cerebellar hyperplasia, macrocephaly and epilepsy

Disorder	**Systemic features**
b)Ciliopathies	
Senior-Loken Syndrome	kidney disease (nephronothisis)
Bardet Biedl syndrome	Mental retardation, polydactyly, obesity and hypogonadism, renal abnormalities
Joubert Syndrome	Cerebellar hypoplasia, oculomotor difficulties and respiratory problems

c)Peroxisomal diseases: present with sensorineural deafness, dysmorphic features, developmental delay, hepatomegaly, early death	
Zellweger disease	Cerebro-hepato-renal syndrome
Neonatal adrenoleuko-dystrophy	Similar in biochemical terms to Zellweger syndrome. It has characteristic facies, adrenal atrophy, and degenerative white matter changes.
Infantile Refsum	Abnormal accumulation of phytanic acid leading to peripheral neuropathy, ataxia impaired hearing, and bone and skin changes

1.5 Molecular genetics of LCA and EORD

The clinical variability of the non-syndromic LCA and EORD spectrum is consistent with the heterogeneous molecular basis for these diseases, with mutations described in nineteen genes. All genes have an autosomal recessive inheritance pattern, except *CRX* and *IMPDH1*. Functional studies of identified genes indicate that they act in strikingly diverse biological pathways, including retina development (*CRB1* [MIM 604210][23], *CRX* [MIM 602225][24-26]), phototransduction (*GUCY2D* [MIM 600179][27]), vitamin A metabolism (*RPE65* [MIM 180069],[28;29] *LRAT* [MIM 604863],[30] *RDH12* [MIM 608830][31]), guanine synthesis (*IMPDH1* [MIM 180105][32]), outer segment phagocytosis (*MERTK* [MIM 604705][33]), cilium formation and function (CEP290 [MIM 610142],[34] *TULP1* [MIM 602280], *IQCB1* [MIM 609237] [35;36;36-38] *RPGRIP1* [MIM 605446],[39;40] *LCA5* [MIM 611408][41]) and *SPATA7* [MIM 609868][42]), an atypical cilium protein, and chaperone activity (*AIPL1* [MIM 604392]),[43]. In addition, the function of *RD3*[44] [MIM 180040] has been postulated to play an important role in retinal maturation;[45] *KCNJ13,*[46] [MIM 603208], encodes a potassium channel subunit at the RPE apical membrane; *NMNAT1* [47-50][MIM 608700], encodes an essential enzyme in NAD biosynthesis and *CABP4* [MIM 608965][51] encodes a calcium channel binding protein.

The genes *OTX2*[52] and *DTHD1*[53] have also been associated with syndromic LCA but they are not described or studied in this thesis due to the non syndromic LCA criteria of this project.

The approximate median frequency of the major genes causing LCA and EOSRD is shown.

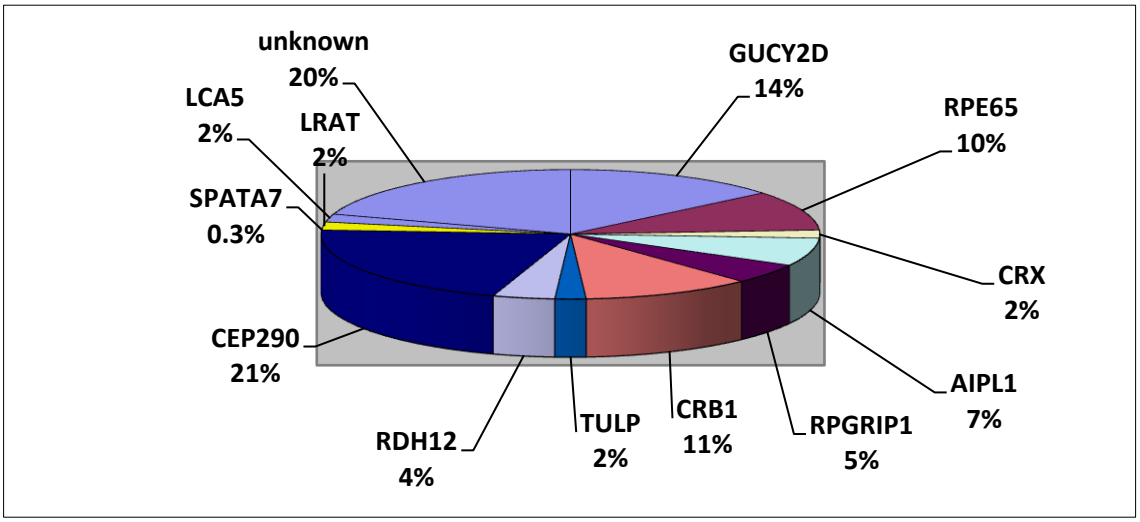

Figure 1.5a Median frequency of disease genes in LCA/ EOSRD [54;55]

Table 1.5 Non syndromic LCA associated genes and their function

Gene	Location	Protein	Function
GUCY2D [27]	17p13.1	Guanylate cyclase 2D	Encodes RetGC-1, phototransduction
RPE65 [29]	1p31	65 kDa RPE localized protein	Retinoid visual cycle
SPATA7 [56]	14q31.3	Spermatogenesis-associated protein	Unknown retinal function
AIPL1 [43]	17p13.1	Aryl hydrocarbon receptor interacting protein-like 1	cGMP-PDE folding, cell cycle progression
LCA5 [41]	6q14.1	Lebercillin	Centrosomal or ciliary function
RPGRIP1 [39;40]	14q11	RP GTPase regulator-interacting protein 1	Ciliary function (Outer segment formation)
CRX [24-26]	9q13.3	Homeodomain transcription factor	Photoreceptor development
CRB1 [23]	1q31	Crumbs like protein 1	Photoreceptor morphogenesis
NMNAT1	1p36.22	NMNAT1	Photoreceptor-neurone protection. NAD biosynthesis
CEP290 [34]	12q21.3	Centrosomal protein	Ciliary protein
IMPDH1 [32]	17q31.3	Inosine monophosphate dehydrogenase	Cell growth
RD3[57]	1q32.3	Retinal degeneration protein	Promyelocytic Leukemia (PML) Nuclear bodies
RDH12 [31]	14q24.1	Retinol dehydrogenase	Retinoid visual cycle
LRAT [30]	4q32.1	Lecithin retinol acyltransferase	Retinoid visual cycle

TULP1[36;36-38]	6p21.3	Tubby-like protein	Ciliary protein and phagocytosis
KCNJ13	2q37.1	Potassium channel subunit Kir7.1	Retinal development and maintenance
MERTK[58]	2q14.1	Receptor tyrosine kinase	Activates cytoskeletal remodelling and phagocytosis
IQCB1[59]	3q13.33	IQ-motif containing protein	Ciliary function
CABP4[51]	11q13.1	Calcium binding protein 4	Modulates synaptic glutamate release in scotopic photoreceptors

The genes *OTX2*[60] and *DTHD1*[61] have also been associated with syndromic LCA but they are not described or studied in this thesis due to the non syndromic LCA criteria of this project.

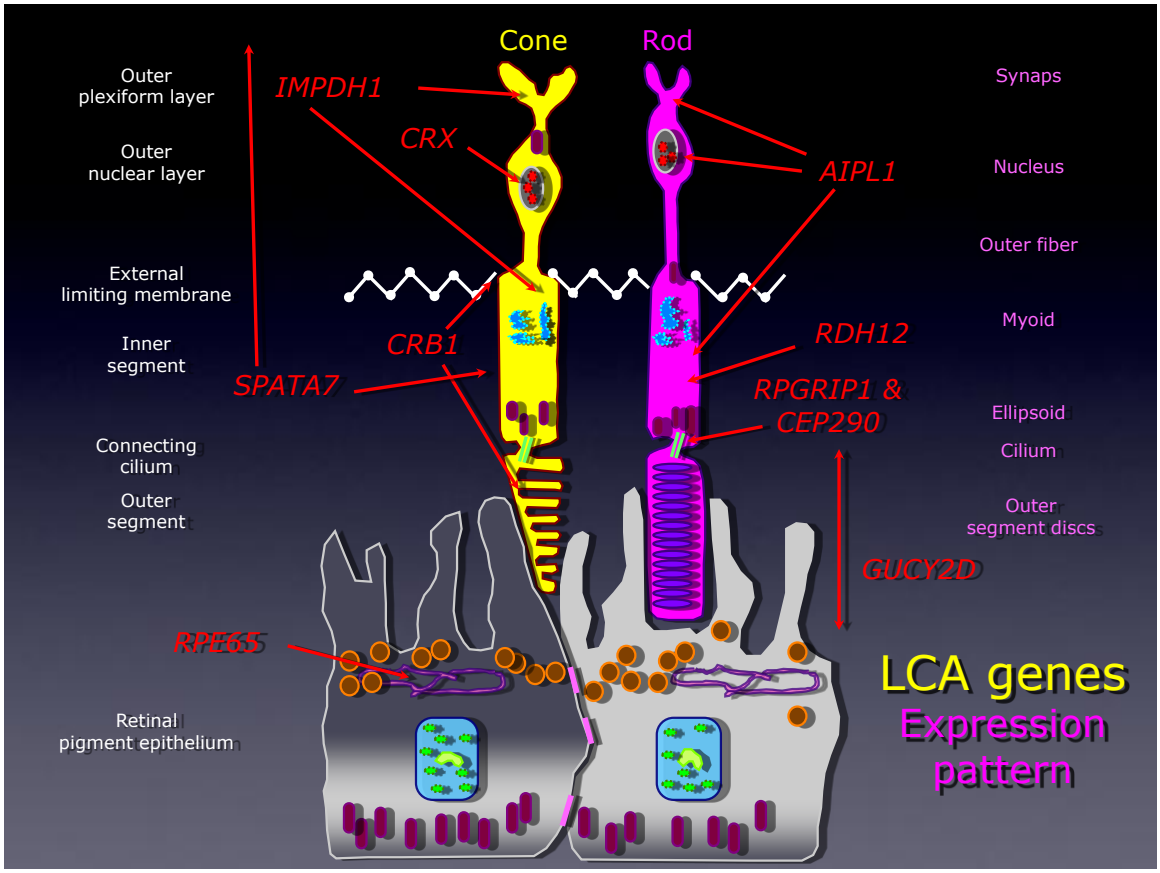

Figure 1.5b (Not all proteins shown). An illustration of several non syndromic LCA-associated proteins (see Table 1.5) and their location in the photoreceptor-RPE complex. Protein functions are outlined in Table 1.5. Proteins altered by LCA-causing mutations affect photoreceptor cells at several levels, including development, outer segment formation, protein trafficking, and photoreceptor–glia connections that form the outer limiting membrane. GUCY2D is a key protein in phototransduction. Additionally, genes expressed in RPE cells are affected, including RPE65, which participates in recycling vitamin A analogues in the visual transduction cycle. AIPL1 is a chaperone protein.

1.5.1(a) Phototransduction and *GUCY2D*

As described in previous sections and below, *GUCY2D* is involved in phototransduction, by coding for a protein that directly catalyses the synthesis of cyclic guanosine monophosphate (cGMP), retinal guanate cyclase-2D or RetGC1. This recycling of cGMP allows recovery of the dark state after phototransduction.

The phototransduction cascade in the rod and cone outer segments is initiated when a photon (h*v*) strikes the visual pigment, rhodopsin in rods, and promotes it into an active state R*, (Step 1 in Fig. 1.5.1, below). Photons are symbolized by *hv*, the energy of a photon, where *h* is Planck's constant and the Greek letter *v* (nu) is the photon's frequency.

Figure 1.5.1 (modified from http://www.ncbi.nlm.nih.gov/books/NBK10806/)

R* interacts with a heterotrimeric G protein (transducin) and guanosine diphosphate (GDP) is released and guanosine triphosphate (GTP) binds to the α subunit of transducin, thereby activating transducin (Step 2). The α subunit in turn disinhibits cyclic guanosine monphosphate (cGMP) phosphodiesterase (PDE), (Step 3), thereby allowing the hydrolysis of cGMP, (Step 4), and the closure of the cyclic nucleotide gated (CNG) channels, (Step 5). The closure of the CNG channels

interrupts the flow of Na^+ and Ca^{2+} into the photoreceptor and hyperpolarizes the membrane potential.

R* deactivation (not shown in Figure 1.5) is required to quench the phototransduction cascade, by the phosphorylation of serine and threonine residues at its C terminus by rhodopsin kinase (RK). Ca^{2+} concentration falls as CNG channels close during the activation of phototransduction and subsequently the phosphorylation of R*. The R* catalytic activity is further quenched by the binding of visual arrestin to phosphorylated R*.

Deactivation of activated PDE requires the hydrolysis of GTP to GDP on subunit α. To re-open CNG channels, retinal guanate cyclase-2D (RetGC1) synthesises cGMP from GTP, a process that is regulated by the Ca^{2+} binding protein, guanylyl cyclase-activating protein 1 and 2 (GCAPs).

1.5.1(b) *GUCY2D*

In 1995, the first gene for LCA (LCA1) was mapped to 17p13.1 by using homozygosity mapping in 15 consanguineous North African families.[62] Subsequently *GUCY2D*, also known as *RetGC-1* (retinal guanylate cyclase-2D), was the first gene identified as causative in LCA.[63] The prevalence of mutations of *GUCY2D* in LCA is 6-20.3%.[64-66] Interestingly, 70% of families with *GUCY2D* mutations originate from Mediterranean countries.[67]

GUCY2D encodes a 1103 amino acid (aa) (120kD) membrane guanylate cyclase, RetGC-1, an enzyme involved in the re-synthesis of cyclic guanosine monophosphate (cGMP), from guanosine triphosphate (GTP). This recycling of cGMP keeps open the gated cation channels allowing recovery of the dark state after phototransduction. Mutations in the gene lead to permanent closure of the cGMP gated cation channels with resultant hyperpolarisation of the plasma membrane.

Many LCA patients carry *GUCY2D* null mutations on both alleles, which are expected to result in the total absence of cyclase activity [27;68]. Causative mutations have been reported in the ligand binding N-terminal segment, transmembrane domain, the internal protein kinase homology region and the C-terminal catalytic domain[69;70]

Heterozygous *GUCY2D* mutations have also been associated with an autosomal dominant form of cone-rod dystrophy (CORD6). [71-74] In patients with this cone rod dystrophy mutational changes are described in GUCY2D at codon 838. [74] Subjects from 4 British families had lifelong poor vision in bright light, with a major reduction in visual acuity occurring after late teenage years. Fundal abnormalities were confined to the central macula and increasing central atrophy was noted with age.

As described, the loss of GUCY2D function prevents restoration of the basal levels of cGMP of cone and rod photoreceptor cells, leading to a situation equivalent to constant light exposure during photoreceptor development. This cellular pathology could explain the retinal degeneration reported in a post mortem, histological study of an 11 year old patient with *GUCY2D*-associated LCA.[75] Rods and cones developed without outer segments in the macula and far periphery. The cones formed a monolayer of cell bodies but the rods were clustered with sprouting neurites. The midperipheral retina was without rods and cones and although the inner nuclear layer appeared normal in thickness, the ganglion cells were reduced in number. The number of rods and cones remaining at this age may permit therapies to restore retinal function.

1.5.2 *GUCY2D* Genotype-phenotype correlations

LCA patients,with mutations in *GUCY2D* have been reported to have poor vision, usually worse than counting fingers, severe hypermetropia, photophobia, early peripheral pigmentation macular atrophy, disc pallor and vessel attenuation. [27] Subsequently there have been reports of more mildly affected patients with less hypermetropia, no photophobia and vision better than 6/60.[64,76]

1.6 The visual cycle and the LCA genes involved (*RPE65, LRAT, RDH12*)

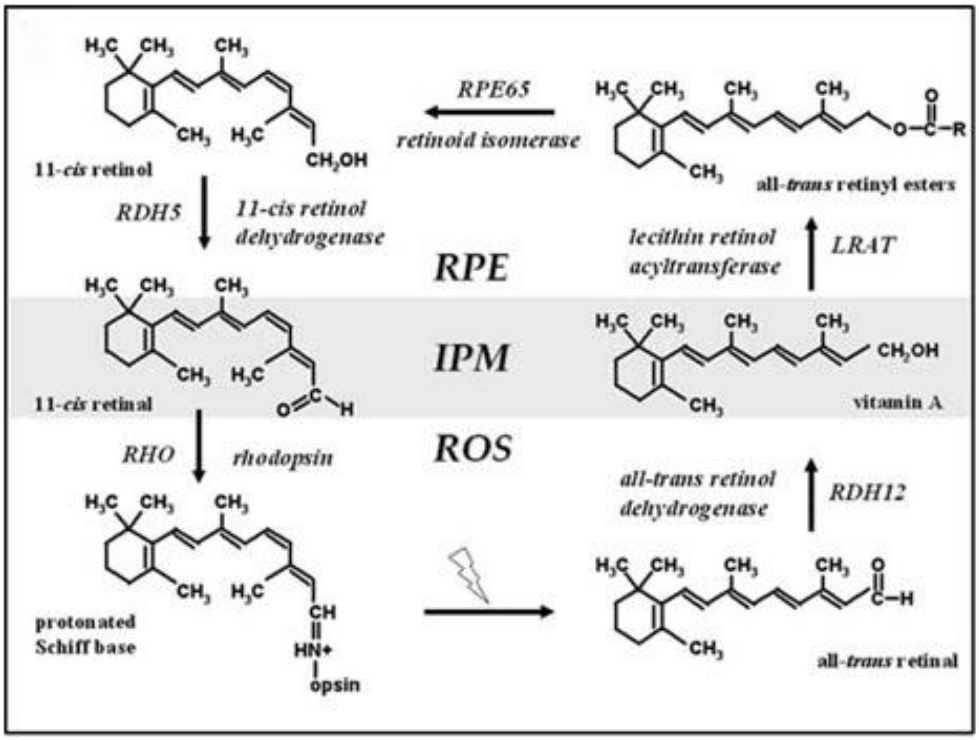

Figure 1.6 Diagram of the reactions of the visual cycle [31]. (Modified from Janecke AR et al. (2004) [31]).

The visual cycle involves the interconversion of vitamin A and 11-*cis* retinal. Illustration above showing the proteins, genes and their corresponding enzymes and retinoids present in photoreceptors and RPE, retinal pigment epithelium. IPM, interphotoreceptor matrix; ROS, rod outer segment.

The visual cycle is a series of enzymatic reactions and transport mechanisms involved in vitamin A metabolism, which is required to facilitate the photopic response of the vertebrate retina. In scotopic conditions, 11-*cis* retinal forms a covalent bond with rod and cone opsins to generate the photoreceptor visual pigments. In light, 11-*cis* retinal is isomerised to all-*trans* retinal, a molecule that stabilises the active signalling configuration of these proteins. After retinal illumination all-*trans* retinal is released from the apoprotein, reduced to all-*trans* retinol (vitamin A), transported to the RPE and esterified. The retinyl esters serve as substrates for a concerted isomerisation/hydrolysis reaction that regenerates 11-*cis retinol,* which is subsequently oxidised to 11-*cis* retinal and returned to the photoreceptors.

1.6.1 *RPE65*

In 1993 Hamel et al. [77] cloned and characterised the unique RPE specific protein, RPE65. The chromosomal locus of *RPE65* was subsequently mapped to 1p31 by linkage analysis in consanguineous families.[78] *RPE65* became the first identified RPE-specific disease gene. In 1997, Marlhens et al. described compound heterozygotes in two LCA siblings.[79] Gu et al.[28] reported mutations of the *RPE65* gene in 5 unrelated families with an autosomal recessive childhood onset retinal dystrophy, that was clinically different to LCA. Subsequently Morimura et al.,[80] screened 45 LCA families and identified nine homozygous or compound heterozygous *RPE65* mutations in seven unrelated families. Mutations in *RPE65* account for 3-30% of LCA / early onset retinal dystrophy (EORD) patients.[39;64;65;80-83] *RPE65* mutations reported in other retinal degenerations are described below.

There are two known forms of RPE65, a 65 kilodalton (kDa) protein, located in smooth endoplasmic reticulum of the retinal pigment epithelium, a membrane associated form (mRPE65) and a lower weight soluble form (sRPE65).[84] RPE65 plays an important role in retinal Vitamin A metabolism. *RPE65* is an isomerohydrolasemerase that catalyses the isomerisation and hydrolysis of all-*trans*-retinyl esters to 11-*cis* retinol within microsomes in the RPE.[85-88] The variants, mRPE65 and sRPE65, were thought to be interconverted by lecithin retinol acyl transferase (LRAT) acting as a palmitoyl transferase with mRPE65 as the palmitoyl donor. Chromophore synthesis has been reported to be blocked when not required by the conversion from membrane bound to soluble RPE65 by LRAT.[89] This conversion between the two RPE65 variants therefore was believed to act as a switch controlling the quantity of chromophore required by the

retinoid visual cycle. However, more recent work has refuted the evidence that LRAT is significant in isomerase activity, beyond the synthesis of retinyl ester substrate, and concluded that both Rpe65 variants (in animal models) have similar isomerase specific activities.[86] This study further suggested that the association of RPE65 with membranes is not dependent upon LRAT or the result of palmitoylation.

Mice whose *Rpe65* gene has been knocked out (*Rpe65*$^{-/-}$) do not generate 11-cis retinal [87] and exhibit rapid cone loss and cone opsin mistrafficking.[90;91] These mice accumulate oil like droplets of all-trans retinyl esters within their retina. However this ester accumulation is not proven to be responsible for photoreceptor cell degeneration. Further experiments in *Rpe65*$^{-/-}$ mice has demonstrated that spontaneous opsin activity may be a key factor in photoreceptor cell death.[92] Furthermore Hamann et al.[93] have also implicated the continuous light-independent activation of the phototransduction cascade that occurs in the *Rpe65*$^{-/-}$ mice, due to the unliganded (no 11-*cis*-retinal) signalling of the opsin, as a mechanism of retinal degeneration. The sequential reduction of the anti-apoptotic Bcl-2 family of proteins and elevated levels of pro-apoptotic Bax and Bak proteins mediated mitochondrial membrane changes leading to rod apoptosis. Knockout out of Bax revealed rescue from apoptosis, indicating that bax inhibition may be an avenue for pharmacological intervention.[93]

Clearly the full understanding of the role of RPE65 in the visual cycle remains incomplete. Although RPE65 has recently shown to be present in the outer segment of human cones, [94] and its role within this cell type is unknown. Interestingly RPE65 in cones does not act as an isomerase, and its possible role as a retinoid binding protein has been postulated.[95] The described mislocalized cone opsins in the absence of the native

chromophore, may have an RPE65 associated mechanism yet to be deduced. Furthermore, the process by which cone opsins are trafficked and why the absence of chromophore inhibits ospin trafficking may be elucidated by an improved knowledge of *RPE65* and its protein.

1.6.2a Genotype-phenotype correlations in *RPE65*

Mutations in *RPE65* were found to be associated with LCA,[28;29;80;96] an autosomal recessive childhood onset retinal dystrophy (or early onset severe retinal dystrophy, EOSRD),[80;97] that was clinically distinct from LCA, and autosomal recessive RP.[80]

Infants with *RPE65* mutations are nightblind from birth and present with nystagmus, pronounced photoattraction and a preference for photopic tasks, [68;97]. There is poor but useful vision in early life, with variable refractive errors[16;64] .Vision declines gradually during school age, and most are severely visually impaired by their early 20s, but may retain residual islands of peripheral vision into their third decade.[83] Visual acuity varies between 6/18 to 6/60 in early childhood but reports of light perception (LP) vision and progressive severe field loss by the fifth decade is a consistent finding. [98] Refractive errors are very variable and emmetropia, myopia, high or low hypermetropia are reported.[16;64] On ERG examination, there is an absence of rod responses but cone responses may be recordable.[83] Patients with compound heterozygous and homozygous RPE65 mutations also have a notable lack of retinal autofluorescence (AF) .[99]

1.6.2b Animal models of RPE65 and RPE65 gene therapy

Animal models have contributed significantly to our understanding of the pathophysiology of LCA and allowed an opportunity to test the safety and efficacy of viral gene therapy. In 1999, Veske et al. reported a natural four base pair deletion of the *Rpe65* gene in the Swedish Briard dog.[100] Similar to humans, these animals are blind at birth with absent ERG responses. Subretinal injections of adeno-associated viruses (AAV) with cytomegalovirus (CMV) promoter and β–actin enhancer in 4 month old dogs resulted in improved ERGs, visual evoked potentials (VEPs), papillary response and vision-dependent behaviours.[101]

Histologic analyses demonstrated 11-*cis* retinal expression in treated photoreceptors, indicating a functional return of the visual transduction pathway.[102]

Gene therapy has also been used to improve vision in Rpe65-deficient mice .Injection of viral vector carrying mouse *Rpe65* gene into the eyes of *Rpe65*$^{-/-}$ embryos *in utero* rescued rhodopsin expression and visual function in these mice.[103]

Prior to human trials, the safety of AAV2 virus in a primate model was evaluated in several studies. Importantly, viral transgene expression was reported for up to 18 months, and no retinal toxicity was noted.[104;105]

In 2008 the first human trials to test the safety of viral vector mediated gene transfer to human LCA patients were reported by three research groups.[106-108] The aims of the initial studies were primarily to test safety and secondarily to test efficacy of viral gene therapy. Each group injected AAV2 viral vectors for *RPE65* expression, into the subretinal space of three patients. Doses of viral particles varied and two of the groups prescribed oral

corticosteroids to limit inflammation. The safety outcomes were acceptable and all immunologic changes and ocular sequelae were self limiting. All three groups reported an improvement in retinal function.

The human *RPE65* gene therapy trials represent the first human gene therapy for inherited retinal disease. Each showed, in its own way, the obstacles in quantifying visual improvement.[109] Furthermore, it remains unclear whether interpretation of retinal function is enough to make a difference to the quality of life of these patients. More research needs to investigate whether viral transduction needs to be optimised or whether gene therapy should be given earlier in the process of retinal degeneration.[110]

1.6.3 *LRAT*

Lecithin retinol acyl transferase (*LRAT*) is located at 4q31.2 and mutations in this gene have been reported in associated with EOSRD[30] , LCA[111] and juvenile RP.[112] LRAT mutations are a rare cause of EOSRD and LCA. LRAT is found in hepatic cells and the RPE where it is involved in the conversion of all-*trans*-retinol into all-*trans*-retinyl esters, replenishing 11-*cis*-retinal in the visual cycle, and facilitating deposition of retinal from the circulation into storage such as retinosome structures in the RPE.[113] LRAT is localized to the endoplasmic reticulum and in eukaryotes, the C-terminal transmembrane domain is essential for catalytic events. As described in the previous section, recent evidence suggests that LRAT is not required for isomerase activity beyond synthesis of retinyl-ester substrate[114] and it is still not understood if RPE65 forms a membrane associated, enzyme complex with LRAT. Despite the expression of LRAT in multiple tissues, the *Lrat*$^{-/-}$ mouse develops normally. However histological analysis and electron

microscopy of the retina for 6-8-week-old *Lrat-/-* mice revealed that the rod outer segments are approximately 35% shorter than those of wild type mice, with apparently normal adjacent neuronal layers and a severely reduced ERG.[115]

1.6.4 Genotype-phenotype correlations for *LRAT*

LRAT mutations in murine models have demonstrated disturbed rod photoreceptor anatomy and attenuated ERGs.[115] The human phenotype includes severe early nyctalopia, poor vision and peripheral field loss with RPE atrophy but an absence of pigment migration.[30;116;117] The LRAT phenotype shares features with RPE65 associated disease, which is consistent with the shared proximity in cellular location and function.

1.6.5 *RDH12*

Homozygous *RDH12* mutations were first identified in three consanguineous Austrian kindreds affected by EORD.[31] Subsequently, in a series of 110 unrelated patients with LCA, *RDH12* mutations were found in 4.1% [118]. *RDH12* maps close to the SPATA7 locus on 14q24.1, [119] although whilst linkage analysis gave a significant lod score at this locus, a maximum lod score was obtained distally. Seven years later haplotype analysis in the family in which LCA3 was mapped excluded RDH12 as the same entity as the SPATA7 gene and it was reported that there was an additional gene in this region.[120]

Retinol dehydrogenase 12 (RDH12) is a 316 amino acid protein with a calculated molecular mass of 35 kD and shares 79% identity with RDH11 . RDH12 is a member of the short chain dehydrogenase / reductase family (SDR) contains two motifs highly conserved within SDRs, the cofactor binding site and catalytic residues . The SDR family of enzymes, contains an amino terminal motif which forms part of the Rossman fold and

interacts with the adenosine monophosphate moiety of the cofactor. Positively charged residues present at the βA-αC and βB-αC motif junctions are important in selectivity for (hydrogenated) nicotinamide adenine dinucleotide, NAD(H), versus (hydrogenated) nicotinamide adenine dinucleotide phosphate, NADP(H), and ensure favourable interaction with NADP(H). [121]

The tissue distribution of RDH12 was deduced from quantitative real time polymerase chain reaction (qRT-PCR) data showing expression in retina, kidney, pancreas, liver, prostate, testes and brain [122]. The highest level of RDH12 expression is in the retina, where it is localised to the inner segment of rod and cone photoreceptors[123]. *In vitro*, RDH12 catalyses the oxidoreductive interconversions of all-trans- and cis-retinoids, and is also active toward medium–chain aldehydes, but with lower affinity. This substrate dual-specificity led to the investigation of the reduction of all trans-retinaldehyde to all-trans retinol in the visual cycle and the detoxification of lipid peroxide products[119;124]. Although bi-directional in vitro, RDH12 acts as a retinal reductase in living cells by shifting the retinoid homeostasis towards increased levels of retinol and decreased levels of bioactive retinoic acid [119;125]. This reductase activity of RDH12 protects cultured cells from death caused by addition of exogenous retinaldehyde, which correlates with lower levels of retinoic acid in RDH12 expressing cells. Deletion of the RDH12 gene in mice increased susceptibility to photoreceptor apoptosis resulting from exposure to high intensity illumination.[123] However, this knockout model expressed normal levels of visual pigments suggesting that other members of the RDHs can compensate for each other in this murine visual model. Although RDH12 is now considered dispensable in the rodent visual cycle, evidence suggests that RDH12 contributes to all trans retinal clearance, as

its loss of function results in slightly increased accumulation of retinotoxic N-retinylidene-N-retinylethanolamine (A2E). [13]

Initially, five RDH12 mutations were found in LCA patients.[31] Additional novel mutations were subsequently identified, some of which were associated with a less severe, early onset autosomal recessive retinal dystrophy.[118;120;120;125] A number of RDH12 mutations have been biochemically evaluated, most of which result in loss-of-function. In one case, a T49M change increases the number of methionine residues that interfere with the binding of the 2'-phosphate group of NADP. [5] Another mutation, A269fsX1, causes a frameshift that results in the formation of a truncated, non-functional protein that lacks part of the Rossman fold, which leads to defective enzymatic activity. [126] The C201R mutation is also a loss of function variant. The Cys residue is located within the catalytic motif (YXXXK), just after the catalytically important Tyr.[126] This change from a hydrophobic residue to a polar residue within the catalytic motif can disrupt important residue alignment involved in catalysis. All these mutations were found in patients with severe loss of retinal function and early onset severe retinal dystrophy.

More disease-associated RDH12 mutants have been shown to retain significant catalytic activity, indicating the existence of additional pathophysiological mechanisms. Lee et al.[127] demonstrated that the catalytically active T49M and I51N mutants undergo accelerated degradation, which results in their reduced cellular levels. Inhibition of proteasome leads to significant accumulation of ubiquitylated T49M and I51N. Furthermore, the degree of ubiquitylation strongly correlates with the half-lives of the proteins. The results suggest that the accelerated degradation of RDH12 mutants by the ubiquitin-proteasome system contributes to the pathophysiology and phenotypic

variability associated with mutations in the RDH12 gene. More recently, exome sequencing has identified RDH12 compound heterozygous mutations in a family with severe retinitis pigmentosa.[128] No regions of shared homozygosity among affected subjects were identified. Exome sequencing in a single patient allowed the detection of two missense mutations in the RDH12 gene: a c.446T>C transition predicting a novel p.L149P substitution, and a c.295C>A transversion predicting a previously reported p.L99I replacement. Sanger sequencing confirmed that all affected subjects carried both RDH12 mutations.

Although RDH12 null mice exhibit normal retinal function at 6 weeks, they show increased susceptibility to retinal cell apoptosis of both cone and rod photoreceptors induced by high intensity illumination.[123] Candidate approaches for the prevention of retinal degeneration may involve reducing exposure to intense light, suppression of the apoptotic pathway and slowing the retinoid cycle.

1.6.6 Genotype-phenotype correlations for *RDH12*

Patients with *RDH12* mutations have early visual loss and nystagmus, intraretinal pigmentary migration, arteriolar attenuation, mild to moderate hypermetropia and macular atrophy.[31;118;120;129] Similarities between the RDH12 and RPE65 phenotype include preservation of visual acuity, peripheral visual fields and electroretinogram responses at young ages. However, significant differences include dense, peripheral bone spicule pigmentation and maculopathy at ages older than 6-7 years old in RDH12 associated retinal dystrophy patients.

1.7 Photoreceptor development and structure (CRX, CRB1)

1.7.1 *CRX*

Freund et al.[130] were attempting to identify retinal homeobox-containing genes when one of the isolated cDNAs was shown to encode a novel gene localizing to 19q13.3, which became known as *CRX* for "cone-rod homeobox-containing gene". The *CRX* gene was initially isolated from murine retina.[131] *CRX* encodes a 299 amino acid protein with a predicted mass of 32 kD that is most similar to the human OTX1 and OTX2 homeodomain proteins. CRX mutations have been reported in autosomal dominant cone-rod dystrophy,[130] autosomal dominant RP,[132] autosomal dominant LCA[24;133] and recessive LCA.[25] CRX has been found to account for between 0.6 and 6% of LCA mutations.[55;64;65;130;134]

Transgenic murine studies suggested that *Otx2* is a direct upstream regulator of *Crx*, via binding to specific consensus sequences in the *Crx* promoter. The findings identified Otx2 as a key regulatory gene in photoreceptor cell development.[135]

Mutations in *CRX* can be significantly atypical, in that of all the 17 genes associated with the development of LCA, only *CRX* and *IMPDH1* have been associated with an autosomal dominant inheritance pattern.[136] Another unusual feature of *CRX* mutations causing LCA is that they are usually *de novo*.[24;137] A recent case report provides further evidence of an autosomal dominant inheritance pattern for LCA and its association with an adenine nucleotide deletion in codon 153 of the CRX gene. This deletion causes a frameshift which affects codons 284-295 and alters the OTX motif encoded at the carboxyl terminus resulting in an abnormal protein (Pro153fsX132).[138]

In vitro, the CRX protein recognizes a specific sequence in the promoter region of known photoreceptor genes such as rhodopsin, arrestin, interphotoreceptor retinoid-binding protein, rod cGMP phosphodiesterase.[139;140] Within cells, these genes require CRX to bind and activate their promoter regions for expression.[141] CRX plays a crucial role at various stage of eye development and is the earliest expressed photoreceptor marker in the retina. It is also expressed in pinealocytes in the pineal gland and regulates photoentrainment.[142] Furthermore, it has an essential role in the differentiation and maintenance of photoreceptor cells and it has been shown that absence of CRX in mice prevents outer segment biogenesis, abolishing the phototransduction pathway in rods and cones.[141] Recently, CRX has also been found to interact with histone acetyl-transferases, suggesting that a mechanism of CRX-mediated transcriptional activation is to recruit these histone processing enzymes in order to stabilize chromatin configurations for transcription.[141;143]

A variety of *CRX* mutations have been described in both dominant and recessive forms of LCA. Reported *CRX* mutations include: a homozygous mutation,[25] a heterozygous deletion,[132] a heterozygous null mutation[133] and a heterozygous frameshift mutation.[144] The speculative explanations for the finding of heterozygous *CRX* mutations in some individuals include the possibility that some *CRX* mutants work in a dominant-negative way to interfere with normal *CRX* function. Alternatively an unidentified mutation on the other CRX allele or a digenic inheritance pattern (with an additional mutation in another gene) may be the causative mechanism.[145]

1.7.2 Genotype-phenotype correlations for *CRX*

Cone rod dystrophy, retinitis pigmentosa and LCA have all been associated with mutations in *CRX*.[132] Variability in phenotype has been reported even for certain identical genotypes. For example c.463del12bp has been reported in LCA and a much milder dystrophy with preservation of visual acuity until adulthood.[132] This suggests that there are likely to be other modifier genes or environmental factors that influence the disease phenotype.

Patients with *CRX* mutations have a severe pigmentary retinopathy, with vessel attenuation, macular atrophy and some patients are reported as having normal fundi in infancy. [64;132;145] It is reported that moderate hyperopia occurs in patients with *CRX* mutations but Rivolta et al. analysed the published refractive data more closely to show a slightly myopic phenotype.[145] This report claimed that hyperopia is more generally associated with poor vision in early childhood rather than the *CRX* mutations.

1.7.3 *CRB1*

The Crumbs homologue 1 gene (*CRB1*) was first described as the causative gene in a form of autosomal recessive RP which exhibited preservation of the para-arteriolar RPE (RP12).[146] Later studies showed that 9-13% of LCA cohorts were found to have CRB1 mutations.[23;55;147;148]. A missense mutation in CRB1 has also been described in a single family with dominant pigmented paravenous chorioretinal atrophy (PPCRA) with variable expressivity.[149]

CRB1, located at 1q31.3, has an important role in many species, ranging from invertebrates to mammals.[150]CRB1 is analogous to the Drosophila Melanogaster Crumbs

protein; it contains 19 epidermal growth factor (EGF)-like domains, a transmembrane domain, 3 laminin A globular-like domains, and a 37-amino acid cytoplasmic tail.[151] Three Crumbs orthologues occur in humans. *Crb1* is only expressed in the brain and retina[152], whereas *Crb2* is also expressed in the kidney, RPE/choroid and at low levels in heart, lung and placenta.[153] *Crb3* is expressed in various epithelial derived tissues, including the retina.[154] The Crumbs transmembrane proteins are responsible for apico-basal cell polarity and adherens junction in embryonic epithelia.[155] Photoreceptors, as epithelial cells, require separation of their apical and basal compartments in order to function in cell-to-cell adhesion, tissue formation, intercellular signalling and directional transport of molecules. The extracellular domain of Crumbs has no known binding partners presently but the intracellular domain has a highly conserved role in macromolecular protein scaffold construction.[150] This scaffold occurs in the photoreceptor cell just apical to the adherens junction at the outer limiting membrane in the retina.[156] Actin filaments attach at adherens junctions, which form the cytoplasmic interface of the plasma membrane. These junctions spatially organize and separate the apical and basolateral membrane. Animal models of *Crb1*$^{-/-}$ mice (*rd8*) have fragmented external limiting membrane and shorter photoreceptor inner and outer segments within 2 weeks of birth, which suggests a developmental pathogenesis.[157] In addition there are an irregular size and number of apical Mueller glial cell villi.[158] Interestingly, adhesion between the photoreceptor cells and the Mueller cells is temporarily lost, after light exposure leading to dramatic structural and functional changes.[156]

Jacobson et al. (2003) characterized the retinal organization *in vivo* of patients with CRB1 mutations and found that, unlike other inherited retinal degenerations, the CRB1

mutant retinas were remarkably thick in cross section and lacked the distinct layers of normal adult retina. There were coarse outer and inner zones and a thick surface layer around the optic nerve. The abnormal retinal architecture in CRB1 mutations resembled that of immature normal retina. The authors concluded that naturally occurring apoptosis may be interrupted by CRB1 dysfunction.[159]

CRB1 mutations in LCA are diverse but an interesting association with high to extreme hyperopia was reported in all 4 affected members of a family of Middle Eastern origin, with *CRB1* mutations. [160] This hyperopic phenotype has been confirmed by other studies.[23;147;161]

1.7.4 Genotype-phenotype correlations for *CRB1*

LCA patients with mutations in *CRB1* have a thickened retina and a lack of the cellular layering of a fully developed adult retina, resembling a more immature normal retina. This has been demonstrated by OCT investigation showing a thickened retina with coarse laminar irregularity.[159] Other features include a higher susceptibility to keratoconus,[162] high hyperopia, white spots at level of the RPE, clumping pigmentation, preservation of peri-arteriolar RPE,[23] and an early macular reorganization. The visual acuity ranges from 6/60 to 6/24 in the first decade of life.[55] A "Coats-like" exudative vasculopathy with a predisposition to tractional retinal detachments has also been reported.[23]

1.8 Ciliopathies and LCA

In mammals, ciliary dysfunction has been linked to a diverse group of phenotypes, from motile cilia defects in Kartagener syndrome to polycystic kidney disease. Recently, the understanding of ciliary dysfunction has been expanded with research showing that

defects in the cilium and its anchoring structure, the basal body, are associated with pleiotropic phenotypes such as Bardet-Biedl, Alstrom and Meckel-Gruber syndromes. [163] The following review of LCA ciliopathies suggests that an improved understanding of the cilium has the potential to explain the molecular and cellular basis of non syndromic, ocular phenotypes. A potent tool for the study of ciliary biology has been published as a ciliary proteome database (http://www.ciliaproteome.org). The authors have integrated all existing ciliary and basal body proteomics data to generate genomic, genetic and functional information to assist ciliary researchers globally.

1.8.1 *TULP1*

TULP1 (6p21.3) encodes a member of the Tubby-like protein family, which consists of 4 proteins in vertebrates.[164;165] TULP1 was reported as a cause of an autosomal recessive degeneration in several isolated families and a large pedigree from the Dominican Republic[37;38;166] In a comprehensive survey it was found that 1.7% of LCA is associated with *TULP1* mutations.[55]

The Tubby-like protein family group have a vital role in the development and function of the retina. Specifically, TULP1 was identified in retinal neuroblasts as early as 8 fetal weeks, [167] suggesting a role in retinal differentiation and consistent with the early onset of the retinal degeneration in LCA caused by *TULP1* mutations. TULP1 contains a C-terminal "tubby domain" that is conserved among the TULP family, and contains a phophatidylinositol-binding region that may anchor the protein to the cell membrane.[168] The tubby domain also exhibits DNA-binding activity which indicates a potential transcription factor of other photoreceptor genes.[169] In the eye, the protein is located in both rods and cones [36;166;170] and mutations of TULP1 in man is associated with loss of

both photopic and scotopic ERG responses.[171] Within the photoreceptors, TULP1 is most abundant in the inner segments, but is also consistently detected in synaptic regions and in connecting cilia.[166] This suggests a role for TULP1 in rhodopsin trafficking from inner to outer segment. Furthermore, the interaction of TULP1 with F-actin [168] could support its role in opsin transport across the cellular actin cytoskeleton from the inner segment through the connecting cilium to the outer segment. More recently, the interaction between TULP1 and neuronal specific dynamin-1 has strengthened hypotheses about its function in vesicle formation and protein transport at retinal synapses.[172]

Tulp1 -/- mice exhibit an early-onset retinal degeneration with a progressive, rapid loss of photoreceptors. Subsequently, *Tulp1*$^{-/-}$ mice were shown to express mislocalized rhodopsin in the plasma membrane of inner segments and within adjacent extracellular vesicles.[166]

Recently *TULP1* mutations have been reported in juvenile retinitis pigmentosa.[173] Homozygosity for a 718+2T>C transition at the splice donor site in IVS7 of the *TULP1* gene was identified in two unrelated Afghan patients. Examination of the asymptomatic heterozygous parents of one of the patients revealed normal visual acuities and electroretinograms, but the mother had striking and easily discernible multiple yellow-white dots just outside of the vascular arcades. The significance of these signs are unclear.

1.8.2 Genotype-phenotype correlations for *TULP1*

Clinical phenotype studies have reported nystagmus, poor vision in infancy ranging from 6/60- light perception (LP), nyctalopia and early unrecordable rod function and impaired

cone function. Yellow macular deposits and pale optic nerves with myopic refractive errors are also described.[166]

1.8.3 *RPGRIP1*

The gene encoding retinitis pigmentosa GTPase Regulator Interacting Protein 1 (*RPGRIP1)* consists of 25 exons, with different splice variants identified, the largest encoding a 1259 amino acid protein with a predicted molecular weight of 144 kDa.[40;174] The gene is localized on 14q11.2. Multiple splice variants of *RPGRIP1* exist, some of which are specifically expressed in the retina.[175-178] The protein contains several structurally conserved motifs including the N-terminal half of the protein, which contains two predicted coiled coil domains, that are homologous to those found in proteins involved in vesicular trafficking,[179] and two leucine zipper motifs. The C-terminal domain contains a bipartite nuclear localization signal, that facilitates shuttling to the nucleus of some isoforms,[180] and an RPGR-interacting domain (RID), by which RPGRIP1 binds RPGR, the protein associated with X-linked retinitis pigmentosa type 3 (RP3).[181;182] Disease associated missense mutations in this regulator of chromosome condensation 1 (RCC1)-like domain of RPGR disrupted the interaction between RPGRIP1 and RPGR, suggesting that this defect could underly the pathogenesis of RP.[179] RPGRIP1 has a single homologue RPGRIP1-like (RPGRIP1L), a basal body protein associated with Jouberts syndrome (JBTS) and Meckel-Gruber syndrome (MKS). Mutations in RPGRIP1 are most commonly associated with LCA, affecting approximately 4-6% of patients with this disease.[39;40;55;183;184] LCA associated mutations in the RID of RPGRIP1 could lead to a loss and gain of binding to RPGR.[185] Most LCA-associated missense mutations have been identified in a conserved, central region of the

RPGRIP1 molecule, a putative calcium binding C2 domain.[180] A homozygous missense mutation in one family with late onset cone-rod dystrophy has also been reported.[40]

The current evidence suggests that the main role of RPGRIP1 is as a scaffold for a protein complex at the connecting cilium, or as a binding site where ciliary proteins can anchor at the base of the cilium. RPGRIP1 function is not fully understood but an *Rpgrip1*$^{-/-}$ mouse, with a retinal phenotype, has been developed.[186] Wild type mice demonstrate that both RPGRIP1 and RPGR localize to the connecting cilium of retina. However RPGR is dependent upon RPGRIP1 to be anchored or transported to the connecting cilium. In the absence of RPGR, RPGRIP1 is still localized to the connecting cilium, but not *vice versa*.[186]

RPGRIP1 knockout mice have a more severe phenotype than RPGR knockouts and RPGRIP/RPGR double knockout mice resemble RPGRIP1 knockouts. The RPGRIP knockout mice are born with a full complement of photoreceptors but the outer segments disorganize rapidly and no recognizable structures are evident by 12 weeks.[186] This evidence supports hypotheses that the presence of RPGRIP1 is essential for RPGR function.[187]

Both RPGRIP1 and RPGR proteins have also been detected in the outer segments of the photoreceptors , in a subset of amacrine cells and in lysosomes.[181;188] Some RPGRIP1 isoforms undergo limited proteolytic processing, yielding a small fragment that can translocate to the nucleus. These isoforms co-localise with RanBP2, a protein in the nuclear pore complex which is implicated in nuclear-cytoplasmic trafficking.[188] Nuclear translocation is not understood presently but RPGRIP1 is not considered to be dependent on microtubules for its centriolar localization.[189]

Recently, the efficacy of replacement gene therapy in a murine model of LCA carrying a targeted disruption of *RPGRIP1* has been evaluated.[190] The replacement construct, packaged in an AAV8 vector, utilized a rhodopsin kinase (RK) gene promoter to drive RPGRIP1 expression. Both promoter and transgene were of human origin. Following subretinal delivery of the replacement gene in the mutant mice, human RPGRIP1 was expressed specifically in photoreceptors, localized correctly in the connecting cilia, and restored the normal localization of RPGR. Electroretinogram and histologic examinations showed better preservation of rod and cone photoreceptor function and improved survival in the treated eyes.

1.8.4 Genotype-phenotype correlations for *RPGRIP1*

RPGRIP1 mutations are associated with severe visual loss so patients have nystagmus, severe visual disability and extinguished electroretinograms from a young age. The earliest phenotypic descriptions report light perception vision, early photophobia, low hyperopia, some vascular attenuation with or without intraretinal pigment. [40;55] In addition, drusen like deposits in the peripheral retina and early photophobia have been reported in patients with *RPGRIP* mutations.[55;82]

1.8.5 *CEP290*

The *CEP290* gene was a strong candidate gene for causing LCA since it was previously found to be mutated in an early onset retinal degeneration mouse model, *rd16*.[191] Mutation analysis in a French Canadian family identified an intronic mutation, C2991+1655A>G (p.Cys998X) that results in the insertion of a cryptic exon in the mRNA and introduces a premature stop codon in the CEP290 protein immediately

downstream of exon 26.[34] The mutation creates a strong splice-donor leading to efficient splicing of the cryptic exon. *CEP290* mutations are the commonest cause of LCA, reported as being found in ~20% of LCA patients.[34]

The *CEP290* gene (93.2kb) is located on chromosome 12q21.32 and spans 54 exons, with a translation initiation codon in exon 2, transcribed to give a multidomain protein containing several predicted motifs that are highly conserved throughout evolution.

The CEP290 is important for centrosome and cilia function. It localises to the centrosomes of mitotic cells and to the nucleus. The protein also localises to the basal bodies at the base of the ciliary apparatus in many different cell types, including the photoreceptor cilium.[191;192] Immunoprecipitation studies of murine retinal extracts demonstrated that CEP290 exists in a complex with several microtubule-based transport proteins of the dynein-dynactin molecular motor, including centrin, dynactin subunit p150, gamma-tubulin, kinesin-associated protein 3 (KAP3), kinesin family member 3A (KIF3A), ninein, p50-dynamitin, pericentrin, RPGR and RPGR-interacting protein 1 (RPGRIP1).[191] The redistribution of RPGR, rhodopsin and rod arrestin in the early onset, retinal degeneration mouse model *rd16* retina suggests an important role for CEP290 in cilia associated transport, although there were no obvious structural defects observed in the connecting cilium of the *rd16* retina.[191]

Atypically for LCA genes, nearly all of the families with *CEP290* mutations were of European descent with the common intronic mutation accounting for 43% of diseased alleles.[69;193;194] Some studies have suggested that this mutation that causes aberrant splicing, resulting in a lower amount of correctly spliced product, which is sufficient for normal cerebellar and renal function but not for functional photoreceptors. [191;192;192;195]

Initially, it was suggested that complete loss of function of both CEP290 alleles leads to Joubert syndrome, characterized by nephronophthsis, retinal degeneration and cerebellar vermis hypoplasia. The retinal-restricted phenotype in LCA could be due to a hypomorphic or residual protein activity.[34] However, the emerging evidence is not clear and two apparent null mutations in CEP290 have been reported in non syndromic LCA,[69] without any diagnosed features of Joubert syndrome. Conversely, patients with other splice-site mutations, such as c.5587-1G>C and c.1711+5G>A, that are also expected to produce abnormally and normally spliced CEP290 transcripts are reported in patients with diagnosed Jouberts syndrome. It seems unlikely that isolated retinal disease could be explained by residual CEP290 activity.

Recently, the pathophysiology of the intronic CEP290 mutation, C2991+1655A>G (p.Cys998X) and the inherent problems of using animal models for human disease research has been highlighted. Garanto et al.[196] generated two humanized knock-in mouse models each carrying ~6.3 kb of the human CEP290 gene, either with or without the intronic mutation. Transcriptional characterization of these mouse models revealed an unexpected splice pattern of CEP290 mRNA, especially in the retina. In both models, a new cryptic exon (coined exon Y) was identified in ~5 to 12% of all Cep290 transcripts. This exon Y was expressed in all murine tissues analyzed but not detected in human retina or fibroblasts of LCA patients. In addition, exon x that is characteristic of LCA in humans, was expressed at only very low levels in the retina of the LCA mouse model. Western blot and immunohistochemical analyses did not reveal any differences between the two transgenic models and wild-type mice. These interesting results show clear differences in the recognition of splice sites between mice and humans, and emphasize

that care is warranted when generating animal models for human genetic diseases caused by splice mutations.

Recent co-immunolabeling experiments demonstrated reduced expression and mislocalization of centrin 3 and disturbed targeting of the Fam161a interactors lebercilin and Cep290, which were restricted to the basal body and proximal connecting cilium in Fam161a$^{GT/GT}$ murine retinas.[197] Misrouting of the outer segment cargo proteins opsin and rds/peripherin 2 in Fam161a$^{GT/GT}$ mice were also identified. The results suggested a critical role for the C-terminal domain of Fam161a for molecular interactions and integrity of the connecting cilium. Fam161a is required for the molecular delivery into the outer segment cilium, a function which is essential for outer segment disk formation and ultimately visual function.

Recently, heterozygous mutations in *CEP290*: the frequent c.2991+1655G>A founder mutation, and a novel nonsense mutation in exon 7 (p.Arg151X), were identified in a proband and two cousins. The proband had nystagmus, hyperopia, a flat electroretinogram, and decreased visual acuity from birth (20/250). The two cousins had minimal scotopic electroretinogram responses at the age of 2. In one of the cousins, the visual acuity reached a level of 6/10 (20/32) at age 5, which is good for patients with CEP290 mutations. The nonsense-associated altered splicing in which either exon 7 or exons 7 and 8 were skipped with a relatively intact open reading frame may explain the less severe phenotype than is expected .[198]

The in-frame deletion of exons 35-39 that causes EORD in the mouse also provided a useful model for studying the CEP290 participation in regulating the transport of specific signaling molecules involved in odorant detection.[199] There has also been reported

abnormal olfactory function in humans, which has been demonstrated in the rd16 murine model.[199] Hypomorphic mutations in the mouse revealed reduced electro-olfactogram recordings and despite the loss of olfactory function, cilia of olfactory sensory neurons (OSNs) remained intact in mice. As in wild type, CEP290 localized to dendritic knobs of rd16 OSNs, where it was in complex with ciliary transport proteins and the olfactory G proteins G(olf) and Ggamma(13). This data implicates distinct mechanisms for ciliary transport of olfactory signaling proteins, with CEP290 being a key mediator involved in G protein trafficking. The assessment of olfactory function may therefore serve as a useful diagnostic tool for genetic screening of certain ciliary diseases.

Most recently, the development of lentiviral vectors carrying full-length CEP290 for the purpose of correcting the CEP290 disease-specific phenotype in human cells have been reported.[200] A lentiviral vector containing CMV-driven human full-length CEP290 was constructed. Following transduction of patient-specific, photoreceptor precursor cells, reverse transcriptase-PCR analysis and western blotting revealed vector-derived expression. As CEP290 is important in ciliogenesis, the ability of fibroblast cultures from CEP290-associated LCA patients to form cilia was investigated. In cultures derived from these patients, fewer cells formed cilia compared with unaffected controls. Cilia that were formed were shorter in patient-derived cells than in cells from unaffected individuals. Importantly, lentiviral delivery of CEP290 rescued the ciliogenesis defect

1.8.6 Genotype-Phenotype Correlations

Patients display a severe rod and cone dysfunction consistent with LCA with high hyperopia, severe and early reduction of visual function, independent of most mutations (except for the less severe p.Arg151X, involved in exon skipping mutation, described

above). A finding of reticular pigment epithelium in the peripheral retina with multiple white dots is consistently reported.[34;69]

A study of differential macular morphology on spectral domain OCT reported poorly defined photoreceptor inner/outer segment junctures (PSJ) and disorganized retinal lamellar structures, where only one to three retinal layers could be observed. Patients with CEP290 mutations tended to have retention of the outer nuclear layer at the fovea and macular thickening, especially at younger ages.[201]

1.8.7 *LCA5*

The *LCA5* gene on chromosome 6q14, which encodes the previously unknown ciliary protein lebercilin was discovered by homozygosity mapping and candidate gene analysis.[41] The *LCA5* gene was previously referred to as 'Lebercilin' but this nomenclature is out of date. 'Lebercilin' should be used for the encoded protein only. Homozygous nonsense and frameshift mutations in *LCA5* in five families affected with LCA were detected. *LCA5* is expressed widely throughout development, although the phenotype in affected individuals is limited to the eye. Lebercilin localizes to the connecting cilia of photoreceptors and to the microtubules, centrioles and primary cilia of cultured mammalian cells. Various proteins that link lebercilin to centrosomal and ciliary functions have been identified.[41] Members of this "interactome" represent candidate genes for LCA and other ciliopathies. *LCA5* mutations are a rare cause of LCA; 1.7% (3/179) of a cohort of LCA patients were found to have mutations in *LCA5*.[202] Similarly, only 1.8% of a Pakistani LCA cohort were reported to have *LCA5* mutations.[203]

There are many reported mutational variants in *LCA5*. Homozygosity for deletion of a cytosine at position 1151, in exon 6 of the *LCA5* gene, results in a frameshift mutation

(P384QfsX17).[41;204] This mutation has been described in a patient with macular staphyloma in a consanguineous Pakistani family. A 1-bp homozygous duplication (1476A) in exon 9 of the *LCA5* gene, resulting in a frameshift mutation (P493TfsX1), and homozygosity for an 835C>T transition in exon 5 of the LCA5 gene, resulting in a null mutation, (Q279X), are also identified to cause LCA.[41] In a study of affected members of the Old Order River Brethren with LCA, a 1,598-bp deletion was described in the LCA5 gene that encompassed 1,077 bp of the promoter region and noncoding exon 1 (g.(-19612)-(-18015)del1598).[205]

Fluorescence-tagged recombinant protein expression demonstrated that lebercilin is expressed in ciliated and non-ciliated cells. [206] Above a critical level, expression of recombinant lebercilin in some non-ciliated cells causes microtubule coalescence and was shown to localize to the centriole indicating its role in mictrotubule dynamics. In ciliated cells, when protein expression was low, lebercilin localized to the transition zone of the cilia.[206] Furthermore, the protein was found to associate intimately with the full ciliary axoneme and microtubule cytoskeleton of cells. The four functional lebercilin-associated, protein groups include molecular adaptors, cytoskeletal structures, various chaperones and cellular signalling cofactors. The complex interplay of these protein groups is still being interpreted in LCA5 disease and the detailed pathogenesis remains unknown.

1.8.8 Genotype-phenotype correlations for *LCA5*

LCA5 patients have been described with a VA range of 6/60 to light perception vision only, a high frequency of photoaversion, hyperopia, nystagmus, nummular pigmentation and a low frequency of keratoconus with late (adult) onset cataracts.[207;208] Prominent central island of retinal pigment epithelium (RPE) surrounded by alternating elliptical-

appearing areas of decreased and increased pigmentation are also reported. Retinal laminar architecture at and near the fovea is abnormal.[184] With increasing eccentricity, there is retinal laminar disorganization. However, regions of pericentral and midperipheral retina retained measurable outer nuclear layer (ONL). In summary, there was evidence of retained photoreceptors mainly in the central retina. Retinal remodelling was present in pericentral regions in patients and the autofluorescence imaging in a younger patient suggested preserved RPE in patchy retinal regions with retained photoreceptors.

More recently the largest *LCA5* study has been reported. Eighteen probands with *LCA5* mutations were identified in 1,008 patients (797 with LCA, 211 with arRP); ~2% of this cohort.[209] Most patients expressed a severe phenotype, typical of LCA. High hypermetropia was common. The visual acuity is reported to range between 0.20 to light perception and there is extensive peripheral field loss. The fundal examinations revealed widespread atrophy of the retina and RPE but with little intraretinal pigment migration. and scattered white dots at the level of the RPE. However, some LCA subjects had better vision and intact inner segment/outer segment (IS/OS) junctions on OCT imaging. In two families with LCA5 variants, the phenotype was more compatible with EORD with affected individuals displaying preserved islands of retinal pigment epithelium. One of the families with a milder phenotype harbored a homozygous splice site mutation; a second family was found to have a combination of a stop mutation and a missense mutation.

1.9 Other LCA disease mechanisms

1.9.1 *AIPL1*

Sohocki et al. (1999) described the fourth of the LCA genes to be identified, *AIPL1*. The gene was localised to 17p13.3, near a retinitis pigmentosa candidate region.[43;210] The protein encoded by this gene was named aryl-hydrocarbon interacting protein-like 1 because of its similarity to AIP (arylhydrocarbon receptor-interacting protein), a member of the FK506-binding protein (FABP) family. The localisation was refined to 17p13.1, approximately 2.5Mb distal to GUCY2D, by fluorescence *in situ* hybridization.[43] *AIPL1* mutations are variably reported as causing 3-11% of LCA.[55;64;211;212]

The predicted 384 amino acid protein contains 3 tetratricopeptide (TPR) motifs and a 56 amino acid proline rich "hinge" region in close proximity to the C terminus that is present only in primate AIPL1.[213] It has been discovered using a polyclonal antibody directed against the protein, that AIPL1 localises within the rod photoreceptor cells of the peripheral and central human retina.[43;214;215;216]

The polyproline-rich region in AIPL1 is imperfectly conserved in primates. It is 56 amino acids in length in humans but varies in length in other primates. The mechanisms whereby AIPL1 alter the farnesylation of proteins has not been completely elucidated. In common with other TPR co-chaperones; the TPR motifs of AIPL1 are required for the interaction with the molecular chaperones Hsp70 and Hsp90. Numerous components of the phototransduction cascade and the visual cycle are modified by prenylation, yet it has been shown in *AIPL1* knockout and hypomorphic mice that none of these components are affected with the exception of the PDE subunits and only PDEα specifically even though

PDEβ is geranylgeranylated.[217] Finally, although it has been shown that AIPL1 is required for the stability of the catalytic PDEα subunit, which is farnesylated, the ability of AIPL1 to moderate the farnesylation of PDEα *per se* has not been shown. *Ex vivo* studies of mouse retinal tissue have shown that AIPL1 is required for the stability of the catalytic α subunit (farnesylated) and consequently assembly of the cGMP PDE holoenzyme, without affecting many other farnesylated proteins (involved in phototransduction) in the retina. Regulation of the stability of PDEα by AIPL1 is therefore complex and requires further elucidation.

A prevalence study of screening 512 unrelated probands for *AIPL1* mutations in inherited retinal degenerative disease, identified 11 Leber congenital amaurosis families whose retinal disorder was caused by null and missense *AIPL1* mutations.[212] This study also identified affected individuals in two apparently dominant families, diagnosed with juvenile retinitis pigmentosa or autosomal dominant cone-rod dystrophy who were heterozygous for a 12-bp deletion in the *AIPL1* gene.

The retinal disease mechanism in *AIPL1* mutations has been well studied. In a murine model of Leber congenital amaurosis (*Aip1*$^{-/-}$), the outer nuclear layer developed normally, but rods and cones then quickly degenerated.[218] The retina showed disorganized, short, fragmented photoreceptor outer segments. Rod cGMP phosphodiesterase (PDE), a farnesylated protein, is absent and cGMP levels are elevated in *Aipl1*$^{-/-}$ retinas before the onset of degeneration. In summary, *AIPL1* mutations are associated with reduced cGMP hydrolysis activity and elevated cGMP, causing rapid degeneration of photoreceptor cells.

Although rod cell death occurs due to rapid destabilization of rod phosphodiesterase, there is a paucity of data regarding the role of AIPL1 in cone photoreceptors. Cone degeneration observed in the absence of AIPL1 was speculated to be due to an indirect 'bystander effect' caused by rod photoreceptor death or a direct role for AIPL1 in cones. However, transgenically expressed hAIPL1 (human AIPL1) exclusively in the rod photoreceptors of the *Aipl1*$^{-/-}$ mouse restored rod morphology and the rod-derived electroretinogram response, but cone photoreceptors were non-functional in the absence of AIPL1.[219] In addition, the cone photoreceptors degenerated, but at a slower rate compared with *Aipl1*$^{-/-}$ mice. This degeneration is linked to the highly reduced levels of cone PDE6 observed in the hAIPL1 transgenic mice. This report demonstrated that AIPL1 is needed for the proper functioning and survival of cone photoreceptors. Furthermore, rod photoreceptors were shown to provide support that partially preserves cone photoreceptors from rapid death in the absence of AIPL1.

Adeno-associated virus (AAV)-mediated gene replacement therapy has been used to improve photoreceptor function and survival in retinal degeneration associated with AIPL1 defects.[220;221] Two mouse models of *AIPL1* deficiency were used: the *Aipl1*-hypomorphic (h/h) mouse (a relatively slow retinal degeneration), and the *Aipl1*-null mouse (with no functional Aipl1 and a very rapid retinal degeneration). The authors demonstrated restoration of cellular function and preservation of photoreceptor cells and retinal function in *Aipl1* h/h mice 28 weeks after subretinal injection of an AAV2/2 vector and in the light-accelerated *Aipl1* h/h model and *Aipl1*-null mice using an AAV2/8 vector.[222]

1.9.2 Genotype-phenotype correlations for *AIPL1*

Despite the promising results of rescue murine models, the severe human phenotype associated with *AIPL1* mutations have caused some doubts regarding a successful gene therapy model in man . However, there does appear to be a subgroup of patients with less severe later onset disease who may also be amenable to therapy, suggesting that later onset cohorts should also be screened for *AIPL1* mutations.[223]

Dharmaraj et al.[224] described a relatively severe phenotype in patients with retinal disease caused by *AIPL1* mutations. In this study visual acuity varied from light perception to 6/120. Patients were moderately hypermetropic and about half reported nyctalopia. Keratoconus and cataracts were identified in 26% (5/19). Variable retinal appearances, ranging from near normal to varying degrees of chorioretinal atrophy and intraretinal pigment migration, were noted. Atrophic and/or pigmentary macular changes were present in 80% (16/20).Varying degrees of optic nerve pallor were noted in all children after the age of 6 years. The ERG findings were mainly undetectable in affected individuals. The ERG of a parent heterozygote missense mutation carrier revealed significantly reduced rod function, while ERGs for 6 other carrier parents were normal.

In a more recent study of LCA associated *AIPL1* mutations, Tan et al. [225] described an increasing degree and extent of retinal pigmentation, including bone spicule formation, with increasing age; with the two youngest subjects having no retinal pigmentation. Two patients were found to have retinal white dots. The severity of maculopathy also increased with age, with patients developing frank full-thickness retinal atrophy over

time. The two youngest subjects had a milder phenotype, with either a normal appearing macula or mild retinal pigment epithelial mottling

1.9.3 *MERTK*

Mutations in *MERTK* were first identified in the Royal College of Surgeons (RCS) rat.[58] This classical model of retinal degeneration arises as RPE fails to phagocytose shed outer segments[58;226] Weier et al. (1999) mapped the human *MERTK* gene to chromosome 2q14.1, using fluorescence in situ hybridization.[227] Subsequently, the human orthologue was screened in a large group of patients with retinal degeneration and it was shown that *MERTK* mutations are associated with RP.[228] The gene is expressed in predominantly phagocytic cells such as RPE and macrophages. *MERTK* encodes a receptor tyrosine kinase that is a member of the Mer-family. There are several members of this family, including Axl and Tyro3, which share two immunoglobulin-like extracellular domains with two fibronectin type III repeats, a transmembrane domain and an intracellular tyrosine kinase domain. This intracellular domain interacts with the SH2 domain of the guanine exchange factor (GEF) Vav1, which post tyrosine phosphorylation, activates GEF/ Vav1 leading to presumed cytoskeletal remodeling and phagocytosis. The majority of *MERTK* mutations in retinal dystrophies represent loss of function alleles in a truncated MERTK lacking the intracellular tyrosine kinase domain.[228-230] Our own group has recently identified a novel 9kb deletion, removing exon 8 between two Alu Y repeats, which is predicted to disrupt the reading frame of *MERTK*, leading to a premature stop codon in exon 9.[229] Only one missense mutation, p.Arg844Cys, has been identified in human retinal disease presumably causing loss of function due to increased protein instability.[33] The missense mutation involving a change from arginine a large, polar,

charged amino acid, to a small, hydrophilic cysteine molecule leads to this probable protein instability.The retinal dystrophy seen in the animal model of MERTK-related disease (the RCS rat) has been successfully rescued with gene replacement therapy.[229;231] In future there may be a window of opportunity for treating young patients with MERKT mutations with gene therapy. Recently preclinical toxicology, potency and biodistribution studies, for AAV2-mediated gene therapy vector in the RCS rat, in the treatment of MERTK associated retinitis pigmentosa, were successful.[232]

1.9.4 Phenotype for *MERTK*

Patients with *MERTK* mutations are described as early onset rod-cone dystrophy with notable nyctalopia, early rod ERG reduction, but preserved visual fields and mild RPE change. A macular bull's eye lesion and recordable autofluorescence are also reported.[33;229;230] Spectral domain OCT shows loss of photoreceptors and hyper-reflective bodies possibly analogous to the debris layer seen in the RCS rat.[229;233] These changes as well as a wavelike appearance of the innermost neurosensory retina might be distinctive OCT findings in patients with mutations in *MERTK*.[229]

1.9.5 *IMPDH1*

Mutations in inosine monophosphate dehydrogenase type I (*IMPDH1*) (7q31.3-q32) were identified in adRP in 2002.[234;235] Heterozygous mutations in IMPDH1 account for approximately 2% of families with adRP.[32] Two IMPDH1 variants, Arg105Trp and Asn198Lys, inherited as single alleles, were subsequently found in two patients with isolated LCA.[32] These were *de novo* mutations (i.e. absent from both parents). None of the novel IMPDH1 mutants identified in this study altered the enzymatic activity of the

corresponding proteins. In contrast, the affinity and the specificity of single-stranded nucleic acid binding were altered for each LCA *IMPDH1* mutation and this may be a poorly understood mechanism of pathogenicity.[236]

Several IMPDH1 retinal isoforms have been detected, which are the result of alternative splicing.[237] IMPDH1 catalyses the rate-limiting step of *de novo* guanine synthesis. During the reduction of NAD, inosine monophosphate is converted into xanthosine monophosphate. Mutations associated with adRP and LCA are located in the second cystathionine beta synthase (CBS) domain of IMPDH1, which may cause misfolding of the protein and thereby abrogate nucleic acid binding affinity and specificity.[32;238] The CBS domains can bind single-stranded nucleic acids and therefore might play a role in transcription, translation, post-translational modification, localization or other aspects of RNA metabolism.[236] Although the exact disease mechanism of *IMPDH1* mutations are still unknown, derangement of RNA metabolism within the photoreceptor may alter posttranscriptional regulation of rhodopsin mRNA. Autosomal dominant RP mutations in *IMPDH1* reduced binding to nucleic acids and reduced association with polyribosomes. If this mutation perturbs the biosynthesis of rhodopsin in some way, this could explain a link between IMPDH and the mechanism of retinal degeneration in patients with LCA too.[239]

1.9.6 Genotype-phenotype correlations for *IMPDH1*

The following descriptions are the only two reported cases of LCA associated with *IMPDH1* mutations in the literature.[32] An affected child with an Arg105Trp single mutation; he was first seen at 8 months of age when he was diagnosed with LCA and

developmental delay with severe hypotonia. He had roving nystagmus with no fixation to light. Macular reflex was present in both eyes with the retina showing diffuse RPE mottling. No pigmentary deposits were present.

An affected female with a Asn198Lys mutation was seen after referral at age 33 months. The parents had noted the child could not see things in her peripheral vision, and she could not find her food in dimly lighted conditions. Refractive error was OD +3.50+1.50 x 85, and OS +3.50+1.50 x 95. By Allen cards, her vision was 6/12 (20/40). On funduscopy, a generalized depigmentation of the fundus, vascular attenuation, pallor of the optic nerve, and a diffuse hypopigmented ring around the discs was reported.

1.9.7 *SPATA7*

In 2009, Wang et al.[240] used homozygosity mapping to identify five LCA families that mapped to the LCA3 locus, on 14q24. Homozygous nonsense and frame shift mutations were found in a positional candidate gene, *SPATA7* (spermatogenesis associated protein 7), by direct Sanger sequencing. Although prevalence data is limited, *SPATA7* mutations have been identified very rarely in families segregating non-syndromic LCA, in less than 0.03% (3/134).[241]

SPATA7 encodes a highly conserved protein containing a single transmembrane domain. The gene that was first identified in human spermatocytes, *SPATA7* may be involved in preparing chromatin in early meiotic prophase nuclei for the initiation of meiotic recombination.[242] In addition to its expression in testis, *SPATA7* is expressed in multiple layers of the mature mouse retina.[243] It is an atypical ciliary protein because it is not enriched at the junction between the inner and outer segments of photoreceptor cells, where the cilium is located, however the protein shows a uniform distribution in the

cytoplasm of the inner segment. The disease mechanism of *SPATA7* mutations remains unknown.

Wang et al. (2009) identified a R108X homozygous mutation in the SPATA7 gene in a LCA family.[244] Homozygosity for different nonsense and frameshift mutations in *SPATA7* were also identified in two patients with juvenile retinitis pigmentosa. Consistent genotype-phenotype correlations were found. The nonsense mutations associated with LCA are located in the middle of the *SPATA7* coding region, whereas those associated with the less severe "juvenile RP" phenotype are located in the last 2 exons of *SPATA7*.

1.9.8 *SPATA7* Genotype-phenotype analysis

At the end of the first decade, the visual acuity of older patients remained stable and comprised between hand motion and ~1/60 (40/200) (age range 13 - 33). [245] Symptoms of LCA began at birth or in the first few months of life with congenital nystagmus and poor pupillary reactions. The fundus of patients was initially normal and gradually displayed a salt and pepper appearance with retinal vascular attenuation and a typical appearance of RP rapidly progressing to retinal atrophy. A transient photophobia was noted by the parents in the first year of life but by the age of three, most complained of nyctalopia. A transient improvement of visual behaviour was regularly noted by the parents by the age of three. The visual field progressively constricted to become severely limited. Most patients have a moderate hyperopia (+1D to +4D).

In one patient, at age 10, fundal autofluorescence imaging showed a parafoveal ring of mildly increased autofluorescence suggesting a relative preservation of parafoveal retinal pigment epithelium but a severely decreased autofluorescence from the paramacular

region to the retinal periphery, including along the arterioles. Another 33 year old patient, presented with complete absence of fundus autofluorescence. This paper reported the diagnosis as an exact definition of "LCA type II " (early and severe rod-cone dystrophy).[246]

1.10 Other genes associated with LCA

1.10.1 Calcium binding protein 4 (CABP4)

Aldahmesh et al. have reported a *CABP4* mutation in a consanguineous family with an LCA phenotype.[51] Homozygosity mapping was performed in this family, with four affected members, to identify regions of homozygosity. Positional candidate gene analysis revealed a novel homozygous single base pair insertion in *CABP4* (11q13.1): c81_82insA (p.Pro28T*fs*X44).

Mutations in *CABP4* which encodes calcium binding protein 4 (CABP4*)* have also been identified in autosomal recessive congenital stationary night blindness (arCSNB).[247] CABP4 is located in close proximity to the synaptic terminals of photoreceptors and modulates the activity of Cav1.4α, a calcium channel that mediates the synaptic release of glutamate from photoreceptors in the dark.[248] *Cabp4*$^{-/-}$ mice manifest a 50% reduction of the "a" wave (generated by photoreceptors), and their "b" wave (generated by bipolar cells) was even more markedly reduced.[249]

The consanguineous family described above, with a LCA phenotype associated with a *CABP4* mutation, had poor vision in infancy with nystagmus, photophobia, best corrected VA of 20/400 in both eyes. Funduscopy was largely normal, apart from decreased foveal

reflex. The ERGs were extinguished for three of the family members under both photopic and scotopic conditions. However, one sibling had normal implicit time on photopic flicker, whereas scotopic ERG was borderline, with normal oscillatory potential. This slightly milder 'normal flicker /borderline scotopic' phenotype is interesting because the mutation reported (p.Pro28Thr*fs*X44) is predicted to result in the most dramatic functional perturbation of the CABP4 molecule reported to date. This mutation is almost certainly a null mutation due to the introduction of novel amino acids early in the transcript, with abolition of all Ca-binding motifs. As a consequence the mutant transcript is unlikely to escape nonsense mediated decay.

1.10.2 IQ-motif containing protein B1 (*IQCB1*)

Mutations in the *IQCB1* gene were identified in three LCA patients using homozygosity mapping supported by positional candidate gene analysis.[250] The *IQCB1* gene was found within one of the regions of homozygosity. The *IQCB1* gene is located on chromosome 3q13.33 and encodes the IQ-motif containing protein B1 (IQCB1). IQCB1 is believed to be involved in cilary function and depletion of either CEP290 or IQCB1 in zebrafish embryos results in hydrocephalus, developmental eye defects, and pronephric cysts.[251] The reported interaction between IQCB1 and CEP290 proteins[252] and the severe retinal dystrophy seen in patients in Senior-Loken syndrome (SLSN) with *IQCB1* mutations (a differential diagnosis of LCA) prompted this hypothesis that mutations in *IQCB1* cause nonsyndromic LCA.

The ocular phenotypes of SLSN and LCA patients with *IQCB1* mutations are similar. [253] The phenotype of LCA patients with *IQCB1* mutations resembles classical LCA with

early onset pendular nystagmus, poor fixation at birth, and a nondetectable rod and cone ERG early in the disease process. In addition, all patients in this cohort were found to have high hyperopic refractions (+3.00 to +7.50 D). The acuities at later ages were variable and ranged from 20/70 at age 15 to light perception at age 10. A striking "lobular" pattern of hypo- and hyperpigmentation outside the retinal arcades was noted in two affected infants. This early lobular pattern is an atypical LCA phenotype.

Subsequently, Stone et al. [254] analyzed the *IQCB1* gene, in LCA patients negative for mutations in 8 known LCA genes, and identified homozygosity or compound heterozygosity for frameshift or nonsense *IQCB1* mutations in 9 patients. None of the patients had overt renal disease in the first decade of life, but 2 of the oldest patients developed severe renal disease changing the presumed LCA diagnosis to Senior-Loken syndrome (SLSN), a syndromic retinal degeneration. (See section 1.4).

1.10.3 *NMNAT1*

In 2012 four studies reported *NMNAT1* (1p36.22) mutations in patients with LCA phenotypes. [255-258] NMNAT1 is an essential enzyme in NAD biosynthesis. However, the mechanism by which NMNAT1 dysfunction causes retinal dystrophy is uncertain and it has been suggested that NMAT1 has a neuroprotective role in the retina. Both NAD synthase domain activity and the presence of other domains are needed in vertebrates for the neuroprotective function of NMNAT1.[259] Koenekoop et al.[260;261] reported that all individuals with biallelic *NMNAT1* mutations had severe LCA but normal physical and mental health. Notably, in addition to the typical LCA phenotype of nystagmus, severe loss of vision and profoundly reduced electroretinogram (ERG), all individuals with

biallelic *NMNAT1* mutations were found to have a peculiar, prominent retinal feature termed 'macular coloboma', which consists of an atrophic lesion in the central retina with a pigmented border, signifying complete loss of neural tissue in the fovea (including photoreceptors, bipolar cells and ganglion cells). This suggests that *NMNAT1* mutations are associated with this severe and rapid foveal degeneration. The rest of the retina was abnormal as well, with pigmentary changes, attenuated retinal blood vessels and optic disc pallor. In addition, other layers of the retina, such as the ganglion cell layer, were also severely affected.

1.10.4 *KCNJ13*

Sergouniotis et al.[262] used a combination of homozygosity mapping and exome sequencing to identify a homozygous nonsense mutation in *KCNJ13*, in siblings with LCA from a consanguineous family. The gene is located on chromosome 2q37.1. In the same study a further 333 unrelated individuals with recessive retinal degeneration were screened. An additional individual proband, from a different family, with LCA and a homozygous missense mutation, c.722T>C (p.Leu241Pro), was identified.

KCNJ13 is a three-exon gene encoding a potassium channel subunit Kir7.1, a 360 amino acid low-conductance inwardly rectifying potassium channel (Kir) that functions as a homotetramer.[263] The protein is localized at the plasma membrane of a variety of ion transporting epithelia and high gene expression occurs widely in different tissues of the body. Within the retina, Kir7.1 is primarily localized to the apical membranes of RPE.[264] The mutant allele identified in the siblings, (c.496C>T, p.Arg166X), would produce a peptide lacking almost the entire C-terminal intracellular segment of 204 amino acids, if

the transcript is not subjected to nonsense-mediated decay. Such a protein product is unlikely to form functional homotetramers, as this portion is known to be critical for Kir channel subunit assembly, and its absence in this mutant would likely lead to mislocalization.[265]

The physiological significance of the p.Leu241Pro change, identified in the individual proband, was demonstrated with homology modelling:[266] Leu241 is located in the cytosolic C-terminal of Kir7.1. Leu241 is the first of six amino acids to form a β sheet.[267] The mutant Pro241 residue does not take part in this β sheet formation and thus induces a considerable conformational protein change.

All identified patients have a distinct and unusual retinal appearance and a similar early onset of visual loss, suggesting both impaired retinal development and progressive retinal degeneration. Both siblings had bilateral cataract surgery in their third decade. Visual acuities were 2.0 logMAR (logarithm of the minimal angle of resolution) in each eye of one sibling and 1.78 logMAR for the right and 1.48 for the left eye of the other sibling. Funduscopy revealed significant pigment in the retinal pigment epithelium (RPE). There was no other family history of retinal disease.

The individual proband from the second family was a 33-year-old man of European descent who was noted to have strabismus, nystagmus, and poor vision before 1 year of age and was diagnosed with LCA at age 2 years. Only mild progression was reported, with night vision having most noticeably deteriorated. He was moderately myopic and underwent bilateral cataract surgery in his early twenties. Examination showed bilateral nystagmus and severe field loss with relative preservation of the inferior field. Funduscopy revealed areas of nummular pigment in the RPE, especially over the

posterior pole. *In vivo* cross-sectional imaging by spectral domain optical coherence tomography (OCT) revealed loss of outer retinal structures, thinning of the hyperreflective band corresponding to RPE/Bruch membrane, and a coarse lamination pattern. The distorted retinal microanatomy in an area of the fundus in which degeneration was not evident, suggested that this might represent disturbance of the early development of the neurosensory retina.

1.10.5 *RD3*

The association of the human *RD3* gene at chromosome 1q32 with retinopathies was reported after a mutation screen of 881 probands was undertaken.[268] In addition to several variants of uncertain significance, a homozygous alteration in the invariant G nucleotide of the *RD3*, exon 2 donor splice site, was identified in two siblings with LCA. This mutation is predicted to result in premature truncation of the RD3 protein, and segregated with the affected individuals. It has been hypothesized that the RD3 protein is part of subnuclear protein complexes involved in diverse processes, such as transcription and splicing.[269]. RD3 is also believed to be able to suppress retinal membrane guanylate cyclase activity, and potentially plays an important role in retinal maturation. [270] However the precise function of RD3 is still unknown. Subsequently Preising et al.[271] excluded seven of nine known LCA/EOSRD genes in a LCA patient, from an extended consanguineous family. Linkage analysis was then performed in the proband's four siblings using a microarray and narrowed the region of interest towards *RD3* (the LCA12 locus). Microsatellite fine mapping and direct sequencing of the region identified a homozygous nonsense mutation (c.180C >A) in *RD3* in all affected members tested.

Best corrected visual acuity (BCVA) was severely reduced from the earliest examinations (as early as 3 months), never exceeding 1.3 LogMAR. The disease presented as cone-rod dystrophy with dystrophic changes in the macula and bone spicules in the periphery.

1.10.6 *RLBP1* – a gene associated with a juvenile onset retinal dystrophy

Two families were referred to this project with a similar early onset retinal dystrophy, but their phenotypes/genotypes are not within the defined LCA/EORD spectrum. Their phenotype and genotype data are included in the project and thesis (Section 3.8) and the introduction to this gene, *RLBP1*, follows.

There is a unique form of retinitis pigmentosa (RP) named Bothnia dystrophy. Bothnia is the region in northern Sweden west of the Gulf of Bothnia, known as Bothnia Occidentalis. Affected individuals show night blindness from early childhood, with clinical features consistent with retinitis punctata albescens (RPA) and macular degeneration. The causative mutation has been shown to reside in *RLBP1* mapped to chromosome 15q26 [272], encoding the human cellular retinaldehyde-binding protein (CRALBP). This protein has been localised to the retinal pigment epithelium (RPE) and Muller cells of the retina, ciliary body pigment epithelium, outer epithelium of the iris, cornea, optic nerve and the pineal gland. In RPE cells CRALBP acts as a carrier protein for endogenous retinoids involved in visual pigment regeneration, returning RPE 11 cis retinol to its retinal equivalent in the photoreceptor outer segment.

Bothnia dystrophy has been associated with a homozygous C to T transition in exon 7 of the RLBP1 gene, leading to an arginine to tryptophan substitution at position 234 of the

protein (R234W).[273] Other mutations in *RLBP1* have also been identified in patients with autosomal recessive RP.[274]

The largest, most recent RLBP1 study reported a progressive decline of VA and VF areas that was age-dependent.[275] Retinal degenerative maculopathy, peripheral degenerative changes and retinitis punctata albescens (RPA) were present. Early retinal thinning in the central foveal, foveal , and inner ring in the macular region, with homogenous, high-reflectance RPA changes, was visualized in and adjacent to the retinal pigment epithelium/choriocapillaris using OCT. Reduced dark adaptation and affected ERGs were present in all ages. Prolonged dark adaptation and ERG (at 24 hr), an increase in final threshold, and ERG rod and mixed rod/cone responses were found. The RLBP1 genotypes presented a phenotypical and electrophysiological expression of progressive retinal disease similar to that previously described in homozygotes for the c.700C>T (p.R234W) RLBP1 mutation. [275]

1.11 Gene identification strategies to identify disease causing mutations

1.11.1 Genetic markers

Genetic markers are inherited variations that can be used to understand genetic events. In the 1960s, it was discovered that the human genome was divided into single copy coding regions of DNA – the genes, which were separated by repetitive regions of spacing DNA. Although the position of genes was unknown, the repeat sequences could be used to indicate a candidate region of interest. These sequences could be used as ‘markers’ of the

gene location because they were genetically linked. If the markers could be organised into maps then the process of identifying the location of a gene would be possible.

1.11.2 Restriction Fragment Length Polymorphisms

The earliest genetic markers were called Restriction Length Fragment Polymorphisms (RLFP) and were based on the presence or absence of a target for a restriction enzyme. DNA is cut into fragments using suitable endonucleases, which only cut the DNA molecule at specific DNA recognition sequences. A variation in the recognised sequence is usually due to a polymorphism at a single base pair, which will change the sequence so the endonuclease does not cut at this DNA sequence. Restriction length fragment polymorphisms were initially typed by preparing Southern blots from restriction digests of the test DNA, and hybridising with radiolabelled probes. Fortunately, RFLPs became simplified with the advancement in PCR allowing a sequence including the variable restriction site to be amplified. The product could then be incubated with the appropriate restriction enzyme and differentiated on a gel to determine if enzymatic truncation occurred. A fundamental limitation is their informativeness. RFLPs have only two alleles at a locus ie the restriction site is either present or absent. The maximum heterozygosity is only 50%. Since genetic markers are only informative when they are heterozygous, on many occasions the RFLP marker will not provide useful information because a key meiosis is unlikely to be informative.

1.11.3 Microsatellite markers

In order to increase the probability of heterozygosity, other naturally occurring multiallelic markers are more useful. Microsatellites are frequently occurring, repeated

sequences of 1-6 base pairs throughout an individual's genome that are often found in the 5' and 3' end of untranslated regions of genes and within introns and non-coding DNA. Commonly used microsatellites are $(CA)_n$ repeats. Tri and tetranucleotide repeats replaced dinucleotide repeats as the markers of choice because cleaner results are achievable. Dinucleotide repeats are prone to replication slippage during PCR amplification and each allele gives a ladder of "stutter bands" on a gel, making interpretation difficult. Compatible sets of microsatellite markers are designed to be amplified together in a multiplex PCR reaction. A universal primer can be directly conjugated with a fluorophore and samples can be resolved together (multiplexed) by capillary electrophoresis using an automated analyser.

On each side of the repeat unit are flanking regions that consist of "unordered" DNA. The flanking regions are critical because they allow the development of locus-specific primers to amplify the microsatellites with PCR. Therefore given a stretch of unordered DNA 30-50 base pairs (bp) long, the probability of finding that particular stretch more than once in the genome is very low. If the four nucleotides occur with equal probability then the probability of a given 50 bp stretch is 0.25^{50}. In contrast, a given repeat unit (say AC_{19}) may occur in thousands of places in the genome. This combination of widely occurring repeat units and locus-specific flanking regions are part of a strategy for finding and developing microsatellite primers. The primers for PCR will be sequences from these unique flanking regions. By having a forward and a reverse primer on each side of the microsatellite, it is possible to amplify a fairly short (100 to 500 bp) locus-specific microsatellite region. If both parents are heterozygous with four distinct alleles at one microsatellite locus the genotype for the progeny is described as fully informative.

1.11.4 Single nucleotide polymorphisms (SNPs)

A single nucleotide polymorphism (SNP), a variation at a single site in DNA, is the most frequent type of variation in the genome. There are approximately 10 million SNPs that have been identified in the human genome. SNPs that are in close proximity to the disease locus will segregate with the disease trait. Specific genomic regions that are linked to phenotypic traits can therefore be identified by following the transmission of a genetic disease with the distribution of SNPs among family members. The advantage of SNPs is that they can be scored on solid state arrays, (e.g. glass or silicon) without the need for gel electrophoresis. The gain in throughput more than offsets the lower informativeness of SNPs, as only 2 alleles usually occur at each tested point.

An international effort has been established to genotype 270 individuals originating from Nigeria, China, Japan and Western Europe for the HapMap (or haplotype) project (http://www.hapmap.org) in order to identify at least 1 million SNPs across the human genome. A haplotype is a set of closely linked alleles that are inherited together during meiosis. The alleles within a haplotype are inherited as a block and their close proximity will make a recombination event less likely, which can be tracked through pedigrees and populations. Haplotype analysis is used to define and refine genetic intervals in order to reduce the possible number of candidate genes once a disease gene has been mapped to a chromosomal region.

When the Project started, 2.8 million SNPs were in the public database (dbSNP). However, many chromosome regions had too few SNPs, and many SNPs were too rare to be useful, so millions of additional SNPs were needed to develop the HapMap. The

Project discovered another 2.8 million SNPs by September of 2003, and SNP discovery continues, producing a very useful resource.

1.11.5 Genomic maps

To perform accurate genetic analysis, it is essential to construct the order, relative distance and the physical relationship between genes. Human genetic mapping depends on markers and their distance between one another. Ideally, it must be comprehensive in order to cover the entire genome with the minimal distance between each marker. Identifying a gene that contributes to an inherited disorder is easier with more genetic markers, as the likelihood that the marker will be linked to the disease gene increases with proximity to the gene. A detailed map with good genomic coverage also allows increased linkage detection between markers. Various well known definitive maps of the human genome exist such as the Marshfield map with 8000 polymorphic markers, the Genethon map of 5264 microsatellite markers and the deCODE map of 5136 microsatellite markers. Panels of markers evenly spaced throughout the genome are available commercially (Illumina, Affymetrix) and can be used to search for genes of interest.

1.11.6 Linkage analysis

During prophase of meiosis I, pairs of homologous chromosomes synapse and exchange segments recombining adjacent regions of a chromosome (recombination). The likelihood of a gene being inherited together with a polymorphic marker depends upon the distance between them. The greater the degree of separation, the more likely that a

recombination will occur during a cross-over event. Recombination frequency (θ) is the frequency with which a chromosomal crossover will take place between two loci (or genes) during meiosis. Recombination frequency is a measure of genetic linkage and is used in the creation of a genetic linkage map. A centimorgan (cM) is a unit to describe a recombination frequency of 1%; i.e. 1 in 100 gametes will be recombinant and the remaining 99 will have the parental configuration. Physically, 1 cM corresponds to approximately 1Mb of DNA sequence although there is much variability between physical and genetic distance for different chromosomal regions. In general, there is more recombination towards the telomeres of chromosomes, while centromeric regions have fewer recombination events.

If a gene is contributing towards the likelihood of developing a disease, then the region of the genome within which the gene is situated will be co-inherited from a common ancestor by affected members of a pedigree more frequently than would be expected by chance. Genome scans attempt to identify polymorphic microsatellite markers in disease affected members of a pedigree. Linkage occurs if polymorphic microsatellite markers segregate with disease statistically more frequently than would be expected by chance.

Statistically a significant degree of linkage exists when the odds of inheriting a locus that segregates with disease rather than chance is greater than 1 in 1000. The Logarithm of this odds ratio, or what is termed the LOD score, is 3 (Z=3). For most statistics $p<0.05$ is used as the threshold of significance, but with 22 pairs of autosomes, it is unlikely that they would be located on the same chromosome (syntenic) or linked and a **prior** probability must be included. In summary, the low probability of syntenic loci means that evidence giving 1000:1 odds in favour of linkage is required to quantify in a Bayesian

calculation, the joint probability (prior x conditional), or overall odds of 20:1. This 20:1 is the conventional p= 0.05 threshold of statistical significance.

1.11.7 Polymerase chain reaction

The Polymerase Chain Reaction (PCR) was developed to amplify a defined sequence length within a source of DNA. A specific target DNA sequence is selectively amplified in a heterogeneous population of DNA sequences, such as genomic DNA. A genomic browser (see later) is used to select sequence information in order to design oligonucleotide primers. A 20-30 base nucleotide sequence (primer) is designed to be complementary to specific sequences at the two ends of the DNA region (amplimer) that requires amplification. Thermally stable DNA polymerase is added to the four deoxynucleoside triphosphates, dATP, dCTP, dGTP and dTTP (DNA building blocks) with the target DNA. The primers bind to the denatured DNA and initiate the synthesis of new DNA strands complementary to the desired amplimer. The synthesized DNA strands act as templates for further DNA synthesis in subsequent cycles. After about 25-35 cycles of DNA synthesis, the PCR products will include about 10^8 copies of the specific target sequence, if 100% efficient.

1.11.8 Genome scans

Genome wide markers are now commercially available and enable investigators to perform a genome-wide scan. Genome scans studying recessive disease are usually based upon affected sibling pairs – two or more sibs in a family who both suffer with the disease. Other unaffected members of the family can also be included in this analysis.

Polymorphic microsatellite markers, near a locus of interest, can be genotyped. This is performed by using PCR with fluorescent tagged primers. At each microsatellite locus there will be two alleles in each subject distinguished by the length of the PCR product. This is determined by using a fluorescent tag attached to one of the primer pair. The height of the electropherogram peak is a reflection of the quantity of PCR product and the size data allows one to distinguish between alleles using a DNA reference ladder.

A genome-wide screen is the genotyping of DNA polymorphisms or microsatellite markers spanning the entire genome. The most important parameters are the type of polymorphisms used and their density. Human genomewide screens involve typing of approximately 350-500 microsatellite markers with an average spacing of approximately 10cM. Human linkage maps are based on typing of relatively few meioses and therefore map distances have limited precision. There is also wide variation in recombination rates among individuals.

1.11.9 The Human Genome Project

The aims of the HGP were to produce a single continuous sequence for all the human chromosomes and to identify the positions of all genes and genetic markers. In 2001, the International Human Genome Sequence Consortium produced the working draft sequence, constructed from fragments of about 100-200 kb of bacterial artificial chromosome (BAC) clones derived from sequences whose chromosomal locatons were known. These analyses were published on websites and updated by the National Centre for Biotechnology Information (www.ncbi.nlm.nih.gov/genome), the Sanger Centre

(www.sanger.ac.uk) and the University of California Santa Cruz (www.genome.ucsc.edu).

More than 10,000 genes have been catalogued in the Online Mendelian Inheritance in Man, which has compiled documentation of all inherited human diseases. The positions of many of the genes annotated as known genes on the database have been determined by alignment of mRNAs with genomic sequences. To analyse the human genome NCBI, Ensembl and UCSC display genomic viewers and datasets to enable access to scientists globally without the need for local software. In addition, the genetics community have created gene prediction programs, SNP detection and novel transcript characterisation programmes to aid discovery of various molecular mechanisms in human disease. For example, "BLAT" at UCSC is a DNA/Protein sequence analysis that identifies the location of a sequence within the genome. It can establish exon/intron organisation rapidly within complementary DNA (cDNA) sequences using up to date genome data. Information on expressed sequenced tags (ESTs) defined from cDNAs and proteins from humans and other organisms provide a quick, accurate resource for gene structure information. The Basic Local Alignment Search Tool (BLAST) is a sequence alignment program that can determine the complete structure of a single gene. Using a nucleotide or amino acid sequence, a query or enquiry to the database with BLAST returns statistical values and a list of possible locations or "hits" recognised within a genome.

1.11.10 Direct sequencing

This is the process of determining the order of nucleotides in a DNA fragment. The dye termination method used today has evolved from the chain termination technique first

described by Frederick Sanger.[276] When a template DNA from a PCR reaction is produced, extension can be initiated with unidirectional oligonucleotide primers, complementary to a specific region. DNA polymerase, the primer and a low concentration of di-deoxynucleotide enables incorporation of this chain terminating nucleotide. The DNA polymerase incorporates the di-deoxynucleotides at a limited frequency due to their lower concentration and subsequently various fragment lengths are produced. Originally, an agarose gel was run to determine the sequences produced.

Fluorescently labelled di-deoxynucleotide chain terminators are used in modern sequencing machines. Each nucleotide is labelled with a different colour dye that fluoresces at various wavelengths when stimulated by differential laser wavelengths. Electrophoretic separation of the fragments occurs in a narrow glass capillary filled with a viscous polymer and the DNA sequence is read using the excitatory laser and software to interpret the emission from the nucleotide dye labels at the termination sites.

Sanger sequencing is still widely used and is often thought of as the ‘gold standard’ but it is being superseded by Next Generation Sequencing (NGS) and other techniques for large scale analyses.

1.11.11 The LCA APEX chip

The Arrayed Primer Extension (APEX) reaction is a sequencing reaction on a solid support. Microarrays were designed and manufactured with APEX technology.[277] 5'-modified, sequence-specific oligonucleotides are arrayed on a glass slide. All variable nucleotides are identified with optimal discrimination at the same reaction conditions. These oligonucleotides are designed with their 3' end immediately adjacent to the variable site. PCR-prepared and fragmented target nucleic acids are annealed to oligonucleotides on the slide, followed by sequence-specific extension of the 3' ends of primers with dye labeled nucleotide analogues (ddNTPs) by DNA polymerase. Consequently, this approach is more specific for multiplex mutation detection and successfully detects single nucleotide polymorphisms (SNPs), deletions, and insertions in heterozygous and homozygous patient samples. APEX also allows good discrimination between genotypes, because the template-dependent extension reactions with four uniquely dye-labeled ddNTPs yield covalent bonds between an oligonucleotide and a dye terminator. This allows stringent washing of slides after APEX, yielding minimal background signal. The time required for complete APEX analysis, including sample preparation, is less than 4 hours. Once designed, these microarrays can be upgraded easily with new variants.

Systematic analysis of all data permits a comprehensive database of LCA-associated variants to be compiled. In September 2008, the number of sequence changes currently considered disease associated exceeded 495 variants. By design, all variants from the coding region and adjacent intronic sequences of the known LCA/early-onset RP genes

reported in the literature are included on the chip. Intronic sequences are included only in cases with predicted or documented involvement in splicing. Several common polymorphisms are also included, mainly from the coding regions to facilitate haplotype assignments. Each sequence change is designed to be queried in duplicate from each sense and antisense strand by the software (Genorama Genotyping Software; Asper Biotech, Ltd.).

1.11.12 Gene identification strategy in LCA

The genetic heterogeneity of LCA and EOSRD has been discovered by various methods, including homozygosity mapping, classical linkage analysis, identity by descent mapping, the candidate gene approach and animal models of retinal degeneration.

Homozygosity mapping is an efficient gene mapping method applicable to rare recessive disorders in inbred populations. The method takes advantage of the fact that inbred affected individuals are likely to have two recessive copies of the disease allele from a common ancestor; i.e. two identical-by-descent (IBD) alleles. Since small chromosomal regions tend to be transmitted whole, unchanged by cross overs in meiosis, affected individuals will also have identical-by-descent alleles at markers located nearby the disease locus and thus will be homozygous at these markers. The basic idea of the method to locate genes involved in rare recessive traits is thus to search for regions of homozygosity that are shared by different affected individuals in the same family.

Linkage analysis with microsatellite markers is very laborious compared with the SNP microarrays, which can contain up to 906,600 SNPs and more than 946,000 copy number probes (SNP array 6.0) and perform linkage analysis in several days. Classical linkage

analysis requires the availability of relatively large families. Linkage data from smaller families can only be combined if there is no genetic heterogeneity. In autosomal recessive LCA, families with at least 6 affected individuals are required for significant linkage. In consanguineous families only 3 or 4 affected individuals may be sufficient, depending on degree of consanguinity.

The *AIPL1, GUCY2D* and *RDH12* genes were identified by classical linkage analysis in relatively large consanguineous and non-consanguineous families. *NMNAT1* and *SPATA7* were also mapped by linkage analysis.

In consanguineous families, another approach involves searching for chromosomal regions that are inherited from both parents through a common ancestor. This approach is known as identity-by-descent and can be powerful in small families that are not large enough for linkage analysis, including isolated patients of consanguineous and non-consanguineous matings. In outbred populations, the homozygous regions are expected to be smaller than in consanguineous populations and SNP arrays may be more useful. The size of chromosome containing a homozygous mutation inherited from a common ancestor of a proband's parents, measures 100 cM/*N (N*= the generations between the common ancestor and the proband). IBD mapping recently led to the identification of both the *CEP290* and *LCA5* genes [34;41]. The CEP290 gene was a strong candidate gene in one of the shared homozygous regions since it was previously found to be mutated in the *rd16* mouse.[19]

A candidate gene approach is another method that has been used to identify LCA genes. LCA only affects the retina and accordingly only genes that are expressed preferentially in the retina or that encode important functional retinal proteins, have been considered as

candidate genes for LCA. Many LCA patients and many candidate genes need to be screened in order to identify new genes. Mutation analysis of such candidate genes in patients with LCA or juvenile retinal dystrophies identified causative mutations in the *LRAT* [30], *RPE65* [28;29;80] and *RPGRIP1* [39;40] genes. The *CRB1*, *CRX* and *IMPDH1* genes were considered candidate genes for LCA since they were previously implicated in other forms of retinal degeneration.[130] [234;278]

Animal models with retinal dystrophies have also been useful to identify genes for LCA or early onset retinal dystrophy. The *MERTK* and *RD3* genes were considered candidate genes for retinal dystrophies since they were found to be causative in the RCS rat and the *rd3* mouse, as described in previous sections.

The identification of ciliary proteins CEP290 and Lebercilin (LCA5) highlights the important role of ciliary proteins in the pathogenesis of LCA. Consequently, the Ciliary Proteome database (http://v3.ciliaproteome.org/cgi-bin/index.php) has become useful as an open resource to explore the role of cilium in disease, identify candidate genes and the mechanisms underlying ciliary biology.

1.11.13 Molecular Diagnosis

A molecular diagnosis is paramount for genetic counselling of affected families. An accurate genetic test can confirm the clinical diagnosis, differentiate the condition from other retinal disorders and inform patients about their visual prognosis, using genotype-phenotype correlation studies in the literature. Genetic testing forms a prerequisite to enrol patients into clinical trials that will be tailored to specific molecular defects, such as the recently successful RPE65 LCA trials. It is also important to identify a molecular

diagnosis in case a severe systemic abnormality is also present, as has recently been established with *CEP290* and Jouberts, Bardet Biedel and Meckel Gruber syndromes.

Establishing a molecular diagnosis for LCA is hampered by the heterogeneity described in the previous section. Systematic sequence analysis or mutation scanning of all the known LCA genes would require an expensive and time consuming analysis of over 230 exons. The cost effective technology that can overcome this exercise includes the LCA mutation chip (Asper Ophthalmics, Estonia), discussed above.[279] The LCA mutation chip is now reported to identify the causative gene in approximately 60% of LCA cases, although there is variation between populations.[81;280-282]

The Carver laboratory at the University of Iowa performs genetic testing using a mutation detection probability distribution, which screens the regions of genes with the most frequent mutations first.[283] This reduces the costs of genetic testing by identifying the common alleles early in the process.

A re-sequencing chip for early onset retinal degenerations has also been reported.[284] The chip is a microarray that allows re-sequencing of 11 genes involved in retinal degeneration. However, the chip detection of new mutations is possible but the chip only covers two of the LCA genes (*CRB1* and *RPE65*), and would therefore be less effective in providing LCA molecular diagnoses.

Next generation sequencing (NGS) represents a major breakthrough in cost-effective sequencing.[285] The cost per base pair for this technology compared with conventional Sanger sequencing is now a thousand times cheaper. To identify novel retinal disease genes, all the exons from a sizable genomic region (e.g., established via linkage analysis or by identity-by-descent mapping) can be sequenced. All the genes on the human

genome (the exome) can be sequenced for less than £5,000. Studies are in progress to tailor next-generation sequencing technology for diagnostic purposes, for example, to sequence the exons of all (approximately 180) human retinal disease genes, or a subset of these genes, for less than £500. With the identification of numerous variants in many putative disease genes, it will be a challenge to discriminate pathologic from benign sequence variants. In addition, nonsyndromic retinal dystrophies in a subset of patients may be caused by the cumulative effect of mutations in more than one gene, and detailed knowledge about the interactions of proteins in networks, such as at the connecting cilium, will be required to begin to understand genetic interactions.

Previously, conventional genetic testing was only applicable to the minority of patients with inherited retinal disease and identifies mutations in fewer than 60% of patients tested (with the LCA APEX chip). NGS includes patients with *de novo* mutations, and those for whom clinical management and prognosis are altered as a consequence of defining their disease at a molecular level. The new NGS approach delivers a change in the diagnosis of inherited eye disease, provides precise diagnostic information and extends the possibility of targeted treatments including gene therapy. The technology will be applied to many conditions that are associated with high levels of genetic heterogeneity.

During genetic testing it is often difficult to determine the pathogenicity of a new variant. This is challenging for amino acid variants, or sequence variants without an amino acid change. Affected siblings would carry both mutant alleles in autosomal recessive disease and cosegregation with phenotype should occur. It is important to check SNP databases and to test control individuals for a variant to determine allele frequency in a normal population. Recent software tools to predict pathogenicity include PolyPhen,[286] SIFT,[287]

PMut,[288] and homology modelling to predict the 3D structure of a protein and the effect on protein function and cellular biology, (see Methods 2.3.6). There are also tests on new variants interruption to splice sites or exonic splice enhancers.[289;290] Bioinformatic progress continues to improve our ability to detect genetic mutations.

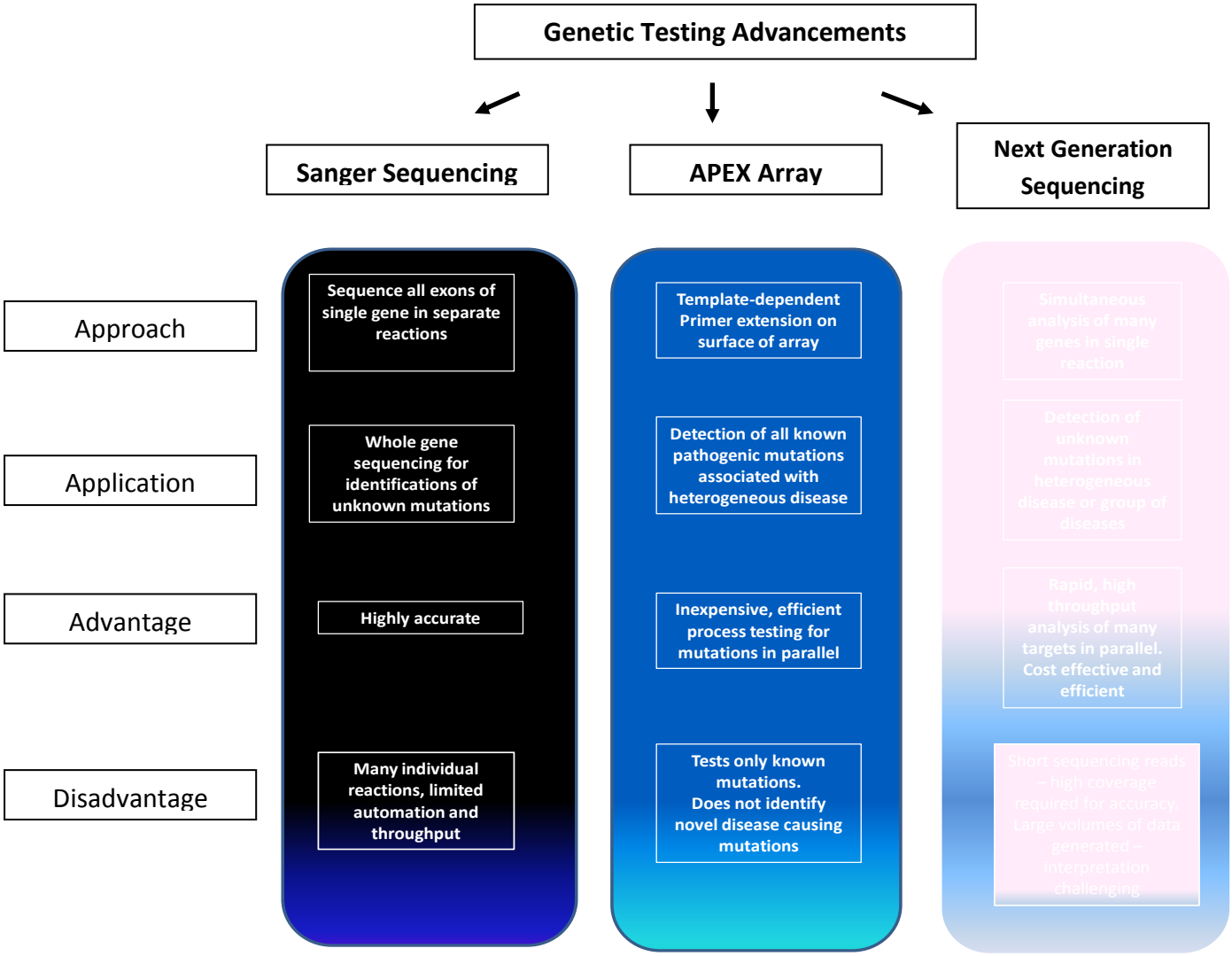

Figure 1.11.13: Testing methods – genetic testing approaches: advantages and limitations

Aims of the project

1. To recruit individuals with Leber Congenital Amaurosis or early onset retinal dystrophies and family members.
2. To obtain detailed phenotypic information from individuals willing to participate in research. (Total number of patients phenotyped in this project: 117 patients, from 115 families).
3. To obtain DNA samples from these individuals and family members for the purposes of identification of the causative genetic mutations. (Total number of patients genotyped in this project: 158 patients)
4. To attempt to identify novel loci and mutations that may be causative of LCA or EORD.
5. To perform genotype-phenotype analysis in order to refine the subtypes of the condition and permit an improved understanding of disease progression.
6. To identify specific patients with disease associated mutations who may be candidates for future gene therapy treatment, including the ongoing RPE65 gene therapy trial.

2 Materials and Methods

2 Methods

2.1.1 Ethical approval for study

Ethical approval was granted from the Multi-centre Research Ethics Committee (MREC). before the study was started in order to protect the dignity, rights, safety and well-being of research participants. This body has been renamed the Central Office for Research Ethics Committee (COREC).

The following patient criteria require ethical approval in an NHS setting:

- Patients and users of the NHS. This includes all potential participants recruited.
- Individuals identified as potential research participants because of their status as relatives, or carers of patients and users of the NHS, as defined above.
- Access to data, organs or other bodily material of past and present NHS patients. *(Research Governance Framework for Health and Community Care)*

Ethical compliance required patient information sheets for children and adults and consent forms (see Appendix).

Our aims were to recruit from two main sites: Moorfields Eye Hospital (MEH) and Great Ormond Street Hospital for Children (GOSH). All phenotyping was conducted at MEH. Site specific assessments were conducted and ethics approval given. (MREC approval number MOOA1005; Great Ormond Street Hospital R&D approval 04-VS-08.).

2.1.2 Database design and registration

A relational Microsoft Access database with necessary encryption for data protection was designed containing a number of tables relating to personal data, clinic visit information, genetic information and clinical history.

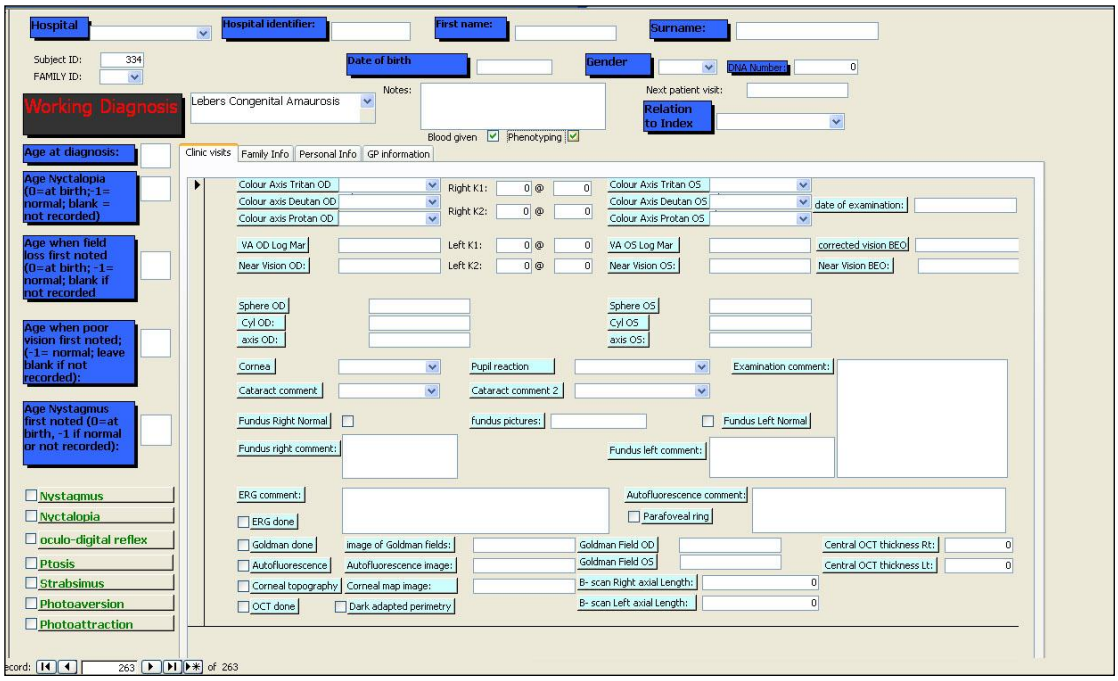

Figure 2.1.2 Screen shot of EORD database

University College London database registration was required under the Data Protection Act (1998). A consent form to keep patient data in the database was created (see appendix). Permission and was granted under registration number: Z6364106, Section 19, Research: Medical Research. (see Appendix for details.)

2.1.3 Patient ascertainment

Leber's congenital amaurosis patients and those with an early onset retinal dystrophy (EORD) were included as research participants. LCA is characterised by its severe visual impairment with onset under 3 months, sensory/wandering nystagmus, amaurotic pupils, and a fundus appearance that is either normal or reveals a pigmentary retinopathy with or without macular atrophy. A severely reduced or non-detectable electroretinogram (ERG) measured early in the disease process is a diagnostic prerequisite.[11-13] For the purposes of this research project, electrophysiological diagnostic verification was used to diagnose early onset retinal dystrophy patients, with symptomatic onset after the first 3 months of infancy but under the age of 5 years, with either a rod-cone dystrophy (RCD) or cone-rod dystrophy (CRD). Those patients that presented with an early retinal dystrophy at presentation, that was too severe for an electrophysiological RCD or CRD diagnosis, and with symptomatic onset after the first 3 months of infancy but under the age of 5 years, were diagnosed as early onset retinal dystrophy with unknown electrophysiology data (Termed 'EORD' in the collected phenotyping data; see Results Chapter 3 in this thesis). Syndromic patients were not included. Initially, all patient ascertainment were planned to be from Moorfields Eye Hospital and Great Ormond Street Hospital.

The Moorfields genetic database, which has 40 years of data for patients in the retinal service, was initially used to search for LCA and EORD. Subsequently new patients with the above diagnoses, or those patients with a probable LCA/EORD diagnosis after electrophysiological verification and verbal consent, were sent a letter to their home

address including a patient information sheet and a reply form with stamped addressed envelope. (See Appendix).

The total number of patients genotyped by thesis author (PM) was 158 patients using the APEX microarray chip and Sanger sequencing. Of these 158 patients genotyped, 117 patients were phenotyped by author (PM) and it is these data that are presented in Results chapter 3.

2.2 Phenotyping

2.2.1 Clinical history

A comprehensive clinical history included age of onset of symptoms, progression of symptoms and visual function history. Visual field impairment , the approximate age of onset of field loss (clumsiness, peripheral field loss), the onset of nystagmus, nyctalopia, photophobia or photoattraction, strabismus, refractive and eye-poking histories (oculodigital reflex) were also ascertained.

A complete past medical history was enquired after to exclude patients with syndromic associations. If necessary previous investigations to diagnose syndromic evidence were sought, including blood work ups and radiological investigations. Further questions were asked concerning developmental milestones, to ensure normal progress. The family history included a full pedigree with ethnicity and consanguinity information.

To assist with diagnostic verification previous electrophysiological data were obtained. The early onset retinal dystrophy (EORD) patients were diagnosed as having a rod-cone dystrophy, or a cone-rod dystrophy. In some cases subjects had a generalised severe photoreceptor dystrophy – both rod and cone systems were severely attenuated on ERG testing. In these patients, if the history was not consistent with LCA and if there was no information as to whether rods or cones were affected initially; a diagnosis of early onset retinal dystrophy (EORD) was documented. (See exact diagnostic criteria described already in sections 1.3, 1.4 and 2.1.3).

Several panels of patient DNA being screened within the Inherited Eye Disease laboratory (Dr Donna Mackay and Dr Zheng Li), but not specifically for this project, included patients with a clinical history and diagnosis of autosomal recessive Retinitis Pigmentosa (arRP), or early onset RP where the age was older than 5 years. The two families with *RLBP1* mutations (see results section 3.8) were included in this study, because the reported history of early onset of this retinal dystrophy overlapped with the larger but distinct EORD/LCA cohort already described.

2.2.2 Visual acuity

LogMar visual acuity was measured if possible. The LogMar test was performed at a distance of 4m with mean transilluminance of 1200 lux. Monocular and binocular visual acuity testing was performed with recent refractive prescription if necessary. The value recorded was dependent upon how many letters were correctly identified on that line, with 0.2 added for each mistake.

Patients unable to see the largest LogMAR letters were moved towards the chart by 1 or 2 metres. Counting finger (CF – Log Mar equivalent value 2.0) detection was performed; if appropriate. Hand movement detection (HM) was recorded as LogMAR equivalent value 3.0. Perception of light (PL) was recorded as a value of 5.0 or no light perception was given a value of LogMAR 6.0.

Vision in infants was recorded from the most recent orthoptic assessment and any Snellen fraction given was converted to LogMar equivalent. If baby or infant was bought for a first assessment, reaction to light was observed with record of the vision appearing central, steady, and maintained. Near vision was tested using the British typesetters Near

Chart (at a distance of 25-33 cm) with both eyes open in standard room lighting. The N value recorded was the lowest at which reading was possible without altering the chart distance.

2.2.3 HRR colour vision testing

Colour vision testing was attempted on patients with vision better than counting fingers. American Optometric Hardy Rand and Rittler (AO H-R-R) pseudoisochromatic plate viewing was conducted in standard room lighting with an angle poised light source at 60 watts.

If the first four demonstration plates shown to the patient were unidentified, the test was discontinued. The screening plates (1-6) were then shown and if the symbol and location on the page were correctly identified, a positive score was recorded. Each page was viewed for 2-3 seconds and only immediate responses were recorded. If all six plates were identified correctly, the subject was found to have normal vision and no further testing was required. If plates 1-2 were incorrect the subject was found to have defective blue-yellow vision. Subsequently plates 17-20 were shown. If plates 3-6 were incorrect then a red-green defect was assumed and plates 7-16 were viewed.

A protan, deutan, or tritan defect was diagnosed if more red, green, or blue-yellow plates were unidentified respectively. The defect was assessed as being mild, moderate, or strong depending upon which plates were failed: mild defect R-G plates 7-11; medium defect R-G plates 12-14; strong defect R-G plates 15-16; Medium defect B-Y plates 17-18; Strong B-Y defect 19-20. The extent of the patient's colour deficiency was given by the last group of plates in which errors occurred.

2.2.4 General examination

An ophthalmic examination was performed on all study subjects. All infants and small children were then refracted with a retinoscope and hand-held neutralising lenses.

The presence of any nystagmus or manifest strabismus was assessed. The pupil size and responses were checked in a darkened room to assess the speed of a direct and consensual response and the presence of a relative afferent pupil defect elicited.

Slit-lamp biomicroscopy was conducted if possible to observe the possibility of keratoconus or cataracts. Dilated fundal examination was carried out using either a Volk superfield fundus lens and a Volk 78D or using the Keeler BIO Vantage indirect ophthalmoscope with a Volk 20D or 28D lens. Recorded features included blood vessel calibre, the colour of the retina including presence, distribution, level and location of any pigment or other notable signs (eg white dots) and the optic disc colour.

All clinical data obtained was recorded on a phenotyping form that was designed for the study (see Appendix for form).

2.2.5 Goldmann Visual Fields

Patients with greater than CF vision performed Goldmann perimetry and if they were capable of test understanding and completion. The perimeter was calibrated according to manufacturer's instructions.

The patient was corrected with a recent prescription and one eye was covered with an eye patch. Using the chin rest, the patient positioned their head and attempted to maintain

fixation at the central dark target. The patient's eye was centred on the cross hairs to allow the examiner to observe maintained target fixation. The V4e target was mobilised from a non seeing area towards fixation with the patient pressing the hand held buzzer on light perception. As the target was moved towards fixation the patient was asked to indicate if the target disappeared for any period.

Nystagmus prevents fixation and if field testing was difficult, an attempt was made to establish field size whilst accepting the possible inaccuracy and limitations of the test.

Analysis of the visual field area was performed by calculating the area contained within the V4e isopter. The Retinal area analysis tool was designed by Fitzke and Halfyard (2002), (see screen shot, Figure 2.2.5). It is a two dimensional planimetry package that allows the user to scale from the optic nerve to the fovea in order to draw around the recorded visible isopter area as a measurement of square degrees.

Figure 2.2.5 Screen shot of the retinal analysis tool displaying number of square degrees inside V4e isopter. Halfyard & Fitzke (2002).

2.2.6 Optical Coherence Tomography (OCT) and Scanning laser ophthalmoscope capture of retinal autofluorescence

The Stratus OCT™ (software version 3; Carl Zeiss Meditec, Inc. Dublin, CA) was used to perform OCT imaging. The fast macula program produced 6 radial tomograms centred on the fovea. Thickness data is calculated using software to subtract the two most reflective layers of the retina, from the RPE to the vitreoretinal surface. A colour map and average thickness values over 9 circumferential areas are available. Acquisition of one radial tomograph in a single plane through the fovea was used in patients with involuntary eye movements when normal OCT image capture was impossible. In this situation, software callipers could be used to quantify measurements.

High resolution spectral domain OCT (SD-OCT; Spectralis spectral domain OCT scanner; Heidelberg Engineering, Heidelberg, Germany) or time-domain (TD-OCT; Stratusoct Model 3000 Scanner; Zeiss Humphrey Instruments, Dublin, CA), and retinal autofluorescence (AF) imaging using a confocal scanning laser ophthalmoscope (Zeiss prototype; Carl Zeiss, Oberkochen, Germany and Heidelberg Retinal Angiograph II, Heidelberg Engineering, Heidelberg, Germany) were performed where nystagmus did not preclude image acquisition and in those who were old enough to cooperate. During fundal autofluorescence capture, ammetropia was corrected by a focus control. The gain function was standardised at 95% to optimise visualisation of 256 greyscale images on the screen. A dilated pupil was required to form a composite of 16 captured frames using software within the ophthalmoscope. Video mode was attempted if nystagmus reduced the quality of still images. These videos were aligned to produce images. During this

project, local specialist OCT interpretation advice (Mr P Keane, IOO) and a systematic method of describing OCT phenotypes was used.[291]

2.2.7 Biometry & keratometry

Axial length and keratometry measurements was attempted if possible and appropriate, depending on nystagmus, using the IOL Master (Carl Zeiss Meditec, Dublin CA).

2.2.8 Autorefraction

An objective cycloplegic refraction using neutralising lenses was carried out in young children or in those patients with nystagmus. Other participants were autorefracted using the Luneau L62-3D autorefractokeratometer (LUNEAU Chartres, France).

2.2.9 Colour fundus photography

The Topcon retinal camera (TRC-50IX with IMAGEnet 2000 system software – TOPCON corporation, Japan) was used to capture fundus images. Composite photographs were exported into Adobe photoshop for editing purposes.

2.2.10 The Smell Identification Test ™ administration

This form of smell identification test (Sensonics, Inc., Haddon Heights, NJ USA) was designed to be self administered by literate people or tested under supervision. Tests occurred supervised in this study. The odorants are embedded in 50 micron urea-formaldehyde polymer microencapsules fixed in a proprietary binder and positioned on brown strips at the bottom of the test booklets. The stimuli were released by scratching strips with a pencil tip in a standardised manner. Above each odorant strip is a multiple

choice question with four alternative responses. The test is forced-choice i.e. the subject is required to mark one of four alternatives even if no smell is perceived. For example, one of the items reads: "This odour smells most like: a) chocolate; b) banana ; c) onion ; d) fruit punch." The subjects were encouraged to sniff the 40 scratch strips immediately after it had been scratched to ensure that the odour had not significantly dissipated. The subject's total number of correct responses (maximal possible = 40) is established by the use of the test's scoring key, a correct odours list. The test score and age of the patient is then used in a separate male and female table to look up the subject's percentile score. For example, in the case of a female subject falling on the 16^{th} percentile, 16% of the group of "normal" females achieved a score at or below that value, with the remainder scoring above. In general, the raw test scores below have been developed for establishing an adult patient's olfactory diagnosis.

Test Score:

0-5	Probable Malingering
6-18	Total Anosmia
19-25	Severe microsmia
26-29	Moderate microsmia (males)
26-30	Moderate microsmia (females)
30-33	Mild microsmia (males)
31-34	Mild microsmia (females)
34-40	Normosmia (males)
35-40	Normosmia (females)

2.2.11 Electrophysiology

Electrophysiological investigation in paediatric clinics is particularly important given the inability of young children to describe their symptoms. Electrophysiological techniques used include full field and pattern electroretinography (ERG;PERG), electro-oculography (EOG), multifocal ERG (mfERG) and cortical visual evoked potentials (VEPs). The International Society for Clinical Electrophysiology of Vision (ISCEV) has published recommendations and minimum standards relating to the performance of these techniques.[292;293]

The ISCEV standard full field ERG is recorded using corneal electrodes with stimuli delivered by a Ganzfeld bowl, an integrating sphere enabling uniform whole field illumination. The Ganzfeld provides both flash stimulation and a diffuse background for photopic adaptation. The reference electrodes should be positioned at the ipsilateral outer canthi if a bipolar contact lens electrode with a built in reference is not used. ISCEV defines a standard flash as 1.5-3.0 $cd.s.m^{-2}$. The response to this flash under scotopic conditions, with a fully dilated pupil, is the maximal or mixed response (Figure 2.2.11 below), which is dominated by the rod system under scotopic conditions.

Cone system ERGs are obtained under photopic conditions using both single flash and 30Hz flicker stimulation superimposed upon a red-saturating background (17-34 cd/m^2). At 30Hz, the poor temporal resolution of the rod system, in addition to the presence of a rod-suppressing background, enables a cone-specific waveform to be recorded.

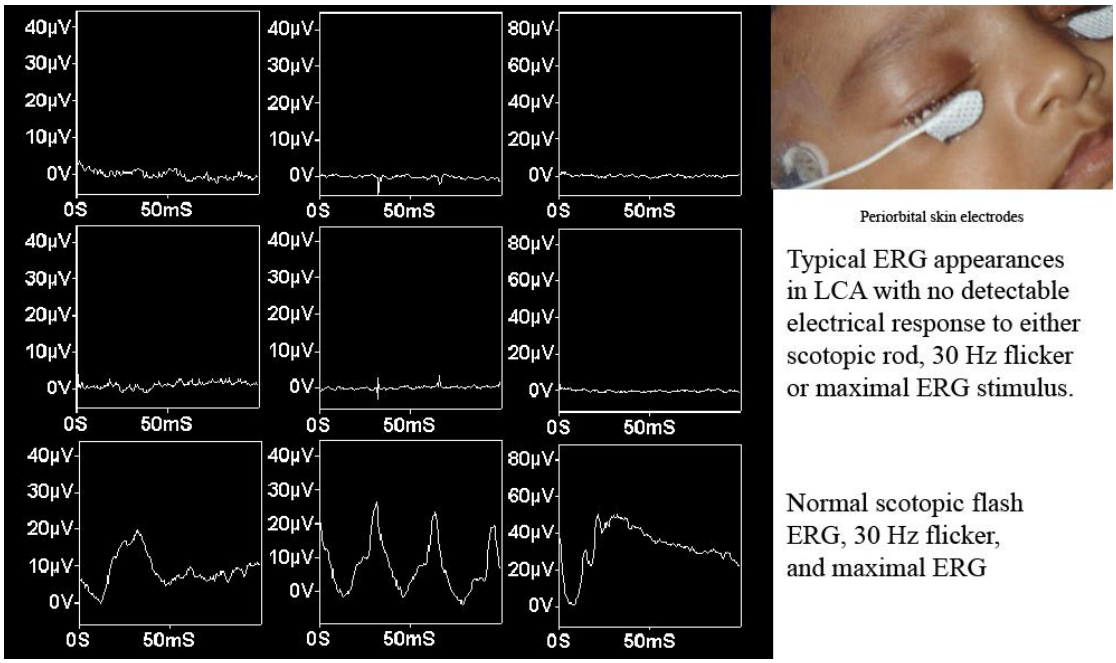

Figure 2.2.11: Top row showing right eye responses of LCA patient. Middle row showing left eye responses of LCA patient. Bottom row showing normal, healthy responses for comparison.

Left to right columns : Left column is the scotopic flash ERG. Middle column is the 30 Hz flicker. Right column is the maximal ERG.

2.3 Molecular genetic methods

2.3.1 DNA extraction

Blood samples were obtained from the proband, and siblings and parents, when possible. Absent family members were sent a letter, blood tubes and consent forms to obtain further family samples.

Two 9ml EDTA (Vacutainer) tubes of peripheral venous blood were considered optimal collection volumes. EMLA cream 5% (AstraZeneca, Macclesfield, UK) was applied to the skin for one hour prior to venepuncture for young children. Blood sample tubes were labelled and stored at 4°C before DNA extraction. Blood samples were logged into the Moorfields database and sent for DNA extraction by the DNA bank service at the Institute of Ophthalmology (Beverly Scott) using the Nucelon BACC-2 kit (GE Healthcare) using manufacturer's instructions.

After extraction, DNA was stored at 4°C if for immediate use or at -20°C if for longer term storage.

2.3.2 LCA chip

Genomic DNA was sent for each proband to Asper Biotech, Tartu, Estonia. Very occasionally, if proband DNA was unavailable, parental DNA was sent for analysis by the LCA chip. The technology and methods have been described in previous Introduction chapter. In 2008, the LCA microarray test contained 461 disease-associated sequence variants identified in 12 LCA or early-onset retinitis pigmentosa genes: *AIPL1, CRB1, CRX, GUCY2D, LRAT, TULP1, MERTK, CEP290, RDH12, RPGRIP1, LCA5, RPE65*.

The only other gene investigated by the author, in this project, was *RLBP1* by direct screening. The genes investigated by direct sequencing on the LCA chip were *RDH12* and *CEP290*.

2.3.3 PCR

Given the time it would take to sequence a large number of probands, especially for the very large gene *CEP290*, mutations were sought and confirmed after the first mutation had been found using the LCA Apex chip. Of the 158 DNA samples included in this study, patient DNA samples were analysed as follows:

LCA chip	Phillip Moradi
CEP290	Phillip Moradi
RDH12	Donna Mackay and Phillip Moradi
CRALBP	Zheng Li and Phillip Moradi

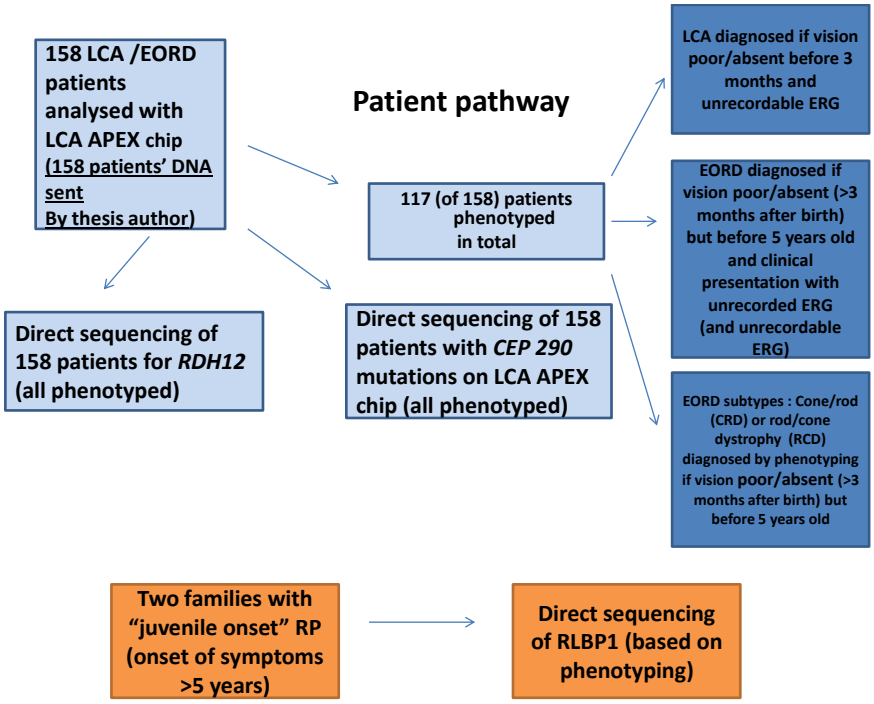

Figure 2.3.3 Flow chart summarising patient pathway in the project and phenotypic diagnoses of LCA, RCD, CRD, EORD and "juvenile onset" RP

Oligonucleotide primer pairs were designed for sequencing the *CEP290*, *RDH12* and *RLBP1* genes using Ensembl (http://www.ensembl.org/index.html) to obtain the reference sequence, and Primer 3 for primer design (Whitehead Institute for Biomedical Research: http://frodo.wi.mit.edu/cgi-bin/primer3/primer3_www.cgi). Primer design was optimised by using a mispriming library within Primer 3; establishing that primers were GC clamped where possible to avoid hairpin aggregations and primer-dimer formation. Amplimers were designed approximately 500 bp apart to coincide with maximal sequence read lengths. Intronic primers were designed at least 50 bases 5' or 3' to the beginning or end of the exon to allow sufficient sequence for full sequencing of the splice sites and coding region.

Oligonucleotides were ordered and manufactured by Sigma Genosys (Sigma-Aldrich Ltd, Haverhill, UK) desalted and deprotected on a 0.05 µm scale of synthesis. Primers were delivered lyophilised and were resuspended in sterile deionised water as per manufacturer's instructions to make 100 µm stock solution. A subsequent 5 µm working dilution was made for PCR amplification and sequencing.

All primers were optimised for PCR using a 20µl mix comprising 10.3µl H_2O; 2µl 10x NH_4 buffer (No $MgCl_2$; Bioline UK); 0.6µl 50µM $MgCl_2$ (for 1.5 µm concentration: Bioline, UK); 2µl [2mMol] dNTPs (from stock solutions of 100mM dATP, dTTP, dCTP, dGTP; Promega, Madison, WI, US); 2µl [5µm] forward and reverse primer; 1µl Biotaq polymerase (Bioline UK); and 50-100ng genomic DNA.

Abgene Reddymix with or without dye (AB795, AB793 – Abgene, Epsom, UK) was also used for convenience. 10µl of reddymix was combined with 5µl of deionised H_2O, 2µl (10pm) of forward and reverse primer and 1µl (50-100ng) of genomic DNA.

Each primer was optimised for ideal Tm on an Eppendorf gradient block (PCR Mastercycler: Eppendorf AG, Barkhausenweg, Hamburg, Germany) using the following cycle:

96°C – 5 min	
94°C – 30 sec	Denaturation
60°C – 30 sec (ramp 3°C/sec; gradient 7°C)	Annealing
72°C – 30 sec	Extension
Go to 2 and repeat 35 cycles	
72°C 10 minutes	Final extension

1% Electrophoresis gels were made by dissolving 1g molecular grade agarose heated in 100ml of TAE (Eppendorf, Germany - 50x concentrate is composed of 2 M Tris-Acetate, 0.05M EDTA, pH 8.3 diluted to 1X). Just before the gel set, dilute Ethidium Bromide 0.5µg/mL was added (usually 2-3µl of lab stock solution per 100mL gel).

Following completion of the PCR 5µl of product was placed in a 1% Agarose (Bioline UK) check gel and run at 120mV for 15 minutes to determine the optimum annealing temperature. A DNA ladder was used (PhiX 174 – Promega, Madison WI, USA) to size the PCR product.

2.3.4 PCR clean up and direct sequencing

The PCR for each amplimer was run at optimal annealing temperature. The DNA fragments were purified using Montage PCR cleanup plates according to the standard protocol (Millipore, Watford, UK). The Big Dye terminator cycle sequencing reaction was then performed using a 10µl reaction mixture containing 0.5µl of BigDye v3.1 (ABI); 2µl of PCR product; 1.5µl of 5pM forward or reverse primer, 3.5µl of H_2O; and 2.5 µl of sequencing buffer. Bidirectional sequencing was performed by 2 sequencing reactions, one with the forward primer and one with the reverse primer.

The sequencing reaction was as follows:

96°C – 5 minutes

96°C – 30 secs

50°C – 30 secs

60°C – 4 minutes

go to step 2 and repeat for 30 cycles

The sequencing reaction mixture was purified using the Montage sequence cleanup (blue) plate as per manufacturer's instructions and run on the ABI 3700 sequencer. DNA sequence was analysed using DNA Star Seqman.

2.3.5 Affymetrix chip (performed by Donna Mackay)

DNA was also sent to the Institute of Child Health for analysis using the Affymetrix 10.2K SNP, single nucleotide polymorphism, chip. The DNA was analysed using the Thermo UV500 spectrophotometer to ensure adequate purity and concentration of DNA (260/280 ratios >1.8 and minimum 400 ng DNA).

Full genome-wide autozygosity scans were also performed in some families. Samples were analysed using the Affymetrix Gene Chip Human Mapping 50k XbaI array following the manufacturer's instructions (Affymetrix, Santa Clara,CA). Genotypes for SNPs were called by the GeneChip DNA Analysis Software (GDAS v3.0; Affymetrix). A macro was written, by Dr Li, in Visual Basic within the Microsoft Excel (Microsoft, Redmond, WA) program to detect genomic regions with a shared haplotype.

Other allele calls were sent back as a text file which was imported into Excel. Significant areas of homozygosity, in which candidate genes could be sought, were also analysed by visually inspecting the data.

2.3.6 Candidate gene identification (by Donna Mackay)

Once the largest and most significant areas of homozygosity were identified, the gene list within the region was downloaded using the BioMart feature of Ensembl. Expression profiles of candidate genes were then examined within NCBI Unigene for EST profiles

within human tissues. Those genes with a high expression level in retina, relative to other tissues, were selected as likely novel candidate genes and further to discussion with colleagues, primers were designed and ordered for further analysis.

2.3.7 Statistical analysis and software

Statistical analysis was performed using GraftPad Prism (GraftPad software Inc). Pedigrees were drawn using Cyrillic 2.1 (FamilyGenetix Ltd, Oxford, UK). Genotyping data was analysed using Genotyper software version 3.7 (Applied Biosystems); DNA sequence analysis was performed using Seqman from the DNA Star package (DNA Star Inc, Madison WI). The Mapdraw and EditSeq components of the DNA Star package were also accessed.

Descriptions of the statistical tests follow.

The two-tailed t test is used to find the two-tailed P value . By assuming the null hypothesis is true, the test calculates the chance that randomly selected samples would have means as far apart as (or further than) observed in this experiment . Two-tailed tests are only applicable when there are two tails, such as in the normal distribution, and correspond to considering either direction significant. This test allows for either group potentially to have the larger mean. It is used to compare the statistically significant difference ($p<0.05$) in this project between two values, comparing two subgroup values, such as age of diagnosis in EORD vs LCA patients (see section 3.1.1).

2.3.8 SIFT (Sorting Intolerant From Tolerance, http://sift.jcvi.org/)

The SIFT algorithm deploys sequence homology to calculate a score, determining the evolutionary conservation status of the amino acid of interest, and predicting whether its substitution will affect protein function. Substitutions at specific positions showing normalized probabilities less than the chosen cutoff value of 0.05 are predicted to be deleterious, and those greater than or equal to 0.05 are predicted to be tolerated. The higher the tolerance index, the less functional impact a particular amino acid substitution is likely to have.

2.3.9 PolyPhen algorithm

(Polymorphism Phenotyping,http://genetics.bwh.harvard.edu/pph/ index.html).

Polyphen evaluates the location of the substitution and the function of that region and whether the substitution is likely to affect the three-dimensional structure of the protein. The prediction is based on the position-specific independent counts (PSIC) score derived from a composite of these calculations. PolyPhen scores greater than 2.0 indicate probably damaging to protein function, scores of 1.5–2.0 as possibly damaging, and scores of lower than 1.5 as benign.

pMUT reference: NN= neural network values from 0-1. >0.5 is predicted as a disease associated mutation. Reliability = values 0-9. >5 is the best prediction

3 Results

3 Results

3.1.1 Recruitment

DNA samples were obtained from at least one parent and contactable siblings in the majority (>95%) of families. A total of 117 affected individuals from 115 families were recruited for phenotyping. Amongst this cohort, 65 patients were male and 52 female, ranging in age from 6 months to 68 years. Mean age was 17.3 years (median 14 years, standard deviation 13.5). The summary by diagnosis (section 3.1.5 and Table 3.1.5) of phenotyped patients included the following: 56 affected individuals diagnosed with LCA, 27 with EORD (early onset retinal dystrophy), 19 with CRD (cone rod dystrophy), 15 with RCD (rod cone dystrophy).

3.1.2 Age at diagnosis

The age that the diagnosis was made was compared between the diagnostic groups. The first analysis compared LCA patients and the combined EORD patients which demonstrated a significant difference ($P<0.0001$ two-tailed t test; Figure 3.1.2).

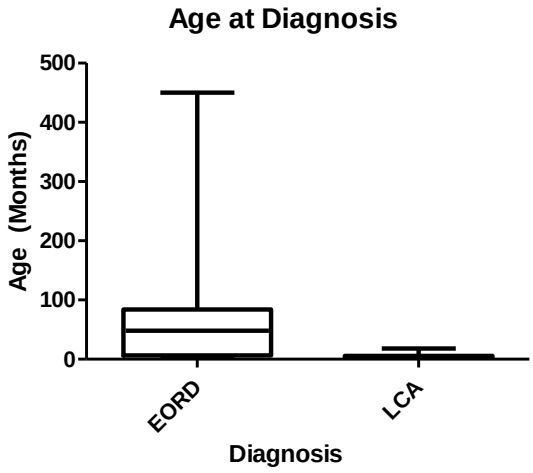

Figure 3.1.2 Box and whisker plot showing age at diagnosis for patients diagnosed with either EORD or LCA. The bottom and top of the box are the first and third quartile value, and the band inside the box is the second quartile value (the median). The ends of the whiskers (vertical lines) represents the minimum and maximum of all of the data for EORD and LCA diagnoses.

Table 3.1.2a: Summary table showing age in months (m) and summary statistics at diagnosis for each group: CRD, EORD, LCA or RCD.

Diagnoses	CRD	EORD	LCA	RCD
Number of patients	16	20	53	12
Minimum age (m)	4	2	0	3
25% Percentile (m)	13.5	5.3	0.0	5.3
Median age (m)	70	39	3	51
75% Percentile (m)	84	60	6	191
Maximum age (m)	200	450	18	360
Mean age (m)	65.81	60.95	3.36	94.75

Comparing and analyzing by different diagnoses (Table 3.1.2b) showed that the greatest differences between ages of diagnosis were seen between LCA groups and the other 3 sub- groups, CRD, RCD and EORD, as expected (Kruskal-Wallis $P<0.0001$).

Table 3.1.2b Dunn's multiple comparison test demonstrating differences in age of diagnosis between different diagnoses.

Dunn's Multiple Comparison Test	P value
CRD vs EORD	>0.05
CRD vs LCA	**< 0.0001**
CRD vs RCD	>0.05
EORD vs LCA	**< 0.0001**
EORD vs RCD	>0.05
LCA vs RCD	**< 0.0001**

3.1.3 Age at examination

This section refers to the age at which patients recruited to this specific study were examined by the author, PM.

A comparison of LCA and EORD groups revealed a significant difference in the age of examination (p=0.0345 two-tailed t test, from data Figure 3.1.3). However, further analysis by specific diagnosis showed no significant difference between groups in terms of the age at which individuals were examined (Kruskal Wallis p=0.190)

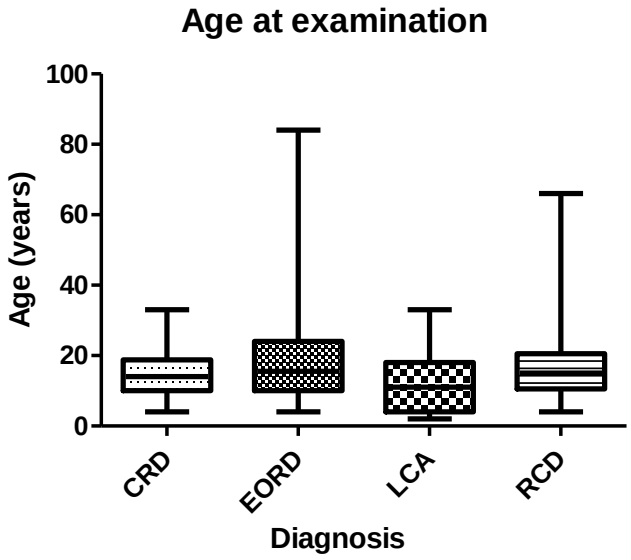

Figure 3.1.3: Box and whisker plot showing median age, interquartile range and highest and lowest observed ages of patients at examination.

3.1.4 Ethnicity and consanguinity

The ethnic diversity represents the tertiary referral clinics and international population at the centre. The majority of the patients studied were ethnically white and British with unrelated parents (62%). Of the 115 families, parental consanguinity occurred in 19.1 %. The consanguineous families were predominantly from India or Pakistan (16/17 families).

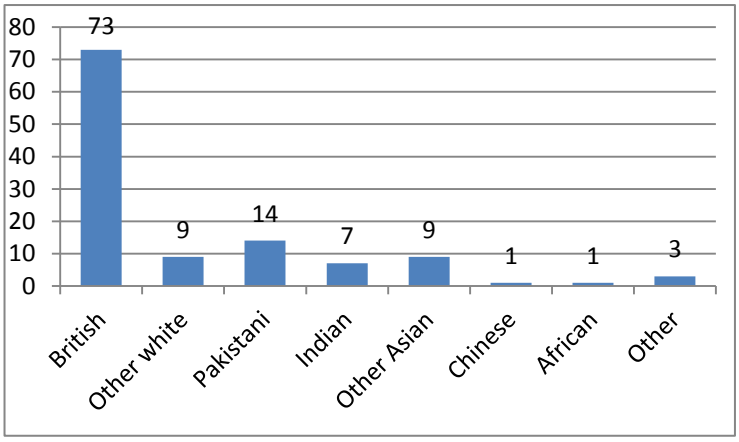

Figure 3.1.4a Graph showing number of individuals recruited in each ethnic group

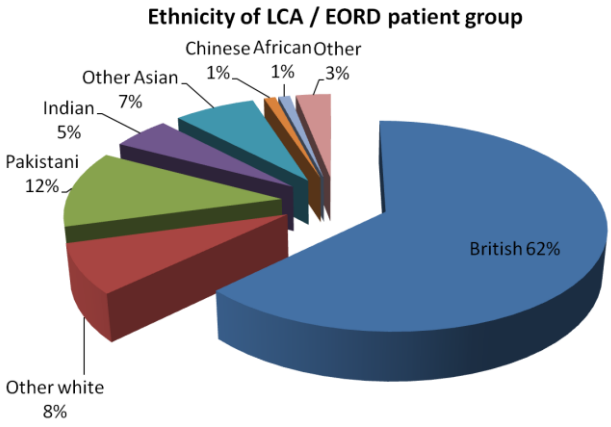

Figure 3.1.4b Pie chart showing percentage of individuals recruited in each ethnic group

3.1.5 Diagnosis

All subjects had a family history consistent with AR inheritance. The literature regarding the "spectrum of LCA" diagnosis is confusing and highlights this phenotypically heterogeneous population. However, for the purposes of this study, patients were diagnosed as having LCA if vision was poor or absent in the first 3 months after birth, and where there was no recordable electroretinogram. A diagnosis of early-onset retinal dystrophy (EORD) was made when symptoms and/or signs were present before the age of 5 years, and subsequently, on electroretinography. For the phenotyping section of this project, those patients with an extinguished ERG were categorised as EORD (with an unknown previous electrophysiology phenotype). The EORD patients that were electrophysiologically diagnosed on the evidence of a severe cone/rod dystrophy (CRD) or rod/cone dystrophy (RCD) phenotype, were decribed as RCD or CRD .

The two families with RLBP1 mutations who were initially referred to our clinic, incorrectly diagnosed as either LCA/ EORD, were diagnosed as 'juvenile onset' retinal dystrophy due to their later onset of symptoms and signs beyond 5 years old (section 3.8.3)..

The diagnosis of each patient was based upon electrophysiological information where available combined with clinical history and examination. LCA was diagnosed in patients with poor vision in infancy, nystagmus, slowly responsive pupils and an undetectable ERG response. Cone-rod dystrophy (CRD) patients reported predominantly central visual

loss, with a relatively reduced cone response relative to rod responses. Conversely, rod-cone dystrophy (RCD) criteria included early onset of night blindness, peripheral visual loss and rod responses reduced more than cone responses on ERG. A group of patients emerged with undetectable ERGs, and where the history did not indicate the predominant cone or rod photoreceptor pathology at presentation. This group was diagnosed as EORD (or EOSRD), early onset severe retinal dystrophy.

Table 3.1.5 The number of patients for whom DNA samples were available for each diagnostic classification, and the number of sampled patients who were phenotyped in this study.

Diagnosis	**DNA Sample obtained**	**No of sampled patients who were phenotyped**
Rod-cone Dystrophy	22	15
Leber Congenital Amaurosis	72	56
Early-onset severe Retinal Dystrophy	39	27
Cone-Rod Dystrophy	24	19
Total	157	117

3.2 Clinical Ascertainment and Clinical Heterogeneity

The subsequent sections, 3.2.1 to 3.2.3, describes age of onset of reported symptoms.

3.2.1 Age of onset of poor vision

Table 3.2.1a Age of onset of poor vision in months (m)

	CRD	EORD	LCA	RCD
Number of patients	16	19	53	12
Minimum age (m)	0	0	0	0
25% Percentile	13.5	2	0	3
Median	66	36	2	36
75% Percentile	81	60	5	114
Maximum	132	200	18	204
Mean	54.75	38.89	3.057	61.25
Std. Deviation	39.73	47.48	3.354	64.11
Std. Error	9.933	10.89	0.4607	18.51

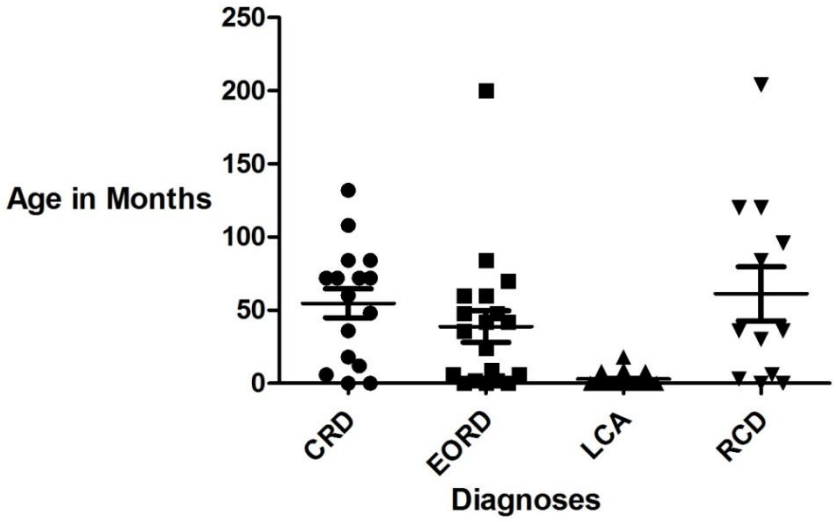

Figure 3.2.1 Vertical scatter plot showing distribution of age at onset of poor vision for each diagnosis. Long horizontal lines within scatter plots showing mean values and whiskers showing standard errors.

LCA patients' reported symptoms of visual loss usually less than 6 months afterbirth (via relatives or observations); (median age of 2 months). The non LCA patients (EORD, CRD and RCD patients) had a median range of onset of poor vision between 36 and 66 months.

The median age of onset of poor vision for all non LCA patient data combined was 44 months, which was significantly different from the LCA group (Table 3.2.1a, and Figure 3.2.1, $p<0.0001$ Mann-Whitney).

In the non LCA patients, central vision in the rod-cone dystrophies was more variable with four patients reporting poor central vision in the second decade. There was a difference between the LCA, CRD, RCD and EORD diagnoses in terms of the age of onset of poor vision reported (Kruskal-Wallis $p<0.0001$). However, this difference was only significant between LCA and the three other diagnoses, as shown below in the Dunn's Multiple Comparison Test (Table 3.2.1b).

Table 3.2.1b Dunn's multiple comparison test for age of onset of poor vision

Dunn's Multiple Comparison Test	P value
CRD vs EORD	P>0.05
CRD vs LCA	P<0.05
CRD vs RCD	P>0.05
EORD vs LCA	P<0.05
EORD vs RCD	P>0.05
LCA vs RCD	P<0.05

3.2.2 Age of onset of nyctalopia

This was reported as the age when navigational problems were noted in low mesopic or scotopic conditions or the age when they were unable to see stars at night.

Comparing the two broad diagnoses, LCA and EORD, the median onset of night blindness was 6 months vs 36 months (P<0.0001 Mann Whitney). Diagnosis specific analysis showed that there was a significant difference between the groups in age at onset of nyctalopia (Kruskal-Wallis p<0.0001). See Figure 3.2.2 and Tables 3.2.2a and 3.2.2b

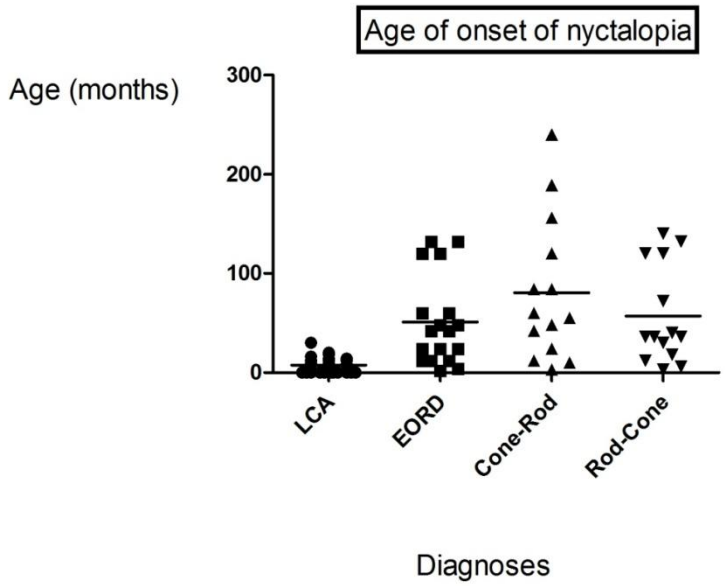

Figure 3.2.2 Vertical scatterplot showing distribution of age of onset (in months) of nyctalopia for each diagnosis. Mean values shown as horizontal lines.

Of the patients with no reported nyctalopia: 10 were diagnosed with CRD, 5 with EORD, 2 with RCD and none with an LCA diagnosis.

Diagnoses	LCA	EORD	CRD	RCD
Number of Patients	55	18	14	14
	Nyctalopia onset (Values in Months)			
Minimum	0	2	3	3
25% Percentile	4	12	21	16.5
Median	6	42	57.5	36
75% Percentile	12	75	129	120
Maximum	30	132	240	140

Table 3.2.2a Age of nyctalopia onset in months with summary statistics shown.

Mean	7.7	51.0	80.5	57.2
Std. Deviation	6.1	44.9	71.8	49.7
Std. Error	0.83	10.59	19.18	13.28

Dunn's Multiple Comparison Test	P value
LCA vs EORD	p<0.0001
LCA vs Cone-Rod	p<0.0001
LCA vs Rod-Cone	p<0.0001
EORD vs Cone-Rod	p>0.05
EORD vs Rod-Cone	p>0.05
Cone-Rod vs Rod-Cone	p>0.05

Table 3.2.2b Post test statistics; Dunn's multiple comparison test for age of onset of nyctalopia.

3.2.3 Age of onset of visual field loss

This symptomatic onset is difficult to verify for both parents and children. Not all parents of affected children were able to report, and patients could not always remember, when the peripheral field problems presented. However memories of peripheral clumsiness or knocking into objects within peripheral vision were recalled. There was a significant difference of age of onset between the overall LCA and combined EORD groupings ($p<0.0001$ Mann Whitney). There was also a significant difference in the median age of onset between the four diagnoses; LCA 9 months, RCD 24 month, EORD 42 months, CRD 84 months (Kruskal-Wallis $p<0.0001$), which were specifically significant between LCA vs EORD and LCA vs CRD, both $p<0.01$.

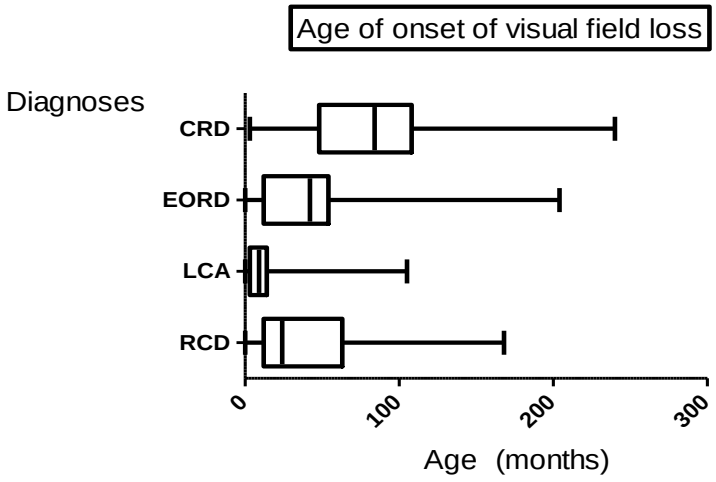

Figure 3.2.3 Horizontal box and whisker plot. The boxes shows inter-quartile range and the vertical lines within box are the median values for each diagnosis. The whiskers denote the range of age of onset of visual field loss for each diagnosis.

Table 3.2.3a Summary statistics of age of onset of visual field loss

	RCD	LCA	EORD	CRD
Number of patients	12	42	17	15
Minimum	0,0	0,0	0,0	3,000
25% Percentile	12,00	3,000	12,00	48,00
Median	24,00	9,000	42,00	84,00
75% Percentile	63,00	14,00	54,00	108,0
Maximum	168,0	105,0	204,0	240,0
Mean	44,00	14,64	52,88	91,27
Std. Deviation	51,06	21,47	61,79	72,86
Std. Error	14,74	3,312	14,99	18,81

Table 3.2.3b: Dunn's multiple comparison test for age of onset of visual field loss

Dunn's Multiple Comparison Test	Summary
RCD vs LCA	p>0.05
RCD vs EORD	p>0.05
RCD vs CRD	p>0.05
LCA vs EORD	P<0.01
LCA vs CRD	P<0.0001
EORD vs CRD	p>0.05

3.2.4 Associated symptoms

LCA was associated with a higher incidence of nystagmus, strabismus and oculodigital reflex than the other diagnoses, as expected. Ninety four percent of LCA patients reported nystagmus, which invariably started within the first months of life. Over two thirds of LCA patients had a form of strabismus, though no predominant pattern noted, and almost half of the LCA group exhibited eye rubbing. Over half the patients in all groups reported nyctalopia and approximately a third of the cohort reported photoaversion. Associated symptoms are summarised in Table 3.2.4.

Table 3.2.4 Associated symptoms reported by different diagnoses

Diagnosis	Nystagmus	Strabismus	Oculo-digital reflex	Nyctalopia	Photoaversion	Photoattraction
RCD	22%	21%	0%	70%	37%	16%
LCA	94%	70%	45%	54%	32%	47%
EORD	55%	25%	0%	62%	28%	51%
CRD	40%	52%	0%	53%	35%	10%

Examining the combined EORD group showed that the highest number of patients suffering from night blindness were those with a rod-cone dystrophy, 70% of whom reported being unable to see stars at night. Photoattraction, or light staring, was experienced by approximately a half of all patients with LCA and EORD. In contrast, light staring occurred in less than 20% in RCD and CRD. The presence of nystagmus correlated with low levels of vision (Figure 3.2.4). Visual acuities worse than 0.7 Log MAR consistently have a greater than 55% chance of being associated with nystagmus.

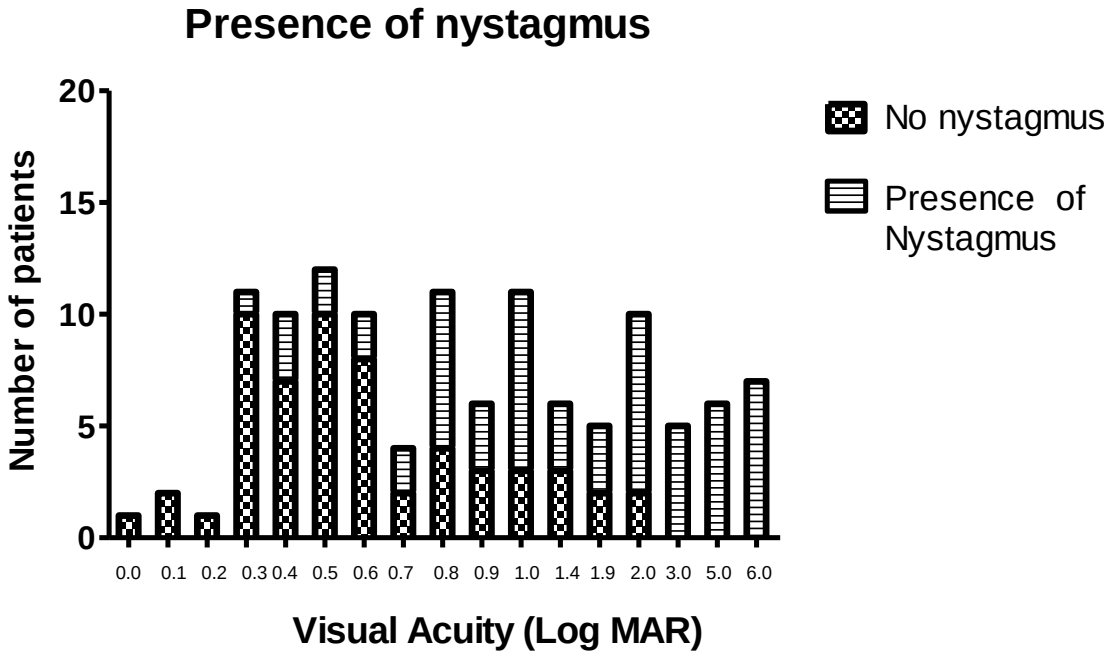

Figure 3.2.4 Bar chart showing increasing incidence of nystagmus with reducing visual acuity.

3.2.5 Visual acuity

The initial comparison of the best corrected visual acuities (VA) from the LCA and EORD subgroups revealed a significant difference with the LCA patients exhibiting worse VA than the EORD groups (Figure 3.2.5 and Table 3.2.5a , $P<0.0001$ Mann Whitney).

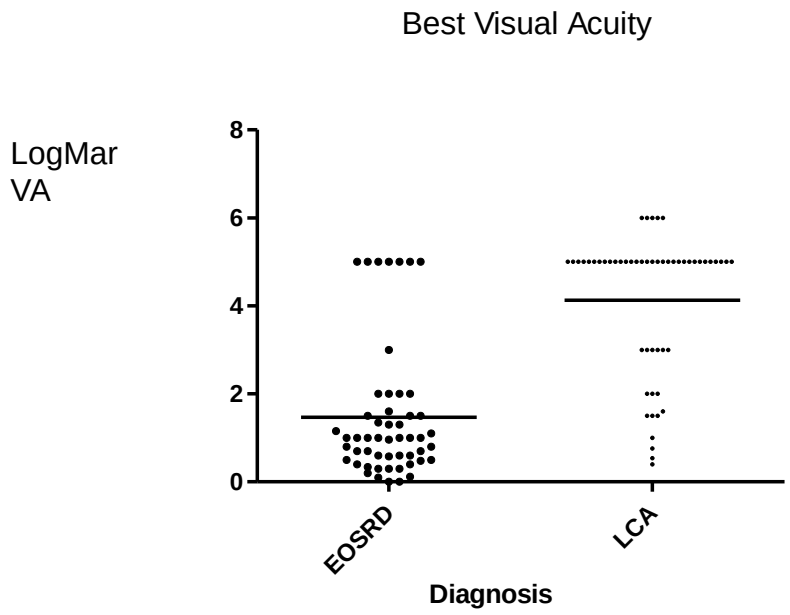

Figure 3.2.5 Best eye visual acuity comparison between LCA and EORD groups. Mean LogMar visual acuity shown as a horizontal line.

Table 3.2.5a Summary of Best Corrected Visual Acuity for each diagnostic subgroup

	CRD	EORD	LCA	RCD
Number of patients	17	20	54	15
Minimum (LogMAR VA)	0,4	0,1	0,4	0,0
25% Percentile	0,70	0,42	3,	0,3
Median (LogMAR VA)	1,0	1,0	5,0	0,70
75% Percentile	1,75	2,75	5,00	1,30
Maximum (LogMAR VA)	5,00	5,00	6,00	5,00
Mean (LogMAR VA)	1,52	1,78	4,03	0,99
Std. Deviation	1,39	1,81	1,53	1,21
Std. Error	0,37	0,40	0,21	0,31

Table 3.2.5b Dunn's multiple comparison test for Best Corrected Visual Acuity (BCVA).

Dunn's Multiple Comparison Test BCVA	Summary
CRD vs EORD	P>0.05
CRD vs LCA	P<0.0001
CRD vs RCD	P>0.05
EORD vs LCA	P<0.0001
EORD vs RCD	P>0.05
LCA vs RCD	P<0.0001

The best corrected visual acuity (BCVA) from either eye was taken and compared between the four subgroups, which demonstrated a significant difference (Table 3.2.5b, Kruskal-Wallis $p<0.0001$). The best visual acuity was observed in the RCD group, median LogMAR 0.7. As shown in Table 3.2.5b, there were significant differences between the LCA cohort and other groups. No significant differences occurred between CRD, EORD and RCD groups. LCA patients had an average visual acuity of 3.4 LogMAR within the first decade approximating hand movements vision. In the second decade, visual acuity was minimally worse at 3.7 LogMAR. After the third decade, the acuities were 4.2 LogMAR on average. However, longitudinal data taken from the patient records of 28 patients with greater than 18 month follow up showed that patients experienced visual deterioration (10 patients), stable vision (10 patients) and slight visual improvement (8 patients).

3.2.6 Refractive error

The spherical equivalent refractive error was calculated by adding the spherical dioptric value to half the cylindrical refractive error. A mean value from the two eyes was calculated (Table 3.2.6a).

Table 3.2.6a Summary of average spherical equivalent refractive error in the four disease subgroups with t test for emmetropia

	Average Spherical equivalent (D) Cone-Rod	Average Spherical equivalent (D) EORD	Average Spherical equivalent (D) LCA	Average Spherical equivalent (D) RCD
Number of patients	17	20	54	13
Percentage of total patients	89%	75%	96%	87%
Minimum	-12,50	-12,50	-7,500	-7,000
25% Percentile	-2,310	-4,720	-0,5600	-0,9400
Median	0,0	-1,180	3,000	0,0600
75% Percentile	1,625	0,0	6,955	3,130
Maximum	6,500	9,500	10,75	4,250
Mean	-0,7571	-1,934	2,879	0,4085
Std. Deviation	3,895	4,570	4,760	2,959
Std. Error	0,9447	1,022	0,6478	0,8206
Lower 95% CI of mean	-2,760	-4,072	1,579	-1,379
Upper 95% CI of mean	1,246	0,2054	4,178	2,196
P value (two tailed)	0,4346	0,0738	< 0.0001	0,6277

LCA patients had a mean refractive error of +2.8D whilst the most myopic group were the EORD patients with a mean of -1.9D. There was significant difference in the spherical refractive error of LCA patients compared to all the other EORD subgroups (Table 3.2.6a and Figure 3.2.6). Furthermore, there was a significant degree of refractive error in the LCA patient group (t test $p<0.0001$) when compared to a hypothetical mean of emmetropia (Table 3.2.6a).

Table 3.2.6b Dunn's multiple comparison test for difference in spherical equivalent refraction between diagnostic groups

Dunn's Multiple Comparison Test	P value
Cone-Rod vs EORD	p>0.05
Cone-Rod vs LCA	p>0.05
Cone-Rod vs Rod-Cone	p>0.05
EORD vs LCA	p<0.05
EORD vs Rod-Cone	p>0.05
LCA vs Rod-Cone	p>0.05

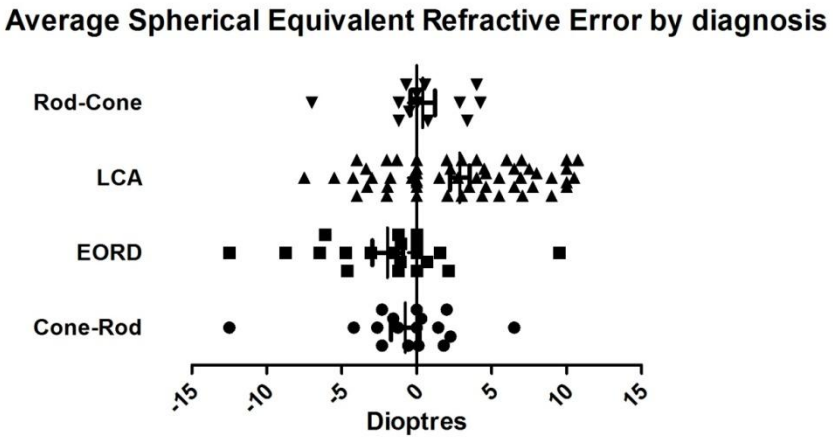

Figure 3.2.6 Horizontal scatter plot of refractive error by diagnosis. Mean values shown as long vertical lines within each of the scattered plots. The shorter vertical lines at the end of the whiskers denote the standard errors of the mean values.

3.2.7 Colour vision

There was no significant colour axis defect in any of the four subgroups of EORD. 95% of LCA patients, 54% of cone-rod dystrophy, 35% of rod cone dystrophy and 20% of early onset dystrophy patients failed the HRR test completely (Table 3.2.7). Conversely normal colour vision was not observed in LCA patients but occurred in 10% of cone-rod patients, 22% of rod cone and 38% of early onset retinal dystrophy patients. Results recorded during phenotyping are noted in Table 3.2.7. There was no statistical significance between protan, deutan and tritan and therefore the data has been simplified to show colour axis defects by diagnosis.

Table 3.2.7: Summary of ability to see colour by diagnostic subtype

	CRD	EORD	LCA	RCD
No colour vision	54%	20%	95%	35%
Strong	10%	4%	3%	12%
Medium	6%	12%	2%	33%
Weak	7%	26%	0%	14%
Normal colour vision	10%	38%	0%	22%

3.2.8 Visual fields

A normal healthy visual field size is a theoretical norm of >15000 square degrees, using the V4e isopter. The mean visual field areas recorded for each group were, from smallest to largest field sizes: 3200 sq. degrees (8 EORD patients), 3660 sq. degrees (21 LCA patients), 7994 sq. degrees (11 RCD patients), 8415 sq. degrees (16 CRD patients).

Mean visual field size using the V4e isopter revealed differences between the subgroups (Table 3.2.8a and Table 3.2.8b and Figure 3.2.8). Each group was also compared to the theoretical norm of >15000 square degrees and was found to be significantly different ($p<0.05$). Analysis of Variance (Kruskal-Wallis) indicated that a significant difference in median visual field size across the diagnoses was detected (Table 3.2.8b, $p=0.0002$). Specifically, there were significant differences between LCA and CRD, and LCA and RCD ($p<0.05$). This significant difference was also noted between EORD and CRD. As expected, all comparisons between left and right eyes were insignificant in inter- and intra-subgroup analysis.

Table 3.2.8a Summary of visual fields, measured in square degrees, between the four diagnostic groups

	LCA	EORD	Cone-Rod	Rod-Cne
Number of patients	21	8	16	11
Percentage of total patients per subgroup	38%	30%	84%	73%
Minimum (sq. degrees)	177,0	187,0	2889	3567
25% Percentile (sq. degrees)	294,5	680,0	6666	4005
Median (sq. degrees)	3200	2084	8387	8776
75% Percentile (sq. degrees)	6470	6419	10873	10010
Maximum (sq. degrees)	10012	7300	13056	14756
Mean (sq. degrees)	3660	3200	8415	7994
Std. Deviation	3236	3000	2949	3473
Std. Error	706,0	1061	737,4	1047

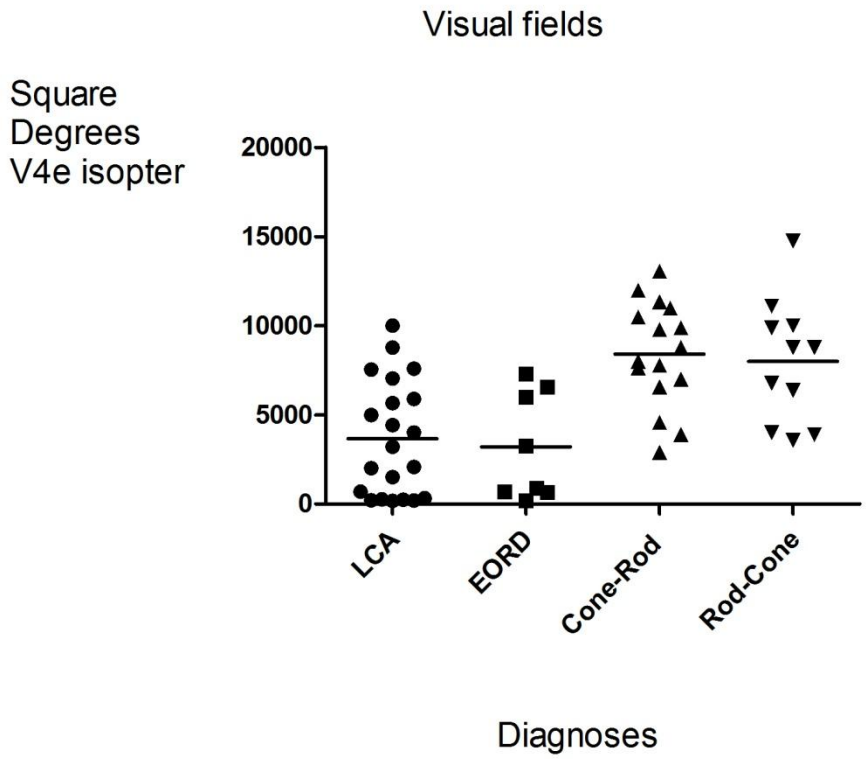

Figure 3.2.8 Mean visual fields measured by planimetry with a V4e isopter for different diagnoses.

Visual field reduced with age in all groups. This was calculated as the mean reduction in square degrees per decade within the V4e isopter for each diagnosis, (Table 3.2.8c).

Table 3.2.8b Showing Dunn's multiple comparison test for statistically significant difference in size of visual fields between diagnoses.

Dunn's Multiple Comparison Test	P value
LCA vs EORD	$p > 0.05$
LCA vs Cone-Rod	$p < 0.05$
LCA vs Rod-Cone	$p < 0.05$
EORD vs Cone-Rod	$p < 0.05$
EORD vs Rod-Cone	$p > 0.05$
Cone-Rod vs Rod-Cone	$p > 0.05$

Table 3.2.8c Visual field reduction per decade by diagnosis

Diagnosis	**Reduction in visual field per decade (square degrees)**
LCA	1111
EORD	2650
CRD	1522
RCD	207

3.2.9 Axial length

Axial length was measured by using the IOL Master. The axial lengths of the four subgroups were not significantly different ($p>0.05$ in Dunn's post test intergroup analysis). The EORD patients had the longest axial length and the LCA group had the shortest axial length (Table 3.2.9 and Figure 3.2.9).

Table 3.2.9 Summary of statistics for axial length by diagnosis

	OD CRD	OS CRD	OD EORD	OS EORD	OD LCA	OS LCA	OD RCD	OS RCD
Number of eyes measured (OD or OS)	11	11	11	11	12	12	9	9
Minimum	21,27	21,00	20,27	19,66	19,27	19,27	20,00	20,00
25% Percentile	21,65	21,86	21,73	21,30	19,70	19,70	20,60	20,60
Median	22,10	22,20	23,06	22,69	20,54	20,50	22,28	22,28
75% Percentile	22,78	22,87	23,66	23,44	24,42	24,39	23,58	23,58
Maximum	24,14	24,28	26,94	28,51	25,22	25,22	24,46	24,46
Mean	22,32	22,37	22,82	22,73	21,68	21,71	22,15	22,15
Std. Deviation	0,9641	0,9212	1,803	2,341	2,394	2,406	1,566	1,566
Std. Error	0,2907	0,2778	0,5436	0,7059	0,6909	0,6946	0,5219	0,5219

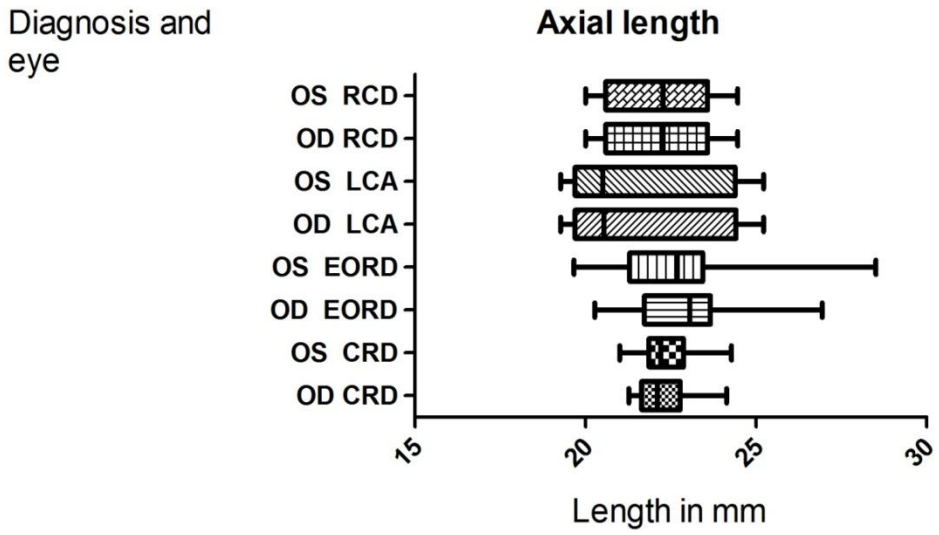

Figure 3.2.9 Box and whisker plot of axial length by diagnosis. The boxes show the interquartile range with median value shown as a vertical line within each box. Whiskers show range (minima to maxima values) of axial lengths (mm) for each diagnosis and each eye.

3.2.10 OCT foveal thickness

Analysis of variance indicated that there was a significant difference in the median OCT thicknesses between the diagnoses (Kruskal-Wallis p=0.007), measured using Stratus OCT-3 (Table 3.2.10, Figure 3.2.10). However, the only significant difference found was between CRD right eyes and LCA right eyes (Dunn's post test $p<0.05$). The LCA patients showed the widest variance and highest mean. Six of these thirteen LCA patients (with a median age of 8 years, range 5-15 years) had CRB1 mutation genotypes. The other seven LCA patients investigated with OCT imaging had unknown genotypes. This majority of CRB1 patients in the (OCT investigated) LCA subgroup are therefore consistent with a known CRB1 mutation associated phenotype of thickened retina and intraretinal cysts in children and adolescents.[294]

Table 3.2.10 Summary of foveal thickness measured by OCT across diagnostic groups and by eye

	CRD OD	CRD OS	EORD OD	EORD OS	LCA OD	LCA OS	RCD OD	RCD OS
Number of patients' eye	11	11	9	9	13	13	10	10
Minimum	104,0	110,0	142,0	140,0	102,0	115,0	133,0	155,0
25% Percentile	131,0	121,0	153,0	152,5	175,0	156,0	159,3	164,8
Median	144,0	153,0	168,0	162,0	212,0	203,0	173,5	180,0
75% Percentile	180,0	184,0	199,0	199,0	314,0	277,5	211,0	215,5
Maximum	227,0	200,0	225,0	228,0	673,0	845,0	378,0	326,0
Mean	152,7	152,8	175,4	174,6	257,4	256,4	196,5	199,2
Std. Deviation	36,76	30,97	27,45	30,34	144,3	188,4	68,95	51,18
Std. Error	11,08	9,337	9,149	10,11	40,01	52,24	21,81	16,18

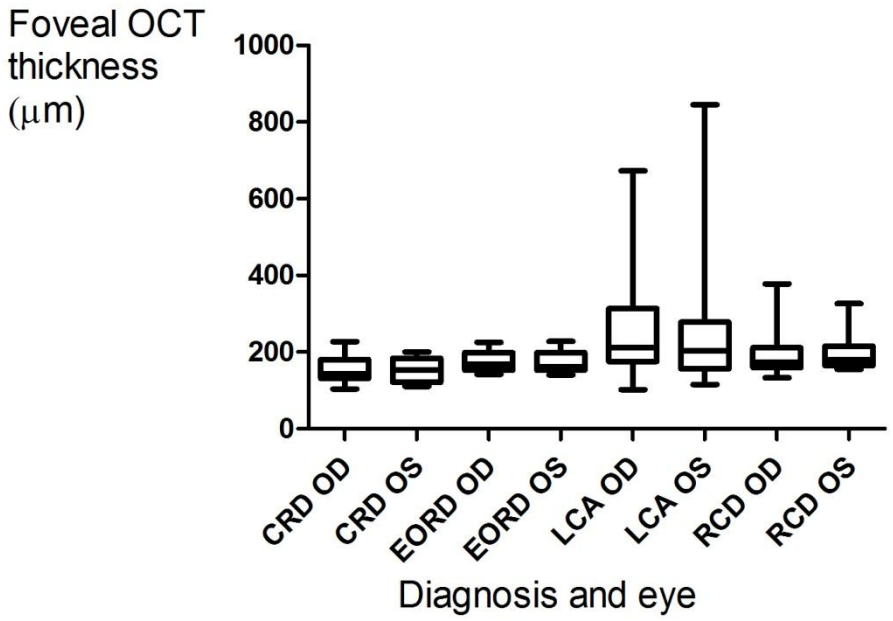

Figure 3.2.10 Vertical box and whisker plot of OCT foveal thickness for each diagnosis with each eye (OD/OS) shown. The boxes show the interquartile range , with lines within boxes showing median values. Vertical whiskers denoting range, from minimal to maximal values.

3.2.11 Funduscopy analysis

Funduscopy data collected included: peripheral pigment migration, macular pigment, the presence of white dots, RPE atrophy and macular atrophy (Table 3.2.11). There were 6 LCA (11%) patients and 5 EORD patients (25%) with no fundal changes evident. Chi-squared testing of each fundal sign did not reveal a significant difference between the diagnoses (data not shown). The fundal phenotypic range of LCA patients ranged from a normal retinal appearance, to mild retinal vessel attenuation, a pseudopapilloedema, and maculopathy with subsequent macular atrophy (or non-developmental/ degenerational

"macular coloboma") in later disease. Bone spicule pigment migration, nummular pigmentation, yellow confluent peripheral spots, white focal lesions at RPE and outer retina levels were also observed. Autofluorescence patterns were variable and could be absent. A hyperfluorescent parafoveal ring was noted in some patients. RPE atrophy and mottling on fundal examination were often consistent with hypofluorescence.

Table 3.2.11 Fundal signs by diagnoses

	Peripheral pigment	White dots	RPE atrophy	Macular atrophy	Macular pigment
LCA (n=54)	55.5%	24.1%	25.9%	44.4%	27.8
CRD (n=21)	33.3%	14.3%	23.8%	28.6%	28.6%
RCD (n=13)	76.9%	7.7%	23.1%	46.1%	38.5%
EORD (n=20)	55%	30%	40%	50%	45%

Rod-cone dystrophy patients had the widest phenotypic spectrum including preserved para-arteriolar RPE (PPRPE) and mid-peripheral RPE mottling and pigment migration. Cone-rod patients had more frequently observed macular pathology, as expected, but the heterogeneity in this group, similar to RCD, EORD and LCA, extended to involve the above described fundal features including generalised rod and cone system dysfunction.

3.3 Using the LCA APEX chip to identify pathogenic mutations

DNA samples from 158 patients were sent to Asper Ophthalmics for LCA chip analysis. Of this group, 22 patients had been phenotyped by a previous research fellow, Dr RH

Henderson and were not therefore included in the preceding phenotypic data section. Direct sequencing of *CEP290* was performed in all patients with one *CEP290* allele identified by the LCA APEX chip.

3.3.1 LCA APEX chip results

A total of 292 patient DNA samples were available at UCL IoO and sent to Asper Biotech, Estonia for LCA APEX chip analysis. During this project 158 patients (158/292) were genotyped by this method (see section 3.1.1). Of this group of 158 patients, there were 66 females and 92 males. Fifty four patients had a diagnosis of LCA whilst the remaining 104 patients had a diagnosis of either early onset rod-cone (combined with the EORD subgroup) or cone-rod dystrophies. Disease associated variants were identified in 49 individuals (31%). Homozygous or compound heterozygous mutations were found in 20 (13%); a further 29 patients (18%) had single mutations. These data are summarised in Table 3.3.1.

Table 3.3.1. Summary of pathogenic mutations identified using the LCA APEX chip

Gene	Number of patients	Single mutation	Two mutations
AIPL1	8	4	4
CEP290	15	8	7
CRB1	10	8	2
GUCY2D	1	1	0
RDH12	7	1	6
RPE65	1	1	0
RPGRIP1	6	5	1
MERTK	1	1	0

LRAT, TULP1, LCA5, *CRX*	No patients	No mutations	No mutations

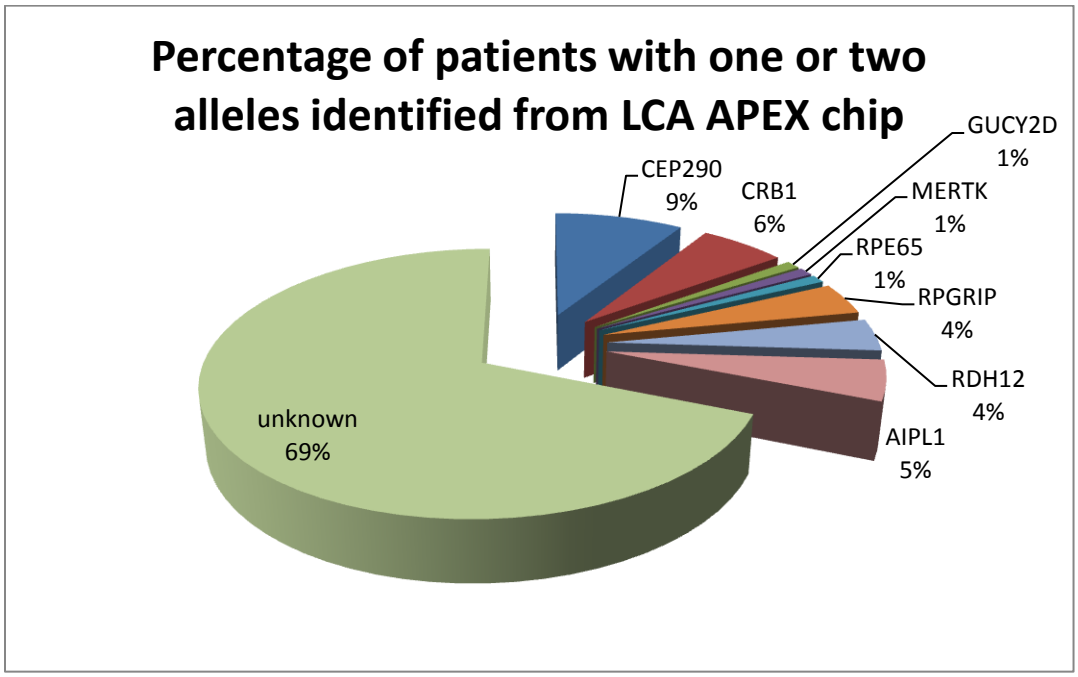

Figure 3.3.1(a): Pie chart showing genotypes, as percentage of cohort (n=158), for either single or both alleles identified by LCA chip

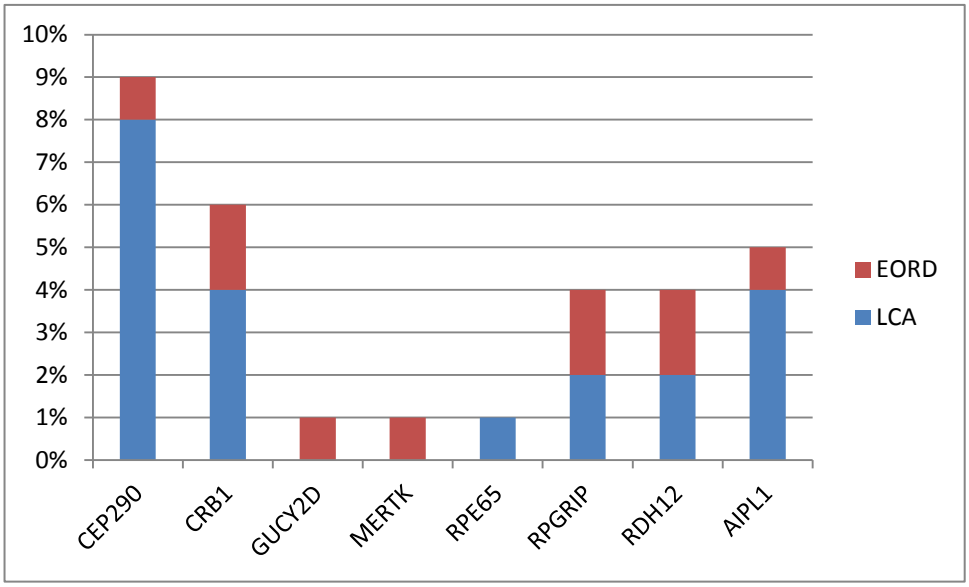

Figure 3.3.1(b) Bar chart showing genotypes and diagnoses, as percentage of cohort (n=158), for either single or both alleles identified by LCA chip

The LCA APEX chip identified 63% (34/54) of the LCA group and 13% (15/104) of the EORD group with at least one mutated allele.

Certain common allelic variants were identified, but were labelled as 'disease associated' by Asper Ophthalmics. However, our analysis showed that some of these 'disease associated' variants were not pathological. These variants are found in normal, healthy populations (dbSNP and other public databases of genetic variants in the population) without EORD and LCA or any other ocular pathology. For example, two *GUCY2D* variants, P701S (9/158 patients positive for this variant on the LCA APEX chip) and W21R (on previous LCA chip versions), are known polymorphisms. [64;279;295] Such variants are termed SNPs (single nucleotide polymorphisms) that occur in normal individuals and therefore are not considered a mutation associated with disease in either the homozygous or compound heterozygous state. SNPs are DNA variants that have withstood evolutionary, natural selection pressures to recur in a significant proportion of the population of a species. The following known SNPs arose in the patient cohort and were discounted from mutation analyses (and these variants were deemed pathogenic by Asper Ophthalmics):

SNP (V66I) in CRX (2/158 patients)

SNP (A132T) in RPE65(2/158 patients)

SNP (A434V) in RPE65 (1/158 patients)

SNP (N321K) in RPE65 (1/158 patients)

SNP (P701S) in GUCY2D (9/158 patients)

SNP (R161Q) in RDH12 (1/158 patients)

3.3.2 LCA APEX chip reliability

Of the 137,704 allele calls made, there were 4,682 uni-directional call failures (3.4%) and 895 bi-directional call failures (0.64%). Call failures occurred when the chip did not detect a signal for a particular allele. Unidirectional failure describes one strand being missed during a chip attempt to genotype an allele, whilst bidirectional means that neither forward nor reverse strand was detected. Bi-directional failures represent a lack of any information at the allele or SNP under chip investigation.The common bi-directional and unidirectional call failures are shown in Table 3.3.2a and Table 3.3.2b:

Table 3.3.2a Common unidirectional call failures from the LCA APEX chip data

Gene	Exon	Nucleotide	Protein	Number call fails	Percent of total 316 calls
CRB1	Ex12	4121_4130del	A1374_G1377delfs	32	10.1%
GUCY2D	IVS9+2	1956+2T>A	SPLICE	33	10.4%
RPE65	13	1418T>A	V473N	56	17.7%
GUCY2D	13	2515A>G	T883A	56	17.7

Table 3.3.2b Common bi-directional call failures from the LCA APEX chip data

Gene	Exon	Nucleotide	Protein	Number call fails	Percent of total 158 subjects
CRB1	5	1148G>A	C383Y	7	4.4%
CRB1	5	1084C>T	Q362X	8	5.1%
RPGRIP1	3	256C>T	R86W	13	8.3%
GUCY2D	4	3236_3237 insACCA	H1079Pinsfs	8	5.1%

All *CEP290* and *RDH12* mutations found on the LCA APEX chip were then directly sequenced to confirm the result, as described in the following sections.

3.4 *RDH12* mutations

The author (PM) sent 158 patients' samples for DNA analysis by the Asper LCA APEX chip. This cohort of 158 patients included the 117 patients phenotyped by author, PM. In August 2008 (project completion date by author), a total of 292 patients, including these 158 patients, had been analysed by the Asper LCA APEX chip. The total 292 DNA samples in the LCA/EORD patient cohort included DNA samples being sent by a previous researcher, Mr R Henderson, during 2004-2006.

Of the 158 DNA samples collected from author's LCA/EORD cohort, *RDH12* mutations were identified in 25 individuals from 22 families. Eight patients were identified using the Asper LCA APEX chip, with at least one mutation in *RDH12*. Direct DNA sequencing (see Methods 2.3.3) confirmed these changes and identified a second *RDH12* mutation in all of them, five of which are novel (see Table 3.4a and 3.4b). Autozygosity

mapping by Donna Mackay, and subsequent direct sequencing of *RDH12* by author, identified three more families with novel homozygous mutations (families 9, 10 and 12). Direct sequencing identified eleven more patients with mutations in *RDH12*, including six novel mutations. Only one coding SNP was identified, rs17852293 (c.482G>A, p.R161Q), located in exon 5.

RDH12 mutation electropherograms

A novel missesnse mutation, c.601 T>C, p.C201R**,** was found in the homozygous state in exon 5 in four unrelated families (Figure 3.4a).

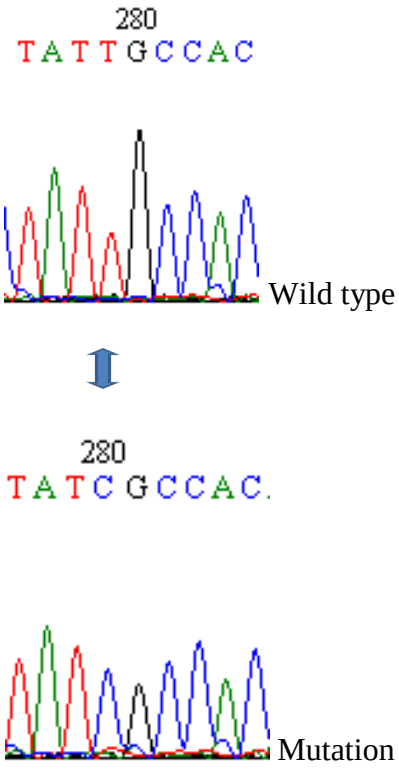

Figure 3.4a Electropherogram of *RDH12* showing a novel homozygous missense mutation, c.601T>C, p.C201R. Top electropherogram is wild type sequence from a control DNA and bottom electropherogram shows patient sequence. This mutation was found in Families 2,15,17 and 21.

A novel missense mutation, c.146C>A , p.T49K, was found in a homozygous state in exon 2 in 2 unrelated families (Figure 3.4b).

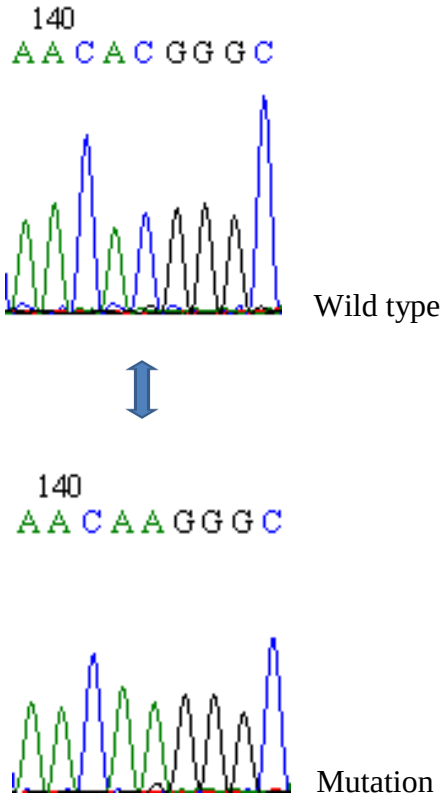

Figure 3.4b Electropherogram of *RDH12* showing a homozygous missense mutation, c.146C>A , p.T49K in *RDH12*. Bottom electropherogram shows patient sequence (family 13) and top is wild type sequence from a control DNA. This mutation was found in Families 13 and 18 (c.146C>T , p.T49M).

A previously reported nonsense mutation, c.193C>T, p.R65X,[129] was found in a homozygous state in exon 2 in one family (Figure 3.4c).

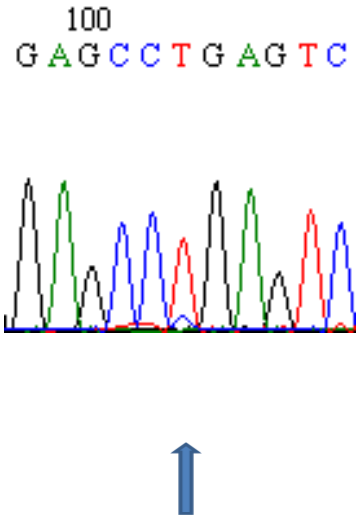

Figure 3.4c Electropherogram of *RDH12* showing a homozygous nonsense mutation, c.193C>T, p.R65X in *RDH12*. Arrow on patient sequence shows position of the mutation.

In two families (Family 8 and 16) a novel homozygous missense mutation was identified in exon 5, c.506G>A, p.R169Q (Figure 3.4d).

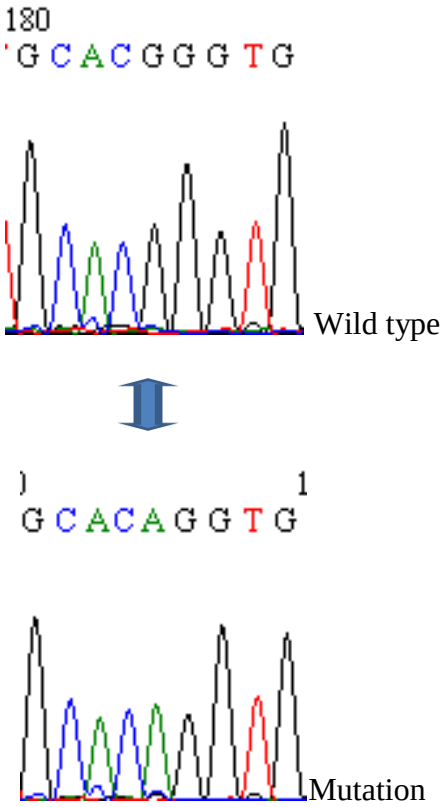

Figure 3.4d Electropherogram of *RDH12* showing a homozygous missense mutation, c.506G>A, p.R169Q. Top electropherogram is wild type sequence from a control DNA and bottom shows patient sequence.

In Family 19, a novel missense mutation was identified in exon 5, c.609C>A, p.S203R (Figure 3.4e).

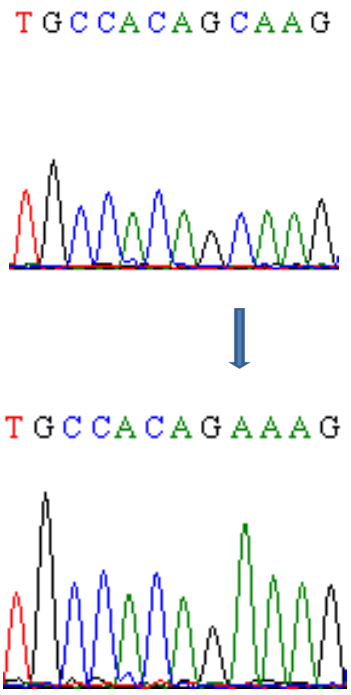

Figure 3.4e Electropherogram of *RDH12* showing a homozygous missense mutation, c.609C>A, p.S203R. Top electropherogram is wild type sequence from a control DNA and bottom shows patient sequence.

In Family 20, a previously reported homozygous nonsense mutation was identified c.379G>T, p.G127X [129](Figure 3.4f).

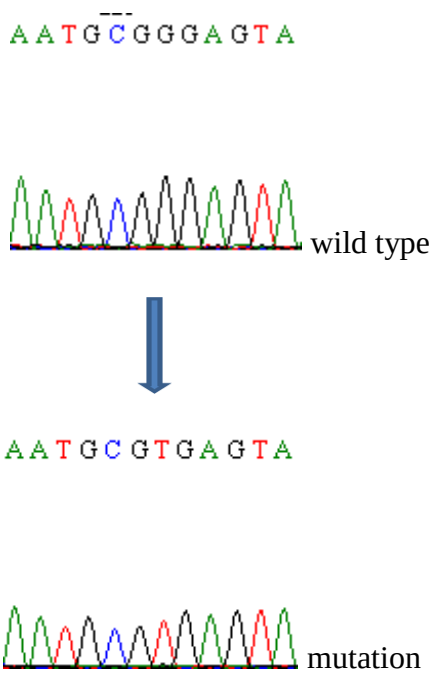

Figure 3.4f. Electropherogram of *RDH12* showing a previously reported homozygous nonsense mutation, c.379G>T, p.G127X.[129] Top electropherogram is wild type sequence from a control DNA and bottom shows patient sequence.

Eight of 22 mutations identified in this study were located in exon 5. All 13 novel mutations were absent in 100 ECACC control DNA samples or in 50 Asian control DNA samples. Where DNA samples from parents and unaffected siblings were available, in four families involving 9 parents and 11 siblings, further analysis demonstrated that the disease segregated with the mutations (data not shown). Analysis of all identified missense mutations using *in silico* methods (methods section 2.3.7) are shown in Table 3.4a. All three programmes identified the p.R169Q, p.R169W, p.Y200C, and p.R239W mutations as being intolerant or damaging to the protein (Table 3.4a). For all of the missense mutations, at least one of the programs considered the protein change to be significant.

In total, 21 different alleles in 22 families from various ethnic origins were identified (Table 3.4b). Eleven families were consanguineous (families 2, 7, 8, 14, 12, 10, 11, 15, 16, 17, 19, 21) and they harboured homozygous mutations. Two other families also had homozygous mutations, even though they did not report consanguinity (families 13 and 20). The most common mutation identified was p.C201R (8/44 alleles, 18%). Overall, missense mutations were the most prevalent mutation identified, affecting 35/44 alleles 80%). Nonsense mutations accounted for 4/44 (9%), and frameshift mutations affected 5/44 alleles (11%). Only one SNP was identified, rs17852293, as described previously.

		SIFT		Polyphen-2		pMUT		
Mutation	**Exon**	**Predict-ion**	**Toler-ance index**	**Predict-ion**	**Var score**	**NN output**	**Reli-ability**	**Predict-ion**
p.T49M	**2**	Intolerant	0	PRD	0.951	0.4152	1	Neutral
p.T49K*	**2**	Intolerant	0.01	POS	0.888	0.6188	2	PATH
p.R65X	**3**	Intolerant	0	PRD	0.996	0.9117	7	PATH
p.R84X*	**3**	NA	NA	NA	NA	NA	NA	NA
p.L99I	**3**	Intolerant	0	PRD	0.991	0.1072	7	Neutral
p.R106X*	**3**	NA	NA	NA	NA	NA	NA	NA
p.G127X	**4**	NA	NA	NA	NA	NA	NA	NA
p.H151D	**5**	Intolerant	0.01	PRD	0.992	0.3323	3	Neutral
p.F152I*	**5**	Intolerant	0	PRD	0.968	0.2127	5	Neutral
p.R161Q	**5**	Tolerant	0.38	Benign	0.018	0.513	0	PATH
p.R169Q*	**5**	Intolerant	0	PRD	0.997	0.5161	0	PATH
p.R169W*	**5**	Intolerant	0	PRD	0.999	0.8159	6	PATH
p.S175L	**5**	Intolerant	0	PRD	0.997	0.2495	5	Neutral
p.Y200C*	**5**	Intolerant	0	PRD	0.998	0.5467	0	PATH
p.C201R	**5**	Tolerant	0.1	POS	0.769	0.5209	0	PATH
p.S203R*	**5**	Intolerant	0	PRD	0.998	0.3381	3	Neutral
p.N207D*	**5**	Intolerant	0.01	PRD	0.994	0.1661	6	Neutral
p.V233L*	**6**	Intolerant	0.02	PRD	0.931	0.1899	6	Neutral
p.R239W	6	Intolerant	0	PRD	0.998	0.9122	8	PATH
p.A269AfsX1	6	NA	NA	NA	NA	NA	NA	NA
p.R295X	7	NA	NA	NA	NA	NA	NA	NA

Table 3.4a *In silico* analysis of RDH12 mutations

Changes highlighted by an asterisk are novel missense mutations identified in this study. SIFT results are reported to be tolerant if tolerance index ≥0.05 or intolerant if tolerance index <0.05.

Polyphen-2 appraises mutations qualitatively as Benign, Possibly Damaging (POS) or Probably damaging (PRD) based on the model's false positive rate.

pMUT is based on the use of different kinds of sequence information to label mutations, and neural networks to process this information NN=neural network values from zero to one. >0.5 is predicted as a disease associated mutation. Reliability=values 0–9. >5 is the best prediction. (PATH = pathological prediction on pMUT analysis)

SIFT and Polyphen2 do not provide prediction scores for stop-gain (a mutation that changes an AA codon to a stop codon) or stop-loss (a mutation that changes a stop codon to an AA codon. For stop codons it is assumed that these mutations will result in truncated proteins and therefore have altered or no function. Also, any stop codons upstream of the last exon usually results in nonsense mediated decay of the transcript so it is expected to result in a loss of signal/message.

Table 3.4b Summary of *RDH12* mutations identified

CH = compound heterozygous, Hom = homozygous

Family	Method of identification	Diagnosis	Ethnic origin British Caucasian	Consanguineous	Mutation Type CH or Hom	Mutation	Reference
1	Asper LCA APEX chip	EORD	British Caucasian	No	CH	c.295C>A, p.L99I* c.883C>T, p.R295X*	(**Ref 109**)
2	Asper LCA APEX chip	LCA	Gujurati Muslim	Yes	Hom	c.601T>C, p.C201R*	(**Ref 110**)
3	Asper LCA APEX chip	EORD	British Caucasian	No	CH	c.715C>T, p.R239W c.806_810del 5bp, p.A269fsX1*	(**Ref 31 , 109**)
4	Asper LCA APEX chip	EORD	British Caucasian	No	CH	c.700G>C, p.V233L c.806_810del 5bp, p.A269fsX1*	Novel to this study (**Ref 31**)
5	Asper LCA APEX chip	EORD	British Caucasian	No	CH	c.316 C>T, p.R106X c.806_810del 5bp, p.A269fsX1*	Novel to this study (**Ref 31**)
6	Asper LCA APEX chip	LCA	unknown	No	CH	c.451C>G, p.H151D c.806_810del 5bp, p.A269fsX1*	(**Refs 31 ; 109**)
7	Direct Sequencing	EORD	Indian	Yes	Hom	c.609C>A, p.S203R	Novel to this study
8	Direct Sequencing	LCA	Pakistani	Yes	Hom	c.506G>A, p.R169Q	Novel to this study

9	Affymetrix	EORD	Indian	No	CH	c.250C>T, p.R84X c.381_delA, p.G127fsX1	Novel to this study Novel to this study
10	Affymetrix	EORD	Irish Caucasian	Yes	Hom	c.454T>A, p.F152I	Novel to this study
11	Direct Sequencing	EORD	unknown	Yes	Hom	c.619A>G , p.N207D	Novel to this study
12	Affymetrix	LCA	Kurdistani Iraqi	Yes	Hom	c.599A>G, p.Y200C	Novel to this study
13	Asper LCA APEX chip	LCA	unknown - prob British caucasian	No	Hom	c.146C>A, p.T49K	Novel to this study
14	Asper LCA APEX chip	EORD	Bangladeshi	Yes	Hom	c.193C>T, p.R65X	**(Ref 111)**
15	Direct Sequencing	EORD	unknown	Yes	Hom	c.601T>C, p.C201R	**(Ref 110)**
16	Direct Sequencing	EORD	Pakistani	Yes	Hom	c.506G>A, p.R169Q	Novel to this study
17	Direct Sequencing	LCA	Gujurati Muslim	Yes	Hom	c.601T>C, p.C201R	**(Ref 110)**
18	Direct Sequencing	LCA	Indian	Unknown	Hom	c.146C>T, p.T49M	(**Ref 31**)
19	Direct Sequencing	LCA	Saudi Arabian	Yes	Hom	c.609C>A, p.S203R	Novel to this study
20	Direct Sequencing	LCA	Kurdistani Iraqi	No	Hom	c.379G>T, p.G127X	**(Ref 111)**
21	Direct Sequencing	EORD	Indian	Yes	Hom	c.601T>C, p.C201R	**(Ref 110)**

22	Direct Sequencing	LCA	British Caucasian	No	CH	c.505C>T, p.R169W c.525C>T, p.S175L	Novel to this study **(Ref 236)**

3.5.1 Clinical phenotype

Clinical features of the 25 patients with confirmed *RDH12* mutations are detailed in Table 3.5.1. Twenty patients (80%) presented with reduced vision. Nyctalopia (6/25) and visual field constriction (5/25) were predominant features. Twenty two patients reported loss of vision that was slowly progressive by age five years and by project defined diagnoses, in section 3.1.5, deemed EORD. Interestingly, 11 patients reported that their vision dramatically deteriorated further and were able to specify the age at which this had occurred, a median age of 26 years. Fundus examination in adults and older children revealed dense intraretinal pigment migration throughout the retina that typically approached the macula from the equator in a concentric manner, with severe RPE atrophy and arteriolar attenuation (Figure 3.5.1b; images A, B and D). The pigmentation showed para-arteriolar sparing in five patients (Figure 3.5.1b; image C). In the younger patients (6/25, age range 5–18 years), widespread RPE atrophy was the predominant feature, with pigment migration, when present, being confined to the retinal periphery (Figure 3.5.1b; image C). Macular atrophy was present in all cases and was associated with striking yellow deposits in 15 patients (60%) (see Figure 3.5.1b; image D).

AF imaging in 10 of 13 patients failed to detect any macular AF, corresponding to the severe macular atrophy. The youngest patients to undergo AF imaging had overall reduced levels of macular AF but also had a hyperautofluorescent signal at the fovea (families 6, and 22; age range of 5–11 years), (see Figure 3.5.1b; image E).

Ten of 13 patients underwent either SD-OCT (7/13) imaging, which showed marked macular thinning (see Figure 3.5.1b; image F). The respective average adult foveal thicknesses observed with SD-OCT was 56 μm (normal adult mean value: 228 μm). In the adults who underwent SD-OCT imaging, there was marked macular excavation, severe retinal thinning, and loss of the laminar architecture (4/5 patients). OCT imaging of the three youngest patients, in whom the macula was better preserved on funduscopy, demonstrated a foveal thickness of 160 μm (TD-OCT, family 6) and 114 μm (SD-OCT, family 17), with some preservation of the laminar architecture.

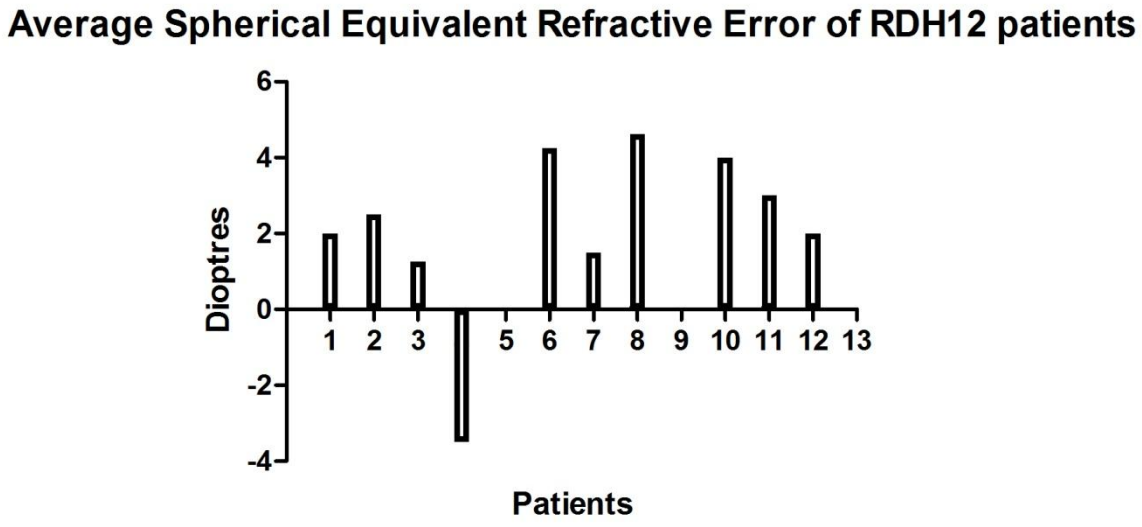

Figure 3.5.1a Each patient with RDH12 mutations, and their spherical equivalent refractive powers (Dioptres). Each patient's refractive error is represented by a single bar.

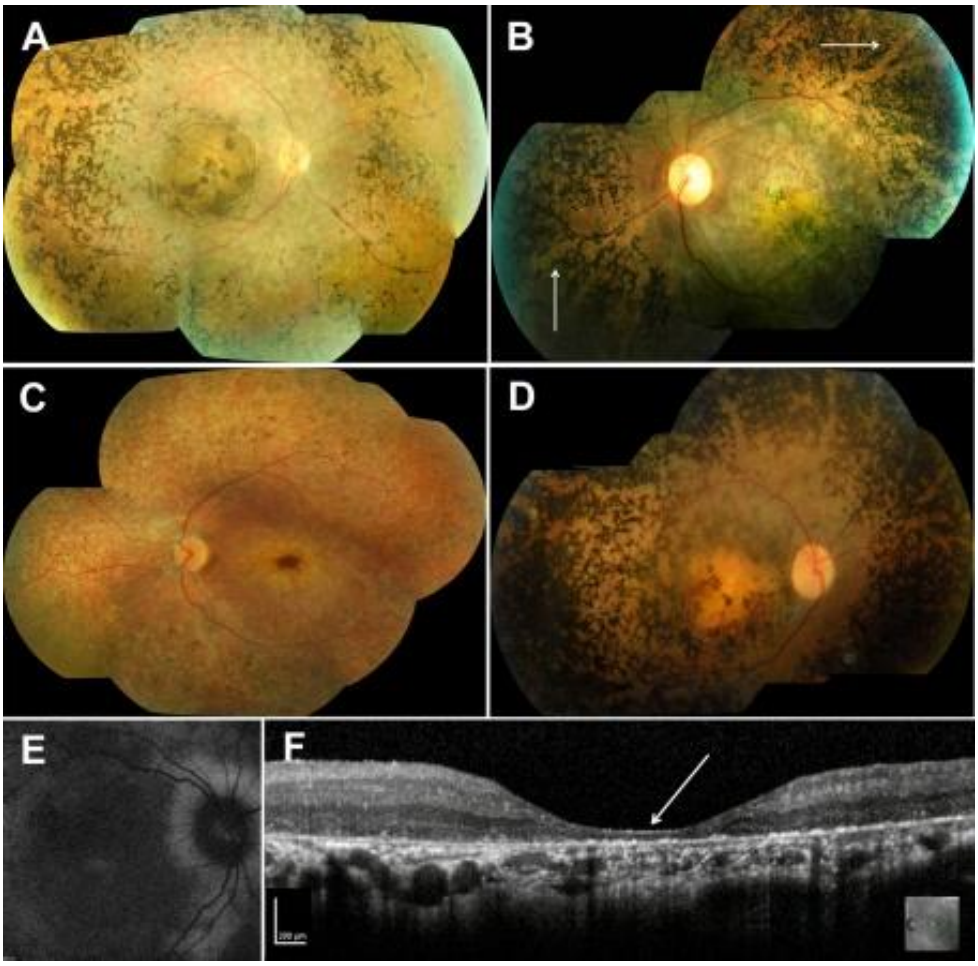

Figure 3.5.1b Phenotype associated with retinal dehydrogenase 12 (*RDH12*) retinopathy. A: Fundus appearance in adults and older children shows dense intraretinal pigment migration, severe retinal pigment epithelium atrophy, and arteriolar attenuation, with a severe atrophic pigmentary maculopathy (family 12, age 20 years). B: Para-arteriolar sparing of the intraretinal pigmentation was evident in six of 32 patients (white arrows, family 17, age 17.5 years). C: In children, retinal pigment epithelium atrophy with macular atrophy and minimal intraretinal pigmentation predominated (family 17, age 8.5 years). D: Macular atrophy was often associated with striking yellow deposits (family 3, age 27 years). E: No detectable macular autofluorescence was visible on fundus autofluorescence imaging, corresponding to the severe macular atrophy (family 11, age 11). F: Spectral domain optical coherence tomography demonstrated severe macular thinning, excavation, and distortion of the laminar architecture (white arrow, family 17, age 17.5 years).[296]

Table 3.5.1 Clinical features of the 25 patients with confirmed *RDH12* mutations

Family (Origin)	Gender	Age initial visual loss, further central visual deterioration (yr)	Age of nyctalopia (yr)	Age at Diagnosis (yr)	Visual Acuity in logMAR (age, yr)	Refraction	Visual Field/ Autofluorescence/ ERG	Anterior segment and fundus
Family 1	F	3,34	7	3 Able to read at school. Most progressive in third decade. (5 episodes CMO)	HM / HM (38)	7.5/7.5	VF: No data AF: No AF ERG: No data	Anterior / Posterior subcapsular cataracts (SC). Macula atrophy (MA). Choroidal atrophy (CA). Bone spicule hyperpigmentation HP.
Family 2	F	1.5, 19	Birth	8	2.30 EE (28)	-1/-6	VF:Residual temporal /nasal field at 50-60 AF/ERG: No data	Ant Segment: Normal. Disc pallor, attenuated vessels, MA, Bone spicule HP
Family 3	F	5, 7	5	5	0.78 RE HM LE (27)	No refraction details		AS: PSCO Dense retinal pigment clumping with para arteriolar sparing, atrophic yellow macula with pigment, arteriolar attenuation
Family 4	M	N/A	N/A	N/A	N/A	N/A	N/A	N/A
Family 5	F	0.5, 26	1	2	PL PL	1.25/ 1.75	VF: Not possible AF: Patchy hypofluorescent AF ERG: Severely attenuated	AS:PSCO Moderate retinal pigment clumping, atrophic yellow macula with pigment, arteriolar attenuation
Family 6	F 0	3	6y	NB, VF / VA loss 3 yrs	6/30 6/30	1.5/ 1.75	VF:Concentric constriction 40 degrees V4e AF: dark SLO with ring of hyperfluorescence around disc ERG: severely attenuated	Ant segment: normal. Healthy disc. Island of macula in atrophic post pole.

Family 7	F M	Birth, 14 4, 29	Birth 4	15 21	CF RE HM LE (27) 1.00 EE (34)	-1.50/+2.00, 85 RE -1.50/+2.25, 95 LE + 0.25/-3.50, 5 RE -1.00/-3.00, 175 LE		F: Moderate retinal pigment clumping, atrophic yellow macula with pigment, arteriolar attenuation M: Moderate retinal pigment clumping, atrophic yellow macula with pigment, arteriolar attenuation,mid-peripheral pericentric spared zone
Family 8	M	4	5	6	1.00 RE 1.20 LE (12)	+5.50/-2.00, 15 RE +5.00/-1.00, 180LE	AF:Patchy hypofluorescence	Anterior Segment: Normal. Minimal retinal pigment clumping, widespread RPE atrophy, atrophic yellowmacula
Family 9	F	3.5	N/A	3.5	0.80 EE (13)	+ 0.50/+4.50, 80 EE	VF: concentric fixation to <5 degrees (V/4e) AF: Patchy	Ant Segment: PSCO. Dense retinal pigment clumping, atrophic macula with pigment,arteriolar attenuation
Family 9	F	1.5,20	10	**3**	HM EE (29)	2.0/3.0	VF: Concentric fixation to <5 degrees (V/4e) AF: Patchy hypofluorescence. Difficult capture ERG: Sco: noise level Pho: noise level	Ant Segment: Normal. Disc drusen, attenuated vessels, MA, Bone spicule HP.
Family 10	M	2.5	8	6	CF EE (29)	N/A		AS:PSCO Moderate retinal pigment clumping, atrophic macula, arteriolar attenuation
Family 11	M F	Teens 8	4 N/A	4 6	HM EE (27) HM EE (25)	N/A	N/A	RE PCIOL; LE PSCLO. Widespread retinal pigment clumping, macular atrophy

Family 11 (contd.)								AS:Normal. Dense retinal pigment clumping, atrophic yellow macula with pigment, arteriolar attenuation
Family 12	F	Birth	N/A	18	HM EE (22)	N/A	N/A	AS: Normal. Dense retinal pigment clumping with para arteriolar sparing, atrophic macula with pigment, arteriolar attenuation
Family 13	M	2	N/A	5	HM EE (34)	N/A	N/A	AS: PSCLO. Dense retinal pigment clumping, atrophic yellow macula with pigment, arteriolar attenuation
Family 14	F	7	6	6	1.00 EE (27)	0.00/+1.5, 90 EE	N/A	Moderate retinal pigment clumping, atrophic macula with pigment, arteriolar attn
Family 15	F	Birth, 27	Birth	30	1.00 RE 0.78 LE (33)	N/A	N/A	AS: PSCLO .Dense retinal pigment clumping with para arteriolar sparing, atrophic yellow macula with pigment, arteriolar attenuation
Family 16	M	N/A	N/A	10	0.78 RE 1.00 LE (18)	+0.25/-1.50, 15 RE +1.00/-1.50, 170 LE	N/A	Moderate retinal pigment clumping, RPE atrophy, atrophic pigmented macula arteriolar attenuation mid-peripheral pericentric spared zone
Family 17	F	2	3	7	1.00 RE 0.78 LE (20)	+1.25/-0.50, 180 RE +1.00/-0.75, 180 LE	N/A	AS: Normal. Dense retinal pigment clumping with para arteriolar sparing, atrophic yellow macula with pigment, arteriolar attenuation

Family 18	F	1	N/A	N/A	PL EE (52)	N/A	N/A	AS:PSCLO. Dense retinal pigment clumping, atrophic yellow macula with pigment, arteriolar attenuation
Family 19	M	2	2	2	HM EE (29)	Emmetropia	VF:Temporal Islands 20 degrees AF: Not recordable	Dense retinal pigment clumping, atrophic yellow macula with pigment, arteriolar attenuation
Family 20	M	Birth	N/A	N/A	PL EE (21)	N/A	N/A	AS:PSCO .Dense retinal pigment clumping with para arteriolarsparing, atrophic yellowmacula with pigment, arteriolar attenuation
Family 21	F	11	11	12	PL EE (30)	N/A	N/A	AS: PSCO. Moderate retinal pigment clumping, widespread macular atrophy and yellowing, arteriolar attenuation
Family 22	M	0.75	0.5	2	1.00 RE 0.90 LE (8)	N/A	N/A	AS:Normal. No retinal pigment clumping, widespread RPE atrophy, atrophic yellow macula

3.5.2 Colour vision and visual field analysis

HRR colour vision testing was only possible in three patients due to poor central vision. In all three patients, families 3,4 and 6 only moderate changes of the tritan axis were demonstrated.

The average number of square degrees for a normal subject within a normal V4e isopter is 15000. Goldmann visual fields were recorded in ten patients and these were constricted symmetrically in eight fields. Two patients' visual fields were recorded as temporal residual islands. Follow up visual field data was less available than longitudinal acuity data however most noted subjective changes before teenage years. The youngest patient, 6 years old, revealed the most preserved field of 40 degrees. This was measured as 10150 square degrees. Eight patients had fields approximating 5-10 degree constrictions although atypically a 25 year old female recorded temporal islands of 20 degrees (family2, C201R).

3.5.3 Autofluorescence

Six patients underwent autofluorescence examination. In the two youngest patients, 6 years old and 8 years old, there was no autofluorescence with a ring of hyperfluorescence around the disc. Autofluorescence in other patients was recorded as either a pattern of patchy, hypofluorescence or an absence of autofluorescence, which could not be captured.

3.5.4 Electrophysiology

Electroretinography was performed at our institution on seven patients (age range of 2–22 years). This showed undetectable or severely attenuated rod and cone responses, demonstrating severe generalized retinal dysfunction from a very young age. This included five of the seven children below age 16 who otherwise had relatively preserved visual acuities (Families 1,2,3,5,6 and 9).

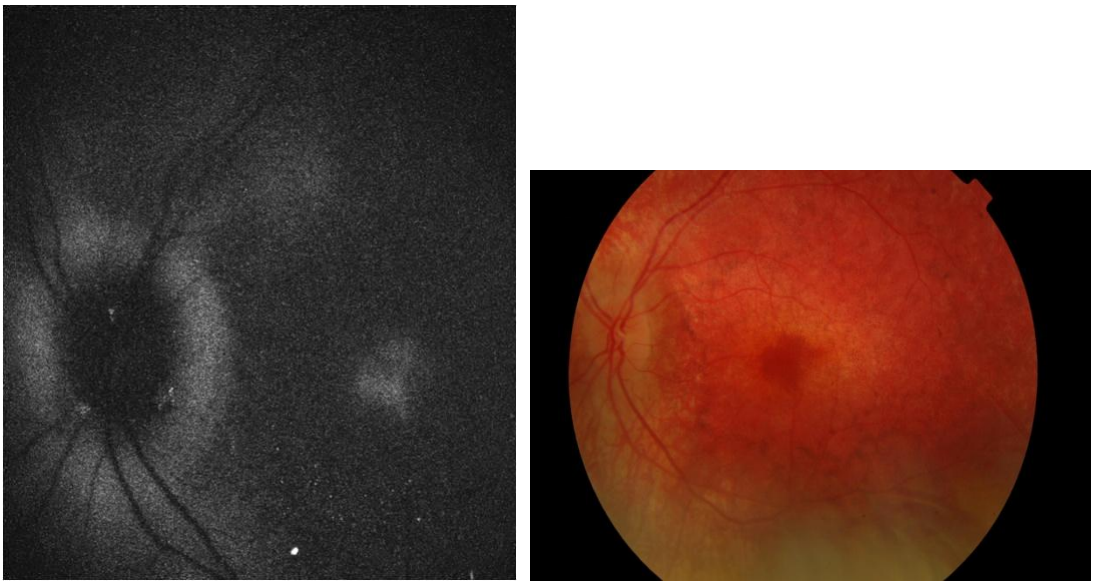

Figure 3.5.3 Autofluorescence imaging and fundus photo of 8 year patient's left eye with a *RDH12* mutation. Hypofluorescence around the the disc and at the macular is shown.

3.6 Summary of *RDH12* phenotype

RDH12 mutations are associated with a characteristic phenotype. There are two distinct patterns of disease progression which did not obviously correlate with the type of associated mutation. There is a phenotype consistent with LCA and a separate less severe EORD, where central and peripheral vision becomes severely affected just after the completion of secondary education in the second and third decade. Both patterns of the RDH12 phenotype are light dependent from an early age and have severe nyctalopia. Visual fields were generally constricted severely and concentrically in the first decade but patients in the less severe EORD reported noting early dramatic peripheral field loss. However, this less severe phenotype retained enough central visual function that did not hinder completion of secondary education in a normal sighted, school environment. Central vision in this group was subjectively reported to decrease rapidly over approximately a 24 month period between the age of 24-32 years. Patients had mainly low hypermetropia. There is a distinctive fundal appearance with extensive retinal atrophy, often affecting the macula, and pigment depositions associated with perifoveal yellow discoloration which allows the recognition of this specific form of retinal degeneration. Autofluorescence was always patchy or absent with a ring of peripapillary hyperfluorescence and a hyperfluorescent fovea noted in some individuals. These features can be used to direct efficient molecular diagnosis. Photoreceptor cell death occurs early and the window for therapeutic intervention appears short, within the first decade.

3.7 *CEP290* genotype and phenotype results

Seventeen patients, of author's cohort of 158 patients genotyped by the LCA APEX chip, from sixteen families, were identified with at least one disease causing allele in *CEP290* (see Table.3.7a). Mutations identified by the chip were then confirmed by PCR amplification of the *CEP290* gene and directly sequenced (methods section 2.3.3) to confirm the LCA APEX chip mutation and to identify the second mutation in patients 2,3,4,6 and 7 (see Table.3.7a).

One proband (patient 3) had a sibling (patient 4) with an identical genotype but a less severe phenotype. Twelve subjects were compound heterozygotes and two subjects were homozygous for *CEP290* mutations. In three patients (5, 8 and 14) only one disease causing mutation could be identified. Four novel variants were identified. The mutations (p.R1754W, K127NfsX35, E2027KfsX5 and p.E994K) were absent from 100 control chromosomes. Fourteen patients had LCA and two patients had a childhood onset rod-cone dystrophy (patient 3 and 5) and the sibling of patient 3 (patient 4) had a less severe adult onset rod-cone dystrophy.

Sixteen patients were white Caucasian, of north European origin, with one patient from the Indian subcontinent having north European maternal grandparents (patient 10). The patients ranged in age from 1-39 years (mean 13.2 years, median 8 years).

Median values for phenotypic findings are tabulated (Tables 3.7c and 3.7d). The majority of patients were moderate hypermetropes (mean +4.3 D, median +6 D) (see Figure 3.7g) which correlated with short axial length (Table 3.7d). The LCA patients had symptoms of poor vision, nystagmus, night blindness and photophobia which was noted in infancy. There were no syndromic features noted in this group. Colour vision was absent in all

LCA patients on HRR plate testing. Only tritan plates were seen by three patients with rod-cone dystrophy (patients 3,4,5). Twelve of the 14 LCA patients (86%) had sluggish or amaurotic pupil responses.

OCT measurements could only be carried out in five patients due to nystagmus or young age (3.7a(iii) showing the OCT of patient 5) . These five patients (clinical details; see table 3.7c, table 3.7d, table 3.7e) were: two individuals with childhood onset rod-cone dystrophy (patient 3 and patient 5); one with adult onset rod-cone dystrophy (patient 4; see fgure 3.7a(iv)) and two patients with LCA (patient 8, see figure 3.7a(iii), and patient 11). Foveal thickness ranged from 186 to 295 microns in the LCA group (median 232 microns) but the fovea were minimally less degenerate in the rod-cone dystrophy group (median 324 microns). Minimal or no autofluorescence was seen in five patients in whom imaging was possible (Figure 3.7a(i): Image C and Image D and Figure 3.7a(ii)). A distinctive hyperfluorescent perimacular ring in patients 5 and 8 was recorded, as shown figure 3.7a(i): images C and D and figure 3.7a(ii).

Examination revealed pale optic discs, attenuated retinal vessels and a loss of the foveal reflex, see Figures 3.7a(i),(ii) and (iii). Only one adult patient had minimal, true bone spicule, peripheral pigmentary migration (patient 4) (Figure 3.7a(iv)). One patient (patient 5) presented with multiple white dots in perifoveal and peripheral distribution (Figure 3.7a(i), image E) and three patients presented with peripheral white dots and choroidal sclerosis (patients 6,8 &10). Electrophysiological investigation showed a non recordable ERG or severe rod and cone dysfunction at diagnosis. Only patient 1 demonstrated residual cone function.

Nine patients with *CEP290* mutations were able to complete clinical olfactory tests and five patients were noted to have reduced, age-adjusted scores (Tables 3.7a and 3.7e). Olfactory status was more severe, termed severe microsmia and anosmia, in patients with two null mutations, (<18% age adjusted olfaction score). Patients with at least 1 missense mutation, shown in Tables 3.7a and 3.7e, had normal olfaction (>50% age adjusted olfaction score). No other patients in our cohort were checked for anosmia.

Spectralis domain OCT images in our study of a 16 year old male (p.K1343RfsX1, unknown second mutation), patient 8 (Figure 3.7a(iii)), showed preservation of the outer retinal layer but evident thinning at the central macular area. This outer retinal layer in normally sighted subjects corresponds to the outer nuclear layer. There was a discrete focal thickening temporal to the central macula. Photoreceptor inner/outer segment junction (PSJ) was visible throughout the macular scan, although they were less defined than in those of visually-normal eyes (Figure 3.7a(iii)). In contrast, a 35 year old male (patient 4) with adult onset rod-cone dystrophy, and with a missense mutation and the common intronic mutation (p.R1754W, p.C998X) showed relatively normal patterns of fluorescence (Figure 3.7a(iv). There was also preservation of the ONL and PSJ at the central macular consistent with the less severe phenotype, adult onset rod-cone dystrophy (see spectral domain OCT of patient 4: Figure 3.7a(iv), lower image).

A **B**

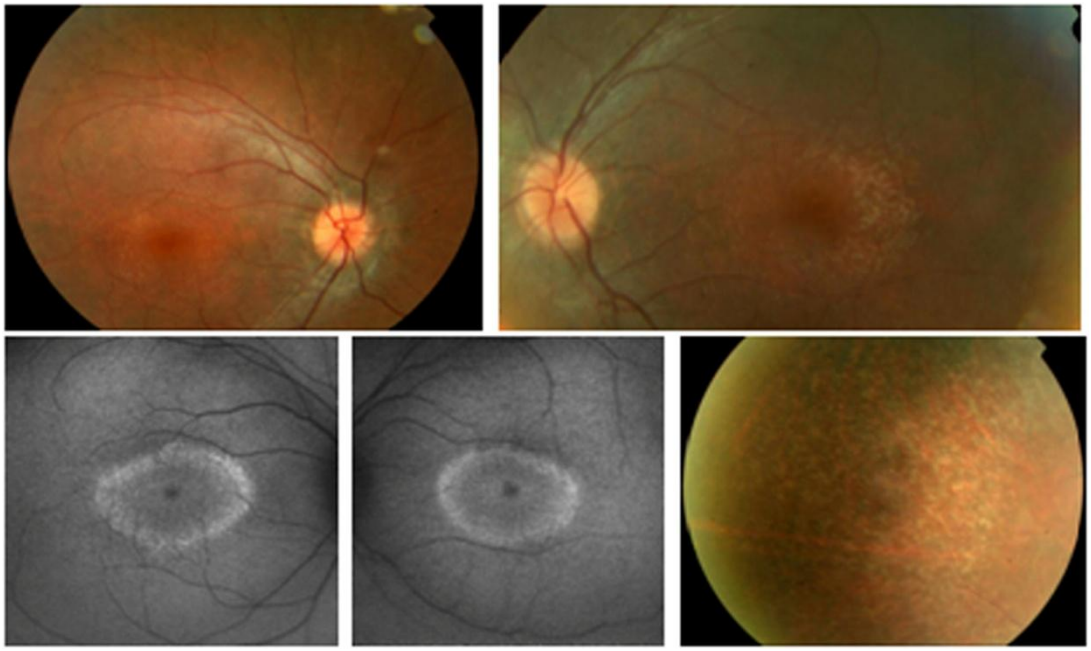

C **D** **E**

Figure 3.7a(i) Images A-E:. Fundus photographs and fundal autofluorescence (FAF) of patient 5. *Images A and B (first row)*: The presence of perifoveal white dots on right and left funduscopy respectively. *Images C and D* (*2nd row, left and middle*): FAF, of patient 5. The presence of perifoveal white dots on photography is consistent with a ring of increased FAF. Background FAF is reduced, suggesting some ability to regenerate chromophore. *Image E* (*2nd row, right*)*:* Peripheral retina white dots, patient 5.[296]

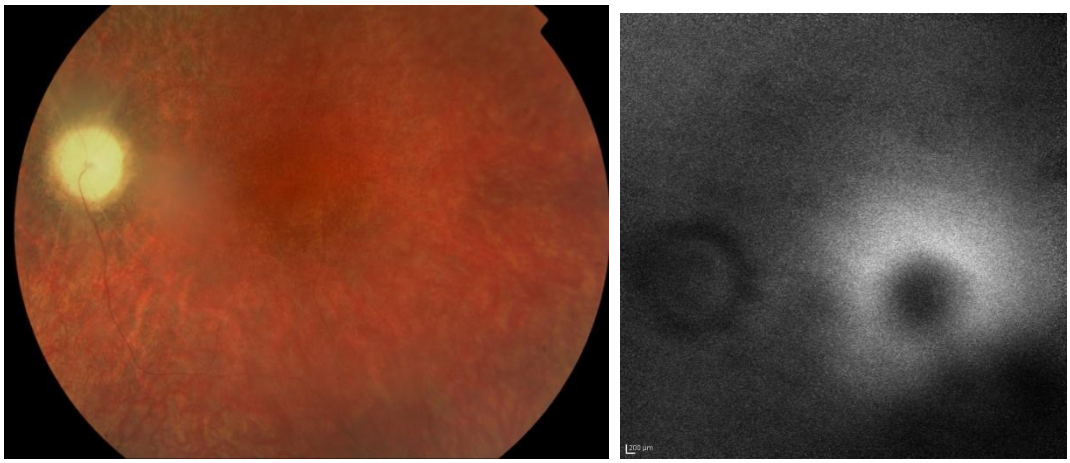

Figure 3.7a(ii) Left fundal photograph and autofluorescence (AF) of 16 year old male, patient 8, with one known *CEP290* nonsense mutation, p.K1343RfsX1. Note the very severe early disc pallor and arteriolar attenuation on fundal photography and the hyperfluorescent ring on AF.

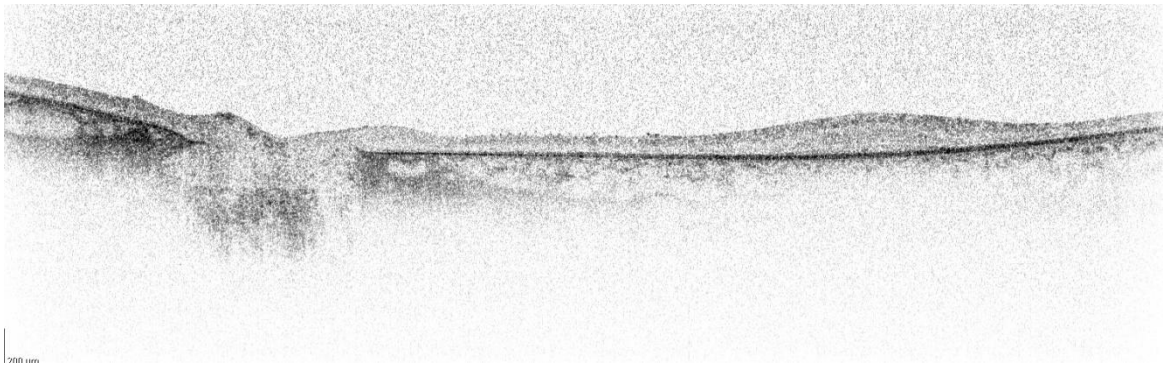

Figure 3.7a(iii) Spectralis Domain OCT in 16 year old male (p.K1343RfsX1, unknown second *CEP290* mutation), patient 8, showing preservation of the outer retinal layer but evident thinning at the central macular area. The outer retinal layer in normally sighted subjects corresponds to the outer nuclear layer. There is a discrete focal thickening temporal to the central macula. Photoreceptor inner/outer segment junction (PSJ) was visible throughout the macular scan, although they were less defined than in those of visually-normal eyes.

Figure 3.7a(iv) Fundal photography, autofluorescence (AF) and SD-OCT of patient 4 (top, middle, bottom rows). AF showing significant lipofuscin levels and chromophore regeneration with mildly reduced levels of fluorescence, distributed within normal ranges. Preservation of the ONL and PSJ at the central macular with less severe phenotype EORD. Patient 4, Milder Rod-Cone dystrophy. VA 6/18 BE (p.C998X , p.R1754W)

Table 3.7a: Phenotype table of *CEP290* patients

Family ID	Age Of examination	Visual Acuity	Refractive Error	Nystagmus/ Photophobia/ Nyctalopia	ERG	Olfaction	Fundus Examination
1	6y	HM// HM	Emmetropia	+ /-/+	Absent rod function ; residual cone function	NA	Normal disc, retina and vessels
2	5y	HM// HM	+6.5/+6.5	+/-/+	Absent rod and cone function	Anosmia <5%	Normal disc and vessels, diffuse,mottled RPE alterations with no intraretinal pigment migration
3	39y	1.3//HM	+7.5/+7.5	+/+/+	Absent rod and cone function	Normosmia >50%	Disc pallor, arteriole attenuation, macular RPE alterations, RP bone spicule migration
4	35y	0.4//0.6	+1.5/+1.0	-/+/+	Adult Onset Milder Rod-Cone dystrophy	Normosmia>50%	Mild disc pallor, no arteriole attenuation, sparse RP migration
6	3y	HM// HM	Emmetropia	+/+/+	Absent rod /cone function	NA	Normal disc, retina and vessels
7	13y	HM// HM	+8/+8	+/-/+	Absent rod and cone function	Normosmia >50%	Healthy disc and vessels. Scarce retinal pigment migration
8	16y	HM/HM	-0.5//-5.25/2.75x14	-/+/+	Absent rod and cone function		Healthy discs and vessels. Scarce peripheral retinal pigment migration

Family ID	Age	Visual Acuity	Refractive Error	Nystagmus/ Photophobia/ Nyctalopia	ERG	Olfaction	Fundus Examination
9	3y	1.5/1.5	+6//+8	+/+/?	NA	NA	Healthy discs, vessels. Normal fundal appearance
10	7y	HM//HM	+10//+9	+/-/+	Absent rod and cone function	Normosmia >50%	Healthy disc, vessels, discrete white dots in retinal periphery
11	8y	PL//PL	3.75/-3x150 // -3.75/-3x35	-/+/+	Absent rod and cone function	NA	Healthy discs, vessels, discrete white dots in retinal periphery
12	4y	HM//HM	+9.5//+8.5	+/+/+	Absent rod and cone function	Normosmia	Disc pallor, healthy vessels and retina
13	24y	HM/HM	-1/+7x115 //+ 5/+2x31	+/+/-	Absent rod and cone function	Microsmia 18%	Disc and vessels healthy, Granular RPE with white dots.
14	10y	HM/HM	emmetropia	+/+/+	Absent rod and cone function	Microsmia 10%	Disc and vessels healthy, early macular RPE atrophy. Peripheral granular RPE
15	36y	0.8/0.8	6.5/1x90//7/1.25x90	+/-/+	Absent rod and cone function	Anosmia <5%	Disc pallor, attenuated vessels, white dots at RPE level,scarce pigment
16	2y	NA	NA	+/+/+	To be repeated	NA	Disc and vessels healthy. No fundal abnormality noted
17	1y	NA	NA	+/-/?	NA	NA	Disc and vessels healthy. No signs

Table 3.7b Identified *CEP290* mutations with Olfactory Status

Patient ID	**Diagnosis**	**Asper Results**	**Mutations**	**Exon**	**Ref**	**Olfactory Status** (see Methods **2.2.10** for scoring)
1	LCA	p.C998X het	c.2991+1665A>G, p.C998X c.1984C>T, p.Q662X	IVS26 Ex20		ND
2	LCA	p.C998X het	c.2991+1665A>G, p.C998X **c.381A>T+382delG, p.K127NfsX35**	IVS26 **EX6**	**Novel**	Anosmia <5%
3	Early onset Rod-Cone dystrophy	ND	c.2991+1665A>G, p.C998X **c.5260C>T p.R1754W**	IVS26 **Ex39**	**Novel**	Normosmia >50%
4	Adult onset Rod-Cone dystrophy	ND	c.2991+1665A>G, p.C998X **c.5260C>T p.R1754W**	IVS26 **Ex39**	**Novel**	Normosmia >50%
5	Early onset Rod-Cone dystrophy	p.C998X het	c.2991+1665A>G, p.C998X	IVS26		ND
6	LCA	p.K1575X het	c.4723G>T, p.K1575X **c.6079delA, p.E2027KfsX5**	Ex34 **Ex44**	**Novel**	ND
7	LCA	p.C998X het	c.2991+1665A>G p.C998X **c.2980G>A, pE994K**	IVS26 **Ex26**	**Novel**	Normosmia >50%
8	LCA	p.K1343fs het	c.4028delA, p.K1343RfsX1	EX31		ND
9	LCA	p.C998X het	c.2991+1665A>G, p.C998X c.6277delG,	IVS26 Ex46		Anosmia <5%

			p.V2093SfsX3			
10	LCA	p.W7C hom	c.21G>T p.W7C c.21G>T p.W7C	Ex2		Normosmia >50%
11	LCA	p.C998X het p.D128Efs het	c.2991+1665A>G p.C998X c.384_387delTAGA, p.D128EfsX33	IVS26 Ex6		ND
12	LCA	p.C998X het	c.2991+1665A>G, p.C998X c.1219_1220delAT, p.M407EfsX13	IVS26 Ex14		ND
13	LCA	p.C998X het p.E1656X het	c.2991+1665A>G, p.C998X c.4966G>T, p.E1656X	IVS26 Ex37		Microsmia 18%
14	LCA	p.C998X het	c.2991+1665A>G, p.C998X	IVS26		Microsmia 10%
15	LCA	p.C998X hom	c.2991+1665A>G, p.C998X c.2991+1665A>G, p.C998X	IVS26 IVS26		Anosmia <5%
16	LCA	p.I1059NfsX1 p.C998X	c.3166_3176 ins 1bp(A) p.I1059NfsX1 c.2991+1655A>G p.C998X	Ex28 IVS26		ND
17	LCA	p.K1575X p.E1656X	c.4723G>T, p.K1575X c.4966G>T, p.E1656X	Ex34 Ex37		ND

3.7.1 Common known mutation p.C998X and other mutations established on direct sequencing of *CEP290*.

The following electropherogram figures and explanatory text demonstrate sequencing results.

Patient 1:

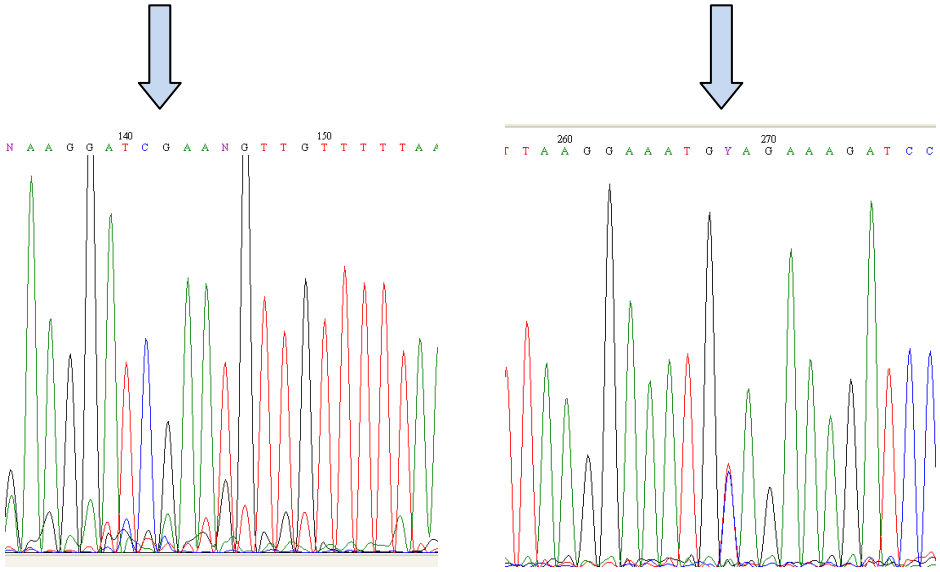

c.2991+1665A>G, p.C998X c. 1984C>T, p. Q662X

Figure 3.7b(i) Electropherograms of *CEP290* showing both mutations of patient 1, a compound heterozygote. Left image p.C998X. Right image p. Q662X

GENOME SEQUENCE: ATG CAG AAA GAT
MUTATED SEQUENCE: ATG YAG AAA GAT, WHERE Y = C or T

Figure 3.7b(ii) (Sequences) A comparison of genome sequence with mutated sequence. Heterozygous C>T change in exon 20 resulting in a codon change from CAG (Gln) to TAG (STOP).

The mutations shown in Figure 3.7b results in a truncated protein of 661 amino acids out of a possible 2479 amino acids. Both mutations result in severely truncated proteins. No stable transcript or functioning protein will remain. These patients have a clinically severe phenotype.

Patient 2:

CEP290

FORWARD PRIMER SEQUENCE REVERSE PRIMER SEQUENCE

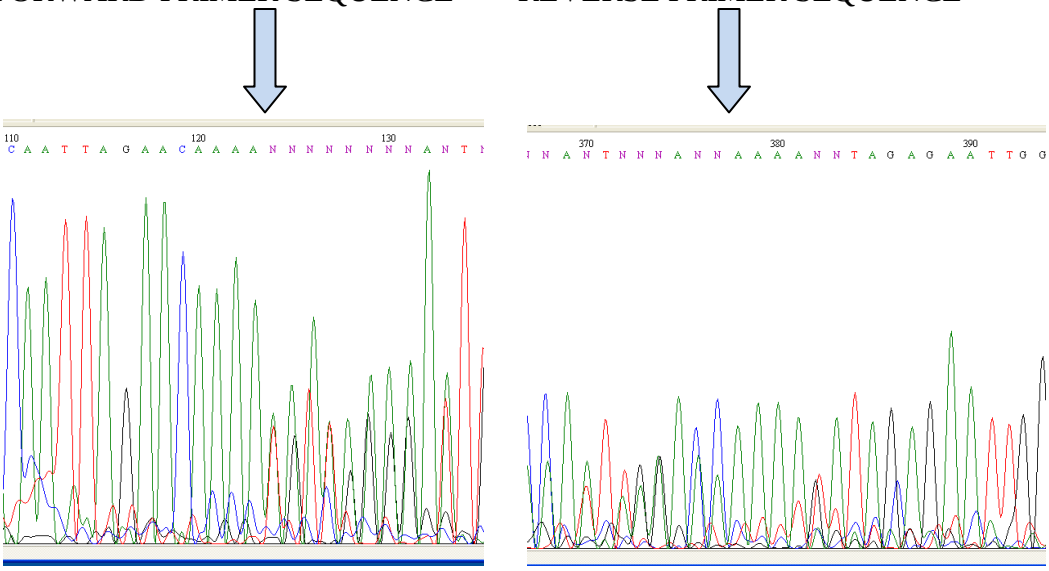

Figure 3.7c Forward and reverse electropherograms of *CEP290*. Patient 2, a compound heterozygote. Images showing the two sequences becoming "mixed" at the mutation position.

c.381A>T+382delG ,p.K127NfsX35

CAA TTA GAA CAA AAA GAT AGA GAA TTG GAG GAC – wildtype

CAA TTA GAA CAA AAT ATA GAG AAT TG – mutated strand

Figure 3.7c When sequences are aligned, they reveal a heterozygous AG>T change in exon 6 resulting in a frameshift and downstream premature STOP codon in exon 7.

This shows that the AG of one of the wildtype strands has been replaced by a single T, with an accompanying single base frameshift. This was confirmed by the reverse sequence. Thus, the mutation is either an A>T change with a delG or delA with a G>T change.

When the mutated strand is continued, the downstream sequence reads:

CAA TTA GAA CAA AAT ATA GAG AAT TGG AGG ACA TGG AAA AGG AGT TGG AGA AAG AGA AGA AAG TTA ATG AGC AA//T TGG CTC TTC GAA ATG AGG AGG CAG AAA ATG AAA ACA GCA AAT TAA, where // denotes the ex6-7 boundary and TAA is the STOP in exon 7.

This mutation, shown above (c.381A>T+382delG ,p.K127NfsX35), results in a truncated protein of 161 amino acids out of a possible 2479 amino acids, 127 amino acids are the same as native CEP290, with an extra 34 amino acids resulting from the frameshift (IENWRTWKRSWRKRRKLMSNWLFEMRRQKMKTAN*).

Patient 3:

CEP290

c.2991+1665A>G, p.C998X

c.5260C>T, p.R1754W

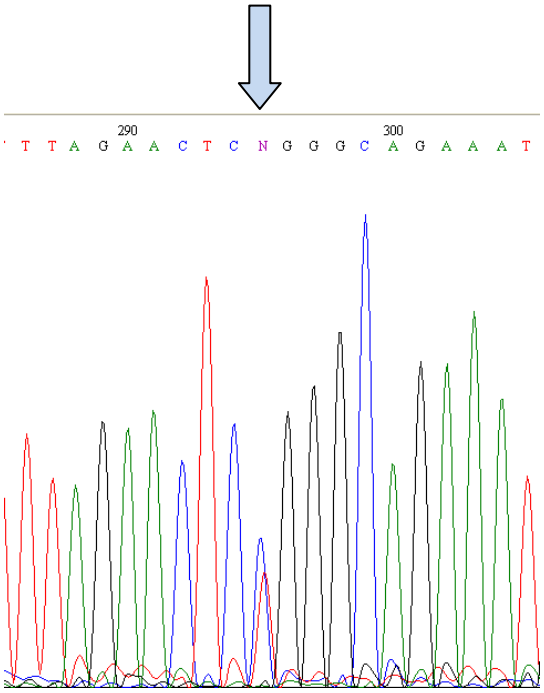

Figure 3.7d Electropherogram of *CEP290* showing second heterozygous mutation in patient 3; mutation designation: c.5260C>T, p.R1754W. Heterozygous missense C>T change in exon 39 resulting in a codon change from CGG (R - arginine) to TGG (W - tryptophan).

GENOME SEQ: T TTA GAA CTC CGG GCA GAA ATG

MUTATN SEQ: T TTA GAA CTC YGG GCA GAA ATG, WHERE Y = C or T

Fig 3.7d (contd.) Wild type genome sequence and mutated sequence below. Position of mutation highlighted with a box.

Patient 6: *CEP290*

c.4723G>T, p.K1575X

c.6079delA, p.E2027KfsX5

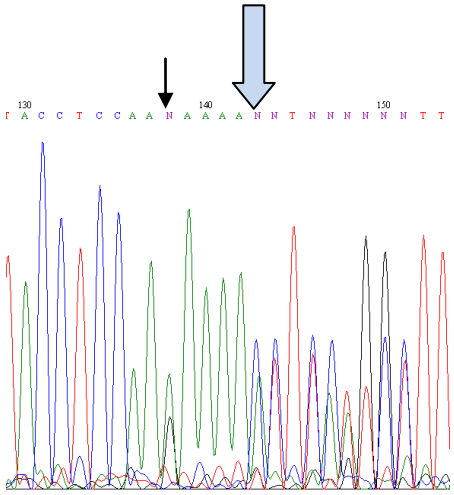

Fig 3.7e Electropherogram of *CEP290* showing a single deletion (c.6079delA, p.E2027KfsX5) has occurred (blue arrow) within one of the wildtype strands and causes a single base frameshift with a STOP codon being generated shortly downstream (see underlined TAG below, Fig 3e (contd.)). There also seems to be a G>A change 5 bases upstream of the deletion (small black arrow), however, this was not confirmed in the reverse sequence and is therefore a sequencing artefact and should be ignored.

Gen: AAT AGA TAC CTC CAA GAA AAA CTT CAT GCT TTA GAA AAA –

Mut: AAT AGA TAC CTC CAA AAA AAC TTC ATG CTT TAG AAA AAA–

Fig 3.7e (contd.) Review of the forward primer for wild type genome sequence (Gen, top) and mutated sequence (Mut, below)showing mutation c.6079delA, p.E2027KfsX5.When aligned this mutation results in a truncated protein of 2031 amino acids out of a possible 2479 amino acids. The initial 2027 amino acids are the same as non-mutated, genomic CEP290, with an extra 4 amino acids resulting from the frameshift (NFML*).

Patient 7: *CEP290*

c.2991+1665A>G, p.C998X (mutational electropherogram, see Figure 3.7b)

c.2980G>A, p.E994K (shown below; Figure 3.7f)

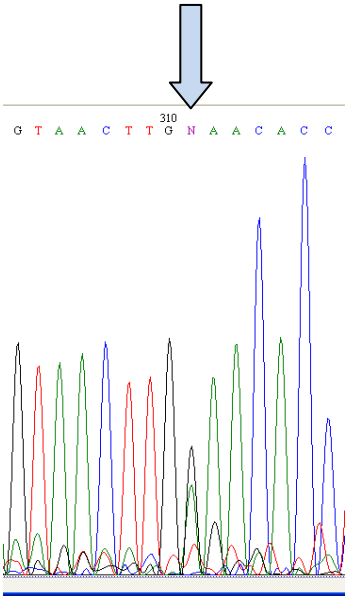

Figure 3.7f Electropherogram of *CEP290* showing a heterozygous mis-sense G>A change in exon 26 resulting in a codon change from GAA (Glu) to AAA (Lys).

GEN: ACA AGT AAC TTG GAA CAC CTG

MUT: ACA AGT AAC TTG RAA CAC CTG, WHERE R = G or A

Figure 3.7f(contd.) This results in a full-length protein of 2479 amino acids out of a possible 2479 amino acids, however, residue 994 has mutated to Lys (K).

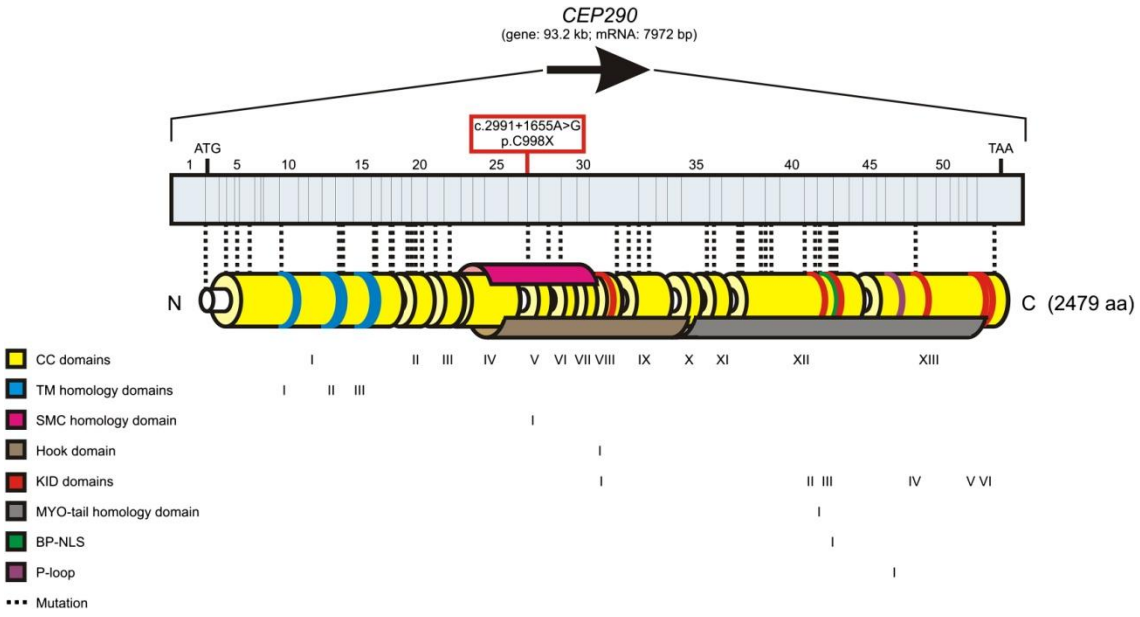

Figure 3.7g (image from Moradi et al.[297])

Top row: The human *CEP290* gene spans 93.2 kb encoding 54 exons. Translation initiation (ATG in exon 2) and termination (TAA in exon 54) codons are indicated (exons are drawn to scale with every fifth exon numbered).

Bottom row: A scale representation of CEP290 protein (2479 residues, white) shows the putative protein motifs in relation to the position of the exons encoding them. Putative protein domains are taken from Sayer et al. [192]

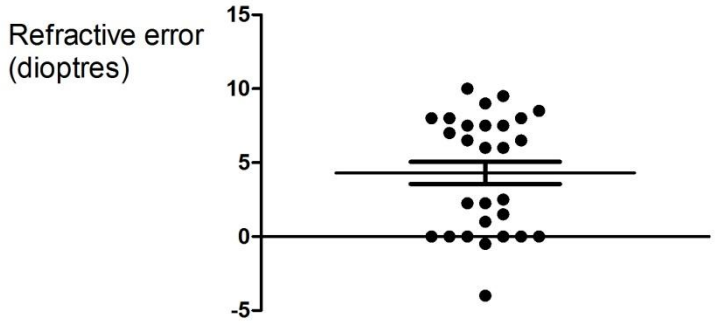

Figure 3.7g Refractive errors in patients with *CEP290* mutations. Long horizontal line within scatter plots showing mean values and whiskers showing standard error.

Table 3.7c Associated signs for patients with CEP290 mutations

	Nystagmus	**Nyctalopia**	**Oculo-Digital reflex**	**Strabismus**	**Photoaversion**	**Photoattraction**
RCD (n=3)	66%	100%	No	No	No	No
LCA (n=14)	81.3%	100%	12.5%	12.5%	64.7%	No

Table 3.7d Median age at onset of symptoms (years) in *CEP290* mutation patients

	(Mean/actual) age examination	**Age at diagnosis**	**Age at nyctalopia**	**Age at field loss**	**Age at poor vision**	**Age at nystagmus**
Juvenile onset RD	17	20	15.2	16	14	NA
LCA	13.2	2	0.7	1	0.7	0.5

Table 3.7e Median values for phenotypic measurements in *CEP290* mutation patients

	LogMar acuity	**Spherical equiv. Refract. (D)**	**Visual field size**	**Axial length (mm)**	**Foveal thickness on OCT (microns)**
RCD	0.7	1.25	1387	23.8	324
LCA	2.35	6	120.6	19.78	232

3.7.2 Summary of *CEP290* phenotype

The majority of the patients with *CEP290* mutations had a diagnosis of LCA with severe, early visual symptoms starting in infancy, although a childhood and adult onset severe rod-cone dystrophy were also evident. Their refraction was low to moderate hypermetropia consistent with a shorter axial length. Fundus examination revealed white dots at the level of the RPE, choroidal vascular sclerosis, sparse pigment migration, pale discs and arteriolar attenuation with a preservation of the outer retinal layer but evident thinning at the central macular area. On spectral domain OCT, photoreceptor inner/outer segment junction (PSJ) was visible throughout the macular scan, although they were less defined than in those of visually-normal eyes. On clinical olfactory testing, asymptomatic but severe microsmia and anosmia were elicited in patients with two null *CEP290* mutations.

3.8 Two families with *RLBP1* mutations

Two familes were referred to our clinic with a diagnosis of EORD or an "early RP". However, in accordance with the project's diagnostic criteria previously defined (section 3.1.5), these two familes had the onset of symptoms and signs of retinal dystrophy greater than 5 years old and were defined as "juvenile onset" RD. The *RLBP1* gene was the first candidate gene sequenced due to the clinical phenotype and pathognomic electrophysiological data described below. *RLBP1* mutations are not on the LCA APEX chip.

3.8.1 *RLBP1* phenotyping results

Two families with *RLBP1* mutations are reported. The first consisted of three female siblings with a retinal dystrophy that resembled gyrate atrophy, a disorder caused by an increased level of serum ornithine consequent upon lack of the enzyme ornithine keto-acid aminotransferase (*OAT*, located on 10q26.13).[298] The second family consisted of two male and one female siblings with a phenotype that was initially thought may be fundus albipunctatus (associated with *RDH5* mutations) or retinitis punctata albescens (associated with *RLBP1* mutations). The clinical phenotype, including the retinal appearance, electrophysiology supporting causative genes and retinal autofluorescence are described (see Figure 3.8.1a-b and 3.8.2.a).

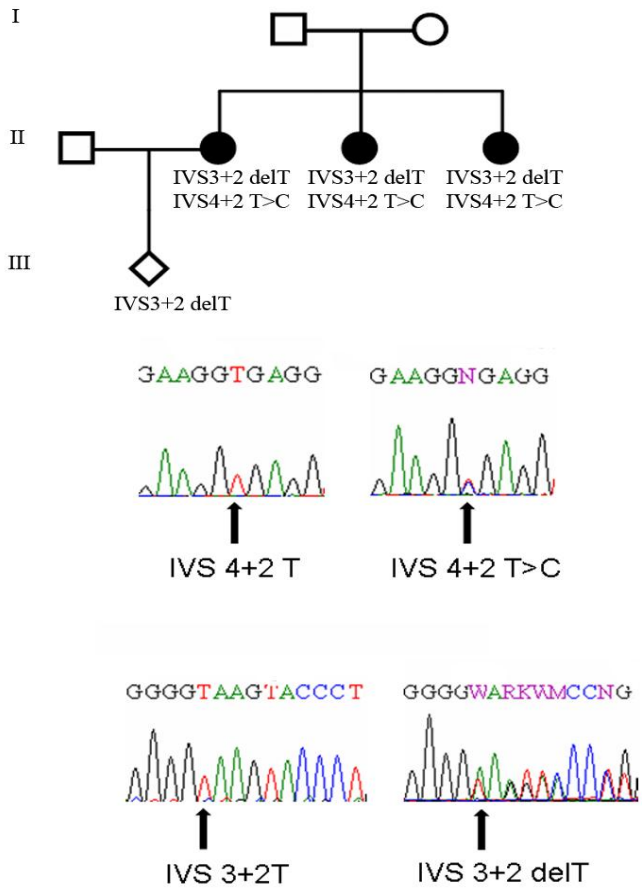

Figure 3.8.1a Family 1 segregated, in trans, a previously published mutation in intron 4 (IVS4+2 T>C), and a novel mutation in intron 3 (IVS3+2 delT).

Family 1

There were no other siblings in the family and no known antecedents with visual problems. Specifically, the parents had normal vision until their death at ages 70 and 68 years. There was no known parental consanguinity. No visual problems were reported in any children of the affected sisters. A drug history of all three siblings included recent hypertensive treatment with daily, oral enalapril and atenolol.

History of Proband

The 67 year old sister had a history of nyctalopia since early childhood, aged approximately 6 years old. Reduced visual acuity and peripheral visual loss was reported during her third decade. On initial ophthalmological examination, aged 39 years, best corrected visual acuity was recorded as 6/36, N18 OD and 6/12, N8 OS (+0.75/-0.5x90 bilaterally). Subtle blue dot cataracts and early posterior subcapsular cataracts were noted. The cataracts slowly deteriorated and underwent phacoemulsification and intraocular lenses 20 years later. Fundal examination is shown in Figure 3.8.1a and demonstrates attenuated vasculature, increasingly pale optic discs, and progressive, widespread retinal pigmentary migration with increasing areas of scalloped chorioretinal and macular atrophy. Kinetic visual fields shown minimal temporal loss aged 40 years. Between the age of 45 and 55 years vision deteriorated to 6/60 OD and 3/60 OS and cystoid oedematous changes affected both maculae for prolonged periods during this time. Ornithine levels were recorded on two separate occasions at only slightly elevated levels 193 μmol /litre and 169 μmol /litre (normal range 20 – 144 μmol /litre) which are not consistent with a diagnosis of gyrate atrophy, caused by *OAT* mutations. The most recent kinetic visual fields were limited to a paracentral island only. Recent autofluorescence imaging is shown in figure 3.8.1a with a minimally hypofluorescent but granular appearance.

Histories of Siblings

The 75 year old sister experienced visual loss in the third decades with a similar slowly progressive course from best corrected visual acuity of 6/18 bilaterally (+0.5/-0.5x75 OD +1 OS) early in the third decade to a VA of light perception bilaterally by the end of the sixth decade. A subtle horizontal nystagmus was present from birth and there were bilateral white cortical lens opacities. The kinetic visual fields were unrecordable.

The 71 year old sister had best corrected VA 3/60 bilaterally (+0.5/0.5x75OD and 0.5D OS). There was no nystagmus evident. Bilateral nuclear sclerotic cataracts were present. Funduscopy is presented within the figures. The kinetic visual fields were limited to a paracentral island only.

Family 2

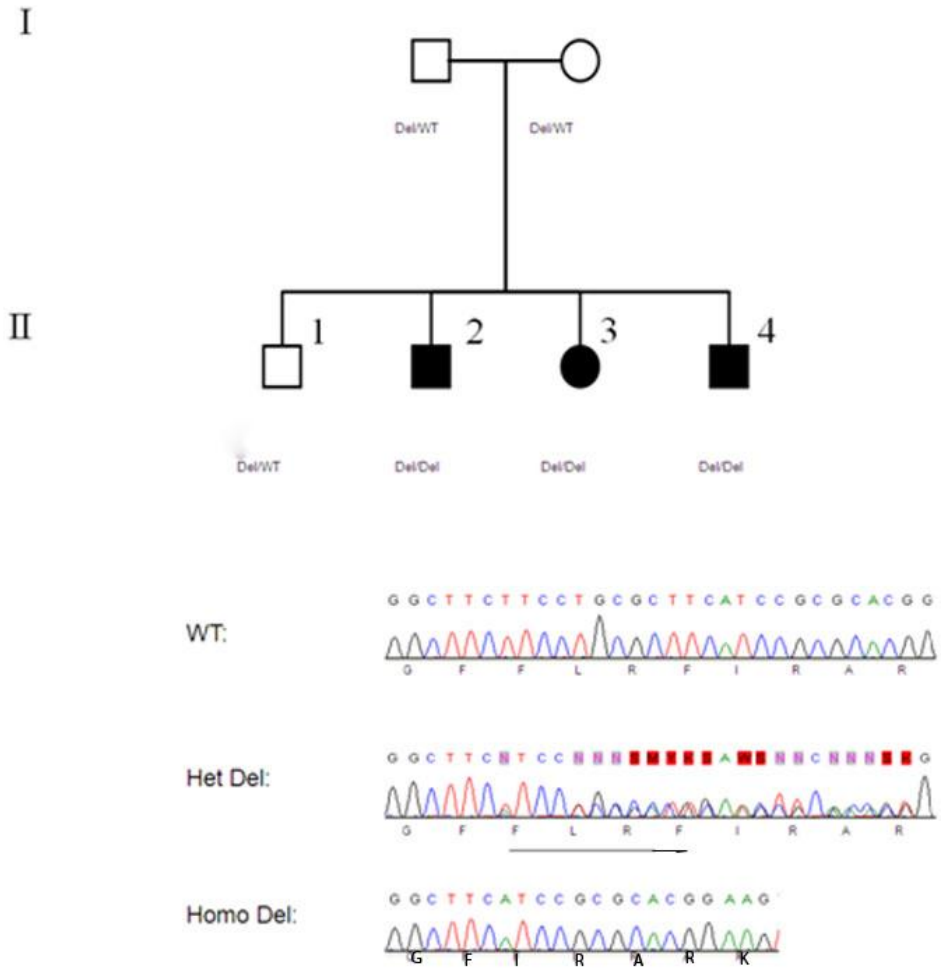

Figure 3.8.1b: Family 2. Affected members of family 2 were homozygous for a novel 12bp deletion in exon 5 (F96_F99del).

In family 2, all three affected siblings experienced night blindness from early childhood however visual fields were within normal range. The 32 year old brother, 24 year old brother and 26 year old sister had corrected visual acuities of 6/6 and N5 with similar low myopic prescriptions of less than 1.5 dioptres bilaterally. Ophthalmic examination

showed clear visual media. On dilated funduscopy, punctate white dots and mild pigment migration was seen in the peripheral retina. The peripheral pigmentary distribution was only seen in the superior retina in the female and in the inferior retina in the 24 year old male. The 32 year old male had a widespread, peripheral distribution. The young patients in family 2 were screened for *RDH5* mutations due to the phenotype showing a similar appearance to fundus albipunctatus. However there were no mutations found within this gene.

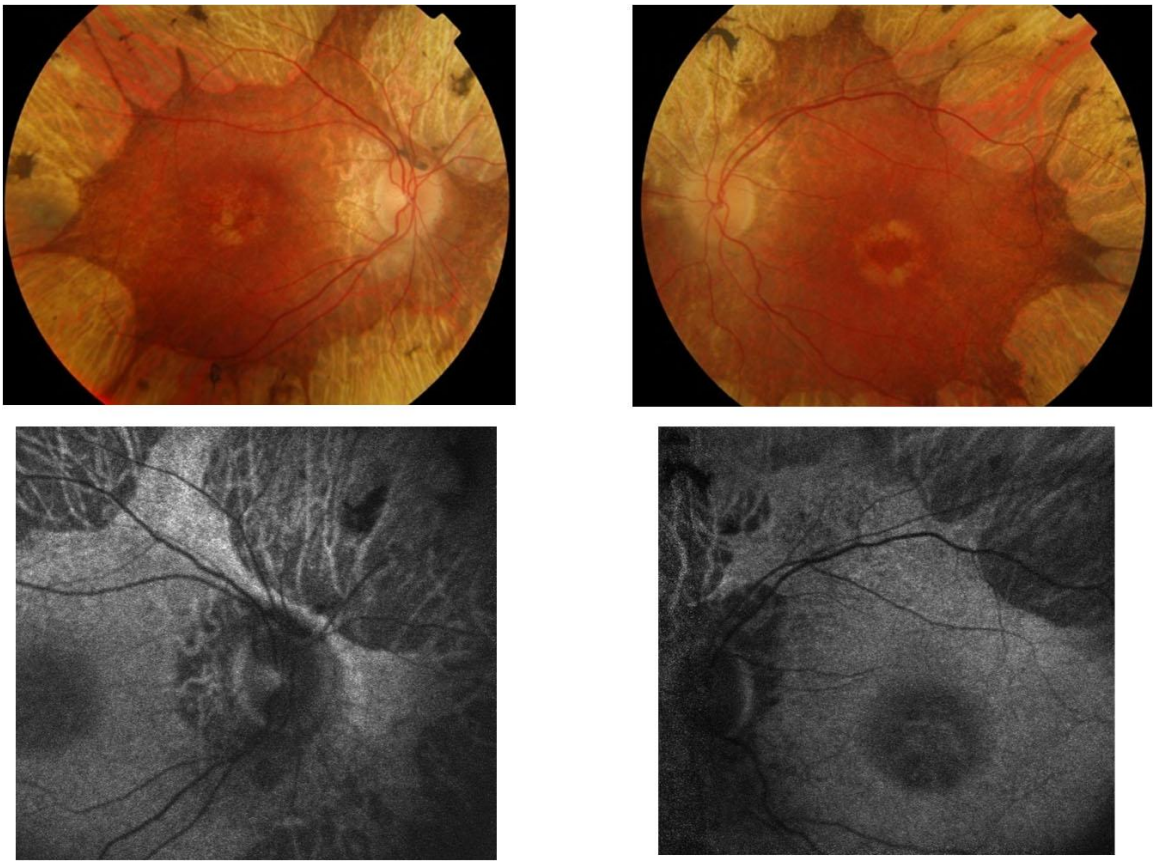

Figure 3.8.1c Fundus photographs (top row) and fundus autofluorescence of proband in family 1. The presence of autofluorescence, although reduced, suggests the ability to regenerate chromophore is retained, in spite of the null mutations.

Figure 3.8.1d Fundus photographs of family 2.

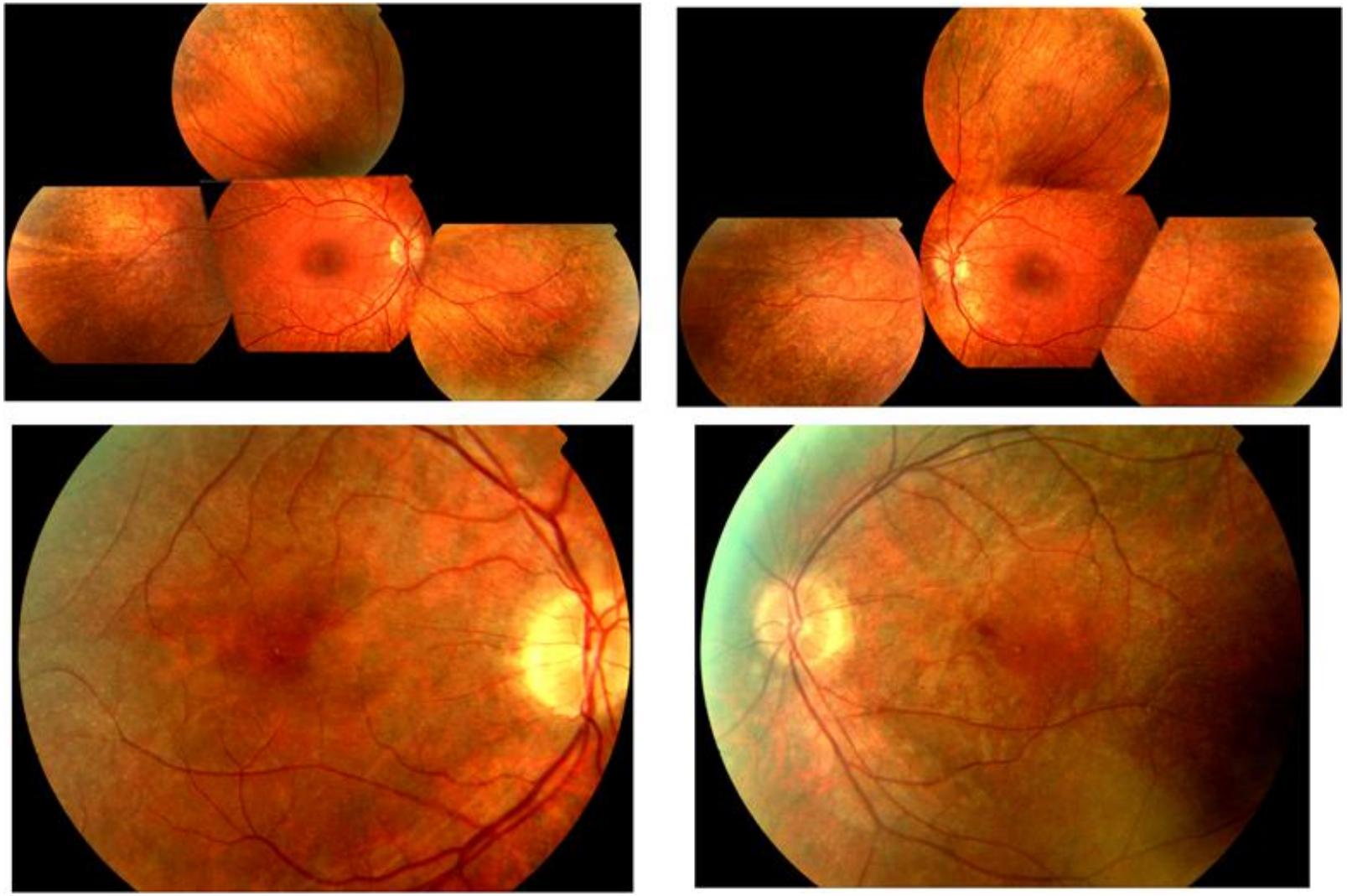

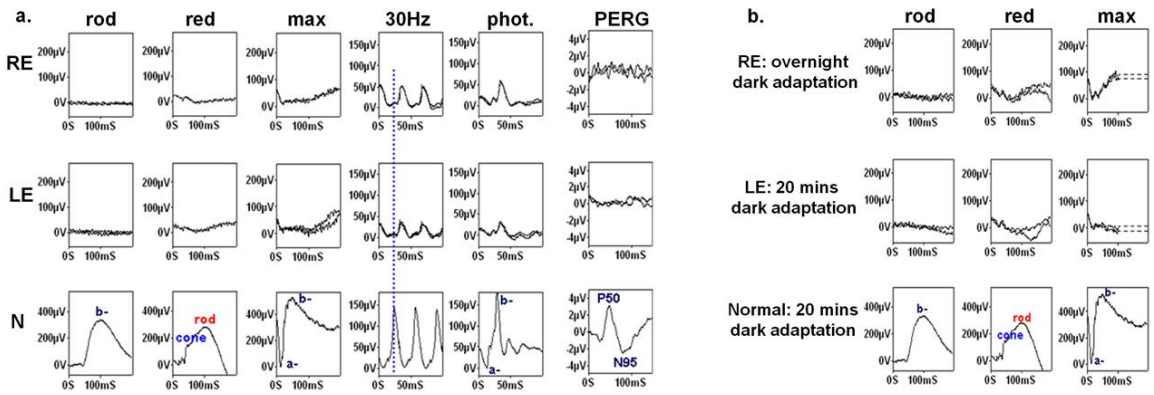

Figure 3.8.2a (left six columns) Full-field and pattern ERGs in subject II-2 (family 2); (see Figure 3.8.3a). Full-field ERGs were initially performed following 20 minutes dark adaptation (both eyes). Bright flash (max) ERGs were recorded to a flash 0.6 log units brighter than the ISCEV standard flash, to better demonstrate the a-wave. The dotted line intersecting the photopic 30Hz flicker ERGs indicates the upper limit of normal timing. Normal examples are shown (N) for comparison.

Figure 3.8.2b (right three columns). Repeat scotopic ERGs recorded after the right eye was dark-adapted for a prolonged period (overnight); left eye for 20 minutes.

3.8.2 Electrophysiology of CRALBP

Representative full-field ERGs, for family 1 and family 2, were consistent with generalised retinal dysfunction affecting rod more than cone photoreceptors with pattern ERG evidence of marked macular involvement. See Figure 3.8.2a, above.

Full data are available for two male siblings, their sister declining to attend for further investigation. The phenotype of early, progressive, nyctalopia, reported in the first decade, with punctate white dots in the peripheral retina were consistent with a retinal dystrophy associated with *RLBP1* mutations. *RDH5* mutations are associated with a stationary nyctalopia, (see Discussion section 4.4). Therefore extended dark adaptation

electrophysiology was performed to identify the more likely candidate gene, which was verified with subsequent genotyping (see Discussion section 4.4, for explicit differences between electrophysiology phenotypes). After a standard period of 25 minutes dark adaptation, rod ERGs were undetectable, in keeping with severe rod-system dysfunction. Bright flash dark-adapted ERGs showed markedly subnormal a-waves, in keeping with loss of rod photoreceptor function, and lower amplitude b-waves. It is likely that this "pseudo-negative" ERG appearance reflects total loss of rod function with preservation of dark-adapted cone function.[299] Photopic 30Hz flicker ERGs were delayed and subnormal in keeping with generalised cone system dysfunction (Fig 3.8.2b). The PERG P50 component was undetectable, consistent with severe macular involvement. Following overnight dark adaptation (right eye) there was partial recovery of dark adapted ERGs in keeping with some recovery of rod function. Both brothers had qualitatively similar findings.

3.8.3 *RLBP1* genotypes

Family 1

Initial diagnoses of fundus albipunctatus (mutations in *RDH5* associated retinal dystrophy) retinitis punctata albescens (mutations in *RLBP1* associated retinal dystrophy) or retinal gyrate atrophy (mutations in *OAT*, ornithine amino transferase, associated retinal dystrophy) were considered. The low plasma ornithine estimation described in family 1 (see 3.8.1), excluded atypical gyrate atophy, and DNA was extracted for *RLBP1* screening (Zheng Li and Phillip Moradi, 60% and 40% respectively of sequencing reactions).

The *RLBP1* gene, which maps to chromosome 15q26,[300] encodes cellular retinaldehyde-binding protein (CRALBP), and was the most likely candidate gene due to the progressive nyctalopia reported, and the lacunar atrophy of RPE that develops over time; see Discussion 4.4 . Conversely, mutations in *RDH5* associated with retinal dystrophy cause a stationary nyctalopia and the cones are less affected and may be normal; [301] see Discussion 4.4 .

Two mutations in *RLBP1* were identified: (IVS4+2T>C) and (IVS3 +2delT). The initial mutation found in family 1 was a previously published mutation in *RLBP1* involving the splice donor site of intron 4 (IVS4+2T>C). Using a splice site prediction programme[302](https://splice.cmh.edu) analysis of this missense mutation revealed a stronger donor splice site, 5 bp downstream, resulting in a frameshift that leads to a premature stop codon in exon 5.[303] The second mutation was a novel deletion of a single nucleotide, abolishing the donor splice site of intron 3 (IVS3+2delT). Prediction analysis of this mutation indicated two stronger splice sites upstream, abrogating *RLBP1* translation. Both mutations co-segregated with disease in all three affected siblings and were not present in unaffected control samples. An unaffected daughter of the oldest sister was a carrier for the novel mutation only; (see Figure 3.8.3a).

Family 2

Affected members of family 2 were homozygous for a novel 12bp deletion in exon 5 (p.F96_F99del) of the *RLBP1* gene. Both unaffected parents and an unaffected brother were found to be heterozygous carriers for this mutation. See Figure 3.8.3b, above.

3.9 Overall results of LCA APEX chip and sequencing strategies

For this project 117 patients were phenotyped (excluding CRALBP families) and 158 patients' DNA samples were sent for Asper LCA chip analysis. A definitive genotype, with two disease causing alleles identified, using the LCA chip and sequencing/ affymetrix chip, has been found in 23% (37/158 patients). The causative genes, where both alleles were identified, is shown in Figure 3.9a(i). The subsequent pie chart and bar chart, Figures 3.9b(i) and (ii) respectively, shows the genotypes with at least one allele identified by percentages and diagnoses. The number of patients identified with only single alleles being identified was 13% (21/158) after further sequencing analysis. The percentage of patients with only one allele identified decreased, as second mutations were discovered, with further sequencing. The most common genes identified in this group were *CEP290 and RDH12.*

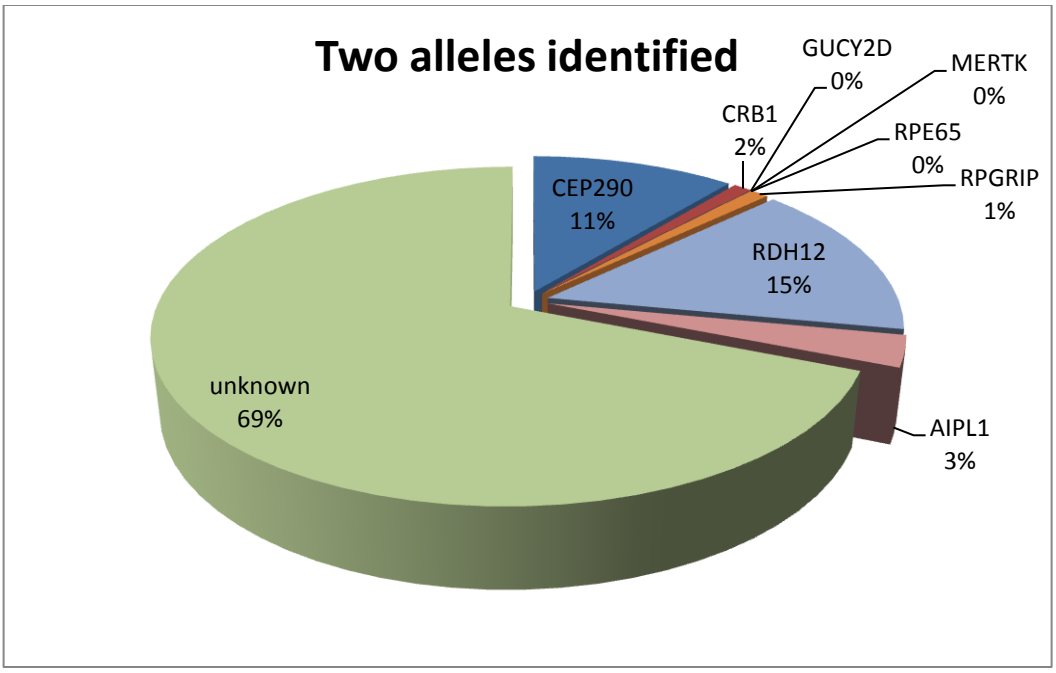

Figure 3.9a(i) Genotype for LCA and EOSRD cohort identified with two mutations by LCA chip and sequencing

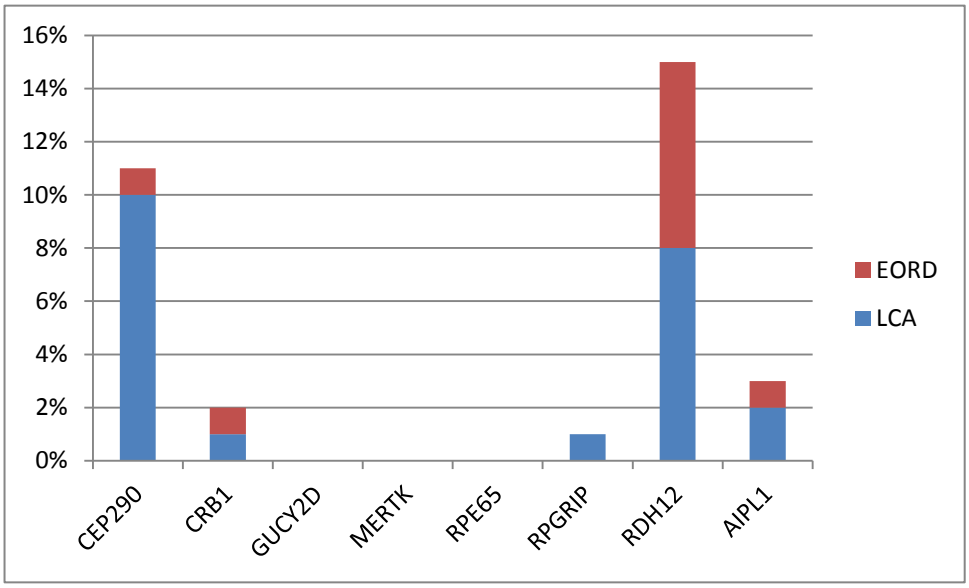

Figure 3.9a(ii) Genotype with diagnosis shown for patients with two mutations identified by LCA chip and further sequencing.

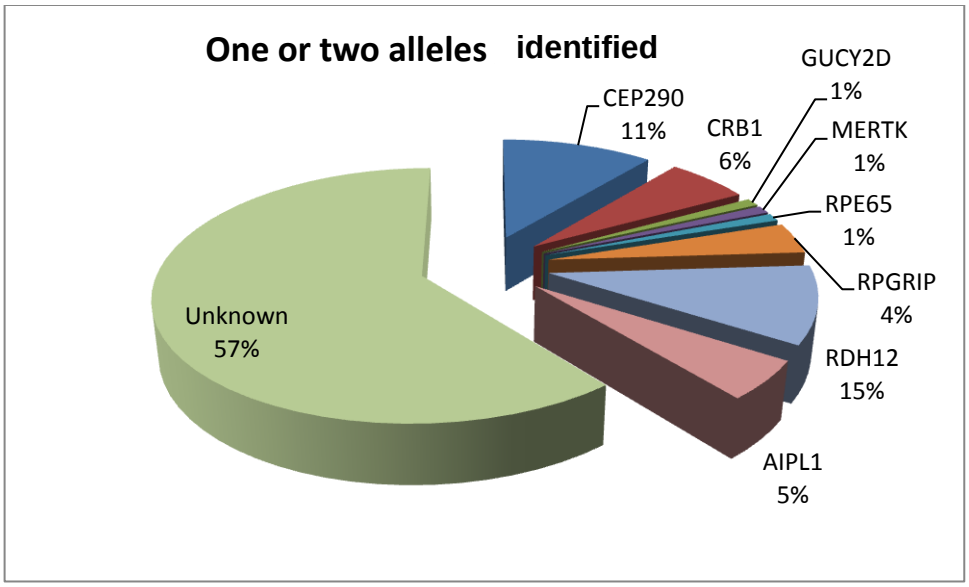

Figure3.9b(i) Genotype for LCA and EORD cohort, with at least one allele identified, by LCA chip and sequencing

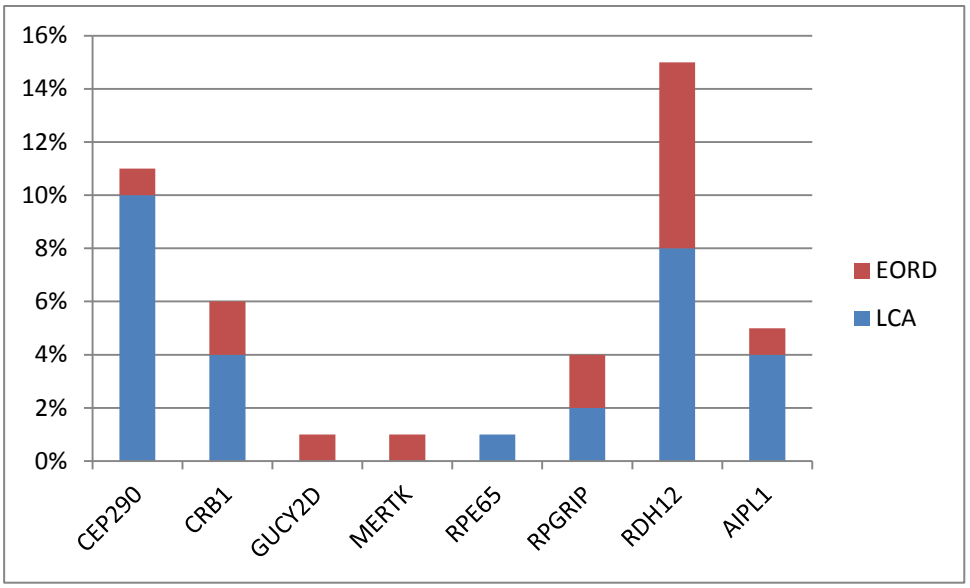

Figure 3.9b(ii) Genotype with diagnosis shown for LCA and EORD cohort, with one or two mutations identified by LCA chip and further sequencing

At the end of the project; 29% of the LCA patients and 15% of the EORD patients had both alleles identified.

4 Discussion

4 Discussion

4.1 The LCA and EORD project and phenotypic summary

The aims of this project were to clinically characterise a cohort of LCA and EORD patients and collect DNA samples for molecular genetic analysis. The primary aim of the study was to obtain a molecular diagnosis and describe genotype-phenotype correlations that will aid in the future diagnosis of patients with these conditions. This project was completed during 2006-8 and it was hoped that a subset of these patients would be candidates for the human *RPE65* gene therapy trial and future inherited eye disease treatment trials. The LCA APEX chip has now been superseded by next generation sequencing but this was a useful technology at the time, during the evolving journey towards large scale targeted genetic testing. This study has added to the limited genotypic and phenotypic data on patients with *RDH12, CEP290 and RLBP1* mutations. It has also highlighted the confusing and inaccurate diagnostic descriptions within the LCA spectrum of diseases, in the literature, and attempted to suggest definitions for LCA, EORD and juvenile onset RD. Inevitably these diagnoses remain phenotypic descriptions which will become less important in this subspecialty with further understanding of the molecular genetic pathogenesis of inherited eye disease, assisted by advancing genotyping and improved comprehension of other genetic and environmental modifiers. Historical studies of LCA reported a very variable phenotype. Theodor Leber, Waardenburg, Alstrom and Franceschetti [3;4;6;304] amongst others recognised that while nystagmus was invariable, some children had residual vision, others exhibited photophobia, and retinal appearances varied from those with typical RP to others with a

normal fundus appearance. This study has confirmed the clinical heterogeneity in both LCA and EORD patients and reported the difference in phenotypic measurements between the diagnosed subgroups.

The natural history of disease varied between the subgroups, with LCA patients reporting earlier visual loss, median 2 months, compared to the other diagnoses; median age 44 months, (see section 3.2.1). LCA patients nearly all had nystagmus (94%) compared with only 39% in the non LCA EORD groups. As expected, squints (70% vs 33%; LCA vs EORD) were more prevalent in the LCA subgroup and oculodigital reflexes were reported in LCA only (45%), (see Results 3.2.4).

Progressive visual loss was noted in LCA during each subsequent decade. However across all EORD subgroups with follow up > 18months, there were equal proportions that lost vision (10 patients), remained stable (10 patients) and deteriorated (8 patients) (see Results 3.5.5). The LCA literature reports conflicting views of stable vision [305] and cohorts with progressive visual loss.[306] *RPE65* mutations have even been reported to improve visual acuity initially before deteriorating.[307] This finding may represent delayed visual maturation rather than a physiological improvement in visual function. There are also inherent inaccuracies in testing visual acuity in infancy, which is additionally difficult in the context of visual impairment. Less recent longitudinal data of visual function in LCA, before accurate genotyping was available, are published. [305;308;309] Snellen visual acuity, grating acuities, dark-adapted visual thresholds, and flash visual evoked potentials were performed in these studies on LCA patients. Visual deterioration was observed in 15%, stability in 75%, and improvement in 10% of the patients (see

Results 3.5.5). Our data are not longitudinally sampled for most patients phenotyped, so it is difficult to comment on the visual acuity progression with these low numbers (n=28, for >18 month follow up data).

This study demonstrated the highest refractive errors were in the LCA group with over a quarter of these patients having a refraction greater than +6.5 D (see Results 3.2.6). This hypermetropic trend was associated with shorter axial lengths . This refractive error could be due to the genetic mutations in these patients influencing the emmetropization process or the size of the infant eye. Consistent published data reveals that LCA patients are known to have high refractive errors and that most patients are high hyperopes. [310] It has been previously suggested that the degree of hyperopia may indicate the presence or absence of associated features in LCA[14] but this association was not substantiated in subsequent research.[311]

Early published LCA phenotypic discussions and detailed "phenotype signs of a genotype" are helpful to direct clinicians but it seems impossible to qualify all criteria set out in flow charts and the more comprehensive detailed genotype-phenotype associations for large cohorts did vary slightly from our observations. [55;64;82;312].

For example, in our study two in three of the LCA patients with *RPGRIP1* mutations did not have hypermetropia > +7D or photophobia,[55] and low myopia was observed in one case. However diagnostic criteria of early peripheral and macular degeneration of the retina with poor vision were consistent with the published *RPGRIP1* mutation phenotype.[40;55;82]

Similarly, of the two patients with *AIPL1* mutations with LCA, photophobia was absent and the -5D myopia in one patient was inconsistent with associated moderate

hypermetropia to low myopia descriptions.[55;224] Consistent with published *AIPL1* phenotypes,[224] variable retinal appearances, with varying degrees of chorioretinal atrophy and intraretinal pigment migration, were noted. Atrophic and/or pigmentary macular changes were also present.

Patients with *CRB1* mutations were very consistent with published phenotypes. All patients had moderate to high hypermetropia, early night blindness, visual fields limited to the central 15 degrees and pan-retinal pigmentation with increased retinal thickness on OCT[23;159] and early macular changes.[55]

Although, some authors have attempted to divide LCA into type I, early cone rod dystrophy with photophobia and type II, early night blindness with rod-cone dystrophy aetiology, over 55% of the LCA patients in this study did not fit these limited, mutually exclusive criteria.[55] The lack of longitudinal data with this young age group, the varying ability of parents to elicit and recall symptoms accurately and the subsequent rapid degeneration of both photoreceptor classes may limit the option to distinguish the chronicity and disparity in rod and cone pathophysiology in an accurate and meaningful way.

The phenotypic data has shown clearly the diverse spectrum of LCA and EORD but as with any phenotype-genotype correlates, there are many overlapping features. Symptoms and signs are helpful but not always definitive. This is to be expected in monogenic disorders when other unknown genetic, molecular and environmental pressures may influence the expected phenotype.

4.2 The LCA APEX chip

Disease associated variants were found in 49 out of 158 individuals (31%) by the LCA APEX chip. Homozygous or compound heterozygous mutations were found in 20 (13%) patients using the LCA APEX chip. A further 29 patients (18%) had single mutations, after using the LCA APEX chip only, without futher analysis with sequencing. The LCA APEX chip identified 63% (34/54) of the LCA group and 13% (15/104) of the EORD group with at least one mutated allele (see Results 3.3.1). Twelve patients of the LCA subgroup (12/54 or 22%) and 8 patients of the EORD subgroup (8/104 or 8%) had a single mutation only identified. Of the 29 patients with both alleles identified, 22 were LCA patients (22/54 or 40%) and 7 were EORD patients (7/104 or 7%). These findings of a higher identification of mutations in the LCA subgroup than the EORD subgroup is consistent with LCA APEX chip development and the manufacturer's aims; "prioritising the genetic identification of LCA mutations".

Three previous studies have reported the results of using the LCA APEX chip in screening for mutations in LCA. Zernant et al. [71] identified mutations in 20.3% to 23.8% of the total number of patients in their cohort. Yzer et al. [214] reported that 24% (14/58) of their subjects had homozygous or compound heterozygous changes and in a further six subjects, a single mutant allele was identified. More recently, Henderson et al.,[313] investigating both LCA and EORD patients, identified a mutation in both alleles in only 11.7% of subjects but in a further 18.3% of subjects one allele was identified.

Zernant et al. [71] reported only the number of alleles identified but did not report the percentage of subjects with both disease associated mutations identified. Reviewing the paper, 22 patients (11%) of their cohort were identified as having two disease associated

alleles. The study by Yzer et al. [214] reported an LCA group with 24% homozygous or heterozygous changes with a further 10% of subjects with a single mutant allele identified. It is important to note that earlier versions of the LCA APEX chip were used for these studies and therefore fewer known mutations and genes were available and this may explain the lower detection levels compared to this study.

The LCA array sensitivity has been criticised that there is a limited capacity to identify novel variants at previously identified SNP sites, as has been reported on other arrays.[314] However no overlap between our novel sequenced mutations and SNP sites were evident.

The Zernant et al. [71] study includes the P701S change in *GUCY2D*. However, this is present in 6.3% of the normal British population and therefore seems unlikely to be a pathological variant.[313] Furthermore an unaffected parent carrying the mutation with SNPs in *GUCY2D* and *RPGRIP1* has been reported which adds to the likelihood that this variant is not pathogenic.[313] For this reason the P701S variant was excluded in this study.

Of the 137,704 allele calls made, there were 4,682 uni-directional call failures (3.4%) and 895 bi-directional call failures (0.64%). Call failures occurred when the LCA APEX chip did not detect a signal for a particular allele. However these are similar to other published chip call failure rates (3.07% and 0.47% for uni- and bi-directional failures). [313]

A comparable, diagnostic microaaray for all the known genes (40 up to now) responsible for the autosomal dominant and recessive RP and Leber congenital amaurosis (LCA) has been published.[315] The shared genes of LCA and RP included were *CRB1*, *CRX*, *IMPDH1*, *LRAT*, *RDH12*, *RPE65*, *TULP1*. This new chip analyzes 240 single nucleotide polymorphisms (SNPs) (6 per gene) on a high-throughput genotyping platform (SNPlex, Applied Biosystems). The six SNPs per gene were selected and prioritisd using the

following criteria: (i) high informativity according to SNPbrowser (2007) and dbSNP (http://www.ncbi.nlm.nih.gov); (ii) position physically close to the gene, and if possible, located in the promoter, intragenic and downstream regions; (iii) that they belonged to different haplotypic blocks. Genetic diagnosis using this microarray is based on the co-segregation analysis of SNP haplotypes (with disease) in independent families. The most important issue of this type of analysis is genetic informativity. This depends on the average heterozygosity of the genetic markers and the number of meioses available. An advantage of this approach is that in a single genotyping step, the number of RP candidates to be screened for mutations is considerably reduced, and in the most informative families, all the candidates are ruled out at once. This analysis allowed exclusion of non-causative genes (~50% in smaller familes, >70% in larger families), thereby diminishing greatly the number of candidates to be sequenced per family .[316]

In summary, this study has demonstrated that the LCA APEX chip is a useful, sensitive technology with a low call failure rate. This has been shown by the 100% sensitivity for detection of known mutations in *CEP290*. The low percentage of call failures are no greater than the artefactual discrepancies that arise with direct sequencing. The continually updated novel mutations and genes on the LCA APEX chip will increase the proportion of patients for whom a molecular diagnosis can be obtained. However the rate of genetic analysis advancement is so rapid that this technology has now been superseded by Next Generation Sequencing (NGS); either exome sequencing or targeted capture of all known retinal genes. This information will improve genetic counselling in affected patients and assist the identification of families who may benefit from future therapeutic trials for early onset retinal dystrophies.

4.3 CEP290

In this study 11% of patients (17 patients) within the cohort of LCA and EORD were found to have *CEP290* mutations on the LCA APEX chip. Of these 17 patients; 14 were diagnosed with LCA, 2 with EORD and 1 with a later onset RD. However in the LCA patient cohort alone, 26% (14/54) of mutations identified occurred in *CEP290*. This is consistent with LCA literature demonstrating *CEP290* mutations causing >20% of LCA.[34;69] Furthermore, all our patients had a north European ancestry which is in contrast to findings in south European studies, where *CEP290* mutations were less prevalent in Italy and Spain, reporting only 4.2% [81] and 8% [317] of LCA patients with mutations. This has led to suggestions that the most prevalent mutation, p.C998X, may be an ancient mutation that arose in the north of Europe several centuries ago.[34]

The most prevalent mutation, p.C998X, is an intronic change that creates a strong splice-donor site that results in the insertion of a cryptic exon in the *CEP290* messenger RNA and competes with the normal splice-donor site. It was initially thought that the residual correctly spliced product is believed to be sufficient for normal cerebellar and renal function but not for correct function of the photoreceptors.[34] However, this hypothesis has been challenged by analysis of *CEP290* mutations with residual, correctly spliced product that has since been associated with the severe non-syndromic LCA phenotype.[69] This genotype-phenotype correlation is consistent with our study. An intronic mutation (IVS50+9T4G [c.6960+9T4G]) has been identified that creates a strong splice (GT) donor site 4 bp upstream of the wild-type splice donor site that consists of a GC sequence. This mutation results in p.C998X.[199] Interestingly, the mRNA has been isolated from mutant cat retina and RPE in a feline model of *CEP290* associated retinal

dystrophy. This feline mutation contained a 4-bp insertion, which created a frameshift resulting in two missense codons, followed by a stop codon.[318]

The variable expression of *CEP290* null mutations, ranging from non-syndromic LCA, Joubert syndrome to a severe, fatal hydrocephalus (MKS or Meckel Gruber syndrome) may demonstrate the significant influence of other genetic factors.[34;69;192;195;319;320] The recent finding of a homozygous *CEP290* nonsense mutation (p.E1903X) together with a MKS3 compound heterozygote in Bardet Biedl Syndrome has highlighted the involvement of triallelic inheritance to explain the diverse, expanding *CEP290* spectrum.[321] The identical genotype but significantly contrasting phenotypes of the siblings (patients 3 and 4) in our cohort may be explained by the epistatic effect of a third mutation in a known or unknown, second LCA/EORD gene (see Results 3.7). Interestingly, family members who carry triallelic mutations have been shown to have more severe LCA phenotypes[279] and further evidence from murine models of epistatic effect have been found as sequence variations in other LCA genes, such as *RPE65*[322] and modifiers of Tubby retinal degeneration 1.[323]

The variability in phenotype within a single genotype has been observed for various *CEP290* mutations. Compound heterozygous mutations in *CEP290* were identified in a female proband and her two less affected cousins[324] with the frequent p.C998X (c.2991+1655A>G) founder mutation and a novel nonsense mutation in exon 7 (c.451C>T, p.Arg151X). One of the cousins had a visual acuity that had reached a level of 20/32 at age 5, which is high for patients with *CEP290* mutations. Analysis of the *CEP290* mRNA in affected individuals revealed altered splice forms in which either exon 7 or exons 7 and 8 were skipped, which code for coiled coil domains.[325] These may have

a less severe phenotypic affect than the heterozygously present *MERTK* mutation, which was found in the most severely affected proband. Similarly the gene *AHI1* encodes a protein that appears to have a similar pathway interaction as shown between CEP290 and rab8a. *AHI1* may have modifying alleles in *CEP290* associated syndromic LCA.[326]

This study has identified a consistent phenotype that is seen in these *CEP290* associated LCA/EORD patients (see Results 3.7).[34;55;327] Patients' vision was very poor from infancy and progressive visual deterioration with age occurred. Fourteen patients had LCA and two patients had a childhood onset rod-cone dystrophy (patient 3 and 5) and the sibling of patient 3 (patient 4) had a less severe adult onset rod-cone dystrophy. The LCA patients had poor vision, nystagmus, night blindness and photophobia which were noted in infancy. Colour vision was absent in all LCA patients on HRR plate testing. Only tritan plates were seen by three patients with rod-cone dystrophy (patients 3,4,5). The degree of photoreceptor degeneration in *CEP290* patients is variable in previous reports. It has been suggested that *CEP290* associated LCA is the cone-rod type, as observed by Perrault et al.[69] although conversely EORD with visual acuity and color vision being relatively well preserved is noted in other patients.[328] In addition, blind retinas have been shown to retain photoreceptor and inner laminar architecture in the cone rich central retina with rapid rod cell death consistent with rod-cone dystrophy.[329]

The majority of patients were moderate hypermetropes (mean +4.3 D, median +6 D) which correlated with short axial length. *CEP290* LCA patients had symptoms of early poor vision, nystagmus, night blindness and photophobia which were noted in infancy (see Results 3.7). These findings correlate well with the early visual reduction, hyperopia

and photoaversion reported in other similar *CEP290* LCA cohorts[34;69;330] and specific visual acuity data reporting 82% of this subgroup with <CF vision .[331]

Variability in visual acuity in four affected siblings has been noted previously, ranging from PL to 20/80 (6/24).[34] Similarly, in our cohort, one proband (patient 3) had a sibling (patient 4) with an identical genotype but a less severely affected phenotype and visual acuity; HM in one sibling compared with LogMAR 0.3 (~6/20) in the other sibling (see Results 3.7). Fundal examination revealed pale optic discs, attenuated retinal vessels and a loss of the foveal reflex. Only one adult patient had minimal, true bone spicule, peripheral pigmentary migration (patient 4). One patient (patient 5) presented with multiple white dots in perifoveal and peripheral distribution and three patients presented with peripheral white dots and choroidal sclerosis (patients 6,8 &10) (see Results 3.7). The limited published fundal descriptions include small white dots or a "marbleised" appearance [69;332]

OCT measurements could only be carried out in five patients due to nystagmus or inappropriate age. Foveal thickness was attenuated in the LCA group (median 232 microns) (see Results 3.7). This finding is consistent with initial description by Chang et al. of CEP290 mutations leading to rapid reduction in outer segment length and outer nuclear layer (ONL) thickness.[191] On spectral domain OCT (SD OCT), in patient 8 with LCA (16 years old) the outer retinal layer was visible throughout the macular scan, although this was thinner than normal in the LCA patient**.** In SD OCT images of Patient 5 with adult onset rod-cone dystrophy, the photoreceptor inner/outer segment junction (PSJ) was visible throughout the macular scan (see Figure 3.7i). The retention of the outer nuclear layer on spectral domain OCT imaging in patients with the common

p.C998X (*CEP290*) mutation has been previously described.[333] Such preservation tended to decline with age. However, patients with another null mutation did not show preservation of the ONL nor any visible PSJ at the central macular area.

Increase in patient age autofluorescence from the accumulation of lipofuscin within the RPE lysosomes during the phagocytosis of rod outer segments is used as an indirect measure of RPE function. Minimal or no autofluorescence was seen in five patients in whom imaging was possible (see Figure 3.7h). Furthermore, the distinctive hyperfluorescent perimacular ring recorded in patients 5 and 8 has been observed in the most recent published CEP290 associated LCA phenotype data.[334]

CEP290 is expressed in the dendritic terminals of olfactory sensory neurons (OSNs), which contain multiple basal bodies that form the base of extending cilia. [199] There is mis-localisation of olfactory cilium G proteins in CEP290 patients and not other proteins involved in olfactory transduction. In this study, patient 15, an individual homozygous for the prevalent mutation, has been previously shown to exhibit severely abnormal olfactory function (section 3.7). However, in contrast, normal olfactory function has been reported previously in compound heterozygotes, with a single missense mutation and the most prevalent *CEP290* mutation, C998X (patient 3, 4 and 7). Furthermore, normosmia was also observed in a patient with another homozygous missense mutation, p.W7C. This mutation has been associated with Joubert's syndrome. Significantly, there have been very few studies that have addressed the olfactory function in the visually impaired. Previous data has implied that blindness, per se, has little effect on chemosensory function in a study comparing sighted and blind subjects to olfactory and gustatory tests.[335] Furthermore, our data may be considered in contrast to a well quoted, but

unproven hypothesis that visually impaired individuals may have increased acuteness in their other senses. This sensory compensatory theory has no rigorous evidence and it is notable that specialized training enhances performance on chemosensory tasks more significantly than any associated visual morbidity.[336] Importantly, our study highlights the significant anosmia associated with this rare cause of congenital blindness.

The altered anosmic status in certain *CEP290* genotypes and the poor visual function, hypermetropia, peripheral subretinal white dots and north European ancestry may guide molecular investigations of *CEP290* in patients with these features. This unusual clinical phenotype may reflect the unique role of *CEP290* in the visual cycle. The study of the various olfactory phenotypes for each genotype could further our understanding of the diverse role of this ciliary protein involved in sensory mechanisms including EORD and LCA. A molecular diagnosis of *CEP290* mutations might have considerable consequences towards the clinical prognosis of an individual. Given the potential involvement of ciliary modifiers and the importance of cilia throughout the body, the development of various additional clinical manifestations should be taken into account. Long-term clinical neurological and nephrological follow-up is appropriate, since some features have a later onset.

4.3 *RDH12* genotype and phenotype

In our cohort, there were two compound heterozygotes and one homozygote variant observed in the later onset phenotype: c.A269fsX1 and p.L99I, (both inherited heterozygously with null mutations likely to be susceptible to nonsense mediated decay; p.R106X and p.R295X respectively) and the homozygous p.F152I. The inheritance of the

L99I mutation together with a nonsense mutation of the second allele, a compound heterozygous, is responsible for a more severe phenotype. *In vivo* variable effects on RDH12 function have been noted with these mutations. Specifically, L99I has shown dramatically reduced ability to convert all-*trans* retinal to all-*trans* retinol in the presence of NADPH, exhibiting <10% wild type levels of activity.[120] In addition, it has been reported that the L99I mutation together with a stop codon is responsible for a more severe phenotype than the p.L99I homozygous mutation.[337]

The c.A269fsX1 mutation causes a frameshift that would result, if translated, in a truncated, non-functional protein, although the mutant transcript would probably be eliminated by nonsense mediated decay.[120] This mutation was found in the compound heterozygous state with another mutation in patients who were all of British Caucasian descent. This mutation was originally described in a German male in the homozygous state,[31] making this a north European mutation. Finally, the p.F152I mutant would change the protein structure to incorporate a hydrophobic, aliphatic amino acid in place of a hydrophobic, aromatic amino acid, which may alter tertiary structure within a beta pleated sheet. It is therefore difficult to explain the later onset of visual loss noted in these individuals given the devastating molecular implications to the RDH12 structure or function.

The p.C201R mutation , the most common mutation, is also a published loss of function variant.[120] This mutation was found to be homozygous in all patients of Gujurati Indian descent and may represent a founder mutation in this population. The Cys residue is located within the catalytic motif (YXXXK), just after the catalytically important Tyr.

This change from a hydrophobic residue to a polar residue within the catalytic motif can disrupt important residue alignment involved in catalysis.

Exon 5 appears to be a mutational hotspot with nine of 21 mutations located within this region. Screening of exon 5 may be a first step in the identification of patients in a large cohort. The novel variant p.R161W affects the same codon as the only SNP seen in the screening of this cohort, rs17852293 (p.R161Q). *In silico* analysis of this variant was inconclusive, but it has been considered by our group as a potential disease variant due to it being found in compound heterozygous state with a frameshift mutation in families published after this project completed.[296]

Deletion of the *RDH12* gene in mice increases the susceptibility to photoreceptor apoptosis resulting from exposure to high intensity illumination.[124] However, this knockout model has normal levels of visual pigments suggesting that either other dehydrogenases can compensate for RDH12 or that RDH12 has a less important role in the visual cycle in the murine eye. RDH12 does, however, contribute to all-trans retinal clearance, as its loss of function results in slightly increased accumulation of retinotoxic N-retinylidene-N-retinylethanolamine (A2E), which accumulates when all-trans retinal is not metabolised normally. However in our study autofluorescence, an indirect measure of A2E, was not significantly raised and patients imaged had hypofluorescent patchy patterns or no autofluorescence evident (section 3.7). This is consistent with low levels of A2E in retina of patients with *RDH12* mutations.

Janecke et al. (2004)[31] first reported that mutations in *RDH12* were associated with Leber congenital amaurosis (LCA) an infantile onset form of severe rod–cone dystrophy. *RDH12* mutations were found subsequently in a less severe form of childhood onset

autosomal recessive retinal dystrophy.[120] A number of *RDH12* mutations have been biochemically evaluated. A prevalent published mutation, a T49M change, would introduce a more hydrophobic side chain that would likely interfere with the binding of the 20-phosphate group of NADP.

In summary, RDH12 protein mutational studies suggest a reduced expression and activity, due to described mutations being widely distributed across the predicted surface of the protein. The missense mutations affect residues that may disrupt functional domains involved in protein interactions, folding and catalytic activity. Further analysis of RDH12 mutations with published programmes SIFT, Polyphen and pMUT shows the predicted intolerance or damaging effect of these variants. However, the mutational analysis highlights the inherent problems arising from theoretical molecular prediction programmes. Firstly, little is known about the exact tertiary structure of RDH12 despite published low resolution models of an apparent globular molecule comprised of alpha helices and beta sheet secondary structures.[120] Furthermore, they take no account of the complexity of the distinct protein interaction involved in the overall process of visual transduction. It is valid to suggest that other components of the visual cycle could modify the functional consequences of these pathogenic mutations. It is also important to acknowledge that the experiments demonstrating that variants, alone or in combination, have a negative effect on *in vitro* RDH12 assays of catalytic activity may not reflect *in vivo* function. Presently, for these reasons the clinical phenotype associated to each mutation is difficult to establish.

In our cohort 7% of all patients had one or two mutations in *RDH12* (see Results 3.4).

This increased to 13% of the LCA patient subgroup. Prevalence data from a large cohort of 1011 patients with autosomal recessive retinal dystrophy (arRD) was comparatively lower with only 2.2% of patients with *RDH12* mutations.[120] Previously, a smaller series of 110 unrelated patients with LCA reported *RDH12* mutations in 4.1% [118]

Schuster et al. (2007)[129] described the RDH12 mutated phenotype as LCA or early onset RP, characterised by poor, yet functional vision in early life, followed by progressive decline due to rod-cone degeneration. The other published symptomatic features [118;129] including nyctalopia, mild-moderate hyperopia, mainly an absence of photophobia, severe colour vision disturbances and field defects in childhood are consistent with our data. Further consistencies included occasional subcapsular cataract, bone spicule and panretinal pigmentation from an early age and macular granularity that rapidly evolved into pronounced macular atrophy in individuals >7 years old. There are limited data explaining the histopathology of intraretinal pigment migration (bone spicules). The rhodopsin knockout mouse (*Rho*$^{-/-}$), a murine model of human retinitis pigmentosa, demonstrated that the migration of RPE cells along blood vessels of the inner retina occurs due to the proximity and contact of the inner retinal vessels with the RPE.[338] Bone spicule pigmentation is caused by pigmented cell clusters forming over the retinal capillaries , except for large surface vessels. This is hypothesised to be a consequence of the thinning retina and the approximation of the inner retinal layers with the RPE. This theory may explain the distribution of intraretinal pigment and para-arteriolar sparing in *RDH12* retinopathy, which is also described in *CRB1* retinopathy.[339]

The disparities noted comparing our data with previous studies include the visual fields in two patients (patients 2 and 7) with temporal island preservation instead of the

symmetrical constriction. In addition, large areas of macular atrophy associated with a yellow pigmentation appeared in all cases older than 6 years old with the exception of a 10 year old patient with pigmentary mottling at the macula bilaterally (see Results 3.4). This unusual macular appearance may be useful in distinguishing the genotype in retinal dystrophy patients. The severe macular atrophy in the *RDH12* phenotype is also consistent with the increased susceptibility at the macula to light-induced photoreceptor apoptosis that has been observed in *RDH12* knockout mice,[340] supporting evidence for the unique role of this enzyme as inner retinal retinoid regulator. However, the disease mechanism is not solely dependent upon loss of enzymatic function and recent evidence has suggested that some missense mutations in *RDH12* retain the protein's function but lead to accelerated degradation by the ubiquitin-proteosome system.[127]

The severe phenotype observed in patients with *RDH12* mutations suggest that its enzyme product has a unique role in the visual cycle despite the presence of other retinol dehydrogenases expressed in photoreceptors, retSDR1 and prRDH, with the similar ability to catalyze the reduction of all-*trans* retinal to *all-trans* retinol.[120;124] The potential for redundancy would be expected to predict a milder phenotype as occurs in *RDH5* mutations, the gene encoding 11-*cis* retinol dehydrogenase of the RPE, which results in fundus albipunctatus, a nonprogressive nyctalopia without retinal dystrophy.

Gene replacement therapy targeting the molecular pathology may be difficult because it is not fully understood if the pathological mechanism is due to a deficit in chromophore production or a deposition of toxic aldehyde intermediates or both. In the latter theory, the exogenous chromophore, 11-cis-retinal that facilitates the phototransduction cascade, possibly exacerbates associated functional loss. Understanding the specific role of

RDH12 in the visual cycle remains an essential prerequisite in the design of therapeutic intervention.

4.4 CRALBP

Two families are described with novel mutations and distinct phenotypes in association with biallelic mutation of *RLBP1,* the gene encoding cellular retinaldehyde binding protein (see Results 3.8). As described previously, both families were referred to the clinic and this study due to an early childhood onset of retinal dystrophy symptoms but after 5 years of age, defined by this study as juvenile onset RD. The clinical, electrophysiological and molecular biological features are described (see 3.8.2).

The first description of autosomal recessive *RLBP1* mutations, associated with retinal degeneration, reported "small white dots" throughout the fundus but no bone spicule pigmentation.[341] Conversely, mild pigmentary migration was evident in all our patients including the youngest sibship (family 2) member. Subsequent published descriptions of patients with *RLBP1* mutations featured a retinitis punctata albescens (RPA) phenotype consistent with a recessive, progressive rod-cone dystrophy that is characterised by nyctalopia and white punctata.[342-344] The older sibship in this study, family 1, is consistent with Swedish phenotypic data reporting a homozygous *RLBP1* mutation (p.R234W), with macular atrophy and circular areas of geographic atrophy in the peripheral retina in patients over 30 years, which has been referred to as Bothnia Dystrophy. [342;345]

No previous autofluorescence (AF) data have been published in CRALBP associated dystrophy and the very reduced levels in the 24 year old patient and less severe AF

reduction in the residual, non atrophic, retina of the 75 year old are significant. The two mutant CRALBP proteins in each sibship in this study are assumed less likely to stimulate the isomerisation of all-*trans* to 11-*cis* retinol, which could account for this AF reduction.

The disorder, in the early stages, can be mistaken for fundus albipunctatus, in which night blindness occurs due to impaired regeneration of rhodopsin consequent upon *RDH5* mutation but unlike that disorder, the retinal degeneration due to *RLBP1* mutation is progressive. There are well known distinctions between RPA (progressive) and fundus albipunctatus. Most patients with FA, show complete recovery of dark adapted ERGs following extended dark adaptation whereas RPA patients only show partial recovery. In addition, cone ERGs are less affected in FA than RPA and may be normal.[346]

Consistent with previously published *RLBP1* patients [342-344;347]; both our families reported nyctalopia from early childhood with progressive loss of peripheral vision in the 3rd-4th decade occurring in the older sibship (see Results 3.8.1). A perimacular ring of white stippling is observed in young patients, and the scallop-bordered, lacunar atrophy of the midperipheral RPE develops over time. This is similar in appearance to gyrate atrophy, however, plasma ornithine levels are normal, early cataracts have not been documented and myopia is not seen.

Our patients have 2 novel mutations and a previously described mutation in *RLBP1,* that segregate with disease in both pedigrees. The novel mutation in Family 1, IVS3 +2 del T, is predicted to interfere with mRNA processing. The splice junction mutation is predicted to activate a cryptic splice site in exon 3. This activation would result in either a truncated protein product or degradation of the incorrectly spliced transcript via

nonsense-mediated RNA decay.[348;349] By contrast, the F96_F99del mutation in Family 2 is a missense mutation, involving 4 amino acids, which may compromise tertiary structure or CRALBP-retinoid molecular dynamics. Three of the four amino acids (R, F, I) are well conserved across several species adding weight to the association with the pathological phenotype. This deletion of four amino acids (L,R,F,I) does not occur in reported functional regions of CRALBP. Several homology models map pathology associated mutations either in or adjacent to the putative ligand-binding cavity (ranging from amino acid 165-244). [350;351] Furthermore, our novel 12 bp deletion does not include six residues, which have been identified as crucial for the hinge-movement of the lipid exchange loop of CRALBP, enabling the binding and release of retinoid.[350] This in frame deletion may be more benign to the function of CRALBP than the novel splice mutation in family 1 consistent with a possible, less severe phenotype in family 2. Importantly, a comparison of phenotypic severity is difficult to assess due to the older age group of family 1 and the progressive nature of CRALBP associated retinal degeneration.

The electrophysiological investigation of the 32 year old brother in family 2 (II-2) demonstrated generalised retinal dysfunction affecting rods more than cones. These findings are consistent with a previous electrophysiological study in Bothnia Dystrophy,[352]demonstrating that the cone b-wave and 30Hz flicker amplitudes were significantly better preserved than were the b-wave amplitudes of the rod and mixed rod-cones responses and the a-wave amplitude of the mixed rod-cone response, indicating later disturbance of the cones compared with the the rods. Hence in *RLBP1* associated disease the glial and inner retinal cell types are affected at a relatively earlier stage

compared with the outer photoreceptor layer. The rods also appear to be influenced before the cone system.

Scotopic ERGs showed partial recovery of rod function following prolonged (overnight) dark adaptation (DA) of the right eye in patient II-2 (see Results 3.8.2). This finding is consistent with a previous study of patients with Bothnia Dystrophy (BD) consequent upon a missense mutation (R233W).[352] The investigators reported the effect of 10 hours DA on the ERG of younger BD patients. In the initial stage of the disease the disturbed retinal function was found to be partially reversible with extended DA. This partial recovery may relate to the 10 hour period of extended DA given that a further study reported normalization of dark adaptometry and scotopic ERG after 20 to 24 hours DA.[353] A slow regeneration of rhodopsin seems to occur at least up to 24 hours. It has been hypothesised that tightened retinoid binding properties in certain CRALBP mutants may be partly responsible for the retardation of RPE visual processing in these patients.[354] A recent study also concluded that extremely long DA (24h) provides significant additional capacity of recovery of rod function and also suggested gain in the activity of the inner retinal layer based on recovery of the b-wave of the dark-adapted ERG.[355] An alternative explanation is that the initial electronegative appearance of the bright flash dark-adapted ERGs merely reflects cone-system origins in a functionally cone isolated retina, such has been described in vitamin A deficiency and also occurs in fundus albipunctatus.[356] The cone system has a property, often (inappropriately) called the “photopic hill phenomenon” in which increasing stimulus intensity of stimulation in a normal retina under photopic conditions eventually results in an increasing a-wave amplitude accompanied by a reducing b-wave amplitude, and thus resembling a

"negative" ERG. The phenomenon reflects an increasing desynchronisation of the On and Off components of the photopic ERG,[357] but can also be observed under dark adapted conditions in the absence of rod function.[356]

The findings in our study extends our knowledge of the disorder, and reports two novel mutations. Molecular screening of *RLBP1* and comprehensive electrophysiological investigations should be considered in patients with early onset white dot nyctalopia or with apparent late-onset gyrate atrophy who do not have severely altered ornithine levels. The moderately slow progression of this disease provides a long window of opportunity for gene-replacement or other novel therapies. The presence of retinal autofluorescence in family 1, albeit reduced, suggests the ability to regenerate chromophore despite null mutations in this gene.

5 Conclusions and future research

The research discovering the molecular causes of LCA in the past 15 years since the first gene LCA1 (*GUCY2D*) mutations were discovered in 1995 has increased our understanding significantly since the early descriptions by Leber. The availability of molecular results, defining the disease associated genetic mutations, and the advantages of modern electrophysiological investigations has significantly advanced the diagnostic information available. Fortunately, this has improved prognostic information and assisted the design of novel therapeutic advances available to our patients.

The aims of the research presented here were fulfilled by recruiting a large cohort of patients, successfully phenotyping the diverse clinical features and achieving a molecular diagnosis in 31% of patients. Some of the patients in this cohort may be recruited in future to gene therapy trials or the present RPE65 gene therapy trial that commenced in 2007.

The LCA APEX chip has been demonstrated as an effective, first pass screening technique for assaying known SNPs in the LCA genes. It is a useful investigative tool in early onset retinal dystrophies, although expanding the clinical diagnostic group to EORD yields a lower detection rate. Genotype-phenotype correlations have been clearly demonstrated for *RPE65, RDH12, CEP290, CRB1* and *RLBP1*. Furthermore novel mutations and phenotypic data have been established including anosmia data in *CEP290* associated disease and electrophysiology in retinitis punctata albescens (RPA) or Bothnia Dystrophy.

It is important to observe that 69% of the patients studied do not have a molecular diagnosis and significant research remains to complete this difficult task. Given that *CEP290* and *RDH12* cause such a large proportion of disease in this project and other studies, it may be useful to prioritise this molecular work. It would also be very interesting to explore the prevalence and genotype-phenotype correlations of other genetic causes of early onset retinal dystrophy, as demonstrated by the novel findings in the families with RPA.

New high throughput next generation sequencing (NGS) methods, which allow the analysis of many gene targets in parallel, are expanding available tests, and recent research assessing their validity in a diagnostic setting demonstrates how such strategies may be developed within a clinical service.[358-360] NGS permits the simultaneous analysis of many DNA templates in one reaction to exponentially increase the sequencing output of a single experiment.[361;362] NGS also offers the capacity to 'pool' DNA preparations from different individuals, providing an additional boost to the throughput of each sequencing run.[363] Whole genome sequencing is now possible, but the expense and amount of data produced means that this is beyond the capacity of most diagnostic laboratories, in terms of data storage and meaningful analysis. Presently, the targeted sequencing of coding regions and regions of the genome implicated in disease are the most pragmatic compromise solution.

After the successful proof of principle in a research environment, O'Sullivan et al.[364] designed an NGS assay covering 105 genes in all forms of RP. Using this NGS strategy, it was reported that testing can identify and improve the mutation pick up rate from 24%, with conventional genetic testing, to over 50%. Importantly, although the cost of NGS

per base of sequencing is dramatically reduced when compared with conventional methods, this is likely to be offset by the increased demands for both genetic testing and genetic counselling as a result of improved mutation detection rates.[365] These huge technological advancements have the potential to revolutionise inherited eye disease service delivery in the near future. Such a resource has significant implications for clinical management, economic modelling and commissioning of services for patients across all medical specialities.

Reference List

1. Leber T. Ueber Retinitis pigmentosa und angeborene Amaurose. *Albert von Graefes Arch Ophthal* 1869;**15**:1-25.

2. FRANCESCHETTI A, Dieterle P. [Differential diagnostic significance of electroretinogram in tapeto-retinal degeneration.]. *Bibl.Ophthalmol.* 1957;161-82.

3. WAARDENBURG PJ. Does agenesis or dysgenesis neuroepithelialis retinae, whether or not related to keratoglobus, exist? *Ophthalmologica* 1957;**133**:454-60.

4. Alstrom CH, Olson O. Heredo-retinopathia congenitalis monohybrida recessiva. *Hereditas* 1957;**43**.

5. SCHAPPERT-KIMMIJSER J. Value of electroretinography in cases of doubtful diagnosis in the blind and partially sighted child. *Ophthalmologica* 1958;**135**:147-54.

6. WAARDENBURG PJ, SCHAPPERT-KIMMIJSER J. ON VARIOUS RECESSIVE BIOTYPES OF LEBER'S CONGENITAL AMAUROSIS. *Acta Ophthalmol.(Copenh)* 1963;**41**:317-20.

7. Rahi JS, Cable N. Severe visual impairment and blindness in children in the UK. *Lancet* 2003;**362**:1359-65.

8. Heckenlively JR, Foxman SG, Parelhoff ES. Retinal dystrophy and macular coloboma. *Doc.Ophthalmol.* 1988;**68**:257-71.

9. Schuil J, Meire FM, Delleman JW. Mental retardation in amaurosis congenita of Leber. *Neuropediatrics* 1998;**29**:294-7.

10. Tabbara KF, Badr IA. Changing pattern of childhood blindness in Saudi Arabia. *Br.J.Ophthalmol.* 1985;**69**:312-5.

11. Foxman SG, Heckenlively JR, Bateman JB *et al*. Classification of congenital and early onset retinitis pigmentosa. *Arch Ophthalmol.* 1985;**103**:1502-6.

12. FRANCESCHETTI A, Dieterle P. [Diagnostic and prognostic importance of the electroretinogram in tapetoretinal degeneration with reduction of the visual field and hemeralopia.]. *Confin.Neurol.* 1954;**14**:184-6.

13. SCHAPPERT-KIMMIJSER J, HENKES HE, Van den Bosch J. Amaurosis congenita (Leber). *AMA.Arch.Ophthalmol.* 1959;**61**:211-8.

14. Wagner RS, Caputo AR, Nelson LB *et al*. High hyperopia in Leber's congenital amaurosis. *Arch Ophthalmol.* 1985;**103**:1507-9.

15. Elder MJ. Leber congenital amaurosis and its association with keratoconus and keratoglobus. *J.Pediatr.Ophthalmol.Strabismus* 1994;**31**:38-40.

16. Paunescu K, Wabbels B, Preising MN *et al*. Longitudinal and cross-sectional study of patients with early-onset severe retinal dystrophy associated with RPE65 mutations. *Graefes Arch.Clin.Exp.Ophthalmol.* 2004.

17. Michaelides M, Hunt DM, Moore AT. The cone dysfunction syndromes. *Br.J.Ophthalmol.* 2004;**88**:291-7.

18. Allen LE, Zito I, Bradshaw K *et al*. Genotype-phenotype correlation in British families with X linked congenital stationary night blindness. *Br.J.Ophthalmol.* 2003;**87**:1413-20.

19. den Hollander AI, Roepman R, Koenekoop RK *et al*. Leber congenital amaurosis: genes, proteins and disease mechanisms. *Prog.Retin.Eye Res.* 2008;**27**:391-419.

20. Russell-Eggitt IM, Clayton PT, Coffey R *et al*. Alstrom syndrome. Report of 22 cases and literature review. *Ophthalmology* 1998;**105**:1274-80.

21. Alsing A, Christensen C. Atypical macular coloboma (dysplasia) associated with familial juvenile nephronophthisis and skeletal abnormality. *Ophthalmic Paediatr.Genet.* 1988;**9**:149-55.

22. Fillastre JP, Guenel J, Riberi P *et al*. Senior-Loken syndrome (nephronophthisis and tapeto-retinal degeneration): a study of 8 cases from 5 families. *Clin.Nephrol.* 1976;**5**:14-9.

23. Lotery AJ, Jacobson SG, Fishman GA *et al*. Mutations in the CRB1 gene cause Leber congenital amaurosis. *Arch.Ophthalmol.* 2001;**119**:415-20.

24. Freund CL, Wang QL, Chen S *et al*. De novo mutations in the CRX homeobox gene associated with Leber congenital amaurosis. *Nat.Genet.* 1998;**18**:311-2.

25. Swaroop A, Wang QL, Wu W *et al*. Leber congenital amaurosis caused by a homozygous mutation (R90W) in the homeodomain of the retinal transcription factor CRX: direct

evidence for the involvement of CRX in the development of photoreceptor function. *Hum.Mol.Genet.* 1999;**8**:299-305.

26. Jacobson SG, Cideciyan AV, Huang Y *et al*. Retinal degenerations with truncation mutations in the cone-rod homeobox (CRX) gene. *Invest Ophthalmol.Vis.Sci.* 1998;**39**:2417-26.

27. Perrault I, Rozet JM, Calvas P *et al*. Retinal-specific guanylate cyclase gene mutations in Leber's congenital amaurosis. *Nat Genet* 1996;**14**:461-4.

28. Gu SM, Thompson DA, Srikumari CR *et al*. Mutations in RPE65 cause autosomal recessive childhood-onset severe retinal dystrophy. *Nat.Genet.* 1997;**17**:194-7.

29. Marlhens F, Bareil C, Griffoin JM *et al*. Mutations in RPE65 cause Leber's congenital amaurosis. *Nat.Genet.* 1997;**17**:139-41.

30. Thompson DA, Li Y, McHenry CL *et al*. Mutations in the gene encoding lecithin retinol acyltransferase are associated with early-onset severe retinal dystrophy. *Nat.Genet.* 2001;**28**:123-4.

31. Janecke AR, Thompson DA, Utermann G *et al*. Mutations in RDH12 encoding a photoreceptor cell retinol dehydrogenase cause childhood-onset severe retinal dystrophy. *Nat.Genet.* 2004;**36**:850-4.

32. Bowne SJ, Sullivan LS, Mortimer SE *et al*. Spectrum and frequency of mutations in IMPDH1 associated with autosomal dominant retinitis pigmentosa and leber congenital amaurosis. *Invest Ophthalmol.Vis.Sci.* 2006;**47**:34-42.

33. McHenry CL, Liu Y, Feng W *et al*. MERTK arginine-844-cysteine in a patient with severe rod-cone dystrophy: loss of mutant protein function in transfected cells. *Invest Ophthalmol.Vis.Sci.* 2004;**45**:1456-63.

34. den Hollander AI, Koenekoop RK, Yzer S *et al*. Mutations in the CEP290 (NPHP6) Gene Are a Frequent Cause of Leber Congenital Amaurosis. *Am.J.Hum.Genet.* 2006;**79**:556-61.

35. Estrada-Cuzcano A, Koenekoop RK, Coppieters F *et al*. IQCB1 mutations in patients with leber congenital amaurosis. *Invest Ophthalmol.Vis.Sci.* 2011;**52**:834-9.

36. Hagstrom SA, North MA, Nishina PL *et al*. Recessive mutations in the gene encoding the tubby-like protein TULP1 in patients with retinitis pigmentosa. *Nat.Genet.* 1998;**18**:174-6.

37. Gu S, Lennon A, Li Y *et al*. Tubby-like protein-1 mutations in autosomal recessive retinitis pigmentosa. *Lancet* 1998;**351**:1103-4.

38. Banerjee P, Kleyn PW, Knowles JA *et al*. TULP1 mutation in two extended Dominican kindreds with autosomal recessive retinitis pigmentosa. *Nat.Genet.* 1998;**18**:177-9.

39. Gerber S, Perrault I, Hanein S *et al*. Complete exon-intron structure of the RPGR-interacting protein (RPGRIP1) gene allows the identification of mutations underlying Leber congenital amaurosis. *Eur.J.Hum.Genet.* 2001;**9**:561-71.

40. Dryja TP, Adams SM, Grimsby JL *et al*. Null RPGRIP1 alleles in patients with Leber congenital amaurosis. *Am.J.Hum.Genet.* 2001;**68**:1295-8.

41. den Hollander AI, Koenekoop RK, Mohamed MD *et al*. Mutations in LCA5, encoding the ciliary protein lebercilin, cause Leber congenital amaurosis. *Nat.Genet.* 2007;**39**:889-95.

42. Wang H, den Hollander AI, Moayedi Y *et al*. Mutations in SPATA7 cause Leber congenital amaurosis and juvenile retinitis pigmentosa. *Am.J.Hum.Genet.* 2009;**84**:380-7.

43. Sohocki MM, Bowne SJ, Sullivan LS *et al*. Mutations in a new photoreceptor-pineal gene on 17p cause Leber congenital amaurosis. *Nat.Genet.* 2000;**24**:79-83.

44. Friedman JS, Chang B, Kannabiran C *et al*. Premature truncation of a novel protein, RD3, exhibiting subnuclear localization is associated with retinal degeneration. *Am.J.Hum.Genet.* 2006;**79**:1059-70.

45. Peshenko IV, Olshevskaya EV, Azadi S *et al*. Retinal degeneration 3 (RD3) protein inhibits catalytic activity of retinal membrane guanylyl cyclase (RetGC) and its stimulation by activating proteins. *Biochemistry* 2011;**50**:9511-9.

46. Sergouniotis PI, Davidson AE, Mackay DS *et al*. Recessive mutations in KCNJ13, encoding an inwardly rectifying potassium channel subunit, cause leber congenital amaurosis. *Am.J.Hum.Genet.* 2011;**89**:183-90.

47. Chiang PW, Wang J, Chen Y *et al*. Exome sequencing identifies NMNAT1 mutations as a cause of Leber congenital amaurosis. *Nat.Genet.* 2012;**44**:972-4.

48. Falk MJ, Zhang Q, Nakamaru-Ogiso E *et al*. NMNAT1 mutations cause Leber congenital amaurosis. *Nat.Genet.* 2012;**44**:1040-5.

49. Koenekoop RK, Wang H, Majewski J *et al*. Mutations in NMNAT1 cause Leber congenital amaurosis and identify a new disease pathway for retinal degeneration. *Nat.Genet.* 2012;**44**:1035-9.

50. Perrault I, Hanein S, Zanlonghi X *et al*. Mutations in NMNAT1 cause Leber congenital amaurosis with early-onset severe macular and optic atrophy. *Nat.Genet.* 2012;**44**:975-7.

51. Aldahmesh MA, Al-Owain M, Alqahtani F *et al*. A null mutation in CABP4 causes Leber's congenital amaurosis-like phenotype. *Mol.Vis.* 2010;**16**:207-12.

52. Ragge NK, Brown AG, Poloschek CM *et al*. Heterozygous mutations of OTX2 cause severe ocular malformations. *Am.J.Hum.Genet.* 2005;**76**:1008-22.

53. bu-Safieh L, Alrashed M, Anazi S *et al*. Autozygome-guided exome sequencing in retinal dystrophy patients reveals pathogenetic mutations and novel candidate disease genes. *Genome Res.* 2013;**23**:236-47.

54. Cremers FP, van den Hurk JA, den Hollander AI. Molecular genetics of Leber congenital amaurosis. *Hum.Mol.Genet.* 2002;**11**:1169-76.

55. Hanein S, Perrault I, Gerber S *et al*. Leber congenital amaurosis: comprehensive survey of the genetic heterogeneity, refinement of the clinical definition, and genotype-phenotype correlations as a strategy for molecular diagnosis. *Hum.Mutat.* 2004;**23**:306-17.

56. Wang H, den Hollander AI, Moayedi Y *et al*. Mutations in SPATA7 cause Leber congenital amaurosis and juvenile retinitis pigmentosa. *Am.J.Hum.Genet.* 2009;**84**:380-7.

57. Friedman JS, Chang B, Kannabiran C *et al*. Premature truncation of a novel protein, RD3, exhibiting subnuclear localization is associated with retinal degeneration. *Am.J.Hum.Genet.* 2006;**79**:1059-70.

58. D'Cruz PM, Yasumura D, Weir J *et al*. Mutation of the receptor tyrosine kinase gene Mertk in the retinal dystrophic RCS rat. *Hum.Mol.Genet.* 2000;**9**:645-51.

59. Estrada-Cuzcano A, Koenekoop RK, Coppieters F *et al*. IQCB1 mutations in patients with leber congenital amaurosis. *Invest Ophthalmol.Vis.Sci.* 2011;**52**:834-9.

60. Ragge NK, Brown AG, Poloschek CM *et al*. Heterozygous mutations of OTX2 cause severe ocular malformations. *Am.J.Hum.Genet.* 2005;**76**:1008-22.

61. bu-Safieh L, Alrashed M, Anazi S *et al*. Autozygome-guided exome sequencing in retinal dystrophy patients reveals pathogenetic mutations and novel candidate disease genes. *Genome Res.* 2013;**23**:236-47.

62. Camuzat A, Dollfus H, Rozet JM *et al*. A gene for Leber's congenital amaurosis maps to chromosome 17p. *Hum.Mol.Genet.* 1995;**4**:1447-52.

63. Perrault I, Rozet JM, Calvas P *et al*. Retinal-specific guanylate cyclase gene mutations in Leber's congenital amaurosis. *Nat Genet* 1996;**14**:461-4.

64. Dharmaraj SR, Silva ER, Pina AL *et al*. Mutational analysis and clinical correlation in Leber congenital amaurosis. *Ophthalmic Genet* 2000;**21**:135-50.

65. Lotery AJ, Namperumalsamy P, Jacobson SG *et al*. Mutation Analysis of 3 Genes in Patients With Leber Congenital Amaurosis. *Arch Ophthalmol* 2000;**118**:538-43.

66. Perrault I, Rozet JM, Gerber S *et al*. Spectrum of retGC1 mutations in Leber's congenital amaurosis. *Eur.J.Hum.Genet.* 2000;**8**:578-82.

67. Hanein S, Perrault I, Olsen P *et al*. Evidence of a founder effect for the RETGC1 (GUCY2D) 2943DelG mutation in Leber congenital amaurosis pedigrees of Finnish origin. *Hum.Mutat.* 2002;**20**:322-3.

68. Perrault I, Rozet JM, Ghazi I *et al*. Different functional outcome of RetGC1 and RPE65 gene mutations in Leber congenital amaurosis. *Am.J.Hum.Genet.* 1999;**64**:1225-8.

69. Perrault I, Delphin N, Hanein S *et al*. Spectrum of NPHP6/CEP290 mutations in Leber congenital amaurosis and delineation of the associated phenotype. *Hum Mutat.* 2007;**28**:416.

70. Rozet JM, Perrault I, Gerber S *et al*. Complete abolition of the retinal-specific guanylyl cyclase (retGC-1) catalytic

ability consistently leads to leber congenital amaurosis (LCA). *Invest Ophthalmol.Vis.Sci.* 2001;**42**:1190-2.

71. Perrault I, Rozet JM, Gerber S *et al*. A retGC-1 mutation in autosomal dominant cone-rod dystrophy. *Am.J.Hum.Genet.* 1998;**63**:651-4.

72. Tucker CL, Woodcock SC, Kelsell RE *et al*. Biochemical analysis of a dimerization domain mutation in RetGC-1 associated with dominant cone-rod dystrophy. *Proc.Natl.Acad.Sci.U.S.A* 1999;**96**:9039-44.

73. Kelsell RE, Gregory-Evans K, Payne AM *et al*. Mutations in the retinal guanylate cyclase (RETGC-1) gene in dominant cone-rod dystrophy. *Hum.Mol.Genet.* 1998;**7**:1179-84.

74. Downes SM, Payne AM, Kelsell RE *et al*. Autosomal dominant cone-rod dystrophy with mutations in the guanylate cyclase 2D gene encoding retinal guanylate cyclase-1. *Arch.Ophthalmol.* 2001;**119**:1667-73.

75. Milam AH, Barakat MR, Gupta N *et al*. Clinicopathologic effects of mutant GUCY2D in Leber congenital amaurosis. *Ophthalmology* 2003;**110**:549-58.

76. Perrault I, Hanein S, Gerber S *et al*. A novel mutation in the GUCY2D gene responsible for an early onset severe RP different from the usual GUCY2D-LCA phenotype. *Hum.Mutat.* 2005;**25**:222.

77. Hamel CP, Tsilou E, Pfeffer BA *et al*. Molecular cloning and expression of RPE65, a novel retinal pigment epithelium-specific microsomal protein that is post-transcriptionally regulated in vitro. *J.Biol.Chem.* 1993;**268**:15751-7.

78. Hamel CP, Jenkins NA, Gilbert DJ *et al*. The gene for the retinal pigment epithelium-specific protein RPE65 is localized to human 1p31 and mouse 3. *Genomics* 1994;**20**:509-12.

79. Marlhens F, Griffoin JM, Bareil C *et al*. Autosomal recessive retinal dystrophy associated with two novel mutations in the RPE65 gene. *Eur.J.Hum.Genet.* 1998;**6**:527-31.

80. Morimura H, Fishman GA, Grover SA *et al*. Mutations in the RPE65 gene in patients with autosomal recessive retinitis pigmentosa or leber congenital amaurosis. *Proc.Natl.Acad.Sci.U.S.A* 1998;**95**:3088-93.

81. Simonelli F, Ziviello C, Testa F *et al*. Clinical and molecular genetics of Leber's congenital amaurosis: a multicenter study of Italian patients. *Invest Ophthalmol.Vis.Sci.* 2007;**48**:4284-90.

82. Galvin JA, Fishman GA, Stone EM *et al*. Clinical phenotypes in carriers of Leber congenital amaurosis mutations. *Ophthalmology* 2005;**112**:349-56.

83. Thompson DA, Gyurus P, Fleischer LL *et al*. Genetics and phenotypes of RPE65 mutations in inherited retinal degeneration. *Invest Ophthalmol.Vis.Sci.* 2000;**41**:4293-9.

84. Ma J, Zhang J, Othersen KL *et al*. Expression, purification, and MALDI analysis of RPE65. *Invest Ophthalmol.Vis.Sci.* 2001;**42**:1429-35.

85. Jahng WJ, David C, Nesnas N *et al*. A cleavable affinity biotinylating agent reveals a retinoid binding role for RPE65. *Biochemistry* 2003;**42**:6159-68.

86. Jin M, Yuan Q, Li S *et al*. Role of LRAT on the retinoid isomerase activity and membrane association of Rpe65. *J Biol.Chem.* 2007;**282**:20915-24.

87. Redmond TM, Yu S, Lee E *et al*. Rpe65 is necessary for production of 11-cis-vitamin A in the retinal visual cycle. *Nat.Genet.* 1998;**20**:344-51.

88. Redmond TM, Poliakov E, Yu S *et al*. Mutation of key residues of RPE65 abolishes its enzymatic role as isomerohydrolase in the visual cycle. *Proc.Natl.Acad.Sci.U.S.A* 2005;**102**:13658-63.

89. Xue L, Gollapalli DR, Maiti P *et al*. A palmitoylation switch mechanism in the regulation of the visual cycle. *Cell* 2004;**117**:761-71.

90. Fan J, Rohrer B, Frederick JM *et al*. Rpe65-/- and Lrat-/- mice: comparable models of leber congenital amaurosis. *Invest Ophthalmol.Vis.Sci.* 2008;**49**:2384-9.

91. Tang PH, Fan J, Goletz PW *et al*. Effective and sustained delivery of hydrophobic retinoids to photoreceptors. *Invest Ophthalmol.Vis.Sci.* 2010;**51**:5958-64.

92. Woodruff ML, Wang Z, Chung HY *et al*. Spontaneous activity of opsin apoprotein is a cause of Leber congenital amaurosis. *Nat.Genet.* 2003;**35**:158-64.

93. Hamann S, Schorderet DF, Cottet S. Bax-induced apoptosis in Leber's congenital amaurosis: a dual role in rod and cone degeneration. *PLoS.One.* 2009;**4**:e6616.

94. Tang PH, Buhusi MC, Ma JX *et al*. RPE65 is present in human green/red cones and promotes photopigment regeneration in an in vitro cone cell model. *J.Neurosci.* 2011;**31**:18618-26.

95. Tang PH, Kono M, Koutalos Y *et al*. New insights into retinoid metabolism and cycling within the retina. *Prog.Retin.Eye Res.* 2013;**32**:48-63.

96. Simovich MJ, Miller B, Ezzeldin H *et al*. Four novel mutations in the RPE65 gene in patients with Leber congenital amaurosis. *Hum.Mutat.* 2001;**18**:164.

97. Lorenz B, Gyurus P, Preising M *et al*. Early-onset severe rod-cone dystrophy in young children with RPE65 mutations. *Invest Ophthalmol.Vis.Sci.* 2000;**41**:2735-42.

98. Al Khayer K, Hagstrom S, Pauer G *et al*. Thirty-year follow-up of a patient with leber congenital amaurosis and novel RPE65 mutations. *Am.J.Ophthalmol.* 2004;**137**:375-7.

99. Lorenz B, Wabbels B, Wegscheider E *et al*. Lack of fundus autofluorescence to 488 nanometers from childhood on in patients with early-onset severe retinal dystrophy associated with mutations in RPE65. *Ophthalmology* 2004;**111**:1585-94.

100. Veske A, Nilsson SE, Narfstrom K *et al*. Retinal dystrophy of Swedish briard/briard-beagle dogs is due to a 4-bp deletion in RPE65. *Genomics* 1999;**57**:57-61.

101. Acland GM, Aguirre GD, Ray J *et al*. Gene therapy restores vision in a canine model of childhood blindness. *Nat.Genet.* 2001;**28**:92-5.

102. Acland GM, Aguirre GD, Bennett J *et al*. Long-term restoration of rod and cone vision by single dose rAAV-

mediated gene transfer to the retina in a canine model of childhood blindness. *Mol.Ther.* 2005;**12**:1072-82.

103. Dejneka NS, Surace EM, Aleman TS *et al*. In utero gene therapy rescues vision in a murine model of congenital blindness. *Mol.Ther.* 2004;**9**:182-8.

104. Jacobson SG, Acland GM, Aguirre GD *et al*. Safety of recombinant adeno-associated virus type 2-RPE65 vector delivered by ocular subretinal injection. *Mol.Ther.* 2006;**13**:1074-84.

105. Le MG, Weber M, Pereon Y *et al*. Postsurgical assessment and long-term safety of recombinant adeno-associated virus-mediated gene transfer into the retinas of dogs and primates. *Arch.Ophthalmol.* 2005;**123**:500-6.

106. Bainbridge JW, Smith AJ, Barker SS *et al*. Effect of gene therapy on visual function in Leber's congenital amaurosis. *N.Engl.J.Med.* 2008;**358**:2231-9.

107. Hauswirth WW, Aleman TS, Kaushal S *et al*. Treatment of leber congenital amaurosis due to RPE65 mutations by ocular subretinal injection of adeno-associated virus gene vector: short-term results of a phase I trial. *Hum.Gene Ther.* 2008;**19**:979-90.

108. Maguire AM, Simonelli F, Pierce EA *et al*. Safety and efficacy of gene transfer for Leber's congenital amaurosis. *N.Engl.J.Med.* 2008;**358**:2240-8.

109. Hufnagel RB, Ahmed ZM, Correa ZM *et al*. Gene therapy for Leber congenital amaurosis: advances and future directions. *Graefes Arch.Clin.Exp.Ophthalmol.* 2012;**250**:1117-28.

110. Hufnagel RB, Ahmed ZM, Correa ZM *et al*. Gene therapy for Leber congenital amaurosis: advances and future directions. *Graefes Arch.Clin.Exp.Ophthalmol.* 2012;**250**:1117-28.

111. Senechal A, Humbert G, Surget MO *et al*. Screening genes of the retinoid metabolism: novel LRAT mutation in leber congenital amaurosis. *Am.J.Ophthalmol.* 2006;**142**:702-4.

112. den Hollander AI, Lopez I, Yzer S *et al*. Identification of novel mutations in patients with Leber congenital amaurosis and juvenile RP by genome-wide homozygosity mapping with SNP microarrays. *Invest Ophthalmol.Vis.Sci.* 2007;**48**:5690-8.

113. Imanishi Y, Gerke V, Palczewski K. Retinosomes: new insights into intracellular managing of hydrophobic substances in lipid bodies. *J Cell Biol.* 2004;**166**:447-53.

114. Jin M, Yuan Q, Li S *et al*. Role of LRAT on the retinoid isomerase activity and membrane association of Rpe65. *J Biol.Chem.* 2007;**282**:20915-24.

115. Batten ML, Imanishi Y, Maeda T *et al*. Lecithin-retinol acyltransferase is essential for accumulation of all-trans-

retinyl esters in the eye and in the liver. *J.Biol.Chem.* 2004;**279**:10422-32.

116. Senechal A, Humbert G, Surget MO *et al*. Screening genes of the retinoid metabolism: novel LRAT mutation in leber congenital amaurosis. *Am.J.Ophthalmol.* 2006;**142**:702-4.

117. den Hollander AI, Lopez I, Yzer S *et al*. Identification of novel mutations in patients with Leber congenital amaurosis and juvenile RP by genome-wide homozygosity mapping with SNP microarrays. *Invest Ophthalmol.Vis.Sci.* 2007;**48**:5690-8.

118. Perrault I, Hanein S, Gerber S *et al*. Retinal dehydrogenase 12 (RDH12) mutations in leber congenital amaurosis. *Am.J.Hum.Genet.* 2004;**75**:639-46.

119. Stockton DW, Lewis RA, Abboud EB *et al*. A novel locus for Leber congenital amaurosis on chromosome 14q24. *Hum.Genet.* 1998;**103**:328-33.

120. Thompson DA, Janecke AR, Lange J *et al*. Retinal degeneration associated with RDH12 mutations results from decreased 11-cis retinal synthesis due to disruption of the visual cycle. *Hum.Mol.Genet.* 2005;**14**:3865-75.

121. Jornvall H, Persson B, Krook M *et al*. Short-chain dehydrogenases/reductases (SDR). *Biochemistry* 1995;**34**:6003-13.

122. Belyaeva OV, Korkina OV, Stetsenko AV *et al*. Biochemical properties of purified human retinol dehydrogenase 12 (RDH12): catalytic efficiency toward retinoids and C9 aldehydes and effects of cellular retinol-binding protein type I (CRBPI) and cellular retinaldehyde-binding protein (CRALBP) on the oxidation and reduction of retinoids. *Biochemistry* 2005;**44**:7035-47.

123. Maeda A, Maeda T, Imanishi Y *et al*. Retinol dehydrogenase (RDH12) protects photoreceptors from light-induced degeneration in mice. *J Biol.Chem.* 2006;**281**:37697-704.

124. Haeseleer F, Jang GF, Imanishi Y *et al*. Dual-substrate specificity short chain retinol dehydrogenases from the vertebrate retina. *J.Biol.Chem.* 2002;**277**:45537-46.

125. Lee SA, Belyaeva OV, Popov IK *et al*. Overproduction of bioactive retinoic acid in cells expressing disease-associated mutants of retinol dehydrogenase 12. *J Biol.Chem.* 2007;**282**:35621-8.

126. Sun W, Gerth C, Maeda A *et al*. Novel RDH12 mutations associated with Leber congenital amaurosis and cone-rod dystrophy: biochemical and clinical evaluations. *Vision Res.* 2007;**47**:2055-66.

127. Lee SA, Belyaeva OV, Kedishvili NY. Disease-associated variants of microsomal retinol dehydrogenase 12 (RDH12)

are degraded at mutant-specific rates. *FEBS Lett.* 2010;**584**:507-10.

128. Chacon-Camacho OF, Jitskii S, Buentello-Volante B *et al*. Exome sequencing identifies RDH12 compound heterozygous mutations in a family with severe retinitis pigmentosa. *Gene* 2013;**528**:178-82.

129. Schuster A, Janecke AR, Wilke R *et al*. The phenotype of early-onset retinal degeneration in persons with RDH12 mutations. *Invest Ophthalmol.Vis.Sci.* 2007;**48**:1824-31.

130. Freund CL, Gregory-Evans CY, Furukawa T *et al*. Cone-rod dystrophy due to mutations in a novel photoreceptor-specific homeobox gene (CRX) essential for maintenance of the photoreceptor. *Cell* 1997;**91**:543-53.

131. Furukawa T, Morrow EM, Cepko CL. Crx, a novel otx-like homeobox gene, shows photoreceptor-specific expression

and regulates photoreceptor differentiation. *Cell* 1997;**91**:531-41.

132. Sohocki MM, Sullivan LS, Mintz-Hittner HA *et al*. A range of clinical phenotypes associated with mutations in CRX, a photoreceptor transcription-factor gene. *Am.J.Hum.Genet.* 1998;**63**:1307-15.

133. Perrault I, Hanein S, Gerber S *et al*. Evidence of autosomal dominant Leber congenital amaurosis (LCA) underlain by a CRX heterozygous null allele. *J.Med.Genet.* 2003;**40**:e90.

134. Rivolta C, Peck NE, Fulton AB *et al*. Novel frameshift mutations in CRX associated with Leber congenital amaurosis. *Hum.Mutat.* 2001;**18**:550-1.

135. Nishida A, Furukawa A, Koike C *et al*. Otx2 homeobox gene controls retinal photoreceptor cell fate and pineal gland development. *Nat.Neurosci.* 2003;**6**:1255-63.

136. Wang P, Guo X, Zhang Q. Further evidence of autosomal-dominant Leber congenital amaurosis caused by heterozygous CRX mutation. *Graefes Arch.Clin.Exp.Ophthalmol.* 2007;**245**:1401-2.

137. Nakamura M, Ito S, Miyake Y. Novel de novo mutation in CRX gene in a Japanese patient with leber congenital amaurosis. *Am.J.Ophthalmol.* 2002;**134**:465-7.

138. Arcot SK, Battista R, Keep RB *et al*. Autosomal-dominant Leber Congenital Amaurosis Caused by a Heterozygous CRX Mutation in a Father and Son. *Ophthalmic Genet.* 2013.

139. Chen S, Wang QL, Nie Z *et al*. Crx, a novel Otx-like paired-homeodomain protein, binds to and transactivates photoreceptor cell-specific genes. *Neuron* 1997;**19**:1017-30.

140. Furukawa T, Morrow EM, Cepko CL. Crx, a novel otx-like homeobox gene, shows photoreceptor-specific expression

and regulates photoreceptor differentiation. *Cell* 1997;**91**:531-41.

141. Furukawa T, Morrow EM, Cepko CL. Crx, a novel otx-like homeobox gene, shows photoreceptor-specific expression and regulates photoreceptor differentiation. *Cell* 1997;**91**:531-41.

142. Furukawa T, Morrow EM, Li T *et al*. Retinopathy and attenuated circadian entrainment in Crx-deficient mice. *Nat Genet* 1999;**23**:466-70.

143. Peng GH, Chen S. Crx activates opsin transcription by recruiting HAT-containing co-activators and promoting histone acetylation. *Hum Mol.Genet* 2007;**16**:2433-52.

144. Klassen HJ, Ng TF, Kurimoto Y *et al*. Multipotent retinal progenitors express developmental markers, differentiate into retinal neurons, and preserve light-mediated behavior. *Invest Ophthalmol.Vis.Sci.* 2004;**45**:4167-73.

145. Rivolta C, Berson EL, Dryja TP. Dominant Leber congenital amaurosis, cone-rod degeneration, and retinitis pigmentosa caused by mutant versions of the transcription factor CRX. *Hum.Mutat.* 2001;**18**:488-98.

146. den Hollander AI, ten Brink JB, de Kok YJ *et al*. Mutations in a human homologue of Drosophila crumbs cause retinitis pigmentosa (RP12). *Nat.Genet.* 1999;**23**:217-21.

147. den Hollander AI, Davis J, van der Velde-Visser SD *et al*. CRB1 mutation spectrum in inherited retinal dystrophies. *Hum.Mutat.* 2004;**24**:355-69.

148. den Hollander AI, Heckenlively JR, van den Born LI *et al*. Leber congenital amaurosis and retinitis pigmentosa with Coats-like exudative vasculopathy are associated with mutations in the crumbs homologue 1 (CRB1) gene. *Am.J.Hum.Genet.* 2001;**69**:198-203.

149. McKay GJ, Clarke S, Davis JA *et al*. Pigmented paravenous chorioretinal atrophy is associated with a mutation within the crumbs homolog 1 (CRB1) gene. *Invest Ophthalmol.Vis.Sci.* 2005;**46**:322-8.

150. Richard M, Roepman R, Aartsen WM *et al*. Towards understanding CRUMBS function in retinal dystrophies. *Hum Mol.Genet* 2006;**15 Spec No 2**:R235-R243.

151. den Hollander AI, Johnson K, de Kok YJ *et al*. CRB1 has a cytoplasmic domain that is functionally conserved between human and Drosophila. *Hum.Mol.Genet.* 2001;**10**:2767-73.

152. den Hollander AI, Ghiani M, de Kok YJ *et al*. Isolation of Crb1, a mouse homologue of Drosophila crumbs, and analysis of its expression pattern in eye and brain. *Mech.Dev.* 2002;**110**:203-7.

153. van den Hurk JA, Rashbass P, Roepman R *et al*. Characterization of the Crumbs homolog 2 (CRB2) gene and

analysis of its role in retinitis pigmentosa and Leber congenital amaurosis. *Mol.Vis.* 2005;**11**:263-73.

154. Makarova O, Roh MH, Liu CJ *et al*. Mammalian Crumbs3 is a small transmembrane protein linked to protein associated with Lin-7 (Pals1). *Gene* 2003;**302**:21-9.

155. Tepass U, Theres C, Knust E. crumbs encodes an EGF-like protein expressed on apical membranes of Drosophila epithelial cells and required for organization of epithelia. *Cell* 1990;**61**:787-99.

156. van de Pavert SA, Kantardzhieva A, Malysheva A *et al*. Crumbs homologue 1 is required for maintenance of photoreceptor cell polarization and adhesion during light exposure. *J.Cell Sci.* 2004;**117**:4169-77.

157. Mehalow AK, Kameya S, Smith RS *et al*. CRB1 is essential for external limiting membrane integrity and photoreceptor

morphogenesis in the mammalian retina. *Hum.Mol.Genet.* 2003;**12**:2179-89.

158. van de Pavert SA, Sanz AS, Aartsen WM *et al*. Crb1 is a determinant of retinal apical Muller glia cell features. *Glia* 2007;**55**:1486-97.

159. Jacobson SG, Cideciyan AV, Aleman TS *et al*. Crumbs homolog 1 (CRB1) mutations result in a thick human retina with abnormal lamination. *Hum.Mol.Genet.* 2003;**12**:1073-8.

160. Abouzeid H, Li Y, Maumenee IH *et al*. A G1103R mutation in CRB1 is co-inherited with high hyperopia and Leber congenital amaurosis. *Ophthalmic Genet.* 2006;**27**:15-20.

161. den Hollander AI, Heckenlively JR, van den Born LI *et al*. Leber congenital amaurosis and retinitis pigmentosa with Coats-like exudative vasculopathy are associated with mutations in the crumbs homologue 1 (CRB1) gene. *Am.J.Hum.Genet.* 2001;**69**:198-203.

162. McMahon TT, Kim LS, Fishman GA *et al*. CRB1 gene mutations are associated with keratoconus in patients with leber congenital amaurosis. *Invest Ophthalmol.Vis.Sci.* 2009;**50**:3185-7.

163. Gherman A, Davis EE, Katsanis N. The ciliary proteome database: an integrated community resource for the genetic and functional dissection of cilia. *Nat.Genet.* 2006;**38**:961-2.

164. Ikeda S, He W, Ikeda A *et al*. Cell-specific expression of tubby gene family members (tub, Tulp1,2, and 3) in the retina. *Invest Ophthalmol.Vis.Sci.* 1999;**40**:2706-12.

165. Ikeda A, Nishina PM, Naggert JK. The tubby-like proteins, a family with roles in neuronal development and function. *J.Cell Sci.* 2002;**115**:9-14.

166. Hagstrom SA, Adamian M, Scimeca M *et al*. A role for the Tubby-like protein 1 in rhodopsin transport. *Invest Ophthalmol.Vis.Sci.* 2001;**42**:1955-62.

167. Milam AH, Hendrickson AE, Xiao M *et al*. Localization of tubby-like protein 1 in developing and adult human retinas. *Invest Ophthalmol.Vis.Sci.* 2000;**41**:2352-6.

168. Xi Q, Pauer GJ, Marmorstein AD *et al*. Tubby-like protein 1 (TULP1) interacts with F-actin in photoreceptor cells. *Invest Ophthalmol.Vis.Sci.* 2005;**46**:4754-61.

169. Boggon TJ, Shan WS, Santagata S *et al*. Implication of tubby proteins as transcription factors by structure-based functional analysis. *Science* 1999;**286**:2119-25.

170. Ikeda S, Shiva N, Ikeda A *et al*. Retinal degeneration but not obesity is observed in null mutants of the tubby-like protein 1 gene. *Hum.Mol.Genet.* 2000;**9**:155-63.

171. Hagstrom SA, Duyao M, North MA *et al*. Retinal degeneration in tulp1-/- mice: vesicular accumulation in the interphotoreceptor matrix. *Invest Ophthalmol.Vis.Sci.* 1999;**40**:2795-802.

172. Xi Q, Pauer GJ, Ball SL *et al*. Interaction between the photoreceptor-specific tubby-like protein 1 and the neuronal-specific GTPase dynamin-1. *Invest Ophthalmol.Vis.Sci.* 2007;**48**:2837-44.

173. den Hollander AI, van Lith-Verhoeven JJ, Arends ML *et al*. Novel compound heterozygous TULP1 mutations in a family with severe early-onset retinitis pigmentosa. *Arch.Ophthalmol.* 2007;**125**:932-5.

174. Lu X, Ferreira PA. Identification of novel murine- and human-specific RPGRIP1 splice variants with distinct expression profiles and subcellular localization. *Invest Ophthalmol.Vis.Sci.* 2005;**46**:1882-90.

175. Kirschner R, Rosenberg T, Schultz-Heienbrok R *et al*. RPGR transcription studies in mouse and human tissues reveal a retina-specific isoform that is disrupted in a patient with X-linked retinitis pigmentosa. *Hum.Mol.Genet.* 1999;**8**:1571-8.

176. Meindl A, Dry K, Herrmann K *et al*. A gene (RPGR) with homology to the RCC1 guanine nucleotide exchange factor is mutated in X-linked retinitis pigmentosa (RP3). *Nat.Genet.* 1996;**13**:35-42.

177. Roepman R, Bauer D, Rosenberg T *et al*. Identification of a gene disrupted by a microdeletion in a patient with X-linked retinitis pigmentosa (XLRP). *Hum.Mol.Genet.* 1996;**5**:827-33.

178. Vervoort R, Lennon A, Bird AC *et al*. Mutational hot spot within a new RPGR exon in X-linked retinitis pigmentosa. *Nat.Genet.* 2000;**25**:462-6.

179. Roepman R, Bernoud-Hubac N, Schick DE *et al*. The retinitis pigmentosa GTPase regulator (RPGR) interacts with novel transport-like proteins in the outer segments of rod photoreceptors. *Hum.Mol.Genet.* 2000;**9**:2095-105.

180. Roepman R, Letteboer SJ, Arts HH *et al*. Interaction of nephrocystin-4 and RPGRIP1 is disrupted by nephronophthisis or Leber congenital amaurosis-associated mutations. *Proc.Natl.Acad.Sci.U.S.A* 2005;**102**:18520-5.

181. Ferreira PA. Insights into X-linked retinitis pigmentosa type 3, allied diseases and underlying pathomechanisms. *Hum Mol.Genet* 2005;**14 Spec No. 2**:R259-R267.

182. Arts HH, Cremers FP, Knoers NV *et al*. Focus on Molecules: RPGRIP1. *Exp.Eye Res.* 2008.

183. Allikmets R. Leber congenital amaurosis: a genetic paradigm. *Ophthalmic Genet.* 2004;**25**:67-79.

184. Koenekoop RK. RPGRIP1 is mutated in Leber congenital amaurosis: a mini-review. *Ophthalmic Genet* 2005;**26**:175-9.

185. Lu X, Guruju M, Oswald J *et al*. Limited proteolysis differentially modulates the stability and subcellular

localization of domains of RPGRIP1 that are distinctly affected by mutations in Leber's congenital amaurosis. *Hum.Mol.Genet.* 2005;**14**:1327-40.

186. Zhao Y, Hong DH, Pawlyk B *et al*. The retinitis pigmentosa GTPase regulator (RPGR)- interacting protein: subserving RPGR function and participating in disk morphogenesis. *Proc.Natl.Acad.Sci.U.S.A* 2003;**100**:3965-70.

187. Pawlyk BS, Smith AJ, Buch PK *et al*. Gene replacement therapy rescues photoreceptor degeneration in a murine model of Leber congenital amaurosis lacking RPGRIP. *Invest Ophthalmol.Vis.Sci.* 2005;**46**:3039-45.

188. Castagnet P, Mavlyutov T, Cai Y *et al*. RPGRIP1s with distinct neuronal localization and biochemical properties associate selectively with RanBP2 in amacrine neurons. *Hum.Mol.Genet.* 2003;**12**:1847-63.

189. Koenekoop RK. RPGRIP1 is mutated in Leber congenital amaurosis: a mini-review. *Ophthalmic Genet* 2005;**26**:175-9.

190. Pawlyk BS, Bulgakov OV, Liu X *et al*. Replacement Gene Therapy with a Human RPGRIP1 Sequence Slows Photoreceptor Degeneration in a Murine Model of Leber Congenital Amaurosis. *Hum.Gene Ther.* 2010.

191. Chang B, Khanna H, Hawes N *et al*. In-frame deletion in a novel centrosomal/ciliary protein CEP290/NPHP6 perturbs its interaction with RPGR and results in early-onset retinal degeneration in the rd16 mouse. *Hum.Mol.Genet.* 2006;**15**:1847-57.

192. Sayer JA, Otto EA, O'Toole JF *et al*. The centrosomal protein nephrocystin-6 is mutated in Joubert syndrome and activates transcription factor ATF4. *Nat Genet* 2006;**38**:674-81.

193. Coppieters F, Casteels I, Meire F *et al*. Genetic screening of LCA in Belgium: predominance of CEP290 and

identification of potential modifier alleles in AHI1 of CEP290-related phenotypes. *Hum.Mutat.* 2010.

194. Coppieters F, Lefever S, Leroy BP *et al*. CEP290, a gene with many faces: mutation overview and presentation of CEP290base. *Hum.Mutat.* 2010;**31**:1097-108.

195. Valente EM, Silhavy JL, Brancati F *et al*. Mutations in CEP290, which encodes a centrosomal protein, cause pleiotropic forms of Joubert syndrome. *Nat Genet* 2006;**38**:623-5.

196. Garanto A, van Beersum SE, Peters TA *et al*. Unexpected CEP290 mRNA splicing in a humanized knock-in mouse model for Leber congenital amaurosis. *PLoS.One.* 2013;**8**:e79369.

197. Karlstetter M, Sorusch N, Caramoy A *et al*. Disruption of the retinitis pigmentosa 28 gene Fam161a in mice affects

photoreceptor ciliary structure and leads to progressive retinal degeneration. *Hum.Mol.Genet.* 2014.

198. Littink KW, Pott JW, Collin RW *et al*. A novel nonsense mutation in CEP290 induces exon skipping and leads to a relatively mild retinal phenotype. *Invest Ophthalmol.Vis.Sci.* 2010.

199. McEwen DP, Koenekoop RK, Khanna H *et al*. Hypomorphic CEP290/NPHP6 mutations result in anosmia caused by the selective loss of G proteins in cilia of olfactory sensory neurons. *Proceedings of the National Academy of Sciences* 2007;0704140104.

200. Burnight ER, Wiley LA, Drack AV *et al*. CEP290 gene transfer rescues Leber congenital amaurosis cellular phenotype. *Gene Ther.* 2014.

201. Pasadhika S, Fishman GA, Stone EM *et al*. Differential Macular Morphology in Patients with RPE65, CEP290,

GUCY2D and AIPL1 Related Leber Congenital Amaurosis. *Invest Ophthalmol.Vis.Sci.* 2009.

202. Gerber S, Hanein S, Perrault I *et al*. Mutations in LCA5 are an uncommon cause of Leber congenital amaurosis (LCA) type II. *Hum.Mutat.* 2007;**28**:1245.

203. McKibbin M, Ali M, Mohamed MD *et al*. Genotype-phenotype correlation for leber congenital amaurosis in Northern Pakistan. *Arch.Ophthalmol.* 2010;**128**:107-13.

204. Mohamed MD, Topping NC, Jafri H *et al*. Progression of phenotype in Leber's congenital amaurosis with a mutation at the LCA5 locus. *Br.J.Ophthalmol.* 2003;**87**:473-5.

205. Dharmaraj S, Li Y, Robitaille JM *et al*. A novel locus for Leber congenital amaurosis maps to chromosome 6q. *Am.J.Hum.Genet.* 2000;**66**:319-26.

206. den Hollander AI, Koenekoop RK, Mohamed MD *et al*. Mutations in LCA5, encoding the ciliary protein lebercilin, cause Leber congenital amaurosis. *Nat Genet* 2007;**39**:889-95.

207. McKibbin M, Ali M, Mohamed MD *et al*. Genotype-phenotype correlation for leber congenital amaurosis in Northern Pakistan. *Arch.Ophthalmol.* 2010;**128**:107-13.

208. Jacobson SG, Aleman TS, Cideciyan AV *et al*. Leber congenital amaurosis caused by Lebercilin (LCA5) mutation: retained photoreceptors adjacent to retinal disorganization. *Mol.Vis.* 2009;**15**:1098-106.

209. Mackay DS, Borman AD, Sui R *et al*. Screening of a Large Cohort of Leber Congenital Amaurosis and Retinitis Pigmentosa Patients Identifies Novel LCA5 Mutations and New Genotype-Phenotype Correlations. *Hum.Mutat.* 2013;**34**:1537-46.

210. Sohocki MM, Malone KA, Sullivan LS *et al*. Localization of retina/pineal-expressed sequences: identification of novel candidate genes for inherited retinal disorders. *Genomics* 1999;**58**:29-33.

211. Koenekoop RK, Loyer M, Dembinska O *et al*. Visual improvement in Leber congenital amaurosis and the CRX genotype. *Ophthalmic Genet.* 2002;**23**:49-59.

212. Sohocki MM, Perrault I, Leroy BP *et al*. Prevalence of AIPL1 mutations in inherited retinal degenerative disease. *Mol.Genet.Metab* 2000;**70**:142-50.

213. Sohocki MM, Sullivan LS, Tirpak DL *et al*. Comparative analysis of aryl-hydrocarbon receptor interacting protein-like 1 (Aipl1), a gene associated with inherited retinal disease in humans. *Mamm.Genome* 2001;**12**:566-8.

214. van der SJ, Kim JH, Yu YS *et al*. The expression of the Leber congenital amaurosis protein AIPL1 coincides with rod and

cone photoreceptor development. *Invest Ophthalmol.Vis.Sci.* 2003;**44**:5396-403.

215. Akey DT, Zhu X, Dyer M *et al*. The inherited blindness associated protein AIPL1 interacts with the cell cycle regulator protein NUB1. *Hum.Mol.Genet.* 2002;**11**:2723-33.

216. van der SJ, Chapple JP, Clark BJ *et al*. The Leber congenital amaurosis gene product AIPL1 is localized exclusively in rod photoreceptors of the adult human retina. *Hum.Mol.Genet.* 2002;**11**:823-31.

217. Liu X, Bulgakov OV, Wen XH *et al*. AIPL1, the protein that is defective in Leber congenital amaurosis, is essential for the biosynthesis of retinal rod cGMP phosphodiesterase. *Proc.Natl.Acad.Sci.U.S.A* 2004;**101**:13903-8.

218. Ramamurthy V, Niemi GA, Reh TA *et al*. Leber congenital amaurosis linked to AIPL1: a mouse model reveals

destabilization of cGMP phosphodiesterase. *Proc.Natl.Acad.Sci.U.S.A* 2004;**101**:13897-902.

219. Kirschman LT, Kolandaivelu S, Frederick JM *et al*. The Leber congenital amaurosis protein, AIPL1, is needed for the viability and functioning of cone photoreceptor cells. *Hum.Mol.Genet.* 2010;**19**:1076-87.

220. Sun X, Pawlyk B, Xu X *et al*. Gene therapy with a promoter targeting both rods and cones rescues retinal degeneration caused by AIPL1 mutations. *Gene Ther.* 2010;**17**:117-31.

221. Tan MH, Smith AJ, Pawlyk B *et al*. Gene therapy for retinitis pigmentosa and Leber congenital amaurosis caused by defects in AIPL1: effective rescue of mouse models of partial and complete Aipl1 deficiency using AAV2/2 and AAV2/8 vectors. *Hum.Mol.Genet.* 2009;**18**:2099-114.

222. Tan MH, Smith AJ, Pawlyk B *et al*. Gene therapy for retinitis pigmentosa and Leber congenital amaurosis caused by

defects in AIPL1: effective rescue of mouse models of partial and complete Aipl1 deficiency using AAV2/2 and AAV2/8 vectors. *Hum.Mol.Genet.* 2009;**18**:2099-114.

223. Jacobson SG, Cideciyan AV, Aleman TS *et al*. Human retinal disease from AIPL1 gene mutations: foveal cone loss with minimal macular photoreceptors and rod function remaining. *Invest Ophthalmol.Vis.Sci.* 2011;**52**:70-9.

224. Dharmaraj S, Leroy BP, Sohocki MM *et al*. The phenotype of Leber congenital amaurosis in patients with AIPL1 mutations. *Arch.Ophthalmol.* 2004;**122**:1029-37.

225. Tan MH, Mackay DS, Cowing J *et al*. Leber congenital amaurosis associated with AIPL1: challenges in ascribing disease causation, clinical findings, and implications for gene therapy. *PLoS.One.* 2012;**7**:e32330.

226. Nandrot E, Dufour EM, Provost AC *et al*. Homozygous deletion in the coding sequence of the c-mer gene in RCS rats

unravels general mechanisms of physiological cell adhesion and apoptosis. *Neurobiol.Dis.* 2000;**7**:586-99.

227. Weier HU, Fung J, Lersch RA. Assignment of protooncogene MERTK (a.k.a. c-mer) to human chromosome 2q14.1 by in situ hybridization. *Cytogenet.Cell Genet.* 1999;**84**:91-2.

228. Gal A, Li Y, Thompson DA *et al*. Mutations in MERTK, the human orthologue of the RCS rat retinal dystrophy gene, cause retinitis pigmentosa. *Nat.Genet.* 2000;**26**:270-1.

229. Mackay DS, Henderson RH, Sergouniotis PI *et al*. Novel mutations in MERTK associated with childhood onset rod-cone dystrophy. *Mol.Vis.* 2010;**16**:369-77.

230. Tschernutter M, Jenkins SA, Waseem NH *et al*. Clinical characterisation of a family with retinal dystrophy caused by mutation in the Mertk gene. *Br.J.Ophthalmol.* 2006;**90**:718-23.

231. Vollrath D, Feng W, Duncan JL *et al*. Correction of the retinal dystrophy phenotype of the RCS rat by viral gene transfer of Mertk. *Proc.Natl.Acad.Sci.U.S.A* 2001;**98**:12584-9.

232. Conlon TJ, Erger K, Porvasnik S *et al*. Preclinical Toxicology and Biodistribution Studies of Recombinant Adeno-Associated Virus 1 Human Acid alpha-Glucosidase. *Hum.Gene Ther.Clin.Dev.* 2013;**24**:127-33.

233. Charbel IP, Bolz HJ, Ebermann I *et al*. Characterisation of severe rod-cone dystrophy in a consanguineous family with a splice site mutation in the MERTK gene. *Br.J.Ophthalmol.* 2009;**93**:920-5.

234. Bowne SJ, Sullivan LS, Blanton SH *et al*. Mutations in the inosine monophosphate dehydrogenase 1 gene (IMPDH1) cause the RP10 form of autosomal dominant retinitis pigmentosa. *Hum.Mol.Genet.* 2002;**11**:559-68.

235. Kennan A, Aherne A, Palfi A *et al*. Identification of an IMPDH1 mutation in autosomal dominant retinitis pigmentosa (RP10) revealed following comparative microarray analysis of transcripts derived from retinas of wild-type and Rho(-/-) mice. *Hum.Mol.Genet.* 2002;**11**:547-57.

236. McLean JE, Hamaguchi N, Belenky P *et al*. Inosine 5'-monophosphate dehydrogenase binds nucleic acids in vitro and in vivo. *Biochem.J.* 2004;**379**:243-51.

237. Bowne SJ, Liu Q, Sullivan LS *et al*. Why do mutations in the ubiquitously expressed housekeeping gene IMPDH1 cause retina-specific photoreceptor degeneration? *Invest Ophthalmol.Vis.Sci.* 2006;**47**:3754-65.

238. Mortimer SE, Hedstrom L. Autosomal dominant retinitis pigmentosa mutations in inosine 5'-monophosphate

dehydrogenase type I disrupt nucleic acid binding. *Biochem.J.* 2005;**390**:41-7.

239. McGrew DA, Hedstrom L. Towards a pathological mechanism for IMPDH1-linked retinitis pigmentosa. *Adv.Exp.Med.Biol.* 2012;**723**:539-45.

240. Wang H, den Hollander AI, Moayedi Y *et al*. Mutations in SPATA7 cause Leber congenital amaurosis and juvenile retinitis pigmentosa. *Am.J.Hum.Genet.* 2009;**84**:380-7.

241. Perrault I, Hanein S, Gerard X *et al*. Spectrum of SPATA7 mutations in Leber congenital amaurosis and delineation of the associated phenotype. *Hum.Mutat.* 2010;**31**:E1241-E1250.

242. Zhang X, Liu H, Zhang Y *et al*. A novel gene, RSD-3/HSD-3.1, encodes a meiotic-related protein expressed in rat and human testis. *J.Mol.Med.* 2003;**81**:380-7.

243. Wang H, den Hollander AI, Moayedi Y *et al*. Mutations in SPATA7 cause Leber congenital amaurosis and juvenile retinitis pigmentosa. *Am.J.Hum.Genet.* 2009;**84**:380-7.

244. Wang H, den Hollander AI, Moayedi Y *et al*. Mutations in SPATA7 cause Leber congenital amaurosis and juvenile retinitis pigmentosa. *Am.J.Hum.Genet.* 2009;**84**:380-7.

245. Perrault I, Hanein S, Gerard X *et al*. Spectrum of SPATA7 mutations in Leber congenital amaurosis and delineation of the associated phenotype. *Hum.Mutat.* 2010;**31**:E1241-E1250.

246. Perrault I, Hanein S, Gerard X *et al*. Spectrum of SPATA7 mutations in Leber congenital amaurosis and delineation of the associated phenotype. *Hum.Mutat.* 2010;**31**:E1241-E1250.

247. Zeitz C, Gruissem BK, Forster U et al. Mutations in CABP4, encoding the Ca- binding protein 4, cause autosomal recessive night blindness. *Am J Hum Genet* 2006.

248. Haeseleer F, Imanishi Y, Maeda T *et al*. Essential role of Ca2+-binding protein 4, a Cav1.4 channel regulator, in photoreceptor synaptic function. *Nat.Neurosci.* 2004;**7**:1079-87.

249. Maeda T, Lem J, Palczewski K *et al*. A critical role of CaBP4 in the cone synapse. *Invest Ophthalmol.Vis.Sci.* 2005;**46**:4320-7.

250. Estrada-Cuzcano A, Koenekoop RK, Coppieters F *et al*. IQCB1 mutations in patients with leber congenital amaurosis. *Invest Ophthalmol.Vis.Sci.* 2011;**52**:834-9.

251. Schafer T, Putz M, Lienkamp S *et al*. Genetic and physical interaction between the NPHP5 and NPHP6 gene products. *Hum.Mol.Genet.* 2008;**17**:3655-62.

252. Schafer T, Putz M, Lienkamp S *et al*. Genetic and physical interaction between the NPHP5 and NPHP6 gene products. *Hum.Mol.Genet.* 2008;**17**:3655-62.

253. Estrada-Cuzcano A, Koenekoop RK, Coppieters F *et al*. IQCB1 mutations in patients with leber congenital amaurosis. *Invest Ophthalmol.Vis.Sci.* 2011;**52**:834-9.

254. Stone EM, Cideciyan AV, Aleman TS *et al*. Variations in NPHP5 in patients with nonsyndromic leber congenital amaurosis and Senior-Loken syndrome. *Arch.Ophthalmol.* 2011;**129**:81-7.

255. Chiang PW, Wang J, Chen Y *et al*. Exome sequencing identifies NMNAT1 mutations as a cause of Leber congenital amaurosis. *Nat.Genet.* 2012;**44**:972-4.

256. Falk MJ, Zhang Q, Nakamaru-Ogiso E *et al*. NMNAT1 mutations cause Leber congenital amaurosis. *Nat.Genet.* 2012;**44**:1040-5.

257. Koenekoop RK, Wang H, Majewski J *et al*. Mutations in NMNAT1 cause Leber congenital amaurosis and identify a new disease pathway for retinal degeneration. *Nat.Genet.* 2012;**44**:1035-9.

258. Perrault I, Hanein S, Zanlonghi X *et al*. Mutations in NMNAT1 cause Leber congenital amaurosis with early-onset severe macular and optic atrophy. *Nat.Genet.* 2012;**44**:975-7.

259. Avery MA, Sheehan AE, Kerr KS *et al*. Wld S requires Nmnat1 enzymatic activity and N16-VCP interactions to suppress Wallerian degeneration. *J.Cell Biol.* 2009;**184**:501-13.

260. Avery MA, Sheehan AE, Kerr KS *et al*. Wld S requires Nmnat1 enzymatic activity and N16-VCP interactions to suppress Wallerian degeneration. *J.Cell Biol.* 2009;**184**:501-13.

261. Koenekoop RK, Wang H, Majewski J *et al*. Mutations in NMNAT1 cause Leber congenital amaurosis and identify a new disease pathway for retinal degeneration. *Nat.Genet.* 2012;**44**:1035-9.

262. Sergouniotis PI, Davidson AE, Mackay DS *et al*. Recessive mutations in KCNJ13, encoding an inwardly rectifying potassium channel subunit, cause leber congenital amaurosis. *Am.J.Hum.Genet.* 2011;**89**:183-90.

263. Doring F, Derst C, Wischmeyer E *et al*. The epithelial inward rectifier channel Kir7.1 displays unusual K+ permeation properties. *J.Neurosci.* 1998;**18**:8625-36.

264. Nakamura N, Suzuki Y, Sakuta H *et al*. Inwardly rectifying K+ channel Kir7.1 is highly expressed in thyroid follicular cells, intestinal epithelial cells and choroid plexus epithelial cells: implication for a functional coupling with Na+,K+-ATPase. *Biochem.J.* 1999;**342 (Pt 2)**:329-36.

265. Hibino H, Inanobe A, Furutani K *et al*. Inwardly rectifying potassium channels: their structure, function, and physiological roles. *Physiol Rev.* 2010;**90**:291-366.

266. Sergouniotis PI, Davidson AE, Mackay DS *et al*. Recessive mutations in KCNJ13, encoding an inwardly rectifying potassium channel subunit, cause leber congenital amaurosis. *Am.J.Hum.Genet.* 2011;**89**:183-90.

267. Tao X, Avalos JL, Chen J *et al*. Crystal structure of the eukaryotic strong inward-rectifier K+ channel Kir2.2 at 3.1 A resolution. *Science* 2009;**326**:1668-74.

268. Friedman JS, Chang B, Kannabiran C *et al*. Premature truncation of a novel protein, RD3, exhibiting subnuclear localization is associated with retinal degeneration. *Am.J.Hum.Genet.* 2006;**79**:1059-70.

269. Friedman JS, Chang B, Kannabiran C *et al*. Premature truncation of a novel protein, RD3, exhibiting subnuclear

localization is associated with retinal degeneration. *Am.J.Hum.Genet.* 2006;**79**:1059-70.

270. Peshenko IV, Olshevskaya EV, Azadi S *et al*. Retinal degeneration 3 (RD3) protein inhibits catalytic activity of retinal membrane guanylyl cyclase (RetGC) and its stimulation by activating proteins. *Biochemistry* 2011;**50**:9511-9.

271. Preising MN, Hausotter-Will N, Solbach MC *et al*. Mutations in RD3 are associated with an extremely rare and severe form of early onset retinal dystrophy. *Invest Ophthalmol.Vis.Sci.* 2012;**53**:3463-72.

272. Burstedt MS, Forsman-Semb K, Golovleva I *et al*. Ocular phenotype of bothnia dystrophy, an autosomal recessive retinitis pigmentosa associated with an R234W mutation in the RLBP1 gene. *Arch.Ophthalmol.* 2001;**119**:260-7.

273. Burstedt MS, Forsman-Semb K, Golovleva I *et al*. Ocular phenotype of bothnia dystrophy, an autosomal recessive retinitis pigmentosa associated with an R234W mutation in the RLBP1 gene. *Arch.Ophthalmol.* 2001;**119**:260-7.

274. Burstedt MS, Sandgren O, Golovleva I *et al*. Effects of prolonged dark adaptation in patients with retinitis pigmentosa of Bothnia type: an electrophysiological study. *Doc.Ophthalmol.* 2008;**116**:193-205.

275. Burstedt M, Jonsson F, Kohn L *et al*. Genotype-phenotype correlations in Bothnia dystrophy caused by RLBP1 gene sequence variations. *Acta Ophthalmol.* 2013;**91**:437-44.

276. Sanger F, Nicklen S, Coulson AR. DNA sequencing with chain-terminating inhibitors. *Proc.Natl.Acad.Sci.U.S.A* 1977;**74**:5463-7.

277. Pastinen T, Kurg A, Metspalu A *et al*. Minisequencing: a specific tool for DNA analysis and diagnostics on oligonucleotide arrays. *Genome Res.* 1997;**7**:606-14.

278. den Hollander AI, Heckenlively JR, van den Born LI *et al*. Leber congenital amaurosis and retinitis pigmentosa with Coats-like exudative vasculopathy are associated with mutations in the crumbs homologue 1 (CRB1) gene. *Am.J.Hum.Genet.* 2001;**69**:198-203.

279. Zernant J, Kulm M, Dharmaraj S *et al*. Genotyping microarray (disease chip) for Leber congenital amaurosis: detection of modifier alleles. *Invest Ophthalmol.Vis.Sci.* 2005;**46**:3052-9.

280. Yzer S, Leroy BP, De Baere E *et al*. Microarray-based mutation detection and phenotypic characterization of patients with Leber congenital amaurosis. *Invest Ophthalmol.Vis.Sci.* 2006;**47**:1167-76.

281. Henderson RH, Waseem N, Searle R *et al*. An assessment of the apex microarray technology in genotyping patients with Leber congenital amaurosis and early-onset severe retinal dystrophy. *Invest Ophthalmol.Vis.Sci.* 2007;**48**:5684-9.

282. Vallespin E, Cantalapiedra D, Riveiro-Alvarez R *et al*. Mutation screening of 299 Spanish families with retinal dystrophies by Leber congenital amaurosis genotyping microarray. *Invest Ophthalmol.Vis.Sci.* 2007;**48**:5653-61.

283. Stone EM. Leber congenital amaurosis - a model for efficient genetic testing of heterogeneous disorders: LXIV Edward Jackson Memorial Lecture. *Am.J.Ophthalmol.* 2007;**144**:791-811.

284. Mandal MN, Heckenlively JR, Burch T *et al*. Sequencing arrays for screening multiple genes associated with early-onset human retinal degenerations on a high-throughput platform. *Invest Ophthalmol.Vis.Sci.* 2005;**46**:3355-62.

285. Ng SB, Buckingham KJ, Lee C *et al*. Exome sequencing identifies the cause of a mendelian disorder. *Nat.Genet.* 2010;**42**:30-5.

286. Ramensky V, Bork P, Sunyaev S. Human non-synonymous SNPs: server and survey. *Nucleic Acids Res.* 2002;**30**:3894-900.

287. Ng PC, Henikoff S. SIFT: Predicting amino acid changes that affect protein function. *Nucleic Acids Res.* 2003;**31**:3812-4.

288. Ferrer-Costa C, Gelpi JL, Zamakola L *et al*. PMUT: a web-based tool for the annotation of pathological mutations on proteins. *Bioinformatics.* 2005;**21**:3176-8.

289. Cartegni L, Wang J, Zhu Z *et al*. ESEfinder: A web resource to identify exonic splicing enhancers. *Nucleic Acids Res.* 2003;**31**:3568-71.

290. Ferrer-Costa C, Gelpi JL, Zamakola L *et al*. PMUT: a web-based tool for the annotation of pathological mutations on proteins. *Bioinformatics.* 2005;**21**:3176-8.

291. Ouyang Y, Walsh AC, Keane PA *et al*. Different phenotypes of the appearance of the outer plexiform layer on optical coherence tomography. *Graefes Arch.Clin.Exp.Ophthalmol.* 2013;**251**:2311-7.

292. Marmor MF, Holder GE, Seeliger MW *et al*. Standard for clinical electroretinography (2004 update). *Doc.Ophthalmol.* 2004;**108**:107-14.

293. Marmor MF, Fulton AB, Holder GE *et al*. ISCEV Standard for full-field clinical electroretinography (2008 update). *Doc.Ophthalmol.* 2009;**118**:69-77.

294. Henderson RH, Mackay DS, Li Z *et al*. Phenotypic variability in patients with retinal dystrophies due to mutations in CRB1. *Br.J.Ophthalmol.* 2011;**95**:811-7.

295. Ito S, Nakamura M, Nuno Y *et al*. Novel complex GUCY2D mutation in Japanese family with cone-rod dystrophy. *Invest Ophthalmol.Vis.Sci.* 2004;**45**:1480-5.

296. Mackay DS, Dev BA, Moradi P *et al*. RDH12 retinopathy: novel mutations and phenotypic description. *Mol.Vis.* 2011;**17**:2706-16.

297. Moradi P, Davies WL, Mackay D *et al*. Focus on Molecules: Centrosomal protein 290 (CEP290). *Exp.Eye Res.* 2010.

298. Mitchell GA, Brody LC, Sipila I *et al*. At least two mutant alleles of ornithine delta-aminotransferase cause gyrate atrophy of the choroid and retina in Finns. *Proc.Natl.Acad.Sci.U.S.A* 1989;**86**:197-201.

299. McBain VA, Egan CA, Pieris SJ *et al*. Functional observations in vitamin A deficiency: diagnosis and time course of recovery. *Eye (Lond)* 2007;**21**:367-76.

300. Burstedt MS, Forsman-Semb K, Golovleva I *et al*. Ocular phenotype of bothnia dystrophy, an autosomal recessive retinitis pigmentosa associated with an R234W mutation in the RLBP1 gene. *Arch.Ophthalmol.* 2001;**119**:260-7.

301. Granse L, Abrahamson M, Ponjavic V *et al*. Electrophysiological findings in two young patients with Bothnia dystrophy and a mutation in the RLBP1 gene. *Ophthalmic Genet* 2001;**22**:97-105.

302. Rogan PK, Faux BM, Schneider TD. Information analysis of human splice site mutations. *Hum Mutat.* 1998;**12**:153-71.

303. Eichers ER, Green JS, Stockton DW *et al*. Newfoundland rod-cone dystrophy, an early-onset retinal dystrophy, is caused by splice-junction mutations in RLBP1. *Am J Hum Genet* 2002;**70**:955-64.

304. FRANCESCHETTI A, FORNI S. [Infantile tapeto-retinal degeneration, Leber type, with marbled aspect of periphery of eye fundus.]. *Ophthalmologica* 1958;**135**:610-6.

305. Fulton AB, Hansen RM, Mayer DL. Vision in Leber congenital amaurosis. *Arch.Ophthalmol.* 1996;**114**:698-703.

306. Pasadhika S, Fishman GA, Stone EM *et al*. Differential Macular Morphology in Patients with RPE65, CEP290, GUCY2D and AIPL1 Related Leber Congenital Amaurosis. *Invest Ophthalmol.Vis.Sci.* 2009.

307. Hamel CP, Griffoin JM, Lasquellec L *et al*. Retinal dystrophies caused by mutations in RPE65: assessment of visual functions. *Br.J.Ophthalmol.* 2001;**85**:424-7.

308. Heher KL, Traboulsi EI, Maumenee IH. The natural history of Leber's congenital amaurosis. Age-related findings in 35 patients. *Ophthalmology* 1992;**99**:241-5.

309. Brecelj J, Stirn-Kranjc B. ERG and VEP follow-up study in children with Leber's congenital amaurosis. *Eye (Lond)* 1999;**13 (Pt 1)**:47-54.

310. Heher KL, Traboulsi EI, Maumenee IH. The natural history of Leber's congenital amaurosis. Age-related findings in 35 patients. *Ophthalmology* 1992;**99**:241-5.

311. Dagi LR, Leys MJ, Hansen RM *et al*. Hyperopia in complicated Leber's congenital amaurosis. *Arch.Ophthalmol.* 1990;**108**:709-12.

312. Koenekoop RK, Lopez I, den Hollander AI *et al*. Genetic testing for retinal dystrophies and dysfunctions: benefits, dilemmas and solutions. *Clin.Experiment.Ophthalmol.* 2007;**35**:473-85.

313. Henderson RH, Waseem N, Searle R *et al*. An assessment of the apex microarray technology in genotyping patients with

Leber congenital amaurosis and early-onset severe retinal dystrophy. *Invest Ophthalmol.Vis.Sci.* 2007;**48**:5684-9.

314. Cremers FP, Kimberling WJ, Kulm M *et al*. Development of a genotyping microarray for Usher syndrome. *J.Med.Genet.* 2007;**44**:153-60.

315. Pomares E, Riera M, Permanyer J *et al*. Comprehensive SNP-chip for retinitis pigmentosa-Leber congenital amaurosis diagnosis: new mutations and detection of mutational founder effects. *Eur.J.Hum.Genet.* 2010;**18**:118-24.

316. Pomares E, Riera M, Permanyer J *et al*. Comprehensive SNP-chip for retinitis pigmentosa-Leber congenital amaurosis diagnosis: new mutations and detection of mutational founder effects. *Eur.J.Hum.Genet.* 2010;**18**:118-24.

317. Vallespin E, Lopez-Martinez MA, Cantalapiedra D *et al*. Frequency of CEP290 c.2991_1655A>G mutation in 175 Spanish families affected with Leber congenital amaurosis and early-onset retinitis pigmentosa. *Mol.Vis.* 2007;**13**:2160-2.

318. Menotti-Raymond M, David VA, Schaffer AA *et al*. Mutation in CEP290 discovered for cat model of human retinal degeneration. *J.Hered.* 2007;**98**:211-20.

319. Baala L, Audollent S, Martinovic J *et al*. Pleiotropic effects of CEP290 (NPHP6) mutations extend to Meckel syndrome. *Am.J.Hum.Genet.* 2007;**81**:170-9.

320. Frank V, den Hollander AI, Bruchle NO *et al*. Mutations of the CEP290 gene encoding a centrosomal protein cause Meckel-Gruber syndrome. *Hum.Mutat.* 2008;**29**:45-52.

321. Leitch CC, Zaghloul NA, Davis EE *et al*. Hypomorphic mutations in syndromic encephalocele genes are associated with Bardet-Biedl syndrome. *Nat.Genet.* 2008;**40**:443-8.

322. Samardzija M, Wenzel A, Naash M *et al*. Rpe65 as a modifier gene for inherited retinal degeneration. *Eur.J.Neurosci.* 2006;**23**:1028-34.

323. Ikeda A, Naggert JK, Nishina PM. Genetic modification of retinal degeneration in tubby mice. *Exp.Eye Res.* 2002;**74**:455-61.

324. Littink KW, Pott JW, Collin RW *et al*. A novel nonsense mutation in CEP290 induces exon skipping and leads to a relatively mild retinal phenotype. *Invest Ophthalmol.Vis.Sci.* 2010.

325. Moradi P, Davies WL, Mackay D *et al*. Focus on Molecules: Centrosomal protein 290 (CEP290). *Exp.Eye Res.* 2010.

326. Coppieters F, Casteels I, Meire F *et al*. Genetic screening of LCA in Belgium: predominance of CEP290 and identification of potential modifier alleles in AHI1 of CEP290-related phenotypes. *Hum.Mutat.* 2010.

327. Littink KW, Pott JW, Collin RW *et al*. A novel nonsense mutation in CEP290 induces exon skipping and leads to a relatively mild retinal phenotype. *Invest Ophthalmol.Vis.Sci.* 2010.

328. Littink KW, Pott JW, Collin RW *et al*. A novel nonsense mutation in CEP290 induces exon skipping and leads to a relatively mild retinal phenotype. *Invest Ophthalmol.Vis.Sci.* 2010.

329. Cideciyan AV, Aleman TS, Jacobson SG *et al*. Centrosomal-ciliary gene CEP290/NPHP6 mutations result in blindness with unexpected sparing of photoreceptors and visual brain:

implications for therapy of Leber congenital amaurosis. *Hum.Mutat.* 2007;**28**:1074-83.

330. Coppieters F, Casteels I, Meire F *et al*. Genetic screening of LCA in Belgium: predominance of CEP290 and identification of potential modifier alleles in AHI1 of CEP290-related phenotypes. *Hum.Mutat.* 2010.

331. Walia S, Fishman GA, Jacobson SG *et al*. Visual acuity in patients with Leber's congenital amaurosis and early childhood-onset retinitis pigmentosa. *Ophthalmology* 2010;**117**:1190-8.

332. Coppieters F, Casteels I, Meire F *et al*. Genetic screening of LCA in Belgium: predominance of CEP290 and identification of potential modifier alleles in AHI1 of CEP290-related phenotypes. *Hum.Mutat.* 2010.

333. Pasadhika S, Fishman GA, Stone EM *et al*. Differential Macular Morphology in Patients with RPE65, CEP290,

GUCY2D and AIPL1 Related Leber Congenital Amaurosis. *Invest Ophthalmol.Vis.Sci.* 2009.

334. Coppieters F, Casteels I, Meire F *et al*. Genetic screening of LCA in Belgium: predominance of CEP290 and identification of potential modifier alleles in AHI1 of CEP290-related phenotypes. *Hum.Mutat.* 2010.

335. Smith RS, Doty RL, Burlingame GK *et al*. Smell and taste function in the visually impaired. *Percept.Psychophys.* 1993;**54**:649-55.

336. Smith RS, Doty RL, Burlingame GK *et al*. Smell and taste function in the visually impaired. *Percept.Psychophys.* 1993;**54**:649-55.

337. Valverde D, Pereiro I, Vallespin E *et al*. Complexity of phenotype-genotype correlations in Spanish patients with RDH12 mutations. *Invest Ophthalmol.Vis.Sci.* 2009;**50**:1065-8.

338. Jaissle GB, May CA, van de Pavert SA *et al*. Bone spicule pigment formation in retinitis pigmentosa: insights from a mouse model. *Graefes Arch.Clin.Exp.Ophthalmol.* 2010;**248**:1063-70.

339. den Hollander AI, Heckenlively JR, van den Born LI *et al*. Leber congenital amaurosis and retinitis pigmentosa with Coats-like exudative vasculopathy are associated with mutations in the crumbs homologue 1 (CRB1) gene. *Am.J.Hum.Genet.* 2001;**69**:198-203.

340. Maeda A, Maeda T, Sun W *et al*. Redundant and unique roles of retinol dehydrogenases in the mouse retina. *Proc.Natl.Acad.Sci.U.S.A* 2007;**104**:19565-70.

341. Maw MA, Kennedy B, Knight A *et al*. Mutation of the gene encoding cellular retinaldehyde-binding protein in autosomal recessive retinitis pigmentosa. *Nature Genetics* 1997;**17**:198-200.

342. Burstedt MS, Sandgren O, Holmgren G *et al*. Bothnia dystrophy caused by mutations in the cellular retinaldehyde-binding protein gene (RLBP1) on chromosome 15q26. *Invest Ophthalmol.Vis.Sci.* 1999;**40**:995-1000.

343. Katsanis N, Shroyer NF, Lewis RA *et al*. Fundus albipunctatus and retinitis punctata albescens in a pedigree with an R150Q mutation in RLBP1. *Clin.Genet* 2001;**59**:424-9.

344. Eichers ER, Green JS, Stockton DW *et al*. Newfoundland rod-cone dystrophy, an early-onset retinal dystrophy, is caused by splice-junction mutations in RLBP1. *Am J Hum Genet* 2002;**70**:955-64.

345. Burstedt MS, Forsman-Semb K, Golovleva I *et al*. Ocular phenotype of bothnia dystrophy, an autosomal recessive retinitis pigmentosa associated with an R234W mutation in the RLBP1 gene. *Arch.Ophthalmol.* 2001;**119**:260-7.

346. Niwa Y, Kondo M, Ueno S *et al*. Cone and rod dysfunction in fundus albipunctatus with RDH5 mutation: an electrophysiological study. *Invest Ophthalmol.Vis.Sci.* 2005;**46**:1480-5.

347. Fishman GA, Roberts MF, Derlacki DJ *et al*. Novel mutations in the cellular retinaldehyde-binding protein gene (RLBP1) associated with retinitis punctata albescens: evidence of interfamilial genetic heterogeneity and fundus changes in heterozygotes. *Arch.Ophthalmol.* 2004;**122**:70-5.

348. Frischmeyer PA, Dietz HC. Nonsense-mediated mRNA decay in health and disease. *Hum Mol.Genet* 1999;**8**:1893-900.

349. Culbertson MR. RNA surveillance. Unforeseen consequences for gene expression, inherited genetic disorders and cancer. *Trends Genet* 1999;**15**:74-80.

350. Liu T, Jenwitheesuk E, Teller DC *et al*. Structural insights into the cellular retinaldehyde-binding protein (CRALBP). *Proteins* 2005;**61**:412-22.

351. He X, Lobsiger J, Stocker A. Bothnia dystrophy is caused by domino-like rearrangements in cellular retinaldehyde-binding protein mutant R234W. *Proc.Natl.Acad.Sci.U.S.A* 2009;**106**:18545-50.

352. Burstedt MS, Sandgren O, Golovleva I *et al*. Retinal function in Bothnia dystrophy. An electrophysiological study. *Vision Res.* 2003;**43**:2559-71.

353. Granse L, Abrahamson M, Ponjavic V *et al*. Electrophysiological findings in two young patients with Bothnia dystrophy and a mutation in the RLBP1 gene. *Ophthalmic Genet* 2001;**22**:97-105.

354. Burstedt MS, Sandgren O, Golovleva I *et al*. Effects of prolonged dark adaptation in patients with retinitis

pigmentosa of Bothnia type: an electrophysiological study. *Doc.Ophthalmol.* 2008;**116**:193-205.

355. Burstedt MS, Sandgren O, Golovleva I *et al*. Effects of prolonged dark adaptation in patients with retinitis pigmentosa of Bothnia type: an electrophysiological study. *Doc.Ophthalmol.* 2008;**116**:193-205.

356. McBain VA, Egan CA, Pieris SJ *et al*. Functional observations in vitamin A deficiency: diagnosis and time course of recovery. *Eye* 2007;**21**:367-76.

357. Ueno S, Kondo M, Niwa Y *et al*. Luminance dependence of neural components that underlies the primate photopic electroretinogram. *Invest Ophthalmol.Vis.Sci.* 2004;**45**:1033-40.

358. Neveling K, Collin RW, Gilissen C *et al*. Next-generation genetic testing for retinitis pigmentosa. *Hum.Mutat.* 2012;**33**:963-72.

359. O'Sullivan J, Mullaney BG, Bhaskar SS *et al*. A paradigm shift in the delivery of services for diagnosis of inherited retinal disease. *J.Med.Genet.* 2012;**49**:322-6.

360. Shanks ME, Downes SM, Copley RR *et al*. Next-generation sequencing (NGS) as a diagnostic tool for retinal degeneration reveals a much higher detection rate in early-onset disease. *Eur.J.Hum.Genet.* 2013;**21**:274-80.

361. Shendure J, Ji H. Next-generation DNA sequencing. *Nat.Biotechnol.* 2008;**26**:1135-45.

362. Metzker ML. Sequencing technologies - the next generation. *Nat.Rev.Genet.* 2010;**11**:31-46.

363. Metzker ML. Sequencing technologies - the next generation. *Nat.Rev.Genet.* 2010;**11**:31-46.

364. O'Sullivan J, Mullaney BG, Bhaskar SS *et al*. A paradigm shift in the delivery of services for diagnosis of inherited retinal disease. *J.Med.Genet.* 2012;**49**:322-6.

365. O'Sullivan J, Mullaney BG, Bhaskar SS *et al*. A paradigm shift in the delivery of services for diagnosis of inherited retinal disease. *J.Med.Genet.* 2012;**49**:322-6.

7 Appendices

7.1 Patient invitation letter

Dear *[parent of patient/patient name]* ,

We are writing to you because you are known to us having been seen at Moorfields Eye Hospital in the past with a history of an early onset retinal dystrophy.

There are a number of different retinal dystrophies as you may well know and we are now starting research into the genetic causes of these. We aim to understand more fully how each disorder manifests itself and how this correlates with each gene defect that we find. Although at present there are unfortunately no curative or preventative measures available for this type of disorder, the collection of this information is important in any attempts to develop new treatments in the future.
We are writing, therefore, to ask whether you would be interested in helping us with this research program. It would mean that [*you/your child]* would need to come to Moorfields for one or maybe two visits to have a number of tests done and to give us a blood sample (or mouth swab in young children) if you have not already provided us with one in the past. Your travel expenses would of course be reimbursed.

We have enclosed some more details about the study and a reply slip should you be able to help us. If you are agreeable the research Registrar - Mr Phillip Moradi - will then contact you to arrange a time for your visit here. We would be extremely grateful for any assistance that you could provide.
With many thanks,
Yours sincerely,

Professor Anthony Moore MA FRCS FRCOphth
Duke Elder Professor of Ophthalmology (UCL)
Consultant Ophthalmologist
Moorfields Eye Hospital & Great Ormond Street Hospital for Children

Mr Andrew Webster MD FRCS FRCOphth

Consultant Ophthalmologist, Moorfields Eye Hospital

7.2 Patient information letter

A clinical and molecular genetic investigation of childhood retinal dystrophies

INFORMATION LEAFLET

PLEASE CONTACT US IF YOU WOULD LIKE THIS LEAFLET IN LARGER TYPE OR THE INFORMATION PROVIDED ON AUDIO CASSETTE TAPE

You are invited to take part in this research study. Before you decide it is important for you to understand why the research is being done and what's involved. Please take time to read the following information carefully and discuss it with your family, friends, hospital specialist or GP if you wish. If you need more information please contact the research team whose telephone number is at the end of this leaflet.

Why the study is being done?

Inherited retinal disorders are an important cause of childhood visual impairment and this research study aims to discover the causes of the retinal problem and to understand the reasons why the retina fails to function normally. Vision is dependent upon the functioning of the cone and rod cells of the retina, a thin membrane at the back of the eye. There are two groups of cells in the retina that detect light. The cones cells are used when light levels are high, and the rods are used when light levels are low. From the way in which night vision, colour vision, central vision and the electrical responses from the

retina are changed we can learn how a condition has affected the cells in the retina. We are able to use this information together with knowledge of the genetic faults causing an eye disorder to build up a picture of what is causing the retinal dysfunction and which approach would be best used in the future to slow down disease progression.

Research has shown that genetic factors have an effect on the risk of someone developing this group of disorders. In other words, some people are at higher risk than others because of their genetic make-up.

This research study is being carried out for two important reasons:

1. We want to find out more about the genetic factors in childhood retinal dystrophies
2. We want to find the genes that affect the risk of developing childhood retinal dystrophies

If we can find which genes affect the risk of childhood retinal dystrophies it would help us understand why the disease occurs and could in the longer term lead to better treatment.

How will the study be carried out?

To find out more about genetic factors in childhood retinal dystrophies we need the help of patients with childhood retinal dystrophies and their relatives. By comparing the genetic make-up of those with childhood retinal dystrophies we can see what genes they have in common and start to work out which genes affect the risk of developing childhood retinal dystrophies. We can also obtain additional information if we have the opportunity of studying unaffected relatives as well.

Why you are being invited to take part

You are being invited to take part because you or your relative has a childhood retinal dystrophies. To give us a good chance of success, we need to study a large number of cases. We hope to recruit at least 60 patients with the disorder and their close relatives.

Do I have to take part?

It is up to you to decide whether or not to take part. If you do decide to take part you will be given this information sheet to keep and be asked to sign a consent form. If you decide to take part you are still free to withdraw at any time and without giving a reason. A decision to withdraw at any time, or a decision not to take part, will not affect the standard of care you receive.

What will happen to me if I take part?

If you decide to take part and have signed a consent form you will be asked to give a 30 ml blood sample (that's about 6 teaspoonfulls) which will be used to extract DNA (the chemical containing your genetic information) which will be used to try and identify genes causing eye disorders. The results of these tests will be kept strictly confidential. You will also be asked to undergo a routine eye examination and have some images taken of the back of your eye using several imaging techniques. The imaging techniques are similar to having a photograph taken of the back of your eyes. You may also have the length of your eye measured with ultrasound (a small probe will touch your eye after a local anaesthetic drop has been instilled). For the imaging we will need to dilate your

pupils. This procedure is conducted routinely in eye clinics. The use of these drops causes some temporary blurring of vision especially for near and as they increase the size of the pupil, they may be associated with increase sensitivity to light. It is advisable that you bring along sunglasses to wear on your journey home. For most people, it takes around 8 hours for the pupil of the eye to return to its normal size following dilation although vision recovers sooner. It is advisable not to drive for 5-6 hours after the drops have been instilled. We will pay your travel expenses to and from London. The tests are quite simple and last approximately 90 minutes although the length of the examination varies from person to person.

In some cases we will ask you to return for additional tests. These tests will involve either the examination of your ability to see targets in your peripheral vision , or measurement of your vision at low light levels (these tests last approximately 2 hours).

As one of the genetic mutations we are studying for your condition could be indicated by an abnormal sense of smell, we will ask you to take a simple "scratch-and-sniff" test. This involves scratching a pre-prepared card to release the scent and then trying to identify the smell. It is entirely non-invasive and takes only a few seconds, but could provide us with valuable information for this study."

What will happen to the blood sample?

The laboratory will extract the genetic material DNA from the cells in the blood sample so that this can be used to study the genes that we think may have an effect on the risk of developing childhood retinal dystrophy..

What will happen to the results of the research study?

All the information from the study will be published in medical journals and presented to relevant health professionals at meetings and conferences. We would also be pleased to provide information about the results of the study to anyone who has taken part. Individual patients will not be identified in any reports or publications arising from the study.

Will information from the study be kept confidential?

All information collected for the study will be kept strictly confidential. The research team will not pass on your personal details to anyone else. The samples will be coded and scientists working in the laboratory will be provided with relevant medical information relating to the samples but will not be given the names of the people from whom the samples were obtained.

Working with other research groups to speed things up

Finding the genes that are important in childhood retinal dystrophy is a major challenge and may take many years. To speed up the research, we may join forces with other research teams in this country or abroad, in which case we may want to provide them

with some of the sample stored from yourself and others for them to work on. In order to make this possible, on the consent form you are asked to agree to donate your sample to the research team as a gift. This means that you give up all rights to the sample and cannot at a later date ask for the sample to be destroyed or returned to you. It also means that at the discretion of the research team your sample can be used by others for research on the causes of childhood retinal dystrophy.

What are the possible benefits of taking part?

It is unlikely that you will benefit personally from helping with this research project, but the results of the research should be of benefit to patients affected by childhood retinal dystrophy in the future.

Will you be told the results of the eye examination or genetic testing?

The purpose of the eye examination is to obtain information we need for the research study. This sort of technical information is unlikely to have any implications for yourself. It is possible but unlikely that in the course of examining your eyes we may discover a problem with your eyes that you were not aware of. Please let us know if you would prefer not to be told if this situation arises. Otherwise we will assume that you would like us to bring it your attention, and with your permission, pass on information to your general practitioner. If you are a car driver, one reason you may choose not to be told about unexpected findings might be the implications this could have for holding a driving licence.

The genetic testing that we will be carrying out will have the aim of identifying the changes in a specific gene which is causing your eye disorder. It may take months or even years before the specific change causing your eye disease is identified. We will inform you if we identify the change in your case. Please let us know if you do not wish to know the result. We will not inform your GP of the result unless you specifically ask us to.

What are the possible disadvantages of taking part?

Your eyes will be photographed, which requires having drops put in your eyes to dilate the pupils. This may cause brief discomfort and some temporary blurring of your near vision so you will not be able to drive a car for the rest of the day. Dilating the pupils is a routine procedure in hospital eye clinics which doesn't usually cause any problem, but you should be aware that a painful rise in the pressure in the eye (acute glaucoma) is a rare but treatable complication. You will be asked to provide a blood sample for the study. This will be done with care by qualified staff but may cause some discomfort and occasionally bruising.

Who is organising and funding the research?

The Special Trustees on Moorfields Eye Hospital using funding donated by the Eranda foundation

What if something goes wrong?

If you are harmed by taking part in this research project, there are no special compensation arrangements. If you are harmed due to someone's negligence, then you may have grounds for a legal action but you may have to pay for it. Regardless of this, if you wish to complain or have any concerns about any aspect of the way you have been approached or treated during the course of this study, the normal National Health Service complaints mechanisms would be available to you.

Contact for Further Information

Professor AT Moore Moorfields Eye Hospital, City Road, London EC1V 2PD

Tel 0207 566 2260

Thank you for reading this information leaflet and for considering taking part in this study

7.3 Consent form

A clinical and molecular genetic investigation of childhood retinal dystrophies

<name of local researcher(s)>

<address>

1. I confirm that I have read and understand the INFORMATION LEAFLET (version [number], dated [ ]) about the above study and have been given a copy to keep. I have had the opportunity to ask questions and understand why the research is being done and any foreseeable risks involved. ☐
2. I understand that my participation in this study is voluntary and that I am free to withdraw at any time, without giving any reason and without my medical care or legal rights being affected. ☐
3. I give permission for my medical records to be looked at and information to be taken and ☐
4. I agree to donate a blood sample as a gift and in so doing give up all legal rights to the sample and its future use. ☐

5. I agree that the sample I have donated and relevant medical information can be used for future projects on the causes of [NAME OF CONDITION] including projects being carried out by other academic or commercial researchers. ☐

6. I understand that I will not benefit financially if this research leads to the development of ☐

CONSENT FORM

I agree to take part in the above study

Full name (BLOCK CAPITALS)	Date	Signature
Name of person taking consent	Date	Signature

1 for patient; 1 for researcher; 1 to be kept with hospital notes

7.4 Data protection form

Data Protection Consent Form

1. I agree to my/my child's personal identifying details (name, address, telephone number) being kept on a secure electronic database.

2. I agree to information regarding my family pedigree (who is related to who) being kept in a secure electronic database

3. I agree to clinical and genetic information about my condition being kept on this database.

4. I understand that this information will be held on a database located at the Institute of Ophthalmology (& Moorfields Eye Hospital). The personal information gathered will only be accessed by the principal researcher and team. Any results published from this information will not contain any personal identifying data.

Name of Patient: …… Date…….

Signature of patient: ……..

Name of Parent (if child)…… Date……

Signature of Parent…….

Relationship to child…….....

Name of researcher…….. Date…….

Signature of researcher…….

1 copy in notes , 1 copy to patient/parent,1 copy to researcher

7.5 Phenotyping records

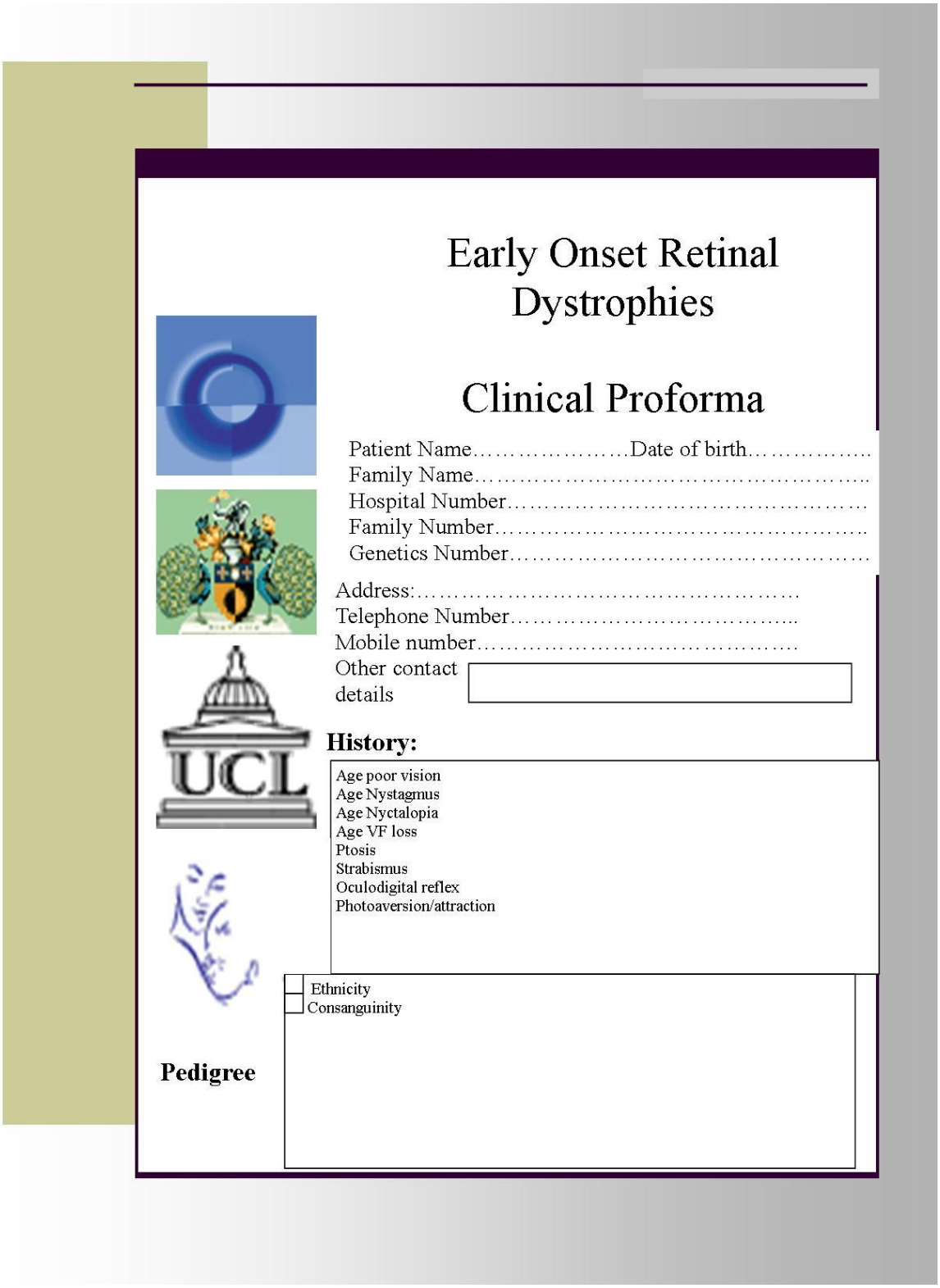

Early Onset Retinal Dystrophies

Clinical Proforma

Patient Name……Date of birth……
Family Name……..
Hospital Number……
Family Number……..
Genetics Number……

Address:……
Telephone Number……..
Mobile number……
Other contact details

History:

Age poor vision
Age Nystagmus
Age Nyctalopia
Age VF loss
Ptosis
Strabismus
Oculodigital reflex
Photoaversion/attraction

Ethnicity
Consanguinity

Pedigree

Phenotyping data

R

Visual Acuity

L

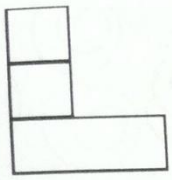

Distance

Near

Colour axis

Adnexae

Cornea

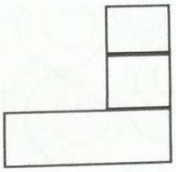

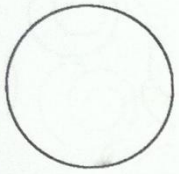

K1 K1 ^{K2}

K– readings ^{K2}

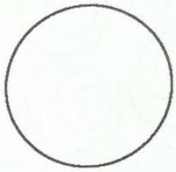

Axial Length

Pupils

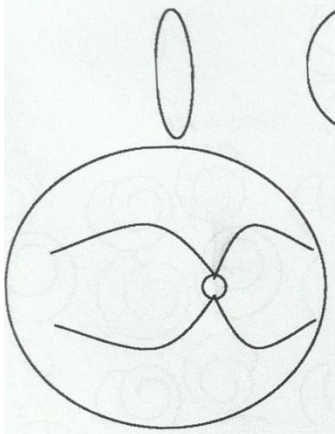

Lens

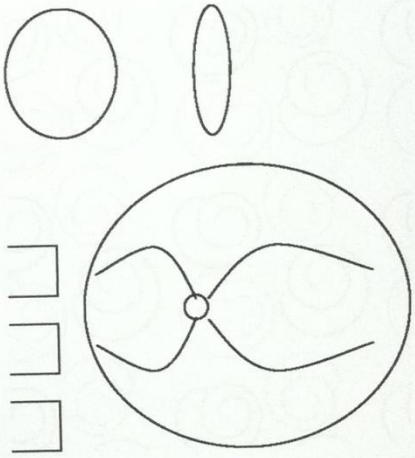

Photographs done?

Autofluorescence?

Fundus

OCT? Goldman

VF?

Electrodiagnostics?

Bloods?

Corneal topography

Dark adapted perimetry

Notes:

Refraction

R

L

7.6 Primers and PCR conditions used in screening RDH12 in this cohort

Exon	Primer	PCR annealing (°C)	Size of fragment (bp)
Exon 1F	TTTCCCCACATTCTCTTTGCC	54	517
Exon 1R	TCCACCATGGTATCCACAACACC		
Exon 2F	TAACGTATCTTAGTGTGAGCTCG	54	306
Exon 2R	TCCTTGAATTTCTAGTCAGAGC		
Exon 3F	TCACTCTACCGTTGAAGGATGG	54	405
Exon 3R	TGTGGCAGAACCTGTCTAGTGG		
Exon 4F	ATAGTTATTGAGTGCTGAGGC	54	459
Exon 4R	TAGACTGATCAGGAGAGGTAC		
Exon 5F	TCAGACCAAACTGACCATTAGAG	54	460
Exon 5R	TGACACGTGCATGTTTGACAGCC		
Exon 6F	TGGTACCTGCTGAATCCTGGG	54	434
Exon 6R	ACCTGGATTGCATCATCAGGC		
Exon 7F	TTAGTTTCTTTGAGTCTGGC	54	884
Exon 7R	TGATTTGTTCCATTTCTCTCC		

7.7 PCR conditions and primers used in screening RLBP1 in this cohort

Exon	Primers	PCR annealing (°C)
1	Non coding	
2F	TGAGATCCACAGTTCTGAGAC	55 C
2R	AGGAGAGCCCTGGAGGACA	
3F	GAACTGAAGGTCTGAGCAGG	60 C
3R	CAGGAGAGAGAATGCAGTCA	
4F	CTCATCACCTGTGTGTGTCCTGCC	58 C
4R	GAGAGCGGATAGCATCCTCATG	
5F	CTTCTGAGTCCCACTAGGAGG	55 C
5R	CCAGTAGAGGCCAGGTTGA	
6F	CCTCAGGACCTCAAGCCTA	55 C
6R	CTGCAAGCACCATGAAAGGA	
7F	AATGAGTGGGAGCCTCTGAG	55 C
7R	CCCTCTTGTCTCATTGTCTGG	
8F	CTCCTGCTCAGTTCTGTCTC	55 C
8R	ACTTGAGAACAGGGTGACACC	

7.8 PCR conditions and primers used in screening *CEP290*

exons	primer sequence (5' to 3')	amplicon size (bp)	PCR annealing temperature
2	ACCAATAATACTGTGTACCTTG CAGATTGTGACAATTATAGTTG	289	58°C
3	CAACTATAATTGTCACAATCTG GTTCCACTAATAGCCAAACC	212	58°C
4	GTGCTTACATTCCAGTATAAAG GTTTAATGAACAAATGGAATTCA	186	58°C
5	ACCTTATAATCATGATGGACTC AATAACCATGATTACAATCATCC	285	58°C
6	TTGTTGACTCATTTGAACCTC AAAAAGCCAGGTAACTTGAAC	264	58°C
7	ACTGCTGAATTTTATCTTCTTC TTAGAAGACTCCAGTCCTGG	208	58°C
8-9	CAAGATAATATGCATCATTTTCCC ATGAAATTAAAGTTTTTAGGAACC	472	60°C
10	AGAGGACACTTATGGCTGCG GTAATGAGATAATATGAAGTCTG	332	54°C
11	CACATATGTAATGTAATGTATCC CTAATAAACGTGTTATAAACCAG	364	54°C
12	GTATCATAAATCTACTAACGGTG ATCGTTCAGAGTTCCAACTG	284	58°C
13	CTTGTACCCACAAGAAAATATG AGAAAACTCAATATTGACTTGAC	341	58°C
14	TGATTTGAAGGAATAAGTAGTC CTGTGAATGGCAAGAATAATTC	282	58°C
15	GTACATTTTCCTTTAGACTTAG ACTTGTAAATCAGGTTGCGC	311	58°C
16-17	CATTTTTGCAGCTTATTTGAATG ATATCCAGACAACTCACTTATC	380	58°C

Exons	primer sequence (5’ to 3’)	amplicon size (bp)	PCR annealing temperature
18	ATTAAAGTGTTGGAATAGTAGG GCAGGAGAATGGCATGAAC	335	58°C
19	ATTGATCAAACTTTTCTTAACTTG ACAGAGGTAATTAGGAGTAAAG	293	58°C
20	CCAATGATGTCTTTGGTATATG AAATATCTCATCAGAAACTATGG	340	58°C
21	GTCCATTTTATTTAAAGACAGAC TTAATTCAAGGGGCATTTTCTC	362	58°C
22	TATGGTTGAGGTAAAATTCCTG AGTACTATCTGCATGCTTTGG	390	58°C
23	TAACTTTCCTATAATGTTGTCAG TAAGTTCCTAACAGTAGTTACC	372	58°C
24	ATACCTCTTGTGTTGAGAAAAC CACAAAGACACATCCATATTAC	300	58°C
25	TATGCAATATTGTACAAAGTAGG TGATACCATCCTATCTTCTGC	368	58°C
26	AAAGTGGCTAGTGCTTGACC TGTTAAATTTATATAAATGCAGGC	358	58°C
27	AACTGGATTGTGAGTTTTAAGG AGGATTATTCATCTGCCTAAG	383	58°C
28	ACAGCATCTAAAATATCTGAGG AGATCCAGACAAACCACTTAAC	369	58°C
29	AAGGCCAAGTAAAGAGGATTG TACTACTAAGAATTGTATACCTG	349	58°C
30	TAGAAAGTGTACTTAATTGTTCC CCCACTCCCAACATCTAATG	231	58°C
31A	AATCTGTGATAACTTTCACTGG TGGAGAACTTTTCCTGTTGTG	356	58°C
31B	CAGGCTCTCTATTATGCTCG TGTTTGCACCACTGAACTCC	372	58°C
32	CATTATCATCAATGGAGGAATG CTTGCAGTGAGCCGAGATC	362	56°C

Exons	Primer sequence (5’ to 3’)	Amplicon size (bp)	PCR annealing temperature
33	CCTGTTATGTGCCTGATGTC TGAGTTAACACTCTAGACTATG	222	58°C
34	ATCTATGTTTTATCATACAGCTG ATCATTCTATGCATTGCCCTC	321	58°C
35	GCATTTTAAAGGGAAAAAGATAC CACTTTAGGGTAAAATAATATTTAG	402	54°C
36	ATATGGAGATACTGTTTCTTCC GCTGAATTTTAATTTACATGGTC	305	58°C
37	AATATGGAATAAGTATGGCATTG AGCAAACACTTATGTTTATCTTC	337	58°C
38	GTGACAGAGTGAGACTGGG ACAACACGGAGATTTATACTAC	397	58°C
39	ATAGTAGGAAGTAATAAAGCTTG TAGTGAATTCTCTTCCAATAGG	305	58°C
40	GTTCCTTTTATCATTGATACTTC AAGTAGAAATAAACTACTACCTC	352	58°C
41	GTGATAGCTTCAGAAAGTTGC CAGAATTAATACAGCCAGGTC	342	58°C
42	AACATATTTACATATTCTCTAGG TAAAGCTATATAATTTCCAGGTC	345	54°C
43	TTTGGTTTGGTAATGAGTATGC TTCAATTTCTAGGGGTCAACC	301	58°C
44	ACACTGAACTTTTCTTTTTTTATC AGATGTAATGCTTTTGGCCAG	320	58°C
45	TATCCAGTATGTCTTTTATGGC ACCATCACCATGATATATTAGG	329	58°C
46	TTTGCCTTTTCTTTTCAATGGC TATCTAAACTTTTCATTTCTGGC	223	58°C
47	TGTTGTATTGTTGGTACTTCG TTAGCCTTGCCTCTCATAAG	394	58°C

Exons	Primer sequence (5’ to 3’)	Amplicon size (bp)	PCR annealing temperature
48	TGGTTTCTAAAACTACTTTGAAG ACTTCCAGTTTTTCCAAGAGG	296	58°C
49	TAGAGCCCCAGGTTATTTTTG TGTTCATCAGGAAGAAACCAG	293	58°C
50	TTAGTACAGTTATTTGAACTGAC ACAATGCAAGGAACATCTTGC	293	58°C
51	ACGCTTTGTTAAAAATGTGTATC ATGCTTGTCTCTAGTTGTAGC	255	58°C
52	TCACTAGTTCATAAGAAATGCC AATTCGATTTTACAGGGAGAC	291	58°C
53	CCATTACCTTGAACTCATTCG TAGGATACGTAGTTAAAGATGG	230	58°C
54	ATTCAGGAATACTTTGGCTTTC TTCGGAGAACTGCTTATTTCC	418	58°C

7.9 LCA APEX chip results

DNA No	initials	Gene	Mutation 1	Mutation 2
March-07				
13412	MI	AIPL1	Ex6 905G>T R302L	Ex6 905G>T R302L
13680	WJ	AIPL1	Ex3 286G>A V96I	
14257	HE	AIPL1	Ex3 286G>A V96I	
14351	AS	AIPL1	Ex6 905G>T R302L	
14401	KC	CRB1	Ex7 2548G>A G850S	Ex12 C>T P1381L
14364	JN	MERTK	Ex14 1951 C>T R651X	
14348	NB	RPE65	Ex12 1301C>T A434V	
13992	TE	RPGRIP	Ex21 3358A>C?G I1120L/V	
14341	AM	RPGRIP	Ex9 1107delA FS	Ex9 1107delA FS
9909	JG	N		
10212	KP	N		
10766	DS	N		
13054	SS	N		
13149	FN	N		
13244	MC	N		
13529	OS	N		
13746	AF	N		
13760	BJ	N		
13765	GM	N		
13781	MR	N		
13842	DS	N		
13864	IR	N		
13956	AB	N		
13973	KL	N		
13989	MY	N		
14017	HS	N		
14076	JS	N		
14088	NG	N		
14090	SI	N		
14171	GH	N		
14208	HK	N		
14210	DS	N		
14214	LC	N		
14245	AM	N		
14267	MA	N		
14271	EDF	N		
14279	CL	N		
14282	RM	N		
14307	FH	N		
14317	NV	N		
14319	GA	N		

14323	AR	N		
14326	RS	N		
14336	IG	N		
14361	CB	N		
14368	AA	N		
14373	JA	N		
14380	CN	N		
14383	TZ	N		
14397	CS	N		
14408	CW	N		
13792	KJ	N		
14639	CF	N		
13841	RB	RDH12	Ex3 193 C>T R65X T/A	Ex3 193 C>T R65X T/A
14688	HA	N		
14682	BM	N		
14657	LH	N		
14663	DW	N		
14777	KAH	AIPL1	Ex4 487C>T Q163X	Ex4 487C>T Q163X
14654	JH	N		
6808	LF	RPGRIP1	Ex14 1767G>T Q589H GT/CA	
14634	JN	N		
14593	DS	RPGRIP1	Ex21 3341A>G D1114G G/C	
14702	SA	N		
14808	HG	N		
14689	RH	CEP290	Ex5 835 C>T Q279X T/A	Ex5 835 C>T Q279X T/A
14695	LB	N		
15014	YHT	N		
15032	OB	N		
15026	FL	RPE65	Ex4 272G>A R91Q GA/CT	
15039	JM	N		
14046	TD	RPGRIP1	Ex21 3402_3404 del GTC M1134I/S1135del GT/GA	
14737	SH	N		
15194	SG	N	Het splice Mutation TULP1 gene (Manchester)	
70815	SK	N		
October-07				
	EH		N	
	SH14479		N	
	AAH14548		N	
	RS14550		N	

	AP14561		N	
	DK14485	**RDH12**		
	RO14553		N	
	AK		N	
	AH		N	
	SK14577	**GUCY2D**	2101C>T P701S CT/GA	
	JT14585			
	AM14474	**RPE65**	963T>G N321K TG/AC	
	ARM14460			
	JH	**CRB1**	2843G>A C948Y GA/CT	
	RS			
Jul-08				
10511	LP		N	
14517	JW		N	
15000	MH	GUCY2D	Ex17 3056A>C H1019P AC/TG HET Mut	
14514	HN		N	
14737	SH		N	
14651	AD	AIPL1	Ex3 341C>T T114I CT/GA	
14650	ES	CRB1	Ex 7 2506C>A P836T CA/GT	
		CRX	Ex3 472G>A A158T GA/CT	
13680	WJ		N	
10679	ES		N	
10183	NW		N	
9694	EH		DEGRADED SAMPLE	
14328	MS		N	
10036	IM		N	
15000	MH	GUCY2D	Ex17 3056A>C H1019P AC/TG	
15001	MH	CRB1	Ex11 3992G>A R1331H A/T	Ex11 3992G>A R1331H A/T
CEP290	CEP290 PANEL			
13576	CM		IVS25 2991+1655 A>G C998X	IVS25 2991+1655 A>G C998X
6794	MS		IVS25 2991+1655 A>G C998X	Ex38 5254C>T K1752N
13467	CS		IVS25 2991+1655 A>G C998X	
14576	BR		IVS25 2991+1655 A>G C998X	2980G>A E994K
416A3	KR		Ex36 K1575X	Ex44 6084delA K2028fs

JP14000	JP		IVS25 2991+1655 A>G C998X	Ex5 381A>T+382delG K127fs
13773	TC		IVS25 2991+1655 A>G C998X	Ex19 1984C>T Q662X
13625	SW		IVS25 2991+1655 A>G C998X	Ex14 M407E fsX13
10785	JM		IVS25 2991+1655 A>G C998X	
13242	HJ		IVS25 2991+1655 A>G C998X	Ex36 4966 G>T E1656X
15286	WB	CEP290	Ex5 384_387delTAGA D128Efs TG/AT	IVS25 2991+1655 A>G C998X AG/TC
14685	GR	CEP290	Ex30 4028delA K1343fs AG/TG	
14736	TH	CEP290	IVS25 2991+1655 A>G C998X AG/TC	Ex46 6277delG V2093fs
14344	RS	CEP290	Ex1 21G>T W7C	Ex1 21G>T W7C
14689	RH	CEP290	Ex5 835 C>T Q279X T/A	Ex5 835 C>T Q279X T/A
13274	MS	RDH12	Ex 1 295C>A L99I	Ex 7 883C>T R295X
10138	SJ	RDH12	Ex 5 601T>C C201R	Ex 5 601T>C C201R
10462	LF	RDH12	Ex 6 715C>T R239W	Ex6 Del 806_810del5bp A269fsX1
13214	SH	RDH12	Ex6 806_810del5bp A269fsX1	Ex6 697G>C V233L
14176	EJ	RDH12	Ex6 806_810del5bp A269fsX1	Ex3 316C>T R106X
14303	RC	RDH12	Ex6 806_810del5bp A269fsX1	Ex5 451C>G H151D
14397	CS	RDH12	Ex5 609C>A S203R	Ex5 609C>A S203R
10812	SS	RDH12	Ex5 R169Q	Ex5 R169Q
14609	NM	RDH12	Ex4 381_delA G127fsX1	Ex3 R84X
14610	JM			
		RDH12		
		RDH12		
		RDH12		
Sept 2008				
15183	FCH	CRB1	2843G>A C948Y GA/CT	
15241	RS	N		
15160	YH	AIPL1		
15160	YH	RPGRIP1	Ex16 2417C>T T806I CT/GA	
15026	FL	RPE65	Ex4 272G>A R91Q GA/CT	
15057	GC	N		
14874	JS	AIPL1	IVS2- 277-2A>G SPLICE AG/TC	

15165	MA	N		
15110	JR	CRB1	Ex7 2401A>T K801X AT/TA	
15144	DH	N		
15066	HA	N		
11359	MG	N		
15240	HP	CRX	Ex2 196G>A V66I GA/CT	
14267	MA	N		
14782	SE	CRB1	Ex7 2401A>T K801X -/TA	
13957	LW	N		
14796	HM	N		
14599	SC	N		
14583	PA	CRB1	Ex7 2401A>T K801X AT/TA	
15033	EW	N		
13469	BS	CRB1	Ex9 2843G>A C948Y GA/CT	
14742	NC	RDH12	Ex2 146 C>T,new146C>A T49M, new T49K	Ex2 146 C>T,new146C>A T49M, new T49K
15070	AC	N		
15172	SS	CRX	Ex2 196G>A V66I GA/CT	
15236	KH	N		
10464	OA	CRB1	Ex7 2536G>A G846R	Ex7 2536G>A G846R
13076/10253	AC	CRB1	Ex7 2401A>T K801X AT/TA	Ex9 2843G>A C948Y GA/CT
1532	JD	N		
	YS	RPE65	Ex5 394G>A A132T GA/CT	
	JAR	GUCY2D	Ex10 2101C>T P701S CT/GA	
15278	AC	N		